NUMERICAL METHODS IN WAVE PROPAGATION IN PERIODIC STRUCTURES

A THESIS

PRESENTED FOR THE DEGREE OF

DOCTOR OF PHILOSOPHY

OF THE

UNIVERSITY OF SOUTHAMPTON

IN THE

FACULTY OF ENGINEERING AND APPLIED SCIENCE

BY

Jose J. de Espindola

May, 1974

ABSTRACT

Faculty of Engineering and Applied Science

Institute of Sound and Vibration Research

Doctor of Philosophy

Numerical Methods in Wave Propagation in Periodic Structures

by Jose J. de Espindola

This work describes a computer oriented study in wave propagation in periodic structures.

A simple introduction is first provided to review the concept of propagation constant and to lay down the basic terminology and ideas for subsequent development.

A general matrix theory of free wave propagation in general linear periodic structures is constructed. A general equation for the propagation constant is derived.

Stringer-stiffened plates and ring-stiffened cylinders undergoing only axi-symmetric motion are analysed by using this general theory.

The effect of coupling between transverse and torsional movement of a support (stringer) is considered.

Numerical methods for the computation of the field transfer matrix are analysed and modifications introduced, where appropriate, to increase accuracy and speed up computation time.

Free wave propagation in stringer-stiffened cylindrical shells and ring-stiffened cylinders undergoing general vibration motion is analysed by using the general method. The frequency dependence of the propagation constant is discussed.

The concept of complex wave component is introduced and used in the construction of a general matrix wave theory of the response of finite

and infinite periodic systems to concentrated harmonic forces. This theory is applied to finite and infinite stringer-stiffened plates and shells.

A general theory of the response of finite and infinite systems to a convected harmonic pressure field is derived and applied to stringer-stiffened plates and shells.

ACKNOWLEDGEMENTS

The author wishes to express his gratitude to the following:

To his wife Elisabeth, for her constant encouragement and preoccupation in keeping him well, both physically and spiritually.

To Dr D. Mead for his constant and interested guidance and help at all stages of this work.

To the University of Santa Catarina and Capes, both organs of the Brazilian Ministry of Education, for their financial support.

To all friends within and outside the ISVR whose interest and warm friendship alleviated the burdens and made his and his family's stay in this country happy and worth remembering.

Finally, to Miss C. Elliott for efficiently typing the manuscript.

CONTENTS

NOTATION

General

$[\ ]$	square matrix
$\{\ \}$	column matrix
$[\ ]^T$	transpose of a matrix
$[\ ]^{-1}$	inverse of a matrix
$[\ ]$	row matrix
Ω	circular frequency
Ω^*	complex non dimensional frequency
Ω_o^*	real non dimensional frequency
μ	complex propagation constant
μ_o	real propagation constant
E	complex modulus of elasticity
E_o	real modulus of elasticity
G	complex modulus of shear rigidity
G_o	real modulus of shear rigidity
ν	Poisson's ratio
ρ	mass density
$[A]$, $[A]_r$	state matrices
$[T(y_2, y_1)]$	transfer matrix, period transfer matrix
$[T_F(y, 0)]$	field transfer matrix
$[P]$	point transfer matrix
$\{z(y)\}$	state vector
x,y,z	spatial variables
$[u]$,$[\ v]$	modal matrices of $[A]$
$[\ \lambda_j\ ]$	diagonal matrix where λ_j are the eigenvalues of $[A]$
u,v,w	displacements in the x, y and z direction, respectively

r number of half waves along a support or number of waves along the circumference of a cylinder

ℓ distance between supports of rings

b distance between frames

ζ a constant

h thickness of plates and shells

K_θ torsional stiffness

K_v stiffness coefficient in the v direction

K_{wv} coupling coefficient between v and w coordinates

$K_{v\theta}$ coupling coefficient between v and θ coordinates

J polar moment of inertia

CW warping constant

P_i coefficients of the characteristic equation of $[T]$

$\{z(y)\}$, $\{x(y)\}$ station vectors

ASP aspect ratio

$[C]$, $[C]_r$ transformation matrix

$[B]$, $[B]_r$ a square matrix transforming $\{x(y)\}'$ into $\{x(y)\}$

K defined in 4.2.10

$\bar{x}$ non dimensional coordinate

R shell radius

A area of a support (stringer, ring) section

A_y, A_z, A_y, C_z defined in fig. 6.1

I_η, $I\zeta$, $I_{\eta\zeta}$ moment of inertia of a stringer

CV convection velocity

Chapter I

ψ	quantity associated with a free harmonic wave
t	time variable
$\{f(t)\}$	input vector

Chapter II

c_1, c_2	arbitrary constants
a_1, a_2, a_3	elements of a square matrix
η_r	stringer loss factor
α_o	a constant
v^*	non dimensional phase velocity
μ_i	imaginary part of the propagation constant
V^*	group velocity

Chapter III

q	generalised displacements
F	generalised forces
t_{ij}	element of the period transfer matrix

Chapter IV

η_1, η_2	elements of the state matrix for a plate element defined in 4.2.9
β	a constant
k	defined in 4.2.10
C	defined in 4.2.12
C_j	coefficients defined in 4.3.1
θ_p	principal argument of a complex number
I_p	polar moment of inertia

$\bar{I}$ a principal moment of inertia defined in eq. (4.4.3)

A area of a ring section

$t^F_{i,j}$ elements of the field transfer matrix

$t^*_{i,j}$ element of the reduced transfer matrix

Chapter V

$[P_j]$ constituent idempotents of $[A]$

$\{x_1\}$, $\{x_2\}$ column matrices defined in 5.3.1

$c_1,..,c_8$ constants

Δ determinant

$[D]$ defined in 5.3.4

$\{v_j\}$, $\{u_j\}$ columns of $[V]$ and $[U]$ respectively

δ_{jm} defined in 5.4.2

Chapter VI

b_{ij} elements of $[B]_r$

η_1, η_2 defined in 4.2.9

η_3 defined in 6.2.8

α a constant defined in 6.2.8

$\{x\}$ a state vector

c_{ij} element of $[C]_r$

d_{ij} element of $[C]_r^{-1}$

α_o, α_1,α_2 defined in 6.3.5

α_4 defined in 6.4.1

ϕ angular coordinate (see fig. 4.1)

F_w,F_v,F_u,F_θ external forces and moments acting on a ring

t_{ij} element of the period transfer matrix

$t^F_{i,j}$ element of the field transfer matrix

$\{S_z(\Omega_o^*)\}$ power spectral density of the response

$S_p(\Omega_o^*)$ power spectral density of the excitation

$< >$ time average

α_k complex constants defined in 8.3.1

Chapter VII

c_j coefficients defined in 7.2.1

$\{c\}_r$ column matrix of coefficients c_j

$[F]$ square matrix defined in 7.2.2

α_m complex coefficients defined in 7.2.16

$\psi_m(y)$ complex wave component

$f(x,y,t)$ exciting harmonic force

γ defined in fig. 7.1

$\{f\}_r$ exciting vector

$[\Sigma(\gamma)]$ a square matrix defined in 7.3.4

$\sigma_{i,k}$ elements of $[\Sigma(\gamma)]$

$q_j(y)$ generalised displacement

s non dimensional coordinate

Chapter VIII

$p(x,y,t)$ harmonic pressure field

p_{or} amplitude of the harmonic pressure field

k wave number

c_j arbitrary constants defined in 8.2.6

$\{c\}$ column matrix of coefficients c_j

$\{c_u\}$ column matrix defined in 8.2.8

$\{X\}$ square matrix defined in 8.2.8

$\{Z_p\}$ column vector defined in 8.2.12

CHAPTER I

1.1 INTRODUCTION

A periodic system is one that consists of identical elements joined together in an identical manner to form the whole system. It is possible to find many such systems in engineering; a large hydroelectric power station pipeline resting on stiffening rings placed at equal distance from each other; a tall building having a uniform structure and identical storeys; an aircraft fuselage consisting of a cylindrical uniform shell stiffened by identical frames and regularly spaced stringers. The modal method of analysing the high frequency forced vibrations of such structures bears inherent shortcomings that are difficult to overcome in practice chiefly when the structure is made up of many periodic elements. For instance, it is well known |6| that the natural frequencies of a periodic structure fall into groups and that each group contain as many natural frequencies as the number of periods of structure. When the number of periods is large (as so often occurs) the natural frequencies are very closely spaced and the modal method becomes complicated to apply to find the response of the structure. Also in these cases the computer time and storage required to find the natural frequencies and normal modes of the structure are very large.

These difficulties may be bypassed by using a wave approach proposed by Mead |9 |. No previous calculations of normal modes or natural frequencies are required to compute the response of the structure to external excitations. Also, no lengthy summation of modal contributions to the response is needed. Damping adds no further complications to the wave method as it does by coupling the normal modes. The wave approach also provides a better insight to the dynamical behaviour of the structure when it is to be excited by a convected acoustic pressure field or

turbulent boundary layer excitations. The wave propagation method is based on a very simple principle (which will be referred to here as 'the basic principle of free wave propagation in spatially periodic systems').

It states that all response quantities ψ associated with a single free harmonic wave in a periodic system (for instance, a transverse displacement, moment, etc.) have values ψ_1, ψ_0 at the extremes of a system period related as:

$$\psi_1 = \psi_0 \, e^{-i\mu} \qquad ..(1.1.1)$$

where μ is the so called propagation constant and it is the change of phase between ψ_1 and ψ_0.

The basic principle expressed by (1.1.1) has extensively been used by Brillouin |7| in connection with crystal structures and electric lines. Its early applications to engineering periodic structures include works by Ungar |40| and Bobrovnitskii and Maslov |41|.

Ungar has derived expressions for the propagation constant for a beam resting on periodic impedances in terms of reflections and transmission coefficients. Bobrovnitskii and Maslov have studied the propagation of waves on a beam with periodic point loading.

The use of receptance functions was first introduced by Mead and Wilby |9|. In |5| Mead reviewed in depth the concept of propagation constants in connection with the free wave propagation in beams on identical, equi-spaced supports. Also the concept of free wave motion as a group is analysed in detail. This concept has later been applied to the response of finite periodic one-dimensional structures |12| and to the analysis of rib-skin structures |11|.

The use of receptance functions has proved adequate to analyse the sort of structures dealt with in |9|, |5|, |12| and |11| but it is apparent that the method would become cumbersome for more complex structures

(for instance, stringer-stiffened shells) or when the supports have more than one degree of freedom coupled together.

It is the purpose of this work to seek a method of wave solution applicable to such complex structures, which, besides being fairly general, requires only a reasonable amount of algebra and is quite adequate for automatic computations.

It has been previously shown |28|, |3|, |4| that transfer matrices can be a powerful tool in analysing periodic structures. It was felt then that by coupling the ability of transfer matrices of handling structures with complex supports with the wave framework of thinking it would provide a good approach to the solution of dynamics problems related to periodic structures.

In chapter II the basic ideas of the method are explained. Generality at that stage was sacrificed in favour of simplicity and the results are valid only for the particular case considered there (a flat plate resting on supports with only one degree of freedom). The notions of propagation constants and wave groups are also reviewed.

In chapter III the general basis of the method is established. This is done with disregard for the particulars of the structure (other than being spatially periodic and linear). A general equation for the propagation constant is derived.

In chapter IV the method is first checked by applying it to the free wave propagation problem of systems with two terminal degrees of freedom. Specifically, a flat plate periodically supported by stringers with two degrees of freedom (rotation and transverse movements) is taken as an example. The effect of coupling is also discussed. Another example, a ring stiffened cylinder undergoing axi-symmetric vibrations, is also considered.

In chapter V the problem of efficiently (in computing time and

accuracy) computing the field transfer matrix for systems with more than two terminal degrees of freedom is considered. Existing methods are reviewed and compared and modifications are suggested, whenever possible, in order to speed up computations and increase accuracy.

In chapter VI two examples are considered (a stringer-stiffened cylindrical shell and a ring-stiffened cylinder) with four terminal degrees of freedom. The general theory established in chapter III is used with three methods of computing the field transfer matrix. It was found that all three methods give virtually the same numerical results but they differ slightly in computing time efficiency.

The general problem of response of infinite and finite periodic structures to concentrated loads is tackled in chapter VI. Again the terminology established in chapter III has proved adequate for a general treatment of this problem. A theoretical background is first constructed leading to the definition of the 'complex free wave components'. The complex free wave components are then used to compute the response of finite and infinite periodic structures. The method is again checked numerically by considering a stringer-stiffened flat plate and a stringer-stiffened circular shell. The role of damping is also analysed in connection with the response.

In chapter VIII a general wave solution is given for the response of infinite and finite periodic structures to a convected harmonic pressure field. This solution is in fact a generalisation of that given by Mead |37| for beams. Again the particulars of the structure (apart from being periodic and linear) are bypassed. The method is checked in a stringer-stiffened flat plate and in a stringer-stiffened shell. Frequency response curves for these structures are presented and discussed.

1.2 TRANSFER MATRIX : THEORETICAL BACKGROUND

1.2.1 The State Equation

The basics of transfer matrices can be found in many texts dealing with engineering structures and automatic controls (see, for instance, |13| and |22|). However, for the sake of completeness and for easy reference a brief account of the theory is provided in this section.

Consider a mathematical model M (i.e. a set of mathematical equations) of a physical system S. The role of the mathematical model is to describe some aspect of the behaviour of the real system. The constituent equations of the mathematical model can be of various form such as algebraic, differential, etc. For the purpose of this work only differential equations need to be considered.

In control theory the concept of state of a physical system (as well as of output) is normally associated with a particular instant of time. For instance, if a certain input is applied to the physical system at an instant to the observed output (as well as the state of the system) at the instant t will depend on the applied input and also on the initial state of the system. Therefore the mathematical model of a system consists of two kinds of equation: those describing the state of the system and those describing the output of the system.

This work will not, of course, be concerned with output equations but only with state equations. For a physical system the state equation can be written as

$$\{z(t)\}^{\bullet} = g(\{z(t)\}, \{f(t)\}, t) \qquad ..(1.2.1)$$

where $\{z(t)\}$ is a column vector representing the state of the system at the instant t and $\{f(t)\}$ is an input vector, and $\{z(t)\}^{\bullet}$ is the time derivative of $\{z(t)\}$.

If the system is linear (1.2.1) can be written as

$$\{z(t)\}^{\bullet} = [A(t)]\{z(t)\} + [B(t)]\{f(t)\} \qquad ..(1.2.2)$$

where $[A(t)]$ and $[B(t)]$ are N x N and N x P matrices, respectively, and $\{f(t)\}$ is a P x 1 column vector.

Now, for the purpose of this work the concept of state must be adapted. Instead of referring to the state of the system at the time t one shall be talking about the state of the system at a particular 'station'. Initial state will mean the state at a reference station. Therefore the time dimension will be substituted for a spatial dimension. When this adaptation is made equation (1.2.2) can be read:

$$\{z(y)\}' = [A(y)]\{z(y)\} + [B(y)]\{f(y)\} \qquad ..(1.2.3)$$

where $\{z(y)\}'$ is the spatial derivative of $\{z(y)\}$.

In many engineering structures matrices $[A(y)]$ and $[B(y)]$ do not depend on y. In these cases the 'state equation' (1.2.3) can be written as:

$$\{z(y)\}' = [A]\{z(y)\} + [B]\{f(y)\} \qquad ..(1.2.4)$$

If no input is applied equation (1.2.4) is further simplified:

$$\{z(y)\}' = [A]\{z(y)\} \qquad ..(1.2.5)$$

Both equations (1.2.4) and (1.2.5) will find their applications in the course of this work.

1.2.2 The transfer matrix

By a transfer matrix $[T(y_2,y_1)]$ it is understood to be a linear operator that transforms the station vector $\{z(y_1)\}$ into $\{z(y_2)\}$. In mathematical notation:

$$\{z(y_2)\} = [T(y_2,y_1)]\ \{z(y_1)\} \qquad ..(1.2.6)$$

Or, for the particular case where $y_1 = 0$ and $y_2 = y$:

$$\{z(y)\} = [T(y,0)]\ \{z(0)\} \qquad ..(1.2.7)$$

Assuming a solution for (1.2.5) of the form $\{z(y)\} = e^{[A]y}$ (see Ref. 27) one can easily see that:

$$[T(y,0)] = e^{[A]y} \qquad ..(1.2.8)$$

It can also be shown that |27| :

$$e^{[A]y} = \sum_{j=0}^{\infty} [A]^j \frac{y^j}{j!} \qquad ..(1.2.9)$$

that is:

$$[T(y,0)] = \sum_{j=0}^{\infty} [A]^j \frac{y^j}{j!} \qquad ..(1.2.10)$$

From expression (1.2.8) some properties of the transfer matrix can be easily derived:

$$[T(0,0)] = [I]$$

$$[T(y_1 + y_2,0)] = [T(y_1,0)]\ [T(y_2,0)] \qquad ..(1.2.11a,b,c)$$

$$[T(y,0)]^{-1} = [T(-y,0)]$$

Other properties of transfer matrices will be listed in Appendix A.

Another expression for the transfer matrix which will be derived in chapter VII is given below:

$$[T(y,0)] = [U]\ [\lambda_j]\ [U]^{-1} \qquad ..(1.2.12)$$

Where $[U]$ is the modal matrix of $[A]$ and $[\lambda_j]$ a diagonal matrix of the eigenvalues of $[A]$.

Expressions (1.2.10) and (1.2.12) will find their applications in chapters V, VI, VII and VIII.

CHAPTER II

Free wave propagation in systems with one terminal degree of freedom

2.1 GENERAL

The purpose of this chapter is to provide an introduction, in a rather simple manner to the basic ideas that form the framework of the methods to be developed in this work, aimed to formulate and solve problems in wave propagations in spatially periodic structures. To this end a thin flat plate, resting on equally spaced flexible supports (or stringers) in one direction and simply supported along an orthogonal direction, is taken as a concrete example. The flexible supports are, for the time being considered infinitely stiff in the transverse direction but can rotate and, consequently, apply both elastic and inertial moments on the plate. The consideration of periodic supports with infinite transverse stiffness might eventually bring severe errors if coupling between transverse and rotational movements of the supports is considerable. But this model is very convenient for the purpose of this chapter due to its inherent simplicity.

For subsequent chapters the ideas introduced here will be extended and a general formulation of the problem of free wave propagation in periodic structures will be presented. In this formulation the peculiarities of the structure (other than being periodic and linear) are by-passed. Restrictions such as that of infinite transverse stiffness, applied to the present model, shall no longer be necessary.

2.2 THE FIELD TRANSFER MATRIX

The sequence of steps toward establishing the basic concepts of this introductory theory will lead to an equation that relates the propagation constant to the frequency.

Consider the model depicted in fig. 2.1 where a uniform flat plate rests on torsionally elastic supports periodically located ℓ units of

length apart and on two other simple supports, orthogonal to the former ones, b being the distance between them. It shall be assumed also that the contact between plate and supports occurs along a line. This is a reasonable assumption since the common area between plate and support is small compared with the area of the bay.

In spite of its simplicity this model can realistically represent an aircraft fusilage structure as it has been shown by Lin |1| and Clarkson |2|.

The simple supports then represent the frames action. The frames have usually very high transverse and torsional stiffness so that they behave as rigid boundaries and panels adjacent across the frames move almost independently. Even so, the hypothesis of simple supports representing frames works, provided the distance between the frames is, say, two and a half times, or greater, the distance between supports (stringers). There is however considerable correlation across the stringers. So, even if the purpose of this chapter is only to bring about ideas that are to be generalized in order to make the theory suitable for more advanced models, the expressions to be obtained are, nevertheless, of value in practice.

Consider now the differential equation of motion of a linear damped flat plate referred to the system of coordinates of fig. 2.1

$$\frac{\partial^4 w}{\partial x^4} + 2\frac{\partial^4 w}{\partial x^2 \partial y^2} + \frac{\partial^4 w}{\partial y^4} = -\frac{h\rho}{D}\frac{\partial^2 w}{\partial t^2} \qquad ..(2.1.1)$$

where w, deflection

h, thickness of the plate,

ρ, mass density,

$D = D_c(1 + i\eta)$, complex flexural stiffness,

where

D_o, flexural stiffness, and

η, loss factor.

If the structure is vibrating harmonically with a frequency Ω, the general solution of equation (2.1.1) can be written as

$$w(x,y,t) = \sum_{r=1}^{\infty} w_r(y) \cdot \sin \frac{r\pi x}{b} \cdot e^{i\Omega t} \qquad ..(2.1.2)$$

where i is the complex unit.

If such solution is introduced into equation (2.1.1) and the expression $e^{i\Omega t}$ eliminated the result is an ordinary linear homogeneous differential equation of fourth order:

$$w_r^{IV}(y) - 2\zeta^2 w_r^{II}(y) + (\zeta^4 - \frac{\rho h \Omega^2}{D}) w_r(y) = 0 \qquad ..(2.1.2a)$$

where $\zeta = \frac{r\pi}{b}$.

The associated characteristic equation is:

$$\lambda^4 - 2\zeta^2\lambda^2 + (\zeta^4 - \frac{\rho h \Omega^2}{D}) = 0 \qquad ..(2.1.3)$$

Equation (2.1.3) has solutions as follows:

$\lambda_1, -\lambda_1, i\lambda_2, -i\lambda_2$, where

$$\lambda_1 = \frac{1}{\ell} \left\{ (\frac{r\pi}{ASP})^2 + \Omega^* \right\}^{\frac{1}{2}} \qquad ..(2.1.4)$$

$$\lambda_2 = \frac{1}{\ell} \left\{ \Omega^* - (\frac{r\pi}{ASP})^2 \right\}^{\frac{1}{2}} \text{ , and}$$

$ASP = b/\ell$, aspect ratio, and

$\Omega^{*2} = \frac{\rho h \ell^4 \Omega^2}{D}$, complex nondimensional frequency.

The solution of equation (2.1.2) is therefore a linear combination of four functions of the type $e^{\lambda y}$. Making use of the simple support

boundary conditions at the frames, it is possible to express two of the arbitrary constants of the linear combination as functions of the other two. Only two arbitrary constants remain.

In the present development, solutions of the form of the expression (2.1.5) will be assumed:

$$W_r(y) = C_1(\sinh \lambda_1 \ell \sin \lambda_2 y - \sin \lambda_2 \ell \sinh \lambda_1 y)$$

$$+ C_2\left[\sinh \lambda_1 \ell \sin \lambda_2 (\ell - y) - \sin \lambda_2 \ell \sinh \lambda_1 (\ell - y)\right] \quad ..(2.1.5)$$

Functions (2.1.5) clearly satisfy the condition of zero deflections at the stringers.

Assume now the following expression for the bending moment :

$$M(y) = \sum_{r=1}^{\infty} M_r(y) \sin \frac{r\pi x}{\ell} e^{-i\Omega t}$$

$$\text{where } M_r(y) = -D\left[\frac{\partial^2 W_r(y)}{\partial y^2} - \nu\zeta^2 W_r(y)\right] \quad ..(2.1.6\ a,b)$$

From (2.1.5) and (2.1.6) the following expressions can be written:

$$W_r'(o) = C_1(\lambda_2 \sin h\lambda_1\ell - \lambda_1 \sin \lambda_2\ell) + C_2(\lambda_1 \sin \lambda_2\ell \cos h\lambda_1\ell$$

$$- \lambda_2 \sin h\lambda_1\ell \cos \lambda_2\ell) \quad ..(2.1.7\ a,b)$$

$$M_r(o) = D.C_2.(\lambda_2^2 \sin h\lambda_1\ell \sin \lambda_2\ell + \lambda_1^2 \sin \lambda_2\ell \sin h\lambda_1\ell)$$

The above expressions can be conveniently written in matrix form:

$$\begin{Bmatrix} W_r'(o) \\ M_r(o) \end{Bmatrix} = \begin{bmatrix} a_1 & a_2 \\ o & a_3 \end{bmatrix} \begin{Bmatrix} C_1 \\ C_2 \end{Bmatrix} \quad .. (2.1.8)$$

and the elements of the 2 x 2 square matrix are:

$$a_1 = \lambda_2 \sin h\lambda_1 \ell - \lambda_1 \sin \lambda_2 \ell$$

$$a_2 = \lambda_1 \sin \lambda_2 \ell \cos h\lambda_1 \ell - \lambda_2 \sin h\lambda_1 \ell \cos \lambda_2 \ell$$

$$a_3 = D \sin \lambda_2 \ell \sin h\lambda_1 \ell \, (\lambda_1^2 + \lambda_2^2)$$

Similar expressions can be written for the slope and displacement at the right end of the bay:

$$\begin{Bmatrix} w_r'(\ell) \\ M_r(\ell) \end{Bmatrix} = \begin{bmatrix} -a_2 & -a_1 \\ a_3 & o \end{bmatrix} \begin{Bmatrix} C_1 \\ C_2 \end{Bmatrix} \qquad ..(2.1.9)$$

Isolating the vector $\begin{Bmatrix} C_1 \\ C_2 \end{Bmatrix}$ from expression (2.1.8) by inverting the square matrix and taking this vector into expression (2.1.9) the result is:

$$\begin{Bmatrix} w_r'(\ell) \\ M_r(\ell) \end{Bmatrix} = \begin{bmatrix} -\frac{a_2}{a_1} & (\frac{a_2^2}{a_1 a_3} - \frac{a_1}{a_3}) \\ \frac{a_3}{a_1} & -\frac{a_2}{a_1} \end{bmatrix} \begin{Bmatrix} w_r'(o) \\ M_r(o) \end{Bmatrix} \qquad ..(2.1.9)$$

The square matrix appearing in the above expression acts as an operator such that, when applied to the vector

$\begin{Bmatrix} w_r'(o) \\ M_r(o) \end{Bmatrix}$ it gives $\begin{Bmatrix} w_r'(\ell) \\ M_r(\ell) \end{Bmatrix}$.

It is in essence a transfer matrix. One can easily see that the determinant of this matrix is one. This happens in accordance with one of the properties of transfer matrices listed in appendix A.

In short, the expression (2.1.9) can be written as:

$$\begin{Bmatrix} w_r'(\ell) \\ M_r(\ell) \end{Bmatrix} = \left[T_F(\ell,0)\right] \begin{Bmatrix} w_r'(0) \\ M_r(0) \end{Bmatrix} \qquad ..(2.1.9\ a)$$

where $\left[T_F(\ell,0)\right]$ is the field transfer matrix and is able to 'transfer' quantities from coordinate 0 to coordinate ℓ along the field. Vectors such as those appearing in equa.(2.1.9) are called station vectors, or state vectors.

2.3 THE POINT TRANSFER MATRIX

In order to apply the basic principle of free wave propagation to a spatially periodic structure an overall transfer matrix must be found that can 'transfer' quantities through a whole period of the structure. Whatever the way a period is considered it must contain a support.

So, an operator has to be found such that when applied to the station vector on the left of a support the station vector on the right of the same support is obtained. This operator is the point transfer matrix.

The supports under consideration in the present chapter have only one degree of freedom, that is, rotation and the point transfer matrix can be derived by applying the compatibility conditions and by knowing that the jump in moment is proportional to the slope:

$$\begin{aligned} w_r'^R(\ell) &= w_r'^L(\ell) \\ M_r^R(\ell) - M_r^L(\ell) &= K_\theta w_r'^L(\ell) \end{aligned} \qquad ..(2.3.1)$$

In the above expression R and L stand for right and left, respectively. In matrix form expression (2.3.1) gives:

$$\begin{Bmatrix} w_r'(\ell) \\ M_r(\ell) \end{Bmatrix}^R = \begin{bmatrix} 1 & 0 \\ K_\theta & 1 \end{bmatrix} \begin{Bmatrix} w_r'(\ell) \\ M_r(\ell) \end{Bmatrix}^L \qquad ..(2.3.2)$$

where $\begin{bmatrix} P \end{bmatrix} = \begin{bmatrix} 1 & 0 \\ K_\theta & 1 \end{bmatrix}$ is the point transfer matrix and its determinant is obviously one.

The point transfer matrix for an open cross section stringer with a line attachment to the plate, or skin, and with the point of attachment and the shear center located on the same perpendicular to the plate was first derived by Lin |3|. Henderson and McDaniel |4| have later dropped this last restriction by allowing a general location of the shear center in relation to the point of attachment (fig. 6.1)

According to Henderson and McDaniel the torsional stiffness K_θ is given by:

$$K_\theta = -GC\zeta^2 - E\zeta^4 CWA + J_A \dot{\alpha}_o \Omega^*{}_o^2 \qquad ..(2.3.3)$$

where:

$E = E_o(1 + i\eta_r)$, complex modulus of elasticity in tension,

E_o, modulus of elasticity in tension,

η_r, loss factor for the stringer,

$G = \dfrac{E}{2(1 + \nu)}$, modulus of elasticity in shear,

C, Saint-Venant's constant for the cross section,

$CWA = CW_o + I_\zeta A_z^2 + I_\eta A_r^2 - 2I_{\eta\zeta} A_r A_z$, warping constant for rotation about point A,

$J_A = J_C + A(C_z - A_z)^2 + A(C_y - A_y)^2$, polar moment of area with respect to point A,

$$\alpha_o = Do/\ell^4 h \quad \text{and} \quad \Omega^{*2}_o = \frac{\rho h \Omega^2 \ell^4}{D_o}$$

In expression (2.3.3) it has been implicitly assumed that both skin and stringer have the same mass density.

2.4 THE EQUATION FOR THE PROPAGATION CONSTANT

Expressions (2.3.2) together with (2.1.9) can be joined in one single expression:

$$\begin{Bmatrix} w_r'(\ell) \\ M_r(\ell) \end{Bmatrix}^R = \begin{bmatrix} -\frac{a_2}{a_1} & \frac{a_2^2}{a_1 a_3} - \frac{a_1}{a_3} \\ -K_\theta \frac{a_2}{a_1} + \frac{a_3}{a_1} & K_\theta\left(\frac{a_2^2}{a_1 a_3} - \frac{a_1}{a_3}\right) - \frac{a_2}{a_1} \end{bmatrix} \begin{Bmatrix} w_r'(o) \\ M_r(o) \end{Bmatrix} \qquad .. (2.4.1)$$

The square matrix in expression (2.4.1) is the overall transfer matrix necessary to the derivation of the equation for the propagation constant and is obtained as a product of the point and field transfer matrices:

$$[T] = [P]\,[T_F(\ell,0)] \qquad ..(2.4.1\ a)$$

Since both point and field transfer matrices have unitary determinant the determinant of the overall transfer matrix is also one.

Now, the application of the basic principle of free wave propagation in spatially periodic structures leads to the following expressions:

$$\begin{Bmatrix} w_r'(\ell) \\ M_r(\ell) \end{Bmatrix}^R = e^{-i\mu} \begin{Bmatrix} w_r'(o) \\ M_r(o) \end{Bmatrix} \qquad ..(2.4.2)$$

which together with (2.4.1) leads to:

$$\left[[T_o] - e^{-i\mu}[I]\right] \begin{Bmatrix} w_r'(o) \\ M_r(o) \end{Bmatrix} = \{0\} \qquad ..(2.4.3)$$

Expression (2.4.3) is in fact an $|2 \times 2|$ eigenvalue problem showing that the eigenvalues of the period transfer matrix are $e^{-i\mu}$. If some damping is present either in the plate or in the supports or in both the period transfer matrix is complex and, accordingly, the propagation constants are complex. When no damping is present the propagation constant might be real or purely imaginary. Only those frequencies for which the propagation constants are real correspond to actually propagating waves.

The characteristic equation associated with the eigenvalue problem (2.4.3) or, in other words, the characteristic equation of the period transfer matrix $[T]$ can easily be seen to be:

$$e^{-i2\mu} - \left\{K_\theta \frac{a_2^2 - a_1^2}{a_1 a_3} - 2\frac{a_2}{a_1}\right\} e^{-i\mu} + 1 = 0 \qquad ..(2.4.4)$$

It is worthwhile looking at equation (2.4.4) and noting that if μ is a solution then $-\mu$ is also a solution. This is in accordance with the physical fact that if the structure allows a wave to propagate, say, to the right, another wave with the same phase velocity should be able to propagate to the left. This fact can also lead to the conclusion that equation (2.4.4) is equivalent to the following:

$$\cos \mu = \frac{K_\theta}{2}\left(\frac{a_2^2 - a_1^2}{a_1 a_3}\right) - \frac{a_2}{a_1} \qquad ..(2.4.5)$$

The above expression is the equation for the propagation constant.

Mead |5| has obtained an equation for the propagation constant for a beam on periodic massless torsional supports using receptance functions. The similarity in the form of his equation and that of (2.4.5) is expected. The case of a beam can be considered by taking $\lambda_1 = \lambda_2 = \lambda$ so that:

$$\begin{aligned} a_1 &= \lambda \sin h\lambda\ell - \lambda \sin \lambda\ell \\ a_2 &= \lambda \sin \lambda\ell \cos h\lambda\ell - \lambda \sin h\lambda\ell \cos \lambda\ell \\ a_3 &= D \sin \lambda\ell \sin h\lambda\ell \, .2\ell^2 \end{aligned} \qquad ..(2.4.6)$$

Miles |6| in an early paper has produced a formula applicable to a beam on simple periodic supports and this formula was derived by making use of difference equations. Miles's formula can be reproduced here by making K_θ equal to zero and substituting (2.4.6) into (2.4.5):

$$\cos \mu = \frac{\sin h\lambda\ell \cos \lambda\ell - \sin \lambda\ell \cos h\lambda\ell}{\sin h\lambda\ell - \sin \lambda\ell} \qquad ..(2.4.7)$$

In expressions (2.4.6) and (2.4.7) λ is given by:

$$\lambda = \frac{1}{\ell} \left(\Omega^*\right)^{\frac{1}{2}} \quad \text{and} \quad \Omega^{*2} = \frac{\rho \ell^4 \Omega^2}{D}$$

Another convenient form of the equation for the propagation constant that is very convenient in analysis is expressed by equation (2.4.8):

$$f(\Omega^*_o, \mu_o) = 0 \qquad ..(2.4.8)$$

In this equation μ_o is considered an independent variable and Ω^*_o an implicit function of μ_o.

The values of μ_o in equation (2.4.8) are restricted to those that make the nondimensional frequency real.

For damped systems the propagation constant must be complex but for non-damped systems there are real values of μ satisfying (2.4.8).

In this work equation (2.4.8) is used in connection with non-damped systems only and it will prove to be interesting both in computations and in the understanding of the phenomenon of free wave propagation in periodic structures. When some damping is present one shall resort to equations of (2.4.4) type.

2.5 PRESENTATION OF NUMERICAL RESULTS; DISCUSSION OF EQUATIONS (2.4.7) AND (2.4.8)

Equations (2.4.7) and (2.4.8) can provide a basis for a discussion from which the fundamentals of the nature of free wave propagation in spatially periodic structures can spring up. Brillouin |7| has first

analysed the phenomenon through discrete spring mass models related to crystals and transmission lines and Mead |5| has thrown further light into it by considering a continuous beam resting on simple periodic supports with massless spring-like torsional restraints. The present discussion rests heavily on these previous works and is introduced here for the sake of completeness and uniformity of wording.

Consider first equation (2.4.7) in connection with a non-damped beam on simple periodic supports.

The right-hand side of equation (2.4.7) is obviously real for any value of the frequency. Those frequencies for which its modulus is equal or smaller than one correspond to real values of the propagation constant. One could call these allowed frequencies, or propagating frequencies. If energy is fed into any point of the structure in one of these frequencies it will propagate in both directions. If the modulus of the right-hand side of (2.4.7) is greater than one the propagation constant is no longer real.

It can either be a pure imaginary number or a complex one, the real part being 0 or π and the imaginary part given by:

$$\mu_i = - \log \left| \cos \mu + (\cos^2 \mu - 1)^{\frac{1}{2}} \right| \qquad ..(2.5.1)$$

One could then talk of a decaying wave and the corresponding frequencies could be called attenuating frequencies.

Fig. (2.2) is a plot of equation (2.4.7) in which the nondimensional frequency Ω^*_o is in the abcissas axis and cos μ, in the ordinate axis.

This figure shows portions of the curve inbetween the $\pm$ 1 lines, these portions meaning bands of propagating frequencies. Also in the graph are shown portions where the curve lies outside the two limiting lines and these represent bands of attenuating frequencies. The figure shows the first three propagation bands numbered 1, 2 and 3, and two attenuation

bands. Therefore a beam on simple periodic supports behaves in a band-pass filter manner and it will be shown in forthcoming chapters that this is, in fact, a common feature of much more complex types of periodical structures. It is worth noting that the crossing points A, B, C, D, E and F correspond to nondimensional frequencies values of π^2, $(\frac{3\pi}{2})^2$, $(2\pi)^2$, $(\frac{5\pi}{2})^2$, $(3\pi)^2$, $(\frac{7\pi}{2})^2$ and $(4\pi)^2$, respectively. In short, the n^{th} pass band starts at the nondimensional frequency $(n\pi)^2$ and finishes at $\left|(2n + 1)\pi/2\right|^2$ These results have first been found by Miles |6|. The previous analysis could also be made by looking at figure (2.3). This is a very interesting kind of graph for the analysis of free wave propagation in periodical structures that will be used throughout this work and is better explained in connection with equation (2.4.8). One can see (for instance, by looking at eqn. 2.4.7) that the frequency is a symmetric function of the propagation constant. This is a general statement applicable to any periodic structure, whatever its degree of complexity. Furthermore, the frequency is a periodic function of the propagation constant, its period being 2π.

These two properties are the basis for the construction of the curves of fig. (2.3) which, for brevity of reference, will be called, from now on, μ_o- Ω^*_o curves.

Symmetry and periodicity properties make it sufficient to draw the curves for half a period only, say, from 0 to π. But one could imagine the graph extending indefinitely to both right and left.

In Fig. (2.3) the first three propagation bands are indicated by numbers 1, 2 and 3.

It is appropriate at this point to define a nondimensional <u>phase velocity:</u>

$$v^* = \frac{\Omega^*_o}{\mu_o} \qquad ..(2.5.2)$$

It is obvious that the phase velocity is dependent on the frequency, that

is, a beam on simple periodic supports, and indeed any periodic structure, is a dispersive medium. As such, only waves that are spatially sinusoidal do not distort as they propagate through the structure. On the other hand, short pulses and short signals always distort as they travel along the structure.

If one thinks of a point harmonically varying force applied to one of the bays of an infinite periodic structure it is easy to understand that the distribution of deflections along the structure does not follow a sinusoidal pattern.

It is particularly easy to visualise this fact by thinking of a static force, i.e. a point harmonic force with zero frequency. The same applies even if the frequency is a propagating one, in which case one could think of a Fourier decomposition of the spatially distributed deflections. To each one of these components there corresponds a propagation constant and, consequently, a phase velocity. In fact one can realise by looking at expressions (2.4.2), or (2.4.5), that if μ_o is the propagation constant corresponding to the frequency Ω^*_o, then $\mu_o \pm j2\pi$, $j = \pm 1, \pm 2 \ldots$, is also a propagation constant corresponding to Ω^*_o. Briefly: the spatially distributed deflections can be decomposed in spatially sinusoidal Fourier components with propagation constants $\mu_o \pm j2\pi$ and nondimensional phase velocities:

$$V^*_j = \frac{\Omega^*}{\mu_o + j2\pi} \quad j = \pm 1, \pm 2, \ldots \qquad ..(2.5.2\ a)$$

If fig. (2.3) is imagined extended to both right and left and if a line parallel to the μ_o-axis is drawn through Ω^*_o (impressed nondimensional frequency of the harmonic point force), this parallel line will cut one of the $\mu - \Omega^*_o$ curves (if the frequency is propagating) at infinite points, each of them corresponding to one of the propagation constants $\mu_o + j2\pi$, $j = \pm 1, \pm 2 \ldots$, that is, corresponding to one of the spatially sinusoidal components. The nondimensional phase velocities will be the quotient of

the impressed nondimensional frequency over these component propagation constants.

The so called nondimensional group velocity is given by

$$V^* = \frac{d\Omega^*_o}{d\mu_o} \qquad ..(2.5.3)$$

When the system shows no dissipation, the group velocity gives the speed of the travelling energy. But if the structure dissipates energy the group velocity becomes less meaningful, physically speaking. Now, if $0 \leq \mu_o \leq \pi$ the slopes at the points $\mu_o + j2\pi$, $j = 0, \pm 1, \pm 2 ..$, are all equal, that is, the group velocity is unique and can be computed by taking any of the sinusoidal wave components.

This means that the set of sinusoidal wave components form, in fact, a group. Similarly, from the point of application of the harmonic force another group of waves is sent to the left (negative direction). It is worth noting that if μ_o is equal to zero or π the slope is zero for any of the values $\mu_o \pm j2\pi$, $j = 0, 1, 2 ...$ This means that the group velocity is zero and no net transfer of energy along the structure does occur. Each bay can be considered as isolated with the extremes either clamped or simply supported and vibrating in one of its fundamental modes. In fig. (2.3) the letter C stands for 'clamped', S, for 'simply supported' and the subscript refers to the particular band or mode.

The conditions of 'clamped' or 'simply supported' ends of a bay for μ_o equals o or π does not necessarily hold for more complicated periodic supports (for instance, supports with more than one degree of freedom). But for any periodic structure (no matter how sophisticated) and what sort of periodic supports it has) the $\mu_o - \Omega^*_o$ curves must be horizontal (that is, have zero slope) at $\mu_o = o$ and π corresponding to zero group velocity.

The concepts of groups of waves and group velocity have only been touched here because it was felt convenient in the discussion of the $\mu_o - \Omega^*_o$ curves. No attempt was made or will be made to elaborate on this subject. A good account of the theory can be found in |7| and a study in depth in |8|.

Another kind of graph that shall be used in this work is shown in fig. (2.4), as yet, for a beam on simple supports . This graph incorporates both real and imaginary parts of the propagation constant and are computed in connection with equations of the (2.4.5) type.

Both damped and nondamped systems can be represented in this form of graph. However, the limits of the passing bands (points S_r^1 and C_r^1) are easier to compute (and indeed with better accuracy) through the method related to the $\mu_o - \Omega^*_o$ curves. Graphs of the type shown in fig. (2.4) have been used to a great extent by Mead |5|, |11|, |12|, Mead and Wilby |9|, and Sen Gupta |10|. In this present work they will be referred to as $\Omega^*_o - \mu$ curves.

Actual computations for plates are not shown in this chapter, although expression (2.4.5) has been derived for a plate. They will appear in chapter IV and it will be shown that the case considered here is just a particular case of a more general one and can be conveniently treated as such, as far as computations are concerned.

CHAPTER III

A general theory of free wave propagation in Periodic Structures

3.1 GENERAL

In chapter II the basic ideas of a matrix method applicable to the free wave propagation phenomenon in spatially periodic structures was introduced. A specific example was necessary to support the ideas and the resultant equations were restricted to that particular structure. If another example of structure is to be taken the whole derivation must be repeated all over again. To this inconvenience it must be added that the derivation is likely to become cumbersome, if not practically impossible to handle, as the consequence of only moderate further complexities appearing in the structure. These shortcomings make the method described in chapter II unsuitable when, for instance, additional degrees of freedom are introduced to the supports and coupling effects are considerable. The same applies to complex structures such as stringer-stiffened cylindrical shells and ring-stiffened cylinders. But the method developed in the previous chapter can easily be generalised and made applicable to such structures. Transfer matrices have been applied to both free and forced vibrations of stiffened beams, plates and shells |3|, |4|, |13|, |14|, |15|, |16|. Its ability to handle several degrees of freedom and the fact that one can obtain a period transfer matrix representative of the whole periodic structure (supposed infinite) suggest its application to more advanced problems in wave propagation. One could argue that the same applies to the stiffness matrix. This is no doubt true and, in fact, the transfer matrix can be obtained from the stiffness matrix, and vice-versa |13|. But, as a general rule, the direct derivation of the period stiffness matrix is far more difficult than the period transfer matrix. Furthermore, general methods for the numerical construction of transfer matrices can conveniently be applied to complex structures, thus avoiding

strenuous algebric manipulations. Some of these methods are to be explored in this work in connection with the wave propagation problem. Besides this numerical advantage, transfer matrices are quite adequate for the theoretical analysis of both free and forced wave propagation problems, as it is to be seen in subsequent chapters.

3.2 THE NATURE OF PROPAGATION CONSTANTS : GENERAL FORMULATION OF THE FREE WAVE PROPAGATION PROBLEM

Consider a spatially periodic linear system. Further peculiarities of the system (apart from being periodical and linear) are immaterial. Such a system can be considered as a chain of identical black boxes (periods) linked and interacting together. Fig. (3.1) shows one of such periods with the interactions resultant at its ends. The interaction resultants are to be referred to as terminal generalised forces. Also shown in the figure are the terminal generalised displacements.

The terms generalised forces and generalised displacements are given here the same usual meaning encountered in the study of Lagrange's equations of classical dynamics.

The number of terminal generalised displacements (forces) equals the number of terminal degrees of freedom.

In addition to the terminal generalised displacements and forces, the system might also exhibit a finite (N) or infinite number of non-terminal generalised displacements. External generalised forces applied by the surrounding environment can also be present but they should not be considered in so far as only free waves are concerned. As a concrete example, the structure of fig. (2.1) has one terminal degree of freedom (rotation) and infinite nonterminal degrees of freedom.

The massless beam with three point masses of fig. (3.2), periodically restrained by longitudinal and tortional massless springs has two terminal

degrees of freedom and three nonterminal degrees of freedom.

The system represented by fig. (3.1) is assumed to have n degrees of freedom and the letters L and R stand for left and right of the period, respectively. The terminal quantities (generalised forces and displacements) on the left and right of a period are related by a period transfer matrix $[T]$ according to expression (3.2.1):

$$\begin{Bmatrix} q \\ F \end{Bmatrix}^R = [T] \begin{Bmatrix} q \\ F \end{Bmatrix}^L \qquad .. (3.2.1)$$

The period transfer matrix appearing in expression (3.2.1) is of order 2n x 2n and is an operator that can 'transfer' a station vector from the left to the right of a period.

The basic principle of free wave propagation in spatially periodic structures states that if a wave is propagating along the system then the station vector in eq. (3.2.1) must be the same, apart from a change in phase. In mathematical form:

$$\begin{Bmatrix} q \\ F \end{Bmatrix}^R = \begin{Bmatrix} q \\ F \end{Bmatrix}^L e^{-i\mu} \qquad .. (3.2.2)$$

Equations (3.2.1) and (3.2.2) can be summarised in eq. (3.2.3) below, where the references R or L have been dropped:

$$\left[[T] - e^{-i\mu}[I]\right] \begin{Bmatrix} q \\ F \end{Bmatrix} = \{0\} \qquad .. (3.2.3)$$

Expression (3.2.3) represents an eigenvalue problem of order 2n x 2n, the eigenvalues being $e^{-i\mu}$. So, a system with n terminal degrees of freedom has 2n propagation constants for each frequency, no matter how many nonterminal degrees of freedom it has. If the system is nondamped some of the propagation constants might be real, some imaginary or complex. One or more real propagation constants means that energy can freely propagate,

that is, the frequency is propagating. The other propagation constants (imaginary or complex) can be thought as representing exponentially decaying waves along the system.

3.3 THE EQUATION FOR THE PROPAGATION CONSTANT

If the system of equation (3.2.3) is to have non-trivial solutions the determinant of its matrix must be zero, that is:

$$\left| [T] - e^{-i\mu} [I] \right| = 0 \qquad .. (3.3.1)$$

This is the equation for the propagation constant, although in a form that is not quite convenient for computations. A first step in transforming (3.3.1) to a more suitable form is to expand it according to eq. (3.3.2):

$$\lambda^{2n} - (p_1\lambda^{2n-1} + p_2\lambda^{2n-2} + \ldots + p_{2n-1}\lambda + p_{2n}) = 0 \quad ..(3.3.2)$$

where $\lambda = e^{-i\mu}$, the eigenvalue of (3.3.1).

Now, this equation can be brought to a far more convenient form (from the computational point of view) by looking at the properties of a transfer matrix listed in appendix A. It can be seen that:

$$p_{2n} = -1 \quad \text{(the determinant of the overall transfer matrix is one)} \qquad .. (3.3.3)$$

$$p_j = p_{2n-j}, \quad j = 1,n$$

The above expressions show that only the n first p_j's coefficients are necessary to be computed. This fact brings considerable simplifications for systems with up to two terminal degrees of freedom and is also an important fact in cutting down computations and round-off errors in systems with higher numbers of terminal degrees of freedom.

The symmetry of the coefficients of eq. (3.3.2), as expressed by

properties (3.3.3), means that if μ is one of its solutions, then $-\mu$ is also a solution.

This property, obvious from the physical point of view, comes out mathematically in a very simple way indeed, thanks to relations (3.3.3). This property can also be used to reduce the order of the eq. (3.3.2) by half, as will be shown in the next section. So far eq. (3.3.2) has been looked upon as a polynomial in λ, that is, in $e^{-i\mu}$ and it was said that, at any frequency, 2n propagation constants are to be found if the system has n terminal degrees of freedom. The number of nonterminal degrees of freedom can be finite (N) or infinite. Now, this equation can also be thought as written in the form (2.4.8) where μ_o is considered an independent variable and Ω^*_o an implicit function. Thinking in this way one reaches the conclusion that eq.(3.3.2) is a polynomial of order N (the number of terminal degrees of freedom) in Ω^*. So, for any value of μ_o (say, between 0 and π) there correspond N real values of Ω^*_o. If one thinks now of an $\mu_o - \Omega^*_o$ graph of (3.3.2) (thought as written in the (2.4.8) form) this will show N $\mu_o - \Omega^*_o$ curves, that is, N bands of propagation. If N is infinite, one shall no longer have a polynomial, but a transcendental equation in Ω^*_o. The number of propagation bands is, accordingly, infinite. In practice only the lower propagation bands (say the first and second) are important and worth being computed.

3.4 PARTICULAR CASES OF EQ.(3.3.2)

3.4.1 Systems with one terminal degree of freedom (n = 1)

For n = 1 eq. (3.3.2) becomes:

$$e^{-i2\mu} - p_1 e^{-i\mu} + 1 = 0$$

The real and imaginary part of the left hand side of the above equation must be zero, that is

$$\cos 2\mu - p_1 \cos \mu + 1 = 0$$

$$\sin 2\mu - p_1 \sin \mu = 0$$

It is easy to show that the above two equations are equivalent to a single one, equation (3.4.1):

$$2 \cos \mu - p_1 = 0 \qquad ..(3.4.1)$$

Where p_1 is the trace of the corresponding period transfer matrix. If one thinks of the structure dealt with in chapter II where the stringers had infinite transverse stiffness, then equations (2.4.5) and (3.4.1) ~~and~~ are equivalent. But eq. (3.4.1) is in fact much more general since it applies to any linear spatially periodical system with only one terminal degree of freedom. For instance, one could think of the structure of chapter II but with the stringers free to move but prevented from rotating transversely. This case was studied by Sen Gupta |19| in a lengthy analysis following a rather different approach. Later in appendix B it will be shown that once the period transfer matrix of a system (in its most general form) is known, the period transfer matrix of any other system derived from it by imposing restraints (singularities) at the terminals can be obtained in an automatic manner, rather conveniently for numerical computations. Particular cases like the one just quoted can be handled without any further work of analysis or complexities.

3.4.2 Systems with two terminal degrees of freedom

If the steps shown in (3.4.1) are repeated for n = 2 one ends up with the following equation:

$$2 \cos 2\mu - 2p_1 \cos \mu - p_2 = 0 \qquad ..(3.4.2)$$

The coefficients p_1 and p_2 in eq. (3.4.2) can be easily found by applying Leverrier's method with Faddeev's modification (see appendix C) |17|, |18|.

According to this procedure p_2 is half the trace of the matrix $[T]$ $([T] - p_1 [I])$. The value of p_1 is, as always, the trace of $[T]$. In mathematical form:

$$p_1 = \sum_{j=1}^{4} t_{jj} \qquad ..(3.4.3)$$

$$p_2 = \frac{1}{2} \left\{ \sum_{j=1}^{4} \left(\sum_{k=1}^{4} t_{jk}\, t_{kj} - p_1 t_{jj} \right) \right\}$$

where the t's are elements of the period transfer matrix $[T]$.

So, for any nondamped periodic system with two terminal degrees of freedom expression (3.4.2) can be interpreted as an equation in which μ is a given real parameter (μ_o) and Ω_o^* is an unknown.

A number of propagation bands can then be found equal to the number of nonterminal degrees of freedom (which can be finite or infinite). Equation (3.4.2) can also be written in the following form:

$$4 \cos^2 \mu - 2p_1 \cos \mu - 2 - p_2 = 0 \qquad ..(3.4.4)$$

In this equation the nondimensional frequency should be considered as a parameter and μ as an unknown. It is worth noting that eq.(3.4.4) is a polynomial of order two in $\cos \mu$. Therefore, instead of working with a polynomial equation of order four in $\lambda = e^{-i\mu}$ property (3.3.3) made it possible to reduce this order by half. Equation (3.4.2) has been used in this work in the computation of $\mu_o - \Omega^*_o$ curves for nondamped stringer-stiffened plates and ring stiffened cylinders, in the case of axisymmetric wave propagation. On the other hand, equation (3.4.4) has been used in the computation of $\Omega^*_o - \mu$ curves for both structures, with and without damping.

3.4.3 Systems with n terminal degrees of freedom

It is now very easy to extend the results of subsections 3.3.1 and 3.3.2. A general equation of the (3.4.2) type can be written:

$$2\cos n\mu - 2p_1\cos(n-1)\mu - 2p_2\cos(n-2) - \ldots 2p_{n-1}\cos\mu - p_n = 0 \qquad \ldots(3.4.5)$$

Again here it is more convenient to regard eq. (3.4.5) as being of the (2.4.8) type, μ being an independent real parameter (μ_o) and Ω^*_o an unknown.

It is always possible to write a polynomial equation in $\cos\mu$ of order n which is more appropriate for the computation of $\Omega^*_o - \mu$ curves.

Two important cases should be noted here for they are related to stringer-stiffened shells and ring-stiffened cylinders:

n = 3:

$$8\cos^3\mu - 4p_1\cos^2\mu - (6 + 2p_2)\cos\mu + 2p_1 - p_3 = 0 \qquad \ldots(3.4.6)$$

n = 4:

$$16\cos^4\mu - 8p_1\cos^3\mu - (4p_2 + 16)\cos^2\mu - (2p_3 - 6p_1)\cos\mu +$$

$$2 + 2p_2 + p_4 = 0 \qquad \ldots(3.4.7)$$

It is worth noting that the coefficients p_j are complex when damping is present.

For n equals or greater than three the p_j coefficients are conveniently found numerically, using a routine based on Leverrier's method with the Fadeev's modification. Of course only half of the coefficients of the period transfer matrix need to be computed, after which the routine should return. This means a considerable saving in numerical computations and, to a certain extent, an increased accuracy. Indeed, if only the first n

coefficients are required the routine needs to perform approximately $(n - 2)(2n)^3 + (2n)^2$ multiplications while $(2n - 2)(2n)^3 + (2n)^2$ multiplications are necessary to compute 2n coefficients. Altogether $n(2n)^3$ multiplications are saved. For instance, an economy of 65% is achieved when n = 4 and 72% when n = 3. The increased accuracy is due to the fact that the process of computing the p_j's, being recurrent, accumulates round-off errors and, consequently, the sooner it is interrupted the better. In fact it is a broad way of speaking. For rather small matrices such as those encountered in this work the accuracy of computing all the 2n coefficients in the usual way (that is without considering property (3.3.3)) would be good anyway. But the fact still remains that there is a great saving in computation time and the need to calculate only half the number of the coefficients of the characteristic equation of the period transfer matrix should be regarded as of important practical value.

CHAPTER IV

Free wave propagation in systems with two terminal degrees of freedom

4.1 GENERAL

In chapter III a general formulation of the problem of free wave propagation in spatially periodic structures was made. A basic step in the solution of this problem is to obtain the period transfer matrix and then the equation for the propagation constant.

The period transfer matrix is generally made up of two factors: the field and the point transfer matrix. In fact, it is not an easy task to obtain the field transfer matrix analytically if its order is, say, greater than four. In these cases convenient numerical procedures must be used. This matter will be dealt with in chapter V.

In the present chapter two classes of structures will be considered as the first applications of the general theory.

The first class consists of thin flat plates (or skins) periodically supported and the second, of cylinders periodically stiffened by rings. The flat plates are considered to be thin and resting along one direction on two parallel simple supports (distant b units of length from each other) and, orthogonally to this direction, on an infinite number of elastic supports (both rotation and vertical translation allowed), distant ℓ apart.

Fig. (2.1) is a sketch of such a structure, the only difference between this and that dealt with in chapter II is that two terminal degrees of freedom are now considered. This makes the plate structure models analysed in this chapter more representative of a real aircraft fuselage, chiefly when coupling between torsional and transverse displacement is strong, or (and) the transverse stiffness is not sufficiently great if compared to the torsional stiffness. The expression 'sufficiently great' will be understood when the numerical results are discussed.

As far as periodically ring-stiffened cylinders are concerned, only axi-symmetrically propagating waves will be considered in this chapter.

The general case of free wave propagation in this class of structures is postponed to chapter V.

4.2 THE STATE TRANSFER MATRIX [A]

The state transfer matrix [A] is the basic element for the computation of the field transfer matrix. It appears in the state equation for the system

$$\{z_r(y)\}' = [A]_r \{z_r(y)\}$$

and it is real for undamped systems and complex if some damping is present.

In this section the state matrix [A] is first derived for a flat plate element and then for the cylinder undergoing axi-symmetric vibrations.

4.2.1 The state matrix [A] for a flat plate element

Select the vector $\lfloor w_r(y),\ w_r'(y),\ w_r''(y),\ w_r'''(y) \rfloor^T$ as a station vector and then resolve the equation (2.1.2) for $w_r^{IV}(y)$:

$$w_r^{IV}(y) = 2\zeta^2 w_r''(y) - \left(\zeta^4 - \frac{\rho h \Omega^2}{D}\right) w_r(y) \qquad ..(4.2.1)$$

It is convenient to remember that equation (4.2.1) is valid for the assumed solution in expression (2.1.2).

Now, looking at equation (4.2.1) it is easy to write:

$$\begin{Bmatrix} w_r(y) \\ w_r'(y) \\ w_r''(y) \\ w_r'''(y) \end{Bmatrix}' = \begin{bmatrix} 0 & 1 & 0 & 0 \\ 0 & 0 & 1 & 0 \\ 0 & 0 & 0 & 1 \\ b_{n1} & 0 & 2\zeta^2 & 0 \end{bmatrix} \begin{Bmatrix} w_r(y) \\ w_r'(y) \\ w_r''(y) \\ w_r'''(y) \end{Bmatrix} \qquad ..(4.2.2)$$

where $b_{41} = -(\zeta^4 - \frac{\rho h \Omega^2}{D}) = \frac{1}{\ell^4}\left\{(\frac{r_\pi}{ASP})^2 - \Omega^{*2}\right\}$

In condensed form the above expression can be written:

$$\{x_r(y)\}' = [B]_r \{x_r(y)\} \qquad ..(4.2.3)$$

One could, of course, define a transfer matrix relating the station vector $\{x_r(y)\}$ at two points of the field (say y_1 and y_2). But the basic principle of free wave propagation calls for relations between generalised forces and displacements (see, for instance expression (3.2.2)) so that a way of transforming vector $\{x_r(y)\}$ into another vector $\{z_r(y)\}$ defined in terms of these quantities ought to be found. The vector $\{z_r(y)\}$ can be conveniently defined as

$$\{z_r(y)\}^T = \lfloor W_r(y),\ W_r'(y),\ M_r(y),\ V_r(y) \rfloor$$

and one shall seek a field transfer matrix relating this vector at two points.

The relation between $\{x_r(y)\}$ and $\{z_r(y)\}$ can be found by first taking the relations

$$\begin{aligned} W_r(y) &= W_r(y) \\ W_r'(y) &= W_r'(y) \\ M_r(y) &= -DW_r''(y) + D\nu\zeta^2 W_r(y) \\ V_r(y) &= -DW_r'''(y) + D(2-\nu)\zeta^2 W_r(y) \end{aligned} \qquad ..(4.2.4)$$

and then rewriting them in matrix form:

$$\begin{Bmatrix} W_r(y) \\ W_r'(y) \\ M_r(y) \\ V_r(y) \end{Bmatrix} = \begin{bmatrix} 1 & 0 & 0 & 0 \\ 0 & 1 & 0 & 0 \\ D\nu\zeta^2 & 0 & -D & 0 \\ 0 & D\zeta^2(2-\nu) & 0 & D \end{bmatrix} \begin{Bmatrix} W_r(y) \\ W_r'(y) \\ W_r''(y) \\ W_r'''(y) \end{Bmatrix} \qquad ..(4.2.5)$$

or, in condensed form:

$$\{z_r(y)\} = [C]_r \quad \{x_r(y)\} \qquad ..(4.2.6)$$

Expressions (4.2.4) have been written by considering expression (2.1.2) for the deflection, expression (2.1.6a) for the moment and

$$V(y) = \sum_{r=1}^{\infty} V_r(y) \sin \frac{r\pi x}{\ell} \; e^{i\Omega t} \qquad ..(4.2.7)$$

for shear and, of course, applying the usual expressions for bending moment and shearing forces per unit length of the ordinary theory of thin elastic plates.

The matrix $[C]_r$ provides the means to transform the station vector $\{x_r(y)\}$into $\{z_r(y)\}$. It shall be called transformation matrix from now on. The state matrix $[A]_r$ can now easily be shown to be

$$[A]_r = [C]_r \, [B]_r \, [C]_r^{-1} \qquad ..(4.2.8)$$

where

$$[C]_r^{-1} = \begin{bmatrix} 1 & 0 & 0 & 0 \\ 0 & 1 & 0 & 0 \\ \nu\zeta^2 & 0 & -\frac{1}{D} & 0 \\ 0 & \zeta^2(2-\nu) & 0 & -\frac{1}{D} \end{bmatrix}$$

Carrying out the product indicated in (4.2.8) the matrix [A] is found in its final form:

$$[A]_r = \begin{bmatrix} 0 & 1 & 0 & 0 \\ \nu\zeta^2 & 0 & -\frac{1}{D} & 0 \\ 0 & \eta_1 & 0 & 1 \\ \eta_2 & 0 & \nu\zeta^2 & 0 \end{bmatrix} \qquad ..(4.2.9)$$

where

$$n_1 = -2D\zeta^2(1 - \nu); \quad n_2 = D\zeta^2(1 - \nu^2) - \beta\bar{\omega}^*{}_o{}^2, \text{ and}$$

$$\beta = \frac{Do}{\ell^4}$$

The state matrix [A] could have been derived in a more straight forward manner by obtaining the derivative of the displacement, slope, moment and shear force as functions of these same quantities. This, in fact, was done by Henderson and Nashif |20|. But the above method seems simpler and involving less algebraic manipulations.

4.2.2 The state matrix [A] for a cylinder element undergoing axi-symmetric motion

Consider the cylindrical shell element of Fig. (4.1). If this element is vibrating in an axi-symmetric mode the tangential displacement (v) as well as the derivatives in relation to ϕ ($\frac{\partial}{\partial\phi}(\ )$) are zero.

The above assumptions lead to the simplified set of Donnell's equations |21|:

$$\frac{\partial^2 u}{\partial \bar{x}^2} + \nu \frac{\partial w}{\partial \bar{x}} - \frac{\rho R^2 h}{K} \frac{\partial^2 u}{\partial t^2} = 0 \qquad ..(4.2.10)$$

$$\nu\frac{\partial u}{\partial \bar{x}} + w + k\frac{\partial^4 w}{\partial \bar{x}^4} + \frac{\rho R^2 h}{K} \frac{\partial^2 w}{\partial t^2} = 0$$

where

R radius of the cylinder element

u longitudinal displacement

$$K = \frac{Eh}{1 - \nu^2}$$

$$k = \frac{h^2}{12R^2}$$

$\bar{x} = \frac{x}{R}$, a nondimensional coordinate.

For the time being it will be assumed that the terms involving u and its derivatives are negligible in eq. (4.2.10) by comparison with the others. This last assumption leads to a single differential equation:

$$\frac{\partial^4 w}{\partial \bar{x}^4} + \frac{1}{k} w + \frac{\rho R^2 h}{D} \frac{\partial^2 w}{\partial t^2} = 0 \qquad ..(4.2.11)$$

If a solution of the form $w(\bar{x}, t) = w(\bar{x})\, e^{i\Omega t}$ is introduced in the above differential equation the result is

$$w^{IV}(\bar{x}) + Cw(\bar{x}) = 0 \qquad ..(4.2.12)$$

where

$$C = R^2\left(\frac{R}{\ell}\right) \frac{12}{h^2} \left(\frac{\ell}{R}\right)^2 - \left(\frac{\Omega^*}{\ell}\right)^2 \quad \text{and}$$

$$\Omega^{*2} = \frac{\rho h \ell^4 \Omega^2}{D}$$

Now, making use of (4.2.12) it is possible to write:

$$\begin{Bmatrix} w(\bar{x}) \\ w'(\bar{x}) \\ w''(\bar{x}) \\ w'''(\bar{x}) \end{Bmatrix}' = \begin{bmatrix} 0 & 1 & 0 & 0 \\ 0 & 0 & 1 & 0 \\ 0 & 0 & 0 & 1 \\ -C & 0 & 0 & 0 \end{bmatrix} \begin{Bmatrix} w(\bar{x}) \\ w'(\bar{x}) \\ w''(\bar{x}) \\ w'''(\bar{x}) \end{Bmatrix}$$

That is the [B] matrix for the cylinder element in axi-symmetric mode of motion.

Making use now of the well known expressions for the bending moment and shear force and applying the assumed solution of eq. (4.2.11), we have:

$$M(\bar{x}) = \frac{D}{R^2} w''(\bar{x})$$

$$V(\bar{x}) = \frac{D}{R^3} w'''(\bar{x}) \qquad ..(4.2.14)$$

It is now very easy to see that:

$$\begin{Bmatrix} w(\bar{x}) \\ \theta(\bar{x}) \\ M(\bar{x}) \\ V(\bar{x}) \end{Bmatrix} = \begin{bmatrix} 1 & 0 & 0 & 0 \\ 0 & \frac{1}{R} & 0 & 0 \\ 0 & 0 & \frac{D}{R^2} & 0 \\ 0 & 0 & 0 & \frac{D}{R^3} \end{bmatrix} \begin{Bmatrix} w(\bar{x}) \\ w'(\bar{x}) \\ w''(\bar{x}) \\ w'''(\bar{x}) \end{Bmatrix} \qquad ..(4.2.15)$$

where

$$\theta(\bar{x}) = \frac{1}{R} \frac{dw(\bar{x})}{d\bar{x}}$$

Expression (4.2.15) shows the transformation matrix [C]. Its inverse is

$$[C]^{-1} = \begin{bmatrix} 1 & 0 & 0 & 0 \\ 0 & R & 0 & 0 \\ 0 & 0 & \frac{R^2}{D} & 0 \\ 0 & 0 & 0 & \frac{R^3}{D} \end{bmatrix} \qquad ..(4.2.16)$$

The state matrix is obtained by carrying out the product $[C][B][C]^{-1}$:

$$[A] = \begin{bmatrix} 0 & R & 0 & 0 \\ 0 & 0 & \frac{R}{D} & 0 \\ 0 & 0 & 0 & R \\ \frac{-CD}{R^3} & 0 & 0 & 0 \end{bmatrix} \qquad ..(4.2.17)$$

It is worth noting that both matrices [A] for the plate element and for the cylinder element are cross-symmetric and of the same order.

4.3 THE FIELD TRANSFER MATRIX

The state matrix [A] is the basic element for the construction of the field transfer matrix. The simplicity of both [A] matrices derived in the previous section suggests the straight forward application of a consequence of the Cayley-Hamilton theorem |13|. It is possible to prove |22| that the field transfer matrix, relating station vectors y units of length apart, can be written as:

$$\left[T_F(y,0)\right] = \sum_{j=1}^{2n} Cj \left[A\right]^{(j-1)} \qquad ..(4.3.1)$$

where the coefficients Cj are the roots of the following system of linear equation:

$$\sum_{j=1}^{2n} Cj \, \lambda_m^{(j-1)} = e^{\lambda m y}; \quad m = 1, 2n \qquad ..(4.3.1a)$$

Generally speaking, the main restriction to this method of finding the field transfer matrix resides in the computation of the power of [A]. This restriction does not apply to the present cases anyway because the extreme simplicity of [A] makes it possible to obtain by hand all the necessary powers of [A].

4.3.1 The Field Transfer Matrix for the Plate Element

The characteristic equation associated with the state matrix [A] for a plate element is given by (2.1.3). If the roots are written in the form λ_1, $-\lambda_1$, λ_2, $-\lambda_2$, where

$$\lambda_1 = \frac{1}{\ell} \left(\frac{r_{\pi}}{ASP}\right)^2 + \Omega^{*\frac{1}{2}}$$

$$\lambda_2 = \frac{1}{\ell} \left(\frac{r_{\pi}}{ASP}\right)^2 - \Omega^{*\frac{1}{2}} \qquad ..(4.3.2)$$

and if these roots are taken into (4.3.1a), the result is:

$$C_1 = \frac{\lambda_1^2 \cos h\lambda_2 y - \lambda_2^2 \cos h\lambda_1 y}{\lambda_1^2 - \lambda_2^2}$$

$$C_2 = \frac{\lambda_2^3 \sin h\lambda_1 y - \lambda_1^3 \sin h\lambda_2 y}{\lambda_1\lambda_2^3 - \lambda_2\lambda_1^3}; \quad C_3 = \frac{\cosh\lambda_1 y - \cosh\lambda_2 y}{\lambda_1^2 - \lambda_2^2}$$

$$C_4 = \frac{\lambda_1 \sin h\lambda_2 y - \lambda_2 \sin h\lambda_1 y}{\lambda_1\lambda_2^3 - \lambda_2\lambda_1^3}$$

Now, obtaining the second and third powers of [A] by hand multiplication and carrying out the linear combination expressed by (4.3.1) the end result is the field transfer matrix for a plate element:

$$\left[T_F(Y,0)\right] = \begin{bmatrix} C_1+C_3\nu\zeta^2 & C_2+C_4(\nu\zeta^2-\frac{\eta_1}{D}) & -\frac{C_3}{D} & -\frac{C_4}{D} \\ C_2\nu\zeta^2+C_4\left\{(\zeta^2\nu)^2-\frac{\eta_2+\nu\zeta^2\eta_1}{D}\right\} & C_1+C_3(\nu\zeta^2-\frac{\eta_1}{D}) & -\frac{C_2}{D}-\frac{C_4}{D}(\frac{\eta_1}{D}-2\nu\zeta^2) & -\frac{C_3}{D} \\ C_3(\eta_1\nu\zeta^2+\eta_2) & C_2\eta_1+C_4(2\eta_1\nu\zeta^2+\eta_2-\frac{\eta_1^2}{D}) & C_1+C_2(\nu\zeta^2-\frac{\eta_1}{D}) & C_2+C_4(\nu\zeta^2-\frac{\eta_1}{D}) \\ C_2\eta_2+C_4\left\{\eta_1(\nu\zeta^2)^2+2\eta_2\nu\zeta^2\right\} & C_3(\eta_2+\nu\eta_1\zeta^2) & C_2\nu\zeta^2+C_4\left\{(\nu\zeta^2)^2-\frac{\eta_2+\eta_1\nu\zeta^2}{D}\right\} & C_1+C_2\nu\zeta^2 \end{bmatrix}$$

..(4.3.3)

where:

$$\zeta = \frac{r_\pi}{b} = \left(\frac{r_\pi}{ASP}\right)\frac{1}{\ell}$$

$$\eta_1 = -2D(1-\nu)\zeta^2 = 2\frac{D}{\ell^2}(1-\nu)\left(\frac{r_\pi}{ASP}\right)^2$$

$$\eta_2 = \frac{D}{\ell^4}\left\{(1-\nu^2)\left(\frac{r_\pi}{ASP}\right)^4 - \Omega^{*2}\right\}$$

4.3.2 The Field Transfer Matrix for the Cylinder Element in axi-symmetric motion

The steps to be given here are basically the same as for the previous section.

The characteristic equation associated with $[A]$ is derived from equation (4.2.12) and is:

$$\lambda^4 + C = 0 \qquad ..(4.3.4)$$

If there is some damping in the cylindrical shell C is complex. If no damping is present C is a real number. One could represent the roots of (4.3.4) by

$$\lambda_j = |C|^{\frac{1}{4}} e^{i\frac{\theta_p + 2(j-1)\pi}{4}}, \quad j = 1,2,3,4, \quad 0 \leq \theta_p \leq 2\pi \qquad ..(4.3.5)$$

where θ_p is the principal argument of C.

It is also easy to show that:

$$\lambda_2 = i\lambda_1$$
$$\lambda_3 = -\lambda_1 \qquad ..(4.3.6)$$
$$\lambda_4 = -i\lambda_1$$

With these relations taken to equations (4.3.1a) the C's coefficients can be found:

$$C_1 = \frac{1}{2}(\cos \lambda_1 \bar{x} + \cos h\lambda_1 \bar{x})$$

$$C_2 = \frac{1}{2}\frac{\sin h\lambda_1 \bar{x} + \sin \lambda_1 \bar{x}}{\lambda_1}$$

$$C_3 = \frac{1}{2}\frac{\cos h\lambda_1 \bar{x} - \cos \lambda_1 \bar{x}}{\lambda_1^2} \qquad ..(4.3.7)$$

$$C_4 = \frac{1}{2}\frac{\sin h\lambda_1 \bar{x} - \sin \lambda_1 \bar{x}}{\lambda_1^3}$$

The above relations are valid only for $|C|$ not equal to zero. For $|C|$ equal to zero one could take the limit values:

$$C_1 = 1$$

$$C_2 = \bar{x}$$

$$C_3 = \frac{1}{2}\bar{x}^2 \qquad ..(4.3.7a)$$

$$C_4 = \frac{1}{6}\bar{x}^3$$

Now it is possible to obtain $[A]^2$ and $[A]^3$ and carry out the linear combination expressed by eq.(4.3.1). The field transfer matrix for a cylindrical element undergoing axi-symmetric vibration is:

$$[T_F(\bar{x}, 0)] = \begin{bmatrix} C_1 & C_2.R & C_3\frac{R^2}{D} & C_4\frac{R^3}{D} \\ -C_4\frac{C}{R} & C_1 & C_2\frac{R}{D} & C_3\frac{R^2}{D} \\ -C_3\frac{DC}{R^2} & -C_4\frac{DC}{R} & C_1 & C_2.R \\ -C_2\frac{DC}{R^3} & -C_3\frac{DC}{R^2} & -C_4\frac{C}{R} & C_1 \end{bmatrix} \qquad ..(4.3.8)$$

For readiness in the computation of (4.3.8) it is good to point out that:

$$\lambda_1 = \frac{|C|^{\frac{1}{4}} \cdot \sqrt{2}}{2} \cdot (1 + i), \quad C > 0$$

$$\lambda_1 = |C|^{\frac{1}{4}} ; \quad C < 0 \qquad ..(4.3.8a)$$

$$\lambda_1 = |C|^{\frac{1}{4}} \cos\left(\frac{\theta_p}{4}\right) + i \sin\left(\frac{\theta_p}{4}\right), \quad C \text{ complex.}$$

It is worth noting that both matrices in expressions (4.3.3) and (4.3.8) are cross symmetric. All the structures to be dealt with in this work have cross symmetric field transfer matrices. The general conditions for a transfer matrix to be cross symmetric is given in |23|.

4.4 THE POINT TRANSFER MATRIX

The reasons to find a point transfer matrix as well as its meaning have been explained in section 2.3. The stiffening elements encountered in the structures dealt with in the present chapter have two degrees of freedom, rotation and transverse displacement.

The point transfer matrix is derived by considering the compatibility conditions for the displacement and slope and the equations for the jumps in moment and shear across the stiffening element:

$$w^R = w^L$$

$$\theta^R = \theta^L$$

$$M^R = K_\theta \beta^L + K_{\theta w} w^L + M^L \qquad ..(4.4.1)$$

$$V^R = K_w w^L - K_{\theta w} \beta^L + V^L$$

In the above expressions θ stands for the slope at the stiffening element and $K_{\theta w}$ is a coupling coefficient between torsional and transverse displacement. The coefficients K_θ, $K_{\theta w}$ and K_w have been computed by

Henderson and McDaniel |4| for the type of support of fig.(6.1) and are:

$$K_{\theta w} = E\zeta^4(A_y I_\eta - A_z I_{\eta\zeta}) + (C_y - A_y).A.\alpha_o.\Omega_o{}^{*2}$$

$$K_w = E\zeta^4 I_\eta - A.\alpha_o.\Omega_o{}^{*2}$$

K_θ, given in expression (2.3.3), and

A, the cross section area of the stringer.

The above expression shall be used in this chapter in connection with stringer-stiffened flat plates.

In matrix form equation (4.4.1) gives the point transfer matrix:

$$\begin{Bmatrix} w \\ \theta \\ M \\ V \end{Bmatrix}_R = \begin{bmatrix} 1 & 0 & 0 & 0 \\ 0 & 1 & 0 & 0 \\ K_{\theta w} & K_\theta & 1 & 0 \\ K_w & -K_{\theta w} & 0 & 1 \end{bmatrix}_r \begin{Bmatrix} w \\ \theta \\ M \\ V \end{Bmatrix}_L \qquad ..(4.4.2)$$

For a ring vibrating axi-symmetrically the elements of the point transfer matrix can be found as follows:

In fig. (4.1) the forces acting on one ring are shown. The sign convention is compatible with that one found in |24| where it was used to derive the cylindrical shell equations.

The differential equations of motion of the ring can be written by applying the hypothesis of axi-symmetry of the vibration to the general equations derived by WAH and Hu |25|. Its results are only two equations:

$$\frac{E\bar{I}}{R^2}\,\theta(t) + \rho I_p \frac{\partial^2\theta(t)}{\partial t^2} = F_\theta(t)$$

$$\frac{EA}{R^2}\,w(t) + \rho A \frac{\partial^2 w(t)}{\partial t^2} = F_w(t) \qquad ..(4.4.3)$$

where:

I_p, the polar moment of area of the section, and

$\bar{I}$, a principal momen of area about an axis parallel to the x axis.

Assuming harmonic expressions for all the quantities involved in equations (4.4.3):

$$\theta(t) = \theta\, e^{i\Omega t}: \quad w(t) = w\, e^{i\Omega t}$$

$$F_\theta(t) = F_\theta e^{i\Omega t}: \quad F_w(t) = F_w\, e^{i\Omega t}$$

and taking these expressions into equation (4.4.3) one finds:

$$F_\theta = \left(\frac{E\bar{I}}{R^2} - \rho I_p \Omega^2\right)\theta$$

$$F_w = \left(\frac{EA}{R^2} - A\Omega^2\right)w \qquad ..(4.4.4)$$

Noting that $F_w = V^L - V^R$ and $F_\theta = M^R - M^L$, equations (4.4.3) give:

$$K_\theta = \frac{E\bar{I}}{R^2} - I_p.\alpha.\Omega_o{}^{*2}$$

$$K_w = -\frac{EA}{R^2} + A.\alpha.\Omega_o{}^{*2} \qquad ..(4.4.5)$$

$$K_{\theta w} = 0$$

The above equations are enough to complete the ring point transfer matrix.

Since there is no coupling between θ and w in the present example of ring the coefficient $K_{\theta w}$ is zero. Of course a more general kind of ring section can be considered.

4.5 THE PERIOD TRANSFER MATRIX

The period transfer matrix is given, as always, by equation (2.4.1a). Looking at the general expression for the point transfer matrix (4.4.2) one can see that the first two lines of the period transfer matrix are equal to the first two lines of the field transfer matrix. The third and fourth lines are obtained as follows:

$$t_{3,j} = K_{\theta w}\, t^{F}_{1,j} + K_{\theta}\, t^{F}_{2,j} + t^{F}_{3,j}$$

$$t_{4,j} = K_{\theta}\, t^{F}_{1,j} - K_{\theta w}\, t^{F}_{2,j} + t_{4,j} \qquad ..(4.5.1)$$

where the t^{F},j are elements of the field transfer matrix $\left[T_F(\ell,0)\right]$. It was implicitly understood that the way the period transfer matrix has been constructed (according to expression (2.4.1a)) corresponds to a definition of period as indicated in fig.(4.2). Of course, there are infinite ways of defining a structural period, the choice being just a matter of convenience. It should be pointed out that whilst the field transfer matrices derived before are cross symmetric the period transfer matrix is not. It is possible, by defining a period symmetrical to its centre, and by proper choise of sign convention to establish a cross symmetrical period transfer matrix (see [23]). However this will not be done in this work and the definition expressed in fig.(4.2) and expression (2.4.1a) will be the only ones used here.

If one assumes that the supports are very stiff either in rotation or translation one terminal degree of freedom can be eliminated by applying the technique described in Appendix B.

When it is done it might be more convenient to apply the reduction technique to the field transfer matrix and then obtain the period transfer matrix by pre-multiplying the reduced matrix by the suitable reduced point

transfer matrix. For instance, in eliminating the transverse movement ($I_1 = 1, I_2 = 4$) the period transfer matrix will be:

$$[T(\ell,0)] = \begin{bmatrix} 1 & 0 \\ K_0 & 1 \end{bmatrix} \begin{bmatrix} t^*_{11} & t^*_{12} \\ t^*_{21} & t^*_{22} \end{bmatrix} = \begin{bmatrix} t^*_{11} & t^*_{12} \\ t^*_{21} + K_0 t^*_{11} & t^*_{22} + K_0 t^*_{12} \end{bmatrix} \quad ..(4.5.2a)$$

If the rotational degree of freedom of the stiffening element is eliminated ($I_1 = 2$, $I_2 = 3$):

$$[T(\ell,0)] = \begin{bmatrix} 1 & 0 \\ K_w & 1 \end{bmatrix} \begin{bmatrix} t^*_{11} & t^*_{12} \\ t^*_{21} & t^*_{22} \end{bmatrix} = \begin{bmatrix} t^*_{11} & t^*_{12} \\ t^*_{21} + K_w t^*_{11} & t^*_{22} + K_w t^*_{12} \end{bmatrix} \quad ..(4.5.2b)$$

The reduced transfer matrix is obtained by eliminating line and column I1 and line and column I2.

It is worth noting that K_{0w} does not appear in any of expressions (4.5.2a) and (4.5.2b). This is obvious for only two terminal movements were possible in the original structure and one has been prevented.

4.6 DISCUSSION OF RESULTS

In this work two examples of stringer-stiffened flat plates are to be considered.

The first example (called here Example I) is taken from a paper by Lin [1] and its pertinent data are listed below in SI units:

Data for Example I

For each panel

b = 50.80 [cm]

E = 0.725×10^6 [N/cm^2]

h = 0.1016 [cm]

ℓ = 20.826 [cm]

ρ = 2.8×10^{-5} [N.sec^2/cm^4]

ν = 0.3

For each stringer

A = 1.485 [cm^2]

A_y = 0.0 [cm]

A_z = 0.208 [cm]

C = 94.20×10^{-4} [cm^4]

CWA = 4.43 [cm^6]

C_y = 0.0 [cm]

C_z = 2.08 [cm]

E = 0.725×10^6 [N/cm^2]

I_η = 5.075 [cm^4]

I_ζ = 3.45 [cm^4]

$I_{\eta\zeta}$ = 0.0 [cm^4]

JA = 10.55 [cm^4]

ρ = 2.8×10^{-5} [N.sec^2/cm^4]

ν = 0.3

In that paper Lin was interested only in the lower and upper limits of each passing band and he developed a method to compute them. These limits are associated with zero group velocity.

It has been shown by Miles |6| that when a periodic structure is finite the natural frequencies fall in groups, the upper and lower frequencies of these groups being independent of the number of periods of the structure. When the structure becomes infinite the frequency groups become continuous frequency bands. So, the limits of a propagating band can be identified as natural resonant frequencies of the infinite periodic

structure, or of any of its periodic substructures, or of an isolated bay. Of course, any frequency falling in a passing band of an infinite periodic structure can also be thought as a 'natural frequency'. The only thing is that if energy is fed into the structure at any of these 'natural frequencies' it will propagate to $\pm \infty$. Infinity can be thought as a sink that absorbs any energy that reaches it. On the other hand, if the vibration is steady at one of the lower or upper limits of a passing band no energy will flow from one bay to the next.

Lin's results are compared in table 4.1 with those obtained by using the technique to compute $\mu_o - \Omega_o^*$ curves (see appendix D).

Table 4.1 Comparison with Lin's results |1| for the lower and upper limits of the Propagation Bands (Example I)

	$\mu_o - \Omega_o^*$ Technique		Lin's Method
μ_o	Ω_o^*	HZ	HZ
π	17.22	98.9	98.9
0	22.681	130.0	130.2
0	39.865	228.9	228.9
π	55.7136	323.0	323.0

The agreement between both sets of results is complete. Fig. (4.3) is a computer plot of the three first $\mu_o - \Omega_o^*$ curves for $r = 1$.

The $\mu_o - \Omega_o^*$ curves of fig. (4.4) were obtained by applying the reducing technique explained in appendix B with I1 = 1, and I2 = 4. This means that the transverse stiffness has been considered infinite. No serious errors have been introduced by applying this technique to this structure for two reasons:

a) The transverse stiffness is in fact very high if compared, say, with the transverse stiffness in the middle of a bay;

b) The coupling coefficient $K_{w\theta}$ is zero since A_y, $I_{n\xi}$ and C_y are zero.

So, the assumption that this system has only the torsional degree of freedom is not too far from reality.

Table 4.2 compares the results with and without the application of the reduction technique:

K_w and K_θ finite		$K_w = \infty$		$K_\theta = \infty$	
μ	Ω_o^*	μ	Ω_o^*	μ	Ω_o^*
π	17.220	π	17.220	0	22.681
0	22.681	0	23.325	π	23.325
0	39.865	0	39.865	π	56.322
π	55.7136	π	55.7136	0	62.920
π	56.322	π	62.920	0	81.300
0	78.192	0	78.192	π	96.211

Table 4.2 Comparison between results obtained for the structure of Example I and derived structures by making either K_w or K_θ infinite.

The small increase in the upper frequency of the first band shown in the second column of table 4.2 is probably due to the greater transverse stiffness of the stringer (infinite, actually). Also shown in table 4.2 are the results obtained when taking I1 = 2, and I2 = 3. This means that the plate is allowed to translate, but not to rotate at the supports, or stringers. In this last case only a special type of flexural waves can exist, namely those for which only transverse displacement of the supports occur.

With the purpose of finding the effect of coupling between transverse and longitudinal displacement another skin-stringer structure (called Example II) is considered below.

In this structure the stringers are not symmetric in relation to the line of attachment so that there is some coupling between transverse and rotational movements.

Data for Example II

For each Panel

$b = 24.39$ [cm]

$E = 20.69 \times 10^6$ [N/cm^2]

$h = 0.122$ [cm]

$\ell = 7.32$ [m]

$\rho = 78.50 \times 10^{-6}$ [N sec^2/cm^2]

$\nu = 0.3$

For each stringer (see sketch below)

$E = 20.69 \times 10^6$ [N/cm^2]

$\rho = 78.50 \times 10^{-6}$ [N.sec^2/cm^2]

$\nu = 0.3$

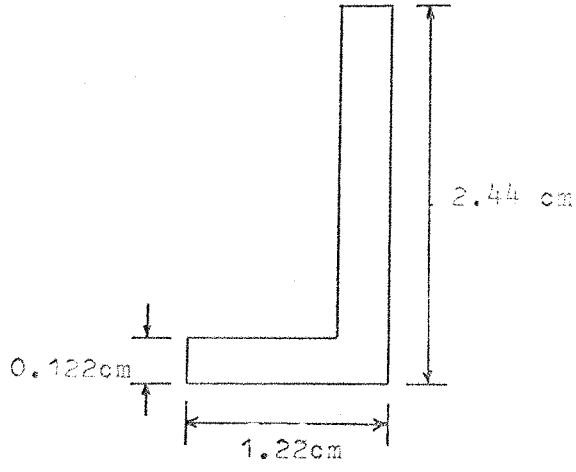

Table 4.3 compares the lower and upper frequencies of the first three passing bands for this structure and figs. (4.6, 4.7 and 4.8) show the corresponding $\mu_o - \Omega_o^*$ plots.

K_w and $K_{w\theta}$ not altered		$K_w = \infty$		$K_{w\theta} = 0$	
μ	$\Omega_o{}^*$	μ	$\Omega_o{}^*$	μ	$\Omega_o{}^*$
0	9.86892	π	11.0327	0	10.3315 (5%)
π	10.03175	0	21.6412	π	11.0327 (10%)
π	16.023	0	22.87324	π	15.3935 (4%)
0	21.71345	π	34.36923	0	21.6412 (0.3%)
0	33.31063	π	62.3386	0	32.9565 (1%)
π	34.596	0	66.9582	π	34.36923 (0.5%)

Table 4.3 Lower and upper band frequencies for Example II and the derived structures for $K_w = \infty$ and $K_{w\theta} = 0$.

Also shown in the same table are the values of the lower and upper band frequencies for $K_w = \infty$.

It can be noticed that by simply ignoring coupling errors(shown in brackets) can be introduced in the first band which incidentally is the most important in many cases. This should be borne in mind if one intended to represent each stringer by one transverse and one torsional spring.

Another feature of this structure is that the stringer transverse stiffness is small compared with the torsional stiffness to the extent that the lower frequency of the first propagating band corresponds to $\mu_o = 0$ (the 'clamped' vibration mode). It is shown in fig. (4.6).

The order of appearance of the limiting band frequencies have reversed here in relation to the order found in the structure called Example I. If the reduction technique is applied to make $K_w = \infty$ the derived system must show the same order as in Example I. This is shown in fig. (4.7) and in table 4.3. But now serious errors are introduced by assuming zero transverse

displacement at the stringer. The departure of these results from those of the original system is in part due to the fact that the stringers are not transversely stiff enough for the hypothesis of zero displacement at their attachment to be a sound one. It is also in part due to the coupling that is automatically eliminated by this hypothesis.

It is interesting to notice that coincident values of frequency such as 11.0327 ($\mu = \pi$), 21.6412 ($\mu = 0$), 34.3692 ($\mu = \pi$) etc. occurs only between columns 2 and 3 in table 4.3. This is expected because both columns show results belonging to derived structures without coupling.

The results discussed above can also be presented in the form of Ω_0^* - μ curves as was explained in chapter II. This is shown in figures (4.9 and 4.10) for $\eta = 0$ and 0.15. All these graphs are divided in two regions, below and above the 0 - 0 line and are related to the original structure of Example I. The imaginary parts of the propagation constants are plotted in the imaginary region and the real parts in the real region.

Figure (4.9) for $\eta = 0$ shows that the 'second' propagation constant is always heavily attenuating. The 'first' propagation constant is sometimes propagating and sometimes attenuating. It is worth noting that the passing bands shown by the first propagation constant coincide with those shown in fig. (4.3).

So if a harmonic point force acts in one of the bays of this structure two waves are sent to the right and two to the left. One of these waves decays strongly along the structure and the other may also decay or propagate, depending on the value of the exciting frequency.

The effect of damping is to introduce a non-zero value for the imaginary part of the propagation constant at all frequencies. Fig. (4.10) shows the Ω_0^* - μ curves for Example I with $\eta = 0.15$. One could notice that the imaginary part of the 2nd propagation constant dips in the region where a propagation band does exist when $\eta = 0$. Cuves like those in

fig. (4.10) have been obtained for some other values of the damping but are not shown here to save space. It is interesting to notice that the same program used to compute curves (4.9) or (4.10) can be used (with minor changes) in case the damping is heavily dependent on the frequency.

In chapter II it was explained that when the infinite periodic structure is excited by a harmonic point force with a propagating frequency two groups of waves are generated; one propagating to the right and the other to the left. It is interesting to plot the phase velocities of one group (the one propagating to the right, say) by using equation (2.5.2a). These sort of plots have been introduced by Mead |5| and have been used by Sen Gupta |10|. Figures (4.11, 4.12 and 4.13) show such graphs for the structure of Example I and they correspond to the first, second and third bands, respectively. Looking at curve (4.11), for instance, one can see that it is divided in positive and negative branches. Positive branches correspond to positive j's in equation (2.5.2a) and negative branches to negative j's and $0 \leq \mu_0 \leq \pi$. In this way positive branches correspond to positive phase velocities and negative branches to negative phase velocities.

So both net waves sent away from the applied harmonic force are combinations of infinite harmonic components with all the possible phase velocities. (For a detailed discussion of this see |5|).

The uppermost branch corresponds to $j = 0$ and this gives the primary component, or primary phase velocity. The wave length of the primary component was called pseudo-wavelength by Mead |26|.

If in fig. (4.11) a vertical line is drawn through a propagating frequency it will cut the branches at points whose ordinates correspond to positive and negative phase velocities.

The junction points shown in fig. (4.11) (marked A, B, C, D, etc.) correspond to the limits of the propagation bands and one can see that

the phase velocities appear in pairs of the same modulus but with different signs. As a result no propagation does occur as was explained in chapter II. The explanation given above applies as well to the curves of figs.(4.12) and (4.13). All the computations carried out for the skin-stringer structures given so far can be repeated for the axi-symmetric wave propagation in ring stiffened cylinders. The computer programs and sub-routines involved are the same, apart from the computation of the state matrix [A]. In the listing below a set of data is given for a ring stiffened structure referred to here as Example III. This set of data is taken from a paper produced by Wah and Hu |25| and converted to SI units.

Data for Example III (cylinder)

For each cylindrical bay:

$R = 103.68$ [mm]

$L = 31.39$ [mm]

$h = 1.19$ [mm]

$E = 2.069 * 10^6$ [N/cm^2]

$\nu = 0.3$

$\rho = 78.50$ [N sec^2/cm^4] x 10^{-6}

For each ring (see sketch):

$b_R = 2.18$ [mm]

$d_R = 5.82$ [mm]

$E = 2.069 * 10^6$ [N/cm^2]

$\nu = 0.3$

$\rho = 78.50 * 10^{-6}$ [N sec^2/cm^4]

Fig. (4.14) shows the μ_0 - Ω_0* curves and table 4.4 presents the limit band frequencies for this structure as well as for the derived structure in which $K_W = \infty$. The μ_0 - Ω_0* curves for the derived structure with $K_W = \infty$ is shown in fig.(4.15).

K_w and K_θ finite		$K_w = \infty$	
μ	Ω_0^*	μ	Ω_0^*
0	27.1153	π	27.73502
π	27.72686	0	35.51674
π	27.73502	0	39.071626
0	39.07163	π	60.76544
0	40.34984	π	67.56043
π	60.76544	0	89.87714

Table 4.4 Limit band frequencies for axi-symmetric wave propagation in ring stiffened cylinders.

Here again the first propagation band starts with $\mu = 0$ as happened in Example II. The reason is that the transverse stiffness of the ring is low if compared to the torsional one.

The application of the reduction technique to make $K_w = \infty$ changes this pattern and the first propagation band comes to start with $\mu_0 = \pi$. Most of the comments made in connection with the structure of Example II apply here.

In fig. (4.16) the $\Omega_0^* - \mu$ curves for the structure of Example III, without the application of the reduction technique, is shown for $\eta = 0$ and in fig. (4.17) for $\eta = 0.15$. It is interesting to consider the curves of fig.(4.15) as the limit of those of fig.(4.17) for η approaching zero. For easy understanding of the curves the Letters I and R, standing for imaginary and real, respectively, appear after the number of the propagation constant. It is interesting to notice that complex conjugate propagation constants do exist for this structure along the bands (0,17.20) and (25.10, 27.115).

Incidentally this last frequency marks the beginning of the first propagation band and above it the curves have a behaviour similar to those of Example II.

CHAPTER V

GENERAL METHODS TO COMPUTE THE FIELD TRANSFER MATRIX

5.1 GENERAL

The general theory developed in chapter III shows that the solution of problems of free wave propagation in spatially periodical structures follows the same lines no matter what the peculiarities of a particular structure or its degree of complexity are. One of the fundamental steps in this theory is the computation of the field transfer matrix from the state matrix.

The state matrix is generally easy to derive (see chapter IV). But if the system concerned has many terminal degrees of freedom (say $n > 2$) the computation of the field transfer matrix can no longer be achieved by following the process employed in chapter IV. One must resort to numerical methods. These methods must be very efficient, both in accuracy and in the amount of computations required. Accuracy in the computation of the field transfer matrix from the state matrix [A] plays an important role since it affects the accuracy of the coefficients p_j's involved in the equation for the propagation constants (see chapter III).

If one is trying to compute $\mu_0 - \Omega_0^*$ curves for the structure the equation (2.4.8) must be solved interactively (it is highly transcendental) and if the p_j's are not accurate enough round-off errors might impair or even prevent the convergence.

Also, because the solution of (2.4.8) is iterative the equation for the propagation constant (consequently the field transfer matrix) must be computed many times and this fact calls for the efficiency (in time) of the computation of the field transfer matrix. So, the two critical factors in the computation of the field transfer matrix are speed and accuracy and they should be one's major preoccupation when selecting or developing a

method.

Henderson and McDaniel |4| have proposed the method based on the constituent idempotents of [A] whose theory is well presented by Frame |27|.

According to this method the field transfer matrix for a bay of length ℓ is given by

$$\left[T_F(\ell,0)\right] = \sum_{j=1}^{2n} e^{\lambda_j \ell} [P_j]$$

where $[P_j]$ are the constituent idempotents of [A] and are computed according to the formula

$$[P_j] = \prod_{\substack{i=1 \\ i \neq j}}^{2n} \frac{[A]_r - \lambda_i [I]}{\lambda_j - \lambda_i}$$

Even for a nondamped bay ([A] real) the constituent indempotents must be computed by using complex arithmetic and $4n(n-1)$ multiplications of complex matrices have to be performed to compute all the $2n$ indempotents of [A], which is equivalent to $16n(n-1)$ products of real matrices. In the case of $n = 4$ it would mean 192 multiplications of 8×8 real matrices. On the top of that the method needs the computation of the roots of the characteristic equation of [A] with great accuracy for they are heavily involved in the computation of $[P_j]$.

At the outset one can see that this method is not very appealing when one is dealing with nondamped systems for, if anything else, it would mean a waste of time in computations. Lin and Donaldson |28| have computed the field transfer matrix for curved panels by lumping the distributed mass of the shell along discrete 'mass lines' running parallel to the stringers and linking each mass line by a massless strip of the shell. The field transfer

matrix of a massless strip and the point transfer matrix of a line mass are then computed and by suitable multiplications the overall field transfer matrix is obtained.

The accuracy of the results depends on the number of mass lines considered.

The method still demands considerable algebraic effort even if the simplest shell theory (Donnell's equation) is used and it must be repeated throughout for each particular kind of structure. Also the numerical computations are kept very high. In this present chapter an effort will be made to select more suitable methods for the computation of the field transfer matrix introducing, whenever possible, modifications in an attempt to reduce the computational task and increase accuracy.

All the methods to be considered here are based upon the state matrix [A] which is the only thing to require algebraic manipulations. As will be seen in chapter VI these algebraic manipulations are usually kept under an acceptable amount.

5.2 THE TRUNCATED SERIES METHOD

In chapter I it was mentioned that the transfer matrix associated with the state matrix [A] can be written in infinite series of the form:

$$\left[T_F(y,0)\right] = e^{[A]_r y} = \sum_{j=0}^{\infty} [A]_r^j \frac{y^j}{j!}$$

The question that arises is whether the above series, when conveniently truncated, provides a good method for the computation of the field transfer matrix. One should expect so because this series is strongly convergent for any matrix $[A]_r$.

Notice, for instance, that $15! = 1.3077 * 10^{12}$ and $20! = 2.4329 * 10^{18}$. This means that by retaining a number of terms of the infinite series of about, say, fifteen to twenty one should get a good accuracy.

If fifteen terms are retained the number of matrix multiplications is thirteen while the indempotent method requires $4n(n - 1)$, that is, fourty eight 8 x 8 matrix multiplications. When no damping is present in the bays the state matrix [A] is real so that the truncated series involves only real operations.

This fact means a two fold advantage upon the constituent indempotent method; first is the obvious economy in computation (the constituent method requires the equivalent of 192 multiplications of real 8 x 8 matrices) and, second, the truncated series method can be programmed for computers in which the complex arithmetic is not available (for instance, the world widespread IBM 1130 computer).

One should recognise another advantage of the truncated series method upon all the others cited previously; it does not require the solution of the characteristic equation of [A], which means further saving in computing time.

In programming the truncated series advantage should be taken from the fact that [A] and its powers are cross-symmetric.

The present method has been used in connection with the computation of $\mu_0 - \Omega_0^*$ curves for the structures dealt with in chapter IV.

The programme was run in the ICL 1907 computer (11 digits in single precision) and in the CDC 7600 computer (14 digits in single precision). The accuracy of the results is virtually the same in both computers. They will be presented later in chapter VI. For computers with seven or eight digits in single precision the method must yet be checked for accuracy and, if necessary, the truncated series should be computed in double precision. In computing the truncated series it is convenient to follow the following steps:

$$[T_1] = [A]_r \, y$$

$$[T_2] = [A]_r \, y \, [T_1]/2$$

$$[T_N] = [A]_r \, y \, [T_{N-1}]/N$$

Then:

$$\left[T_F(\ell,0)\right] = \sum_{j=1}^{N} [T_j] + [I].$$

5.3 THE METHOD BASED ON CAYLEY-HAMILTON THEOREM

The method described in chapter IV and summarized in expressions (4.3.1) and (4.3.1a) can conveniently be programmed if attention is paid to some details to improve efficiency and accuracy.

According to this method - which is a consequence of Cayley-Hamilton theorem - the field transfer matrix is a linear combination of powers of [A] and the coefficients of the linear combination are solutions of a system of linear equations given by (4.3.1a).

The first step towards the application of this method is to solve the characteristic equations of the state matrix. That is a fourth order polynomial equation in λ^2 and give solutions in the form $\pm \lambda_1$, $\pm \lambda_2$, $\pm \lambda_3$ and $\pm \lambda_4$. Accuracy is necessary in computing these roots. Also, because the computation of the field transfer matrix is a step inserted in an iterative process aiming to find μ_0 - Ω_0* curves (propagation bands), it is essential that the method used to solve the characteristic equations be always convergent. Muller's method [29] has proved to satisfy both requirements of accuracy and convergence besides being extremely fast.

It is interesting to point out here that no formal proof has ever been provided for the convergence of Muller's method but no failures have been reported by Muller in his papers or has it happened in this work.

So this method has been used here whenever a polynomial equation (with real or complex coefficients) had to be solved.

Now, it is faster to solve two systems of four linear equations than one system of eight ones. Due to the nature of the roots of the characteristic equation of [A] it is possible to split the system of eight linear equations represented in (4.3.1a) into two systems of four equations each. It can be easily shown that the two smaller systems are:

$$\left[1 \quad \lambda_m^2 \quad \lambda_m^4 \quad \lambda_m^6\right] \left\{X_1\right\} = \left\{\cos h\lambda_m y\right\} \qquad ..(5.3.1)$$

$$\left[\lambda_m \quad \lambda_m^3 \quad \lambda_m^5 \quad \lambda_m^7\right] \left\{X_2\right\} = \left\{\sin h\lambda_m y\right\}$$

$$m = 1, 2, 3, 4$$

In the above systems of equations one has:

$$\left\{X_1\right\} = \begin{Bmatrix} C_1 \\ C_3 \\ C_5 \\ C_7 \end{Bmatrix}; \qquad \left\{X_2\right\} = \begin{Bmatrix} C_2 \\ C_4 \\ C_6 \\ C_8 \end{Bmatrix}$$

The square matrices of the two systems in (5.3.1) are very closely related indeed, for:

$$\left[\lambda_m \quad \lambda_m^3 \quad \lambda_m^5 \quad \lambda_m^7\right] = \left[\lambda_j\right] \left[1 \quad \lambda_m^2 \quad \lambda_m^4 \quad \lambda_m^6\right]$$

where $\left[\lambda_j\right]$ is the square matrix:

$$\left[\lambda_j\right] = \begin{bmatrix} \lambda_1 & 0 & 0 & 0 \\ 0 & \lambda_2 & 0 & 0 \\ 0 & 0 & \lambda_3 & 0 \\ 0 & 0 & 0 & \lambda_4 \end{bmatrix}$$

In this way the two systems (5.3.1) can be represented by:

$$\begin{bmatrix} 1 & \lambda_m^2 & \lambda_m^4 & \lambda_m^6 \end{bmatrix} \{x_1\} = \{\cos h\lambda_m y\}$$

$$\begin{bmatrix} 1 & \lambda_m^2 & \lambda_m^4 & \lambda_m^6 \end{bmatrix} \{x_2\} = \left\{\frac{\sin h\lambda_m y}{\lambda_m}\right\} \qquad ..(5.3.2)$$

Noticing that the determinant of the above square matrix is

$$\Delta = (\lambda_2^2-\lambda_1^2)(\lambda_3^2-\lambda_1^2)(\lambda_4^2-\lambda_1^2)(\lambda_3^2-\lambda_2^2)(\lambda_4^2-\lambda_2^2)(\lambda_4^2-\lambda_3^2) \qquad ..(5.3.3)$$

the sole condition for the systems (5.3.2) to have determinate solutions is that

$$\lambda_m^2 \neq \lambda_j^2 \text{ for } m \neq j.$$

Now, the matrix appearing in system (5.3.2) is of the simple alternant type. This can be easily seen by noting that its determinant is an alternating function of the variables λ_1^2, λ_2^2, λ_3^2 and λ_4^2, that is, it changes its sign (but preserves its absolute value) when two of the variables are interchanged. It can be shown [30] that the inverse of a simple alternant matrix can be obtained by following a very simple rule.

The elements of the j^{th} column of the inverse are quotients of which the numerators are elementary symmetric functions of the variables λ_1^2 λ_2^2, λ_3^2, λ_4^2 with the λ_j^2 omitted and the denominators are products of all the factors of the form $(\lambda_j^2 - \lambda_m^2)$, $m \neq j$. Following this rule the inverse of the matrix of the systems (5.3.2) can easily be written down:

$$[D] = \begin{bmatrix} -\frac{\lambda_2^2\lambda_3^2\lambda_4^2}{D_1} & -\frac{\lambda_1^2\lambda_3^2\lambda_4^2}{D_2} & -\frac{\lambda_1^2\lambda_2^2\lambda_4^2}{D_3} & -\frac{\lambda_1^2\lambda_2^2\lambda_3^2}{D_4} \\ \frac{\lambda_2^2\lambda_3^2+\lambda_2^2\lambda_4^2+\lambda_3^2\lambda_4^2}{D_1} & \frac{\lambda_1^2\lambda_3^2+\lambda_1^2\lambda_4^2+\lambda_3^2\lambda_4^2}{D_2} & \frac{\lambda_1^2\lambda_2^2+\lambda_1^2\lambda_4^2+\lambda_2^2\lambda_4^2}{D_3} & \frac{\lambda_1^2\lambda_2^2+\lambda_1^2\lambda_3^2+\lambda_2^2\lambda_3^2}{D_4} \\ -\frac{\lambda_2^2+\lambda_3^2+\lambda_4^2}{D_1} & -\frac{\lambda_1^2+\lambda_3^2+\lambda_4^2}{D_2} & -\frac{\lambda_1^2+\lambda_2^2+\lambda_4^2}{D_3} & -\frac{\lambda_1^2+\lambda_2^2+\lambda_3^2}{D_4} \\ \frac{1}{D_1} & \frac{1}{D_2} & \frac{1}{D_3} & \frac{1}{D_4} \end{bmatrix}$$

..(5.3.4)

where:

$$D_1 = (\lambda_1^2-\lambda_2^2)(\lambda_1^2-\lambda_3^2)(\lambda_1^2-\lambda_4^2)$$

$$D_2 = (\lambda_2^2-\lambda_1^2)(\lambda_2^2-\lambda_3^2)(\lambda_2^2-\lambda_4^2)$$

$$D_3 = (\lambda_3^2-\lambda_1^2)(\lambda_3^2-\lambda_2^2)(\lambda_3^2-\lambda_4^2)$$

$$D_4 = (\lambda_4^2-\lambda_1^2)(\lambda_4^2-\lambda_2^2)(\lambda_4^2-\lambda_3^2)$$

The solution of system (5.3.2) is then found to be:

$$\begin{Bmatrix} C_1 \\ C_3 \\ C_5 \\ C_7 \end{Bmatrix} = [D] \left\{\cos h\lambda_m y\right\} \; ; \; \begin{Bmatrix} C_2 \\ C_4 \\ C_6 \\ C_8 \end{Bmatrix} = [D] \left\{\frac{\sin h\lambda_m y}{\lambda_m}\right\} \qquad ..(5.3.5)$$

As a last remark one should point out that the matrix [D] does not contain the length of the field for which the field transfer matrix is to be computed. It does appear only in expression (5.3.5). This fact is of convenience when the field transfer matrix has to be computed for several lengths of field, for instance, when computing the state vectors along many points in a bay.

So, instead of solving in the computer a system of eight linear equations with complex coefficients one has only to calculate matrix [D] and then the C_j's by applying expression (5.3.5). The economy in computation is considerable. One should always bear in mind that the field transfer matrix has to be computed many times in the process of calculation of the propagation bands to have an idea of the importance of this saving.

Having determined the coefficients C_j's one is now able to form the linear combination (4.3.1).

Instead of computing the powers of [A] it is advisable to follow the

scheme shown below:

$$[T_1] = C_8[A] + C_7[I]$$

$$[T_2] = [T_1]\,[A] + C_6[I]$$

$$[T_7] = [T_6]\,[A] + C_1[I]$$

$$[T_F(y,0)] = [T_7]$$

In following the above scheme advantage should be taken from the cross-symmetry of the state matrix.

5.4 THE METHOD BASED ON THE EIGENVECTORS OF [A]

The third method to be explored in this work is quite straight forward and is based on the eigenvectors and eigenvalues of the state matrix.

It shall be seen in chapter VII that the field transfer matrix can be expressed by

$$[T_F(y,0)] = [U]\,[e^{\lambda j y}]\,[V]^T \qquad ..(5.4.1)$$

where $[U]$ is the matrix of the right eigenvectors of $[A]$ and $[V]$ is the matrix of the left eigenvectors that is, the eigenvectors of the transpose of $[A]_r$.

Expression (5.4.1) is valid on the condition that the eigenvalues are normalized according to expression (5.4.2):

$$\{V_j\}^T \{U_m\} = \delta_{jm} \qquad ..(5.4.2)$$

where δ_{jm} is one when $j = m$ and zero otherwise. It is also assumed that

$$\lambda j \neq \lambda_m, \qquad j \neq m.$$

As a consequence of (5.4.2) one can write:

$$[V]^T \; [U] \;=\; [I] \qquad ..(5.4.3)$$

which means that:

$$[V]^T \;=\; [U]^{-1} \qquad ..(5.4.4)$$

Taking this result to (5.4.1) the final expression for the field transfer matrix will be:

$$[T_F(y,0)] \;=\; [U] \; [e^{\lambda j y}] \; [U]^{-1} \qquad ..(5.4.5)$$

The eigenvectors and eigenvalues of the state matrix can, of course, be computed by using a standard subroutine. There are some shortcomings in following this approach. First, standard subroutines to solve eigenvalue problems with a general complex matrix are not generally available in many computing systems. Second, a general feature of most (if not all) the standard iterative methods to solve eigenvalue problems is that the accuracy of the eigenvectors is somehow lower than the accuracy of the eigenvalues. This is, of course, inconvenient in the present case since the computation of the field transfer matrix is only an intermediate step towards the calculation of the propagation constants. Consequently the accuracy of the eigenvectors should also be great, of the same order as the accuracy of the eigenvalues.

Further, the standard iterative methods mentioned above are, in general, too time consuming for the present purposes.

In appendix C the Leverrier's method with Fadeev's modification will be described. This is a direct method giving the characteristic equation of [A] and can also be applied to compute both its right and left eigenvectors.

This method is very efficient and accurate for small matrices (say

up to 15 x 15) and has no restrictions related to the nature of the square matrix. One must only assume that the eigenvalues are distinct. The method also permits advantage to be taken from the fact that [A] is cross symmetric and that $a_{ij} = 0$ when $i + j$ is even.

The method described in this section enjoys the same advantage pointed out in the end of section 5.3. One can see by looking at expression (5.4.5) that the size of the field (y) can easily vary because it is not involved in the modal matrices appearing in this expression. So, once the matrices [U] and $[U]^{-1}$ have been obtained (for a certain frequency) the field transfer matrix for any length of field can be calculated.

One shall see, later in this work, applications of this property.

CHAPTER VI

FREE WAVE PROPAGATION IN STRINGER-STIFFENED SHELLS AND RING-STIFFENED CYLINDERS

6.1 GENERAL

Having developed a general theory to solve problems of free wave propagation in periodic structures (chapter III) and discussed suitable techniques to compute the field transfer matrix from the state matrix (chapter V) one is now prepared to tackle some specific examples.

Two kinds of structures will be considered in this chapter and they will be referred to as stringer-stiffened shell and ring-stiffened cylinder.

The main element in both structures is a thin cylindrical elastic shell, damped or not.

In the first structure referred above the shell is supposed to be simply supported along two circular frames distance b units apart and orthogonal to the axis of the shell. The stringers are also supposed to be simply supported at the frames and run parallel to the axis of the shell. This structure is supposed to represent a section of a cylindrical aircraft fuselage (see fig. 6.1). The attachment between shell and stringer is considered to be along a line.

The comments related to the representativeness of this model of a real structure could follow the same lines as those made in chapters II and IV for the stringer-stiffened plate structure. The circular frames are considered as acting as simple supports in spite of their high transverse and torsional stiffness.

As pointed out in |2| this is a sound hypothesis for high aspect ratio, say, greater than two and a half.

Since panels adjacent across the frame move almost independently and since there is considerable correlation across the stringers one shall

examine wave propagation around the circumference of the shell (y direction in fig. (6.1)) only.

The second structure to be dealt with in this chapter consists of an infinitely long circular cylinder stiffened by rings distant b units apart. All the rings are assumed to be identical and attached to the shell along a line. Ring-stiffened cylinders have been a subject of vibration research for a long time, which is shown by the considerable number of publications available.

Most of these works are concerned with finding the eigenvalues and modal shapes of ring-stiffened shells. Bushnell |31| has developed a finite difference analysis of a general shell of revolution by using Novoshilov's kinematic relations for these shells.

Hu and Wah |25| have analysed a ring-stiffened circular cylinder by considering the interaction forces between shell and rings as forcing functions on the rings and the problem is treated as one of the forced response of a series of rings.

Forsberg |32| has tackled the problem by introducing the ring characteristics (stiffness and inertia) through the boundary conditions at each junction and at the ends of the shell. Finite element has also been used |32| but it has been pointed out by Forsberg and Warburton |33| |34| that for cylindrical shells there is no inherent advantage of finite elements upon other methods.

When all the bays and ring-stiffeners are identical the structure can be thought as periodical, each period including a cylindrical shell bay and a ring. In this case the theory developed in chapter III can be conveniently applied to examine the wave propagation along the structure.

In the next two sections the state matrix related to both structures dealt with in this chapter will be derived. For simplicity Donnell's equations will be taken in both cases but a more advanced theory could be

used without increasing too much the algebraic work to derive the state matrices. As explained before, as soon as the state matrix is derived the task of finding the field transfer matrix is left to the computer.

6.2 The state matrix for the shell element associated with stringer-stiffened shells

The method adopted in chapter IV to find the state matrix for a flat plate element can be applied here for the shell element.

As was said in the previous section the dynamic counterpart of Donnell's equations will be used for both stringer-stiffened shell and ring-stiffened cylinder. The reason for this choice is simplicity, though a more general shell theory would not increase too much the amount of algebra.

Considering the sign convention established in fig. (6.1) the Donnell's equation can be written:

$$\frac{\partial^2 u}{\partial x^2} + \frac{1-\nu}{2}\frac{\partial^2 u}{\partial y^2} + \frac{1+\nu}{2}\frac{\partial^2 v}{\partial x \partial y} - \frac{1}{R}\frac{\partial w}{\partial x} - \frac{\rho h}{K}\frac{\partial^2 u}{\partial t^2} = 0$$

$$\frac{1+\nu}{2}\frac{\partial^2 u}{\partial x \partial y} + \frac{1-\nu}{2}\frac{\partial^2 v}{\partial x^2} + \frac{\partial^2 v}{\partial y^2} - \frac{1}{R}\frac{\partial w}{\partial y} - \frac{\rho h}{K}\frac{\partial^2 v}{\partial t^2} = 0 \qquad ..(6.2.1)$$

$$\frac{\nu}{R}\frac{\partial u}{\partial x} + \frac{1}{R}\frac{\partial v}{\partial y} - \frac{w}{R^2} - \frac{h^2}{12}\left(\frac{\partial^4 w}{\partial x^4} + 2\frac{\partial^4 w}{\partial x^2 \partial y^2} + \frac{\partial^4 w}{\partial y^2}\right) - \frac{\rho h}{K}\frac{\partial^2 w}{\partial t^2} = 0$$

In equations (6.2.1) R is the radius of the shell element and $K = \frac{Eh}{1-\nu^2}$. Assuming solutions of the form:

$$u(x,y,t) = \sum_{r=1}^{\infty} u_r(y) \cos \zeta x \, e^{i\Omega t}$$

$$v(x,y,t) = \sum_{r=1}^{\infty} v_r(y) \sin \zeta x \, e^{i\Omega t} \qquad ..(6.2.2)$$

$$w(x,y,t) = \sum_{r=1}^{\infty} w_r(y) \sin \zeta x \, e^{i\Omega t} \; ; \; \zeta = \frac{r\pi}{b}$$

and taking them to equations (6.2.1) and solving each of the resulting equations for the highest derivative it contains one ends up with:

$$u_r''(y) = \frac{2}{1-\nu}(\zeta^2 - \frac{\rho h\Omega^2}{K})u_r(y) - \frac{1+\nu}{1-\nu}\cdot\zeta\cdot v_r'(y) + \frac{2\nu}{1-\nu}\cdot\frac{\zeta}{R}\cdot w_r(y)$$

$$v_r''(y) = (\frac{1-\nu}{2}\cdot\zeta^2 - \frac{\rho h\Omega^2}{K})v_r(y) + \frac{1+\nu}{2}\cdot\zeta\cdot u_r'(y) + \frac{1}{R}w_r'(y)$$

$$w_r^{IV}(y) = \frac{12}{h^2R}v_r'(y) - \frac{12\nu}{h^2R}\cdot\zeta\cdot u_r(y) - \left\{\zeta^4 + \frac{12}{h^2}(\frac{1}{R^2} - \frac{\rho h\Omega^2}{K})\right\}w_r(y)$$

$$+ 2\zeta^2 w_r''(y) \qquad ..(6.2.3)$$

Equations (6.2.3) can be used to construct the following matrix differential equation:

$$\begin{Bmatrix} u \\ v \\ w \\ w' \\ w'' \\ w''' \\ v' \\ u' \end{Bmatrix}' = \begin{bmatrix} 0 & 0 & 0 & 0 & 0 & 0 & 0 & 1 \\ 0 & 0 & 0 & 0 & 0 & 0 & 1 & 0 \\ 0 & 0 & 0 & 1 & 0 & 0 & 0 & 0 \\ 0 & 0 & 0 & 0 & 1 & 0 & 0 & 0 \\ 0 & 0 & 0 & 0 & 0 & 1 & 0 & 0 \\ b_{61} & 0 & b_{63} & 0 & b_{65} & 0 & b_{67} & 0 \\ 0 & b_{72} & 0 & b_{74} & 0 & 0 & 0 & b_{78} \\ b_{81} & 0 & b_{83} & 0 & 0 & 0 & b_{87} & 0 \end{bmatrix} \begin{Bmatrix} u \\ v \\ w \\ w' \\ w'' \\ w''' \\ v' \\ u' \end{Bmatrix} \qquad ..(6.2.4)$$

Equation (6.2.4) can be written in condensed form:

$$\{x\}_r' = [B]_r \{x\}_r \qquad ..(6.2.4a)$$

The elements of matrix $[B]_r$ are given below:

$$b_{61} = -\frac{12}{h^2R}\cdot\zeta; \quad b_{63} = -\left\{\zeta^4 + \frac{12}{h^2}(\frac{1}{R^2} - \frac{\rho h\Omega^2}{K})\right\}; \quad b_{65} = 2\zeta^2;$$

$$b_{67} = \frac{12}{h^2 R} \; ; \quad b_{72} = \frac{1-\nu}{2} \cdot \zeta^2 - \frac{\rho h \Omega^2}{K} \; ; \quad b_{74} = \frac{1}{R} \; ; \quad b_{78} = \frac{1+\nu}{2} \cdot \zeta$$

$$b_{81} = \frac{2}{1-\nu}\left(\zeta^2 - \frac{\rho h \Omega^2}{K}\right); \quad b_{83} = \frac{2\nu}{1-\nu} \cdot \frac{\zeta}{R} \; ; \quad b_{87} = -\frac{1+\nu}{1-\nu} \cdot$$

Here again it must be said that it is convenient to find another vector different from $\{x\}_r$ and more suitable to our purpose. The vector to be chosen is;

$$\{z\}_r^T = \left\lfloor u_r(y), v_r(y), w_r(y), w'_r(y), M_r(y), V_r(y), -N_r(y), T_r(y) \right\rfloor_r ;$$

Vectors $\{x\}_r$ and $\{z\}_r$ are linked by a transformation matrix $[C]_r$ that can be found by making use of the expressions for the stress resultants in accordance with the sign convention defined in fig.(6.1):

$$\begin{aligned} N_y &= K\left(\frac{\partial v}{\partial y} + \nu \frac{\partial u}{\partial x} - \frac{w}{R}\right) \\ M_y &= -D\left(\frac{\partial^2 w}{\partial y^2} + \nu \frac{\partial^2 w}{\partial x^2}\right) \\ V_y &= -D\left\{\frac{\partial^3 w}{\partial y^2} + (2-\nu)\frac{\partial^3 w}{\partial x^2 \partial y}\right\} \\ T_y &= \frac{K(1-\nu)}{2}\left(\frac{\partial u}{\partial y} + \frac{\partial v}{\partial x}\right) \end{aligned} \qquad \ldots(6.2.5)$$

Applying expressions (6.2.2) to expressions (6.2.5) one can write the following transformation matrix equation in which $[C]_r$ is the transformation matrix:

$$\begin{Bmatrix} u \\ v \\ w \\ w' \\ M \\ V \\ -N \\ T \end{Bmatrix} = \begin{bmatrix} 1 & 0 & 0 & 0 & 0 & 0 & 0 & 0 \\ 0 & 1 & 0 & 0 & 0 & 0 & 0 & 0 \\ 0 & 0 & 1 & 0 & 0 & 0 & 0 & 0 \\ 0 & 0 & 0 & 1 & 0 & 0 & 0 & 0 \\ 0 & 0 & D\nu\zeta^2 & 0 & -D & 0 & 0 & 0 \\ 0 & 0 & 0 & D(2-\nu)\zeta^2 & 0 & -D & 0 & 0 \\ \nu\zeta K & 0 & K/R & 0 & 0 & 0 & -K & 0 \\ 0 & \zeta\frac{K(1-\nu)}{2} & 0 & 0 & 0 & 0 & 0 & \frac{K(1-\nu)}{2} \end{bmatrix} \begin{Bmatrix} u \\ v \\ w \\ w' \\ w'' \\ w''' \\ v' \\ u' \end{Bmatrix} \quad ..(6.2.6)$$

or

$$\{z(y)\}_r = [C]_r \{x(y)\}_r \quad ..(6.2.6a)$$

The inverse of matrix $[C]_r$ can easily be found by applying expressions (6.2.2) to expressions (6.2.5) solving the results for the highest derivatives:

$$w_r''(y) = -\frac{M_r(y)}{D} + \nu\zeta^2 w_r(y)$$

$$w_r'''(y) = -\frac{V_r(y)}{D} + (2-\nu).\zeta^2.\, w_r'(y)$$

$$v_r'(y) = -\frac{N_r(y)}{K} + \nu\zeta u_r(y) + \frac{W_r(y)}{R}$$

$$u_r'(y) = \frac{2}{K(1-\nu)}\, T_r(y) - \zeta V_r(y)$$

and writing

$$\begin{Bmatrix} u \\ v \\ w \\ w' \\ w'' \\ w''' \\ v' \\ u' \end{Bmatrix} = \begin{bmatrix} 1 & 0 & 0 & 0 & 0 & 0 & 0 & 0 \\ 0 & 1 & 0 & 0 & 0 & 0 & 0 & 0 \\ 0 & 0 & 1 & 0 & 0 & 0 & 0 & 0 \\ 0 & 0 & 0 & 1 & 0 & 0 & 0 & 0 \\ 0 & 0 & \nu\zeta^2 & 0 & -\frac{1}{D} & 0 & 0 & 0 \\ 0 & -\frac{1}{D} & 0 & \zeta^2(2-\nu) & 0 & 0 & 0 & 0 \\ \nu\zeta & 0 & \frac{1}{R} & 0 & 0 & 0 & -\frac{1}{K} & 0 \\ 0 & -\zeta & 0 & 0 & 0 & 0 & 0 & \frac{2}{K(1-\nu)} \end{bmatrix}_r \begin{Bmatrix} u \\ v \\ w \\ w' \\ M \\ V \\ -N \\ T \end{Bmatrix} \quad ..(6.2.7)$$

or

$$\{x(y)\} = [C]^{-1} \{z(y)\} \quad ..(6.2.7a)$$

Now, the state matrix appearing in the state equation $\{z(y)\}' = [A]\{z(y)\}$ is given by $[C]\ [B]\ [C]^{-1}$. The matrices $[C]$, $[C]^{-1}$ and $[B]$ are very sparse indeed which makes the above product extremely easy to be carried out by hand.

If this is done the result is:

$$[A]_r = \begin{bmatrix} 0 & -\zeta & 0 & 0 & 0 & 0 & 0 & \frac{2}{K(1-\nu)} \\ \nu\zeta & 0 & \frac{1}{R} & 0 & 0 & 0 & -\frac{1}{K} & 0 \\ 0 & 0 & 0 & 1 & 0 & 0 & 0 & 0 \\ 0 & 0 & \nu\zeta^2 & 0 & -\frac{1}{D} & 0 & 0 & 0 \\ 0 & 0 & 0 & \eta_1 & 0 & 1 & 0 & 0 \\ 0 & 0 & \eta_2 & 0 & \nu\zeta^2 & 0 & \frac{1}{R} & 0 \\ 0 & \alpha\Omega^{*2} & 0 & 0 & 0 & 0 & 0 & -\zeta \\ \eta_3 & 0 & 0 & 0 & 0 & 0 & \nu\zeta & 0 \end{bmatrix} \quad ..(6.2.8)$$

where $\alpha = D/\ell^4$, and $\eta_3 = K(1-\nu^2) - \rho h \Omega^2$

Again it must be said that the above matrix could have been derived by finding the expressions for the derivatives of the stress resultants as functions of the stress resultants themselves. This has in fact been done by Henderson and McDaniel|4| but the method produced above seems more elegant, systematic and the intermediate steps are easier to check. The algebra required is also extremely simple.

6.3 THE STATE MATRIX FOR THE SHELL ELEMENT ASSOCIATED WITH THE RING-STIFFENED STRUCTURE

To compute the state matrix for the shell element associated with the ring-stiffened cylindrical structure (that is, the state matrix associated with the x direction (see fig. 4.1) one shall follow, as always, the procedure used in chapter IV and in the previous section.

The same set of Donnell's equations will be used here with the sign convention established in fig.(4.1) so that the proper sign adaptations should be performed in equations (6.2.1).

Assuming the following set of solutions:

$$u(\bar{x},\phi,t) = \sum_{r=1}^{\infty} u_r(\bar{x}) \sin r\phi \, e^{i\Omega t}$$

$$v(\bar{x},\phi,t) = \sum_{r=1}^{\infty} v_r(\bar{x}) \cos r\phi \, e^{i\Omega t} \qquad ..(6.3.1)$$

$$w(\bar{x},\phi,t) = \sum_{r=1}^{\infty} w_r(\bar{x}) \sin r\phi \, e^{i\Omega t}$$

and taking

$$\{x\}^T = \left\lfloor -v, u, w, w', w'', w''', v', u' \right\rfloor$$

and following the same steps given in the previous sub-section one finds

$$[B] = \begin{bmatrix} 0 & 0 & 0 & 0 & 0 & 0 & -1 & 0 \\ 0 & 0 & 0 & 0 & 0 & 0 & 0 & 1 \\ 0 & 0 & 0 & 1 & 0 & 0 & 0 & 0 \\ 0 & 0 & 0 & 0 & 1 & 0 & 0 & 0 \\ 0 & 0 & 0 & 0 & 0 & 1 & 0 & 0 \\ b_{61} & 0 & b_{63} & 0 & b_{65} & 0 & 0 & b_{68} \\ b_{71} & 0 & b_{73} & 0 & 0 & 0 & 0 & b_{78} \\ 0 & b_{82} & 0 & b_{84} & 0 & 0 & b_{87} & 0 \end{bmatrix}_r \qquad ..(6.3.2)$$

or

$$\{x(\bar{x})\}_r = [B]_r \{x(\bar{x})\}_r \qquad ..(6.3.2a)$$

where

$$b_{61} = -\frac{r}{K}; \quad b_{63} = -r^4 - \frac{1}{K} + \frac{\rho h R^2}{kK}\Omega^2; \quad b_{65} = 2r^2; \quad b_{68} = -\frac{\nu}{K}$$

$$b_{71} = -\frac{2}{1-\nu}\left(r^2 - \frac{\rho h R^2}{K}\Omega^2\right); \quad b_{73} = -\frac{2r}{1-\nu}; \quad b_{78} = -\frac{1+\nu}{1-\nu} r$$

$$b_{82} = \frac{1-\nu}{2} r^2 - \frac{\rho h R^2}{K}\Omega^2; \quad b_{84} = -\nu; \quad b_{87} = r\frac{1+\nu}{2}$$

$$k = \frac{h^2}{12R^2}$$

The transformation matrix is found by taking expressions (6.3.1) into Donnell's expressions for the stress resultants and assuming:

$$\{z(\bar{x})\}_r^T = \left[-v(\bar{x}), u(\bar{x}), w(\bar{x}), \theta(\bar{x}), M(\bar{x}), V(\bar{x}), N(\bar{x}), T(\bar{x})\right]_r$$

The result is:

$$[C]_r = \begin{bmatrix} 1 & 0 & 0 & 0 & 0 & 0 & 0 & 0 \\ 0 & 1 & 0 & 0 & 0 & 0 & 0 & 0 \\ 0 & 0 & 1 & 0 & 0 & 0 & 0 & 0 \\ 0 & 0 & 0 & \frac{1}{R} & 0 & 0 & 0 & 0 \\ 0 & 0 & C_{53} & 0 & C_{55} & 0 & 0 & 0 \\ 0 & 0 & 0 & C_{64} & 0 & C_{66} & 0 & 0 \\ C_{71} & 0 & C_{73} & 0 & 0 & 0 & 0 & C_{78} \\ 0 & C_{82} & 0 & 0 & 0 & 0 & C_{87} & 0 \end{bmatrix}_r \quad ..(6.3.3)$$

or

$$\{z(\bar{x})\}_r = [C]_r \{x(\bar{x})\} \quad ..(6.3.3a)$$

where

$C_{53} = -\nu r^2 D/R^2$; $C_{55} = D/R^2$;

$C_{64} = -(2-\nu)r^2 D/R^3$; $C_{66} = D/R^3$;

$C_{71} = r\nu K/R$; $C_{73} = \nu K/R$;

$C_{78} = K/R$; $C_{82} = rK(1-\nu)/2R$;

$C_{87} = K(1-\nu)/2R$

The inverse of $[C]_r$ is found by the usual process shown in the previous sub-section and is:

$$[C]_r^{-1} = \begin{bmatrix} 1 & 0 & 0 & 0 & 0 & 0 & 0 & 0 \\ 0 & 1 & 0 & 0 & 0 & 0 & 0 & 0 \\ 0 & 0 & 1 & 0 & 0 & 0 & 0 & 0 \\ 0 & 0 & 0 & R & 0 & 0 & 0 & 0 \\ 0 & 0 & d_{53} & 0 & d_{55} & 0 & 0 & 0 \\ 0 & 0 & 0 & d_{64} & 0 & d_{66} & 0 & 0 \\ 0 & d_{72} & 0 & 0 & 0 & 0 & 0 & d_{78} \\ d_{81} & 0 & d_{83} & 0 & 0 & 0 & d_{87} & 0 \end{bmatrix}_r \quad ..(6.3.4)$$

where

$$d_{53} = \nu r^2; \quad d_{55} = R^2/D; \quad d_{64} = R(2-\nu)r^2; \quad d_{66} = R^3/D;$$

$$d_{72} = -r; \quad d_{78} = 2R/(1-\nu)K; \quad d_{81} = -r\nu; \quad d_{83} = -\nu;$$

$$d_{87} = R/K$$

Now, performing the product $[C]\ [B]\ [C]^{-1}$ the state matrix comes out:

$$[A]_r = \begin{bmatrix} 0 & r & 0 & 0 & 0 & 0 & 0 & -2R/K(1-\nu) \\ -r\nu & 0 & -\nu & 0 & 0 & 0 & \frac{R}{K} & 0 \\ 0 & 0 & 0 & R & 0 & 0 & 0 & 0 \\ 0 & 0 & \nu r^2/R & 0 & \frac{R}{D} & 0 & 0 & 0 \\ 0 & 0 & 0 & 2Dr^2(1-\nu)/R & 0 & R & 0 & 0 \\ -rK(1-\nu^2)/R & 0 & \alpha_1 & 0 & \nu r^2/R & 0 & -\nu & 0 \\ 0 & -R\alpha_o\Omega^*{}_o^2 & 0 & 0 & 0 & 0 & 0 & r \\ \alpha_2 & 0 & -rK(1-\nu^2)/R & 0 & 0 & 0 & -r\nu & 0 \end{bmatrix} \quad ..(6.3.5)$$

where

$$\alpha_1 = -\frac{D}{R^3}(r^4 + \frac{12R^2}{h^2})(1-\nu^2) + R\alpha_o\Omega_o^{*2}$$

$$\alpha_2 = -\frac{K}{R}r^2(1-\nu^2) + R\alpha_o\Omega_o^{*2}$$

$$\alpha_o = D_o/\ell^4$$

ℓ, distance between stiffening rings.

One should notice that all the state transfer matrices derived in this and in chapter IV share the common properties of being cross-symmetric and having $a_{ij} = 0$ if $i + j$ is an even number. Their properties lead to a cross-symmetric field transfer matrix. This fact is of convenience for checking purposes and also because it provides means of time saving in the numerical computation of the field transfer matrix.

General methods for the computation of the field transfer matrix have been considered in chapter V. One can see that for the structures dealt with in this present chapter one has to resort to one of those methods because the order of the state matrix is too high to follow the approach found in chapter IV.

The next section will deal with the point transfer matrix.

6.4 THE POINT TRANSFER MATRIX

As pointed out in chapters II and IV the point transfer matrix for an open section stringer has been developed by Lin [3] and made more general by Henderson and McDaniel [4].

In these derivations the inertia in the directions of y, z and θ (see fig. 6.1) is considered. The displacements in these directions are considered small and the effects of variations of u along the stringer, negligible.

According to the above stated assumptions the jump in bending momement, radial shear V_r and in plane force N_r across the stringer are given by:

$$
\begin{aligned}
M_r^R &= K_{V\theta} v_r + K_{w\theta} w_r + K_\theta \theta_r + M_r^L \\
V_r^R &= K_{vw} v_r + K_w w_r - K_{w\theta} \theta_r + V_r^L \qquad \text{..(6.4.1)} \\
-N_r^R &= K_v v_r - K_{vw} w_r + K_{v\theta} \theta_r - N_r^L
\end{aligned}
$$

where

$$K_{V\theta} = E\zeta^4 (A_y I_{\eta\zeta} - A_z I_\zeta) - (C_z - A_z)\, A\, \alpha_4 \Omega_o{}^{*2}$$

$$K_{vw} = E\zeta^4 I_{\eta\zeta}$$

$$K_v = E\zeta^4 I_\zeta + A\alpha_4 \Omega_o{}^{*2}$$

where

$$\alpha_4 = D_o / h\ell^4$$

The other coefficients appearing in (6.4.1) are given in 2.3.3 and 4.

From equations (6.4.1) Henderson and McDaniel's point transfer matrix is derived:

$$
\begin{Bmatrix} u \\ v \\ w \\ \theta \\ M \\ V \\ -N \\ T \end{Bmatrix}_r^R
=
\begin{bmatrix}
1 & 0 & 0 & 0 & 0 & 0 & 0 & 0 \\
0 & 1 & 0 & 0 & 0 & 0 & 0 & 0 \\
0 & 0 & 1 & 0 & 0 & 0 & 0 & 0 \\
0 & 0 & 0 & 1 & 0 & 0 & 0 & 0 \\
0 & K_{V\theta} & K_{w\theta} & K_\theta & 1 & 0 & 0 & 0 \\
0 & K_{vw} & K_w & -K_{w\theta} & 0 & 1 & 0 & 0 \\
0 & K_v & -K_{vw} & K_{v\theta} & 0 & 0 & 1 & 0 \\
0 & 0 & 0 & 0 & 0 & 0 & 0 & 1
\end{bmatrix}_r
\begin{Bmatrix} u \\ v \\ w \\ \theta \\ M \\ V \\ -N \\ T \end{Bmatrix}_r^L
\qquad \text{..(6.4.2)}
$$

Neither Lin nor Henderson and McDaniel were interested in wave propagation through periodic structures but in the forced response and natural frequencies of a finite stringer-stiffened shell using the classical transfer matrix approach |13|.

Stringer-stiffened shells have been considered in this work because it provides a good example to check the numerical procedures related to the method established in chapter III.

In order to derive the point transfer matrix for a ring, resort will be made to the general equations produced by Wah and Hu |25|:

$$\frac{EI}{R^4}\left(\frac{\partial^4 w}{\partial\phi^4} - \frac{\partial^3 v}{\partial\phi^3}\right) + \frac{EA}{R^2}\left(w + \frac{\partial v}{\partial\phi}\right) + \rho A \frac{\partial^2 w}{\partial t^2} = F_w(\phi,t)$$

$$\frac{EI}{R^4}\left(\frac{\partial^3 w}{\partial\phi^3} - \frac{\partial^2 v}{\partial\phi^2}\right) - \frac{EA}{R^2}\left(\frac{\partial w}{\partial\phi} + \frac{\partial^2 v}{\partial\phi^2}\right) + \rho A \frac{\partial^2 v}{\partial t^2} = F_v(\phi,t) \qquad ..(6.4.3)$$

$$\frac{E\bar{I}}{R^4}\left(\frac{\partial^4 u}{\partial\phi^4} - R\frac{\partial^2\theta}{\partial\phi^2}\right) - \frac{GJ}{R^4}\left(\frac{\partial^2 u}{\partial\phi^2} + R\frac{\partial^2\theta}{\partial\phi^2}\right) + \rho A \frac{\partial^2 u}{\partial t^2} = F_u(\phi,t)$$

$$\frac{E\bar{I}}{R^2}\left(R - \frac{\partial^2 u}{\partial\phi^2}\right) - \frac{GJ}{R^2}\left(\frac{\partial^2 u}{\partial\phi^2} + R\frac{\partial^2\theta}{\partial\phi^2}\right) + \rho I_p R \frac{\partial\theta}{\partial t^2} = RF_\theta(\phi,t)$$

In equation (6.4.3) I is a principal moment of area of the ring cross-section about an axis parallel to the radial direction. The quantities F_w, F_v, F_u and F_θ are the external forces and twisting moment per unit length acting on the ring (see fig. 4.1).

The other constants appearing in equations (6.4.3) have already been explained in chapters II and IV. It will be assumed here that rings and cylindrical shells have both the same mass density, an assumption that can easily be dropped if necessary.

Now applying expressions (6.3.1) to the differential equations (6.4.3) assuming that

$$F_w(\phi,t) = \sum_{r=1}^{\infty} F_{wr} \sin r\phi \, e^{i\Omega t}$$

$$F_v(\phi,t) = \sum_{r=1}^{\infty} F_{vr} \cos r\phi \, e^{i\Omega t}$$

$$F_u(\phi,t) = \sum_{r=1}^{\infty} F_{ur} \sin r\phi \, e^{i\Omega t}$$

$$F_\theta(\phi,t) = \sum_{r=1}^{\infty} F_{\theta r} \sin r\phi \, e^{i\Omega t}$$

and noting that

$$F_{wr} = V_r^L - V_r^R$$

$$F_{vr} = T_r^R - T_r^L$$

$$F_\mu = N_r^R - N_r^L$$

$$F_\theta = M_r^R - M_r^L$$

the result is:

$$M_r^R = M_r^L + K_{u\theta} u_r + K_\theta \theta_r$$

$$V_r^R = V_r^L + K_{vw} v_r - K_w w_r$$

$$N^R = N^L + K_u u_r + K_{\mu\theta} \theta_r$$

$$T^R = T^L + K_v v_r - K_{vw} w_r$$

..(6.4.4)

where

$$K_{u\theta} = r^2 \left(\frac{E\bar{I}}{R^3} + \frac{GJ}{R^3}\right)$$

$$K_\theta = \frac{E\bar{I}}{R^2} + r^2 \frac{GJ}{R^2} - I_p \cdot \alpha_4 \cdot \Omega_o{}^{*2}$$

$$K_{vw} = r^3 \frac{EI}{R^4} + r \frac{EA}{R^2}$$

$$K_w = r^4 \frac{EI}{R^4} + \frac{EA}{R^2} - A \cdot \alpha_4 \cdot \Omega_o{}^{*2}$$

$$K_u = r^4 \frac{E\bar{I}}{R^4} + r^2 \frac{GJ}{R^4} - A \cdot \alpha_4 \cdot \Omega_o{}^{*2}$$

$$K_v = r^2 \frac{EI}{R^4} + r^2 \frac{EA}{R^2} - A \cdot \alpha_4 \, \Omega_o{}^{*2}$$

and

$$\alpha_4 = D_o / \ell^4 h$$

Notice that the coupling coefficients $K_{u\theta}$ and K_{vw} in the above expressions vanish when r = 0 (axi-symmetric case). Expressions (6.4.4) can now be used to determine the ring point transfer matrix:

$$\begin{Bmatrix} -v \\ u \\ w \\ \theta \\ M \\ V \\ N \\ T \end{Bmatrix}_R = \begin{bmatrix} 1 & 0 & 0 & 0 & 0 & 0 & 0 & 0 \\ 0 & 1 & 0 & 0 & 0 & 0 & 0 & 0 \\ 0 & 0 & 1 & 0 & 0 & 0 & 0 & 0 \\ 0 & 0 & 0 & 1 & 0 & 0 & 0 & 0 \\ 0 & K_{u\theta} & 0 & K_\theta & 1 & 0 & 0 & 0 \\ -K_{vw} & 0 & -K_w & 0 & 0 & 1 & 0 & 0 \\ 0 & K_u & 0 & K_{u\theta} & 0 & 0 & 1 & 0 \\ -K_\theta & 0 & -K_{vw} & 0 & 0 & 0 & 0 & 1 \end{bmatrix}_r \begin{Bmatrix} -v \\ u \\ w \\ \theta \\ M \\ V \\ N \\ T \end{Bmatrix}_L \quad ..(6.4.5)$$

The square matrix appearing in (6.4.5) is the point transfer matrix for a ring.

6.5 THE PERIOD TRANSFER MATRIX

The period transfer matrix is obtained, as always, by performing the product $[P]_r\ [T]_F$, where $[P]_r$ is the point transfer matrix. For easy computation the elements of the period transfer matrix can be written as:

a) for stringer-stiffened shell:

$$t_{i,j} = t^F_{i,j} \; ; \quad i \leq 4,\ i = 8,\ j = 1,8$$

$$t_{5,j} = t^F_{5,j} + K_{v\theta} t^F_{2,j} + k_{w\theta} t^F_{3,j} + t^F_{4,j}$$

$$t_{6,j} = t^F_{6,j} + K_{vw} t^F_{2,j} + K_w t^F_{3,j} - K_{w\theta} t^F_{4,j} \qquad ; j = 1,8 \qquad ..(6.5.1)$$

$$t_{7,j} = t^F_{7,j} + K_v t^F_{2,j} - K_{vw} t^F_{3,j} - K_{v\theta} t^F_{4,j}$$

b) for ring stiffened cylinder:

$$t_{i,j} = t^F_{i,j} \; ; \quad i \leq 4,\ j = 1,8$$

$$t_{5,j} = t^F_{5,j} + K_{u\theta} t^F_{2,j} + K_\theta t^F_{4,j}$$

$$t_{6,j} = t^F_{6,j} - K_{vw} t^F_{1,j} - K_w t_{3,j}$$

$$t_{7,j} = t^F_{7,j} + K_u t^F_{2,j} + K_{u\theta} t^F_{4,j} \qquad ; \quad j = 1,8 \qquad ..(6.5.2)$$

$$t_{8,j} = t^F_{8,j} - K_v t_{1,j} - K_{vw} t_{3,j}$$

If the situation is such that one decides to assume that the transverse displacement is zero the period transfer matrix can be written as

a) for stringer-stiffened shell:

$$t^*_{i,j} = t^{*F}_{i,j} \; ; \quad i \leq 3,\ i = 6; \quad j = 1,6$$

$$t^*_{4,j} = t^{*F}_{4,j} + K_{V\theta} t^{*F}_{2,j} + K_{\theta} t^{*F}_{3,j} \qquad \text{..(6.5.3)}$$

$$: j = 1,6$$

$$t^*_{5,j} = t^{*F}_{5,j} + K_V t^{*F}_{2,j} + K_{V\theta} t^{*F}_{3,j}$$

b) for ring-stiffened cylinder:

$$t^*_{i,j} = t^{*F}_{i,j} \; ; \quad i \leq 3; \; j = 1,6$$

$$t^*_{4,j} = t^{*F}_{4,j} + K_{u\theta} t^{*F}_{2,j} + K_{\theta} t^{*F}_{3,j}$$

$$\text{..(6.5.4)}$$

$$t^*_{5,j} = t^{*F}_{5,j} + K_u t^{*F}_{2,j} + K_{u\theta} t^{*F}_{3,j} \quad ; \; j = 1,6$$

$$t^*_{6,j} = t^{*F}_{6,j} - K_V t^{*F}_{1,j}$$

In expressions (6.5.1) to (6.5.4) F stands for 'field' and the star means 'reduced', that is the reducing technique described in appendix B has been applied to the original field transfer matrix to obtain $[T_F^*]$.

6.6 NUMERICAL RESULTS

In this section a ring-stiffened cylinder (fig.4.1) and a stringer-stiffened shell (fig. 6.1) are considered for numerical computations. The data for the ring-stiffened cylinder are the same as Example III listed in chapter IV. The data for the stringer-stiffened shell is the same as Example I with the additional data for the radius which is R = 182.88 cm .

All three methods of computation of the field transfer matrix have been used to compute μ_o - Ω_o^* curves. The numerical results are virtually

the same. As far as computing time is concerned the method based on the eigenvalues and eigenvectors of $[A]_r$ shows an advantage of 20% over the truncated series method but is practically equivalent to the modified method based upon Cayley-Hamilton Theorem.

6.6.1 Stringer-stiffened shell results

Table 6.1 lists the lower and upper limits for the first three bands of the stringer-stiffened shell.

Also shown on table 6.1 are Lin's results |1| and the lower limit of the first band computed by Henderson and McDaniel |4|. This last figure refers to a closed skin-stringer shell made up of 56 bays.

Henderson and McDaniel had applied the traditional transfer matrix approach |4| to find the first natural frequencies of closed skin-stringer structures. One can see by looking at table 6.1 how close their computed first natural frequency is to the lower limit of the first band found in this work.

On the other hand, apart from the lower limit of the first band, the results obtained in this work are very different from those shown by Lin. Fig.(6.2)shows the first three propagating bands as computed in this work and fig. (6.3) represents the numerical results produced by Lin. The dashed lines linking the limits of the bands is to remind that the intermediate frequencies have not actually been computed by Lin. One could see that the two bands shown in fig. (6.3) actually overlap, a fact not shown in fig. (6.2) in the first two bands.

Table 6.1 Comparison of results obtained by Lin, Henderson and McDaniel and the technique developed in this work. Stringer-stiffened structure with ASP = 2.44.

μ_o- Ω_o^* technique			Lin's Method	Henderson and McDaniel
μ_o	Ω_o^*	Hz	Hz	Hz
π	19.9975	114.3	104.5	112.3
0	39.45826	226.0	414.0	
π	55.9429	321.0	232.3	
0	63.23307	362.0	496.6	
0	78.4660	450.0		
π	96.21064	550.2		

To boost the confidence in the numerical methods and techniques used in this work further runs have been done with increased values of the radius. Radius of 2.5R, 10R, 100R and 1000R have been considered. The aim was to see whether the above results would steadily converge to those of the flat plate when the radius gets bigger and bigger. Table 6.2 shows that it actually happens. This fact is believed to be a necessary check on the techniques used in this chapter.

One should point out here that the results produced in table 6.1 have been obtained in three different ways, that is, each time one of the techniques for the construction of the field transfer matrix described in chapter V has been used.

Lin's method for curved structures is radically different from that for flat ones. Instead of using the 'exact' approach developed for flat structures (which would be extremely laborious) he derives an approximate energy method.

Table 6.2 Lower and upper frequency limits of passing bands for different radius. Stringer-stiffened structure with ASP = 2.44, R = 182.88 [cm]

μ	R	2.5R	10R	100R	1000R	Flat Plate*
π	19.997	17.595	17.209	17.217	17.221	17.222
0	39.458	34.505	23.610	22.690	22.681	22.681
π	55.943	55.813	55.711	55.697	55.695	55.714
0	63.233	39.662	39.781	39.819	39.823	39.865

* Results obtained in chapter IV

The numerical results seen in tables 6.1 and 6.2 were obtained by making use of a state matrix based on the more general set of Flugge's equations. The simplified equations (Donnell's equations) used to derive the state matrix in expression (6.2.8) have proved to be just as good for the computation of the first two passing bands as one can see by looking at table 6.3.

Table 6.3 Stringer-stiffened structure. Comparison of results from Donnell's and Flugge's general equations.

Simplified Flugge's equations (Donnell's eq)	General Flugge's Theory
20.0132	19.9975
39.4645	39.4583
55.9335	55.9429
63.2510	63.2331

The reducing technique explained in appendix B has been applied here with

$I_1 = 3$ and $I_2 = 6$, that is, the transverse stiffness was considered infinite.

In table 6.4 a comparison is made between the original results and those for the reduced structure.

Table 6.4 Stringer-stiffened shell. Variation of results when the stringer transverse stiffness is considered infinite.

Original structure	$K_W = \infty$
20.0132	20.0132
39.4645	39.4653
55.9335	55.9486
63.2510	66.0664

As can be seen the results for $K_W = \infty$ are good enough to represent the original structure. For other kinds of stringers a careful analysis must be made on the grounds of the discussion presented in chapter IV. The main advantage of elimination of degrees of freedom (when it is justifiable) is some time saving in computations. For instance, it took 40.046 seconds in a CDC 7600 computer to calculate the two first passing bands of the original structure when the method based on the eigenvectors and eigenvalues of $[A]$ was applied. With the reduction technique applied as explained above the time was 35.953 seconds which means an economy of just over eleven percent. Fig. (6.4) and fig. (6.5) show $\Omega_o^* - \mu$ curves for the stringer-stiffened shell corresponding to $\eta = 0.0$ and $\eta = 0.15$ and with an aspect ratio equal to three. The propagation constants have been numbered for easy understanding of the graphs. A number refers to the real or imaginary part of the corresponding propagation constant if it is below or above the 0-0 line, respectively. Again it is convenient to

consider fig. (6.4) as a limit to which fig. (6.5) tends to when damping tends to zero.

Considering now fig. (6.4) one can see that propagation constants 1 and 2 are complex conjugates up to point A(Ω_0^* = 39.130) and propagation constants 2 and 3 are complex conjugates from Ω_0^* = 39.130 to 44.736 (point B).

This same graph shows two complete propagation zones the first being associated with the propagation constant numbered three. The second propagation band can be considered in three parts. The first part is associated with propagation constants 3 and 2, that is, these are 'propagating' propagation constants. So, associated with any frequency within this first part there are two propagating waves. The second part of the second band is associated with propagation constant number three only. In this part of the propagation band the propagation constant number two becomes 'attenuating'. The third part of the second propagation band is also associated only with propagation constant number three, but one can see that there is an overlap with the third propagation band (propagation constant number two starts propagating again). The reason for usinghhere aspect ratio equals 3 (instead of 2.44 used before) is to enlarge the second part of the second propagation band for easier visualisation. If the aspect ratio of 2.44 were used this region would almost disappear as one can understand by looking at fig. (6.2). The aspect ratio was increased by holding ℓ constant and increasing b (distance between frames).

Fig. (6.6) and (6.7) show Ω_0^* - v* curves (that is non-dimensional phase velocity plotted against the non-dimensional frequency) for the stringer-stiffened shell with ASP = 2.44. Fig. (6.6) corresponds to the first propagation band and fig. (6.7) to the second one. It is again very clear from fig. (6.7) that for any frequency within the band (47.736,

55.943) there correspond two groups of free propagating waves. In fact, since the second and third bands overlap in the way shown in fig. (6.2) one could say that for most frequencies within the second band there correspond two groups of waves.

6.6.2 Numerical Results for ring-stiffened cylinders

Computations of $\mu_o - \Omega_o^*$ and $\Omega_o^* - \mu$ curves have been carried out for the ring-stiffened cylinder mentioned in the beginning of this section. Different numbers of circumferential waves have been considered and fig. (6.8) and (6.9) are typical plots.

Fig. (6.8) was computed for five circumferential waves and fig.(6.9) for two. Comparison of results is difficult because of the lack of comparable data available. Wah and Hu [25] have considered fifteen bays of the above ring-stiffened structure simply supported on two 'half-rings' placed at both ends. They have computed the first natural frequency for some circumferential wave numbers.

If their ring-stiffened cylinders were infinite the first natural frequency (for any circumferential wave number) would have to coincide with the lower limit of the first propagating band. For finite structures supported at the ends the comparison is not always so straight forward.

Wah and Hu have shown that the transverse displacement along the structure (15 bays) follows an overall semi-sinusoidal pattern with some inter-ring displacement superimposed upon it.

If the number of circumferential waves is large (say greater than three) there is considerable inter-ring motion and the potential energy of the structure is very little due to the overall semi-sinusoidal displacement. In this case and if the number of bays is large the first natural frequency of the finite structure (for $r \geq 3$) should compare with the lower limit of the first propagation band of the infinite structure.

Table 6.5 makes such a comparison.

Table 6.5 Circular frequencies (rd/sec). Comparison between the lower limit of the first propagation band with the first natural frequency of a 15 bay structure.

μ	r	Wave propagation method	Wah and Hu
0	3	4.140	4.615
0	4	7.860	7.982
0	5	12.590	12.660

Note that for three circumferential waves the discrepancy between the results is about 12% while for five waves they differ by only about 1%. For higher numbers of circumferential waves the agreement is expected to be still better.

When the number of circumferential waves is small (say one or two) the inter-ring motion decreases in importance so that the elastic energy of the finite structure is due mainly to the overall semi-sinusoidal displacement.

The rings participate with more inertia than elasticity. In these cases ($r \lesssim 2$) comparison with the infinite structure is obviously out of the question. This is particularly true when $r = 1$ (rigid body motion for the infinite structure and 'beam' mode for the finite one). The potential elastic energy for the infinite structure is zero in this case so is the lower limit of the first band. For the finite ring-stiffened cylinder the 'beam mode' means that some potential energy plays a role so that the first natural frequency is well above zero.

Wah and Hu computed natural frequency for $r = 2$ is 4235|rd/sec| and

the lower limit of the first band as computed here is 1510 [rd/sec].

In table 6.5 one can see that the lower limit of the first propagation constant corresponds to $\mu = 0$. This is in agreement with the computed mode shapes by Wah and Hu which shows that the inter-ring displacements follow a modified sine wave pattern with localised effect at the rings so that $\partial w/\partial x = 0$.

Fig. (6.10) shows the Ω_o^* - μ curves for the ring-stiffened cylinders without damping and for five circumferential waves and fig. (6.11) was obtained for a skin damping of $\eta = 0.15$.

As was explained previously it is easier to understand the curves of fig. (6.10) if they are considered as a limit of those of fig. (6.11) when the damping is brought to zero.

For easy understanding the propagation constants have been numbered. A number refers to the real or imaginary part of the corresponding propagation constant if it is below or above the 0-0 line, respectively.

For instance, the number 1 just below the 0-0 line (look within the first propagation band) means that the real part of the first propagation band is zero (at that frequency). The number 2 just above the 0-0 line means that the second propagation constant is zero. With this convention the graph becomes almost self-explanatory.

One could notice that propagation constants 1 and 2 are complex conjugates up to the lower limit of the first propagation band.

Propagation constants 3 and 4 are complex conjugates for frequencies ranging from zero to 8.320 (point A(A')) and from 20.410 (point B(B')) to 38.090 (point C(C')).

Two complete propagation bands are included in fig. (6.10) as well as part of the third band.

It is interesting to notice that for this structure (and for the range of frequencies shown in the figure) propagation constant number 2 is

the only one associated with actual wave propagation.

Propagation constants 3 and 4 are very attenuating for all the range of frequencies shown in the figure.

Propagation constant 1 is much less attenuating than 3 and 4. It is interesting to notice that at the beginning of the first propagation band both propagation constants 1 and 2 have zero real and imaginary parts. At this frequency both propagation constants correspond to standing waves.

CHAPTER VII

RESPONSE OF SPATIALLY PERIODIC STRUCTURES TO CONCENTRATED FORCES

7.1 GENERAL

The previous chapters have dealt with free wave propagation in periodic structures. In this chapter it will be shown that the same matrix language used before can successfully be applied to the problem of response to point harmonic forces. The propagation constants of the structure are supposed to be known for the frequency (or frequencies) of interest. The case of a single harmonic force applied anywhere in a bay of an infinite periodic structure is first considered. The problem can easily be extended to the case of several concentrated harmonic forces by super position (the structure is supposed to be linear). As far as the structure is concerned the only requirements are that it is spatially periodic and linear. Other peculiarities of the structure are by-passed in the theory leading to the response to concentrated forces to be developed in this chapter.

The response of finite periodic structures will be developed in sequence and other cases of interest shall be briefly discussed.

The analytical computation of the response of infinite and finite structures to concentrated harmonic forces can be a powerful tool in the interpretation of results from experiments. It will be shown that the method developed in this chapter applies in fact to both deterministic and random forces as well. Before tackling the problem of finding the response of an infinite periodic structure to a harmonic force some theoretical background must be explored. This will be done in the next section.

7.2 WAVE SHAPE - COMPLEX WAVE COMPONENTS

Broadly speaking, to each terminal degree of freedom there correspond a pair of free waves, one directed to the positive and another directed to the negative direction. Of course all of these waves, or some of them, can be attenuating, depending on the particular frequency considered. In any case the spatial distribution of the deflections along one bay can be expressed as a linear combination of functions $e^{\lambda j y}$ where the λj are the eigenvalues of the state matrix. For simplicity (but without sacrificing the generality of language) a flat structure will be considered as a way of introduction. Equations (4.2.4) can thus be written:

$$
\begin{aligned}
w_r(y) &= \sum_j C_j\, e^{\lambda j y} \\
\theta_r(y) &= \sum_j \lambda_j\, C_j\, e^{\lambda j y} \\
M_r(y) &= -D \sum_j C_j(\lambda_j{}^2 - \varsigma_r{}^2 \nu)\, e^{\lambda j y} \\
V_r(y) &= -D \sum_j C_j\, \lambda_j \left\{\lambda_j{}^2 - (2-\nu)\varsigma_r^2\right\}\, e^{\lambda j y}
\end{aligned}
\qquad ..(7.2.1)
$$

where C_j are complex constants.

Equations (7.2.1) can be written in matrix form as shown in expression (7.2.2):

$$
\{z(y)\}_r = [F]_r \left[e^{\lambda j y}\right]_r \{C\}_r \qquad ..(7.2.2)
$$

where

$$
\{C\}_r = \left\lfloor C_1, C_2, C_3, C_4 \right\rfloor^T ; \quad \{z(y)\}_r = \left\lfloor w_r(y), \theta_r(y), M_r(y), V_r(y) \right\rfloor^T
$$

and

$$[F]_r = \begin{bmatrix} 1 & 1 & 1 & 1 \\ \lambda_1 & \lambda_2 & \lambda_3 & \lambda_4 \\ -D(\lambda_1^2-\zeta_r^2\nu) & -D(\lambda_2^2-\zeta_r^2\nu) & -D(\lambda_3^2-\zeta_r^2\nu) & -D(\lambda_4^2-\zeta_r^2\nu) \\ -D(\lambda_1^2-(2-\nu)\zeta_r^2)\lambda_1 & -D(\lambda_2^2-(2-\nu)\zeta_r^2)\lambda_2 & -D(\lambda_3^2-(2-\nu)\zeta_r^2)\lambda_3 & -D(\lambda_4^2-(2-\nu)\zeta_r^2)\lambda_4 \end{bmatrix}$$

For the particular case of $y = 0$ expression (7.2.2) reads:

$$\{z(0)\}_r = [F]_r \{C\}_r \qquad ..(7.2.3)$$

Equations (7.2.2) and (7.2.3) can be combined on the condition that the inverse of $[F]_r$ exists:

$$\{z(y)\}_r = [F]_r \left[e^{\lambda_j y}\right] [F]_r^{-1} \{z(0)\}_r \qquad ..(7.2.4)$$

Expression (7.2.4) shows clearly that the coefficient of $\{z(0)\}_r$ is precisely the field transfer matrix for a field length y. Therefore one can write:

$$[T_F(y,0)] = [F]_r \left[e^{\lambda_j y}\right] [F]_r^{-1} \{y(0)\}_r \qquad ..(7.2.5)$$

Now, expression (7.2.4) can be thought of as the solution of the state equation $\{z(y)\}' = [A] \{z(y)\}$. Substituting $\{z(y)\}$ in the state equation for the expression (7.2.4) and noting that $\left[\lambda_j e^{\lambda_j y}\right] = \left[\lambda_j\right] \left[e^{\lambda_j y}\right]$ one ends up with the following expression:

$$[F]_r \left[\lambda_j\right] [F]_r^{-1} [F]_r \left[e^{\lambda_j y}\right] [F]_r^{-1} \{z(0)\}_r = [A]_r [F]_r \left[e^{\lambda_j y}\right] [F]_r^{-1} \{z(0)\}_r$$

from which one concludes that

$$[A]_r = [F]_r \left[\lambda_j\right] [F]_r^{-1} \qquad ..(7.2.6)$$

The interesting conclusion that springs up from expression (7.2.6) is that matrix $[F]_r$ is in fact the modal matrix of $[A]_r$, that is, the matrix whose columns are the right eigenvectors of $[A]_r$. In chapter V the matrix of the right eigenvectors of $[A]_r$ was denoted by $[U]_r$ and for uniformity of notation equations (7.2.4) and (7.2.6) are re-written here:

$$\{z(y)\}_r = [T_F(y,0)]_r \{z(0)\}_r \qquad ..(7.2.7)$$

and

$$[T_F(y,0)]_r = [U]_r \left[e^{\lambda_j y}\right] [U]_r^{-1} \qquad ..(7.2.8)$$

Expression (7.2.8) has been considered in chapter V as providing a very convenient method of computing the field transfer matrix.

It is not convenient to invert $[U]_r$ to compute the field transfer matrix. Instead it is preferable to find the modal matrix of the left eigenvector, that is, the matrix whose columns are the eigenvectors of the transpose of $[A]_r$. It is well known from linear algebra that the transpose of the matrix of the left eigenvectors is the inverse of $[U]_r$. In mathematical notation:

$$[V]_r^T = [U]^{-1} \qquad ..(7.2.9)$$

where $[V]_r$ is the matrix of the eigenvectors of $[A]_r^T$, provided the eigenvectors are normalised such that $\{v\}_m^T \{u\}_j = \delta_{mj}$.

Matrix $[V]_r$ can conveniently be computed by using the same subroutine that calculates $[U]_r$ (see appendix C). Now apply the basic principle of free wave propagation in spatially periodical structures by taking $y = \ell$ in expression (7.2.2) and considering expression (7.2.3):

$$[P]_r \{z(\ell)\}_r = [P]_r [U]_r \left[e^{\lambda_j \ell} \right] [U]_r^{-1} [U]_r [C]_r = e^{-i\mu} [U]_r \{C\}_r, \text{ or}$$

$$[P]_r [T_F(\ell,0)] [U]_r \{C\}_r = e^{-i\mu} [U]_r \{C\}_r, \text{ or}$$

$$[U]^{-1} [T] [U] \{C\}_r = e^{-i\mu} \{C\}_r \qquad ..(7.2.10)$$

Therefore the complex coefficients appearing in expressions (7.2.1) can be found by solving the eigenvalue problem expressed in (7.2.10). Note that there are 2n eigenvalues, that is, 2n sets of complex coefficients C_j.

One can easily see that since $\{z(0)\} = [U]\{C\}_r$ expression (7.2.10) can be transformed into

$$[T] \{z(0)\} = e^{-i\mu} \{z(0)\} \qquad ..(7.2.11)$$

which is the basic eigenvalue problem dealt with in chapter III.

The relation between $\{C\}_r$ and $\{z(0)\}_r$ is given by (7.2.3) from which one can write:

$$\{C\}_r^m = [U]^{-1} \{z(0)\}^m = [V]^T \{z(0)\}^m, \text{ so that}$$

$$C_j^m = \{v_j\}^T \{z(0)\}^m, \; j, m = 1,2 \ldots 2n \qquad ..(7.2.12)$$

So the quantities appearing in (7.2.1) can be written as functions of the eigenvectors of the period transfer matrix.

Next, represent $[T_F(y,0)]$ as follows:

$$[T_F(y,0)] = \begin{bmatrix} \lfloor t_1^F(y,0) \rfloor \\ \vdots \\ \lfloor t_{2n}^F(y,0) \rfloor \end{bmatrix}$$

so that any component of a state vector $\{z(y)\}_r$ can be written as (see expression (7.2.7)):

$$z_j^m(y) = \lfloor t_j^F(y,0) \rfloor \{z(0)\}^m \qquad ..(7.2.13)$$

The total value of $z_j(y)$ will be:

$$z_j(y) = \sum_m z_j^m(y) = \lfloor t_j^F(y,0) \rfloor (\Sigma\{z(0)\}^m) \qquad ..(7.2.14)$$

More generally a state vector can be written as:

$$\{z(y)\} = [T_F(y,0)] (\sum_m \{z(0)\}^m) , \quad m = 1, 2n \qquad ..(7.2.15)$$

remembering that $\{z(0)\}^m$ are the eigenvectors of the period transfer matrix.

Note that the state vector in expression (7.2.15) is not completely determined because the eigenvectors of the period transfer matrix are only computed within an arbitrary constant. Therefore expression (7.2.15) can be written in another very convenient form for computations:

$$\{z(y)\} = \sum_{m=1}^{2n} \alpha_m \{\psi_m(y)\} \qquad ..(7.2.16)$$

where α_m are arbitrary complex constants and

$$\{\psi_m(y)\} = [T_F(y,0)] \quad \{z(0)\}_m \qquad ..(7.2.17)$$

The vectors $\{\psi_m(y)\}$ shall be called complex wave components.

In the beginning of this section a flat periodic structure was taken as a way of illustration. By following the steps given above it is easy to realise that the theory developed here is indeed very general and not at all restricted to flat structures.

In fact after writing down expression (7.2.2) all the subsequent steps could have been done without referring to any particular kind of structure.

Such expression can also be written by thinking of a more complicated structure. In fact it has been done for a curved shell by using Donnell's equations and the modal matrix $[U]_r$ has been written down but is not included here. In practice it is far more convenient to compute the modal matrix numerically (as explained in appendix C) when the number of terminal degrees of freedom exceeds two. (For two terminal degrees of freedom the method used in chapter IV should be used).

Therefore, as a closing remark, one should say that expression (7.2.2) can be regarded as general and also is the theory developed in this section.

7.3 RESPONSE OF INFINITE AND FINITE PERIODIC STRUCTURES TO CONCENTRATED HARMONIC FORCES

The theoretical background developed in the previous section will be applied here to find the response of spatially periodic infinite structures to concentrated harmonic forces.

In fig. (7.1) an infinite periodic structure is depicted where a harmonic force represented as $f(x,y,t) = \sum_{r=1}^{\infty} f_r(y) \sin \frac{r\pi x}{b} e^{i\Omega t}$ is applied at bay numbered zero.

Starting at the point of application of the force two sets of waves are sent away, one to the right (positive direction) and another to the left (negative direction).

Some or all of these waves might actually be decaying along the structure, depending on the nature of the propagation constants at the frequency Ω. Without loss of generality the response at bay 0 can be represented by expressions (7.3.1 a and b):

$$\{z(y)\}^{+} = \sum_{m=1}^{n} \alpha_m \{\psi_m(y)\} \; ; \quad y \geq \gamma$$

$$\{z(y)\}^{-} = \sum_{m=n+1}^{2n} \alpha_m \{\psi_m(y)\} ; \; y < \gamma \qquad ..(7.3.1\ a,b)$$

In the above set of expressions it was assumed that the propagation constants $\mu_1, \mu_2, \ldots \mu_n$ are associated with waves propagating (or decaying) to the right. The propagation constants $\mu_{n+1}, \mu_{n+2}, \ldots \mu_{2n}$ are in turn related to waves propagating (or attenuating) to the left.

Now the station vectors just left and just right of the point of application of the force are related as shown in expression (7.3.2):

$$\{z(\gamma)\}_r^{+} = \{z(\gamma)\}_r^{-} - \{f\}_r \qquad ..(7.3.2)$$

where $\{f\}_r$ is the applied force vector. For instance, in the case of a flat structure the applied force vector is

$\{f\}_r = \lfloor 0, 0, 0, \underline{f_r} \rfloor^T$, where f_r is the amplitude of the applied harmonic force. For the case of a general time varying force and response an equation similar to (7.3.2) can be written with vectors $\{z(\gamma)\}_r e^{i\Omega t}$ and $\{f\}_r e^{i\Omega t}$ replaced by their Fourier transforms. Consequently the present theory can be applied to both deterministic and random problems [35].

Combining (7.3.1a,b) and (7.3.2) one has:

$$\sum_{m=1}^{\infty} \alpha_m \{\psi_m(\gamma)\} = \sum_{m=n+1}^{2n} \alpha_m \{\psi_m(\gamma)\} - \{f\}_r \text{ , or}$$

$$\left[\{\psi_1(\gamma)\} \ldots \{\psi_n(\gamma)\} - \{\psi_{n+1}(\gamma)\} \ldots -\{\psi_{2n}(\gamma)\}\right] \begin{Bmatrix} \alpha_1 \\ \alpha_2 \\ \vdots \\ \alpha_{2n-1} \\ \alpha_{2n} \end{Bmatrix} = \{f\}_r \quad ..(7.3.3)$$

Expression (7.3.3) represents a system of 2n linear equations that can be solved for the coefficients α_m. It is worth noting that the square matrix appearing in the above expression is nonsingular since the vectors $\{\psi_j(\gamma)\}$ are linearly independent as can be seen by their definition in expression (7.2.17).

Therefore, by solving the system of equations (7.3.3) one is able to find the response within the bay 0. For easier reference expression (7.3.3) shall be written in a more compact form:

$$\left[\Sigma(\gamma)\right] \{\alpha_m\} = -\{f\}_o \quad ..(7.3.3.a)$$

where

$$\begin{Bmatrix} \sigma_{1,K(\gamma)} \\ \sigma_{2,K(\gamma)} \\ \vdots \\ \sigma_{2n,K(\gamma)} \end{Bmatrix} = \begin{cases} \{\psi_K(\gamma)\} & \text{if } 1 \leq K \leq n \\ -\{\psi_K(\gamma)\} & \text{if } n+1 \leq K \leq 2n \end{cases} \quad -.(7.3.4)$$

Now, the station vector at any point of the structure can be partitioned as shown, for instance, in expression (3.2.1), that is, in generalised displacement and generalised forces. The generalised displacement does not change when 'transferred' across a support (compatibility condition), so that one can write:

$$\{q(\ell)\}_0 = \{q(0)\}_1$$

where the subscripts 0 and 1 stand for bay 0 and bay 1.

It is convenient to remember that

$$q_j(y) = z_j(y) \; ; \qquad j = 1, n.$$

With the above considerations made it is possible to write:

$$\{q(\ell)\}_0 = \{q(0)\}_1 = \sum_{m=1}^{n} \alpha_m \begin{Bmatrix} \sigma_{1,m}(0) \\ \sigma_{2,m}(0) \\ \\ \sigma_{n,m}(0) \end{Bmatrix} \qquad ..(7.3.5)$$

In general for the bay numbered N one has:

$$\{q(y)\}_N = \sum_{m=1}^{n} \alpha_m \begin{Bmatrix} \sigma_{1,m}(y) \\ \sigma_{2,m}(y) \\ \\ \sigma_{n,m}(y) \end{Bmatrix} \cdot e^{-i(N-1)\mu_m} \qquad ..(7.3.6)$$

One should note that expression (7.3.5) represents a set of linear equations that can be solved for α_m, that is:

$$\begin{bmatrix} \sigma_{1,m}(0) \\ \sigma_{2,m}(0) \\ \cdot \\ \cdot \\ \cdot \\ \sigma_{n,m}(0) \end{bmatrix} \begin{Bmatrix} \alpha_1 \\ \alpha_2 \\ \\ \\ \alpha_n \end{Bmatrix} = \begin{Bmatrix} q(\ell) \\ \\ \\ \\ \\ \end{Bmatrix}_0 \qquad ..(7.3.5a)$$

Note that $\{q(\ell)\}_0$ is computed by using (7.3.1a).

In expression (7.3.6) y is a local variable varying between 0 and ℓ and $\{q(y)\}_N$ means the general co-ordinates within bay number N.

Having solved equations (7.3.5a) the complete state vector at bay N can be computed by using (7.3.7):

$$\{z(y)\}_N = \sum_{m=1}^{n} \alpha_m \begin{Bmatrix} \sigma_{1,m}(y) \\ \sigma_{2,m}(y) \\ \cdot \\ \cdot \\ \cdot \\ \sigma_{2n,m}(y) \end{Bmatrix} e^{-i(n-1)\mu_m} \qquad ..(7.3.7)$$

Obviously what was explained above for a bay on the right of bay numbered zero (this will be called a positive bay) can be applied 'mutatis mutandis' to a bay on the left (negative bay) of bay zero. Therefore the above theory gives the response at any point of a spatially periodic infinite structure. The main role in this theory is played by the complex wave components defined in expression (7.2.17). Since the system has been considered linear the response to several concentrated harmonic forces can, obviously, be obtained by superposition.

7.4 RESPONSE OF FINITE SPATIALLY PERIODIC STRUCTURES TO CONCENTRATED HARMONIC FORCES

Section 7.3 has dealt with the response of infinite periodic structures

to harmonic concentrated forces.

The response of a finite periodic structure can be obtained by taking the response of the structure as if it was infinite and adding the effects of the boundaries. The effects of the boundaries are the reflections of the free waves at the corresponding frequency. In mathematical form the response can be described as (see fig. 7.2):

$$\{z(y)\}_j = \{z(y)\}_{j\infty} + \sum_{m=1}^{2n} \alpha_m \{\psi_m(y)\}\, e^{-(j+M)\mu_m} \qquad ..(7.4.1)$$

where j is the number of the bay where the response is computed. The application of expression (7.4.1) to the boundaries gives a system of 2n linear equations from which α_m are computed.

As a way of illustration a stringer stiffened plate (fig. 7.2) will be considered. Shear force and bending moment at the ends of the structure are zero.

For the right hand side of the first and last stringers one can write:

$$\begin{Bmatrix} z_1(0) \\ \\ z_2(0) \end{Bmatrix}_{-M} = \begin{Bmatrix} z_{\infty 1}(0) \\ \\ z_{\infty 2}(0) \end{Bmatrix}_{-M} + \sum_{m=1}^{2n} \alpha_m \begin{Bmatrix} \psi_{1,m}(0) \\ \\ \psi_{2,m}(0) \end{Bmatrix}$$

$$\begin{Bmatrix} 0 \\ \\ 0 \end{Bmatrix} = \begin{Bmatrix} z_{\infty 3}(0) \\ \\ z_{\infty 4}(0) \end{Bmatrix}_{N+M+2} + \sum_{m=1}^{2n} \alpha_m \begin{Bmatrix} \psi_{3,m}(0) \\ \\ \psi_{4,m}(0) \end{Bmatrix} \cdot e^{-(N+M+1)\mu_m} \qquad ..(7.4.2a,b)$$

The slight modification of subscript notations introduced in (7.4.2) is self-explanatory.

The state vector at the right of the first stringer can be written as:

$$\begin{Bmatrix} z_1(0) \\ z_2(0) \\ z_3(0) \\ z_4(0) \end{Bmatrix}_{-M} = \begin{bmatrix} 1 & 0 & 0 & 0 \\ 0 & 1 & 0 & 0 \\ K_{w\theta} & K_{\theta} & 1 & 0 \\ K_w & -K_{w\theta} & 0 & 1 \end{bmatrix} \begin{Bmatrix} z_1(0) \\ z_2(0) \\ 0 \\ 0 \end{Bmatrix}_{-(M+1)}$$

from which

$$\begin{Bmatrix} z_3(0) \\ z_4(0) \end{Bmatrix}_{-M} = \begin{bmatrix} K_{w\theta} & K_{\theta} \\ K_w & -K_{w\theta} \end{bmatrix} \begin{Bmatrix} z_1(0) \\ z_2(0) \end{Bmatrix}_{-M} \qquad ..(7.4.3)$$

But

$$\begin{Bmatrix} z_3(0) \\ z_4(0) \end{Bmatrix}_{-M} = \begin{Bmatrix} z_{\infty,3}(0) \\ z_{\infty,4}(0) \end{Bmatrix}_{-M} + \sum_{m=1}^{2m} \alpha_m \begin{Bmatrix} \psi_{3,m}(0) \\ \psi_{4,m}(0) \end{Bmatrix} \qquad ..(7.4.4)$$

Substitutions of (7.4.2a) and (7.4.4) in (7.4.3) and using (7.4.2b) lead to a system of four linear equations from which the coefficients can be found, that is

$$
\begin{bmatrix}
\lfloor K_{\theta w}\psi_{1,m}(0) + K_{\theta}\psi_{2,m}(0) - \psi_{3,m}(0)\rfloor \\
\lfloor K_{w}\psi_{1,m}(0) - K_{\theta w}\psi_{2,m}(0) - \psi_{4,m}(0)\rfloor \\
\lfloor \psi_{3,m}(0)\, e^{-i(N+M+1)\mu_m}\rfloor \\
\lfloor \psi_{4,m}(0)\, e^{-i(N+M+1)\mu_m}\rfloor
\end{bmatrix}
\begin{Bmatrix} \alpha_1 \\ \alpha_2 \\ \alpha_3 \\ \alpha_4 \end{Bmatrix}
=
\begin{Bmatrix}
\begin{Bmatrix} z_{\infty,3}(0) \\ z_{\infty,4}(0) \end{Bmatrix}_{-M}
-
\begin{bmatrix} K_{w\theta} & K_{\theta} \\ K_{w} & -K_{w\theta} \end{bmatrix}
\begin{Bmatrix} z_{\infty,1}(0) \\ z_{\infty,2}(0) \end{Bmatrix}_{-M} \\
-
\begin{Bmatrix} z_{\infty,3}(0) \\ z_{\infty,4}(0) \end{Bmatrix}_{(N+M+2)}
\end{Bmatrix}
$$

..(7.4.5)

Having determined the coefficients α_m the response can be found by taking them to (7.4.1).

The steps given in this section can be repeated for other kinds of boundary conditions as well as for more advanced structures.

The knowledge of the complex wave components permits the computation of the response of periodic structures in many other cases. For instance, a semi-infinite or finite periodic structure with base (ground) excited motion can easily be dealt with.

7.5 NUMERICAL RESULTS

In this section some computer results for stringer-stiffened plates and shells will be presented and commented on.

A harmonic force of unit amplitude is applied at a point of a bay and the response is either plotted along the structure (for a certain value of the frequency) or plotted at a single point for a suitable range of frequencies (frequency response plot).

When plotting the response along the length of the structure a non-dimensional co-ordinate is defined such that:

$$s = (j + 1)y/\ell \quad , \qquad j = 0, 1, 2 \ldots.$$

$$s = jy/\ell \quad , \qquad j = -1, -2 \ldots.$$

where j numbers the bay where s lies.

In this section both finite and infinite structures are considered and the results commented on. The stringer-stiffened plate considered here is the same as called Example I in chapter IV and the stringer-stiffened shell is the same as that appearing in chapter VI.

7.5.1 Stringer-stiffened plate

As a first example an infinite stringer-stiffened flat plate is taken and a harmonic force of unit amplitude is applied in the middle of a bay.

Fig. 7.3 and 7.4 show the amplitude response of the displacement and moment of an undamped infinite stringer-stiffened plate for two values of the non-dimensional frequency. Curve 1 is for $\Omega_0^* = 18.175$, a propagating frequency, and curve 2 is for $\Omega_0^* = 0.10$ which is an attenuating frequency.

The response is plotted only at bays 0, 1, 2, 3 and 4. There is no need to plot the response at the left of bay 2 because of the symmetry of the structure and load. The displacement and moment are made non-dimensional by multiplying them by 1/h and h/D, respectively. It can be seen that for the propagating frequency (18.175) the moment has its peaks at the stringers but the displacement amplitude is greater in the middle of a bay. The response at the frequency 0.10 resembles that of a beam on an elastic foundation acted upon by a static force |36|.

Figs. 7.5 and 7.6 show the amplitude response along the structure at the frequencies $\Omega_0^* = 49.363$ (a propagating frequency) and $\Omega_0^* = 34.10$ (an attenuating frequency). Frequency 49.363 falls within the second propagation band and frequency 34.10 lies inbetween the first and the second propagation bands.

One can see that the response at these high frequencies tends to be very small if compared with the response, say, for frequencies belonging to the first propagation band (figs. 7.3 and 7.4). What was said above refers to an infinite non-damped stringer-stiffened flat plate (Example I in chapter IV).

Figs. 7.7 and 7.8 show the response of the same structure but with some damping ($\eta = 0.15$) in the skin for the frequency 18.175.

The main effect of this amount of damping is to introduce an amplitude

decay along the structure (note that 18.175 is a propagating frequency for $\eta = 0.0$). The decay is due to the fact that damping makes the imaginary part of μ_1 (zero for $\eta = 0.0$) different to zero.

The reduction in the amplitude level in the first bay is very small indeed. Notice that the peak value of the non-dimensional moment for the non-damped structure is 2.448×10^{-3} while for the damped structure it is 2.213×10^{-3}.

Computations for the same structure excited at the same frequency (18.175) with a damping level of $\eta = 0.25$ shows that the maximum moment is 1.793×10^{-3}. When damping is increased from 0.15 to 0.25 the reduction in the maximum moment amplitude is about 22% and in the maximum displacement about 27%.

To have an idea of the effectiveness of damping in reducing the response level one could think that for the same increase in damping (0.15 to 0.25) a single degree of freedom system would have its amplitude of vibration level reduced by about 65%. But damping in the stiffened plat structure is extremely important when the exciting frequency coincides with one of the lower or higher limits of a propagation band. In these particular cases the steady state amplitudes of the response would be theoretically infinite if no damping was present in the structure.

The results shown so far refer to an infinite stringer-stiffened plate.

In figures 7.9 and 7.10 one can see the amplitude response for a finite stringer-stiffened plate with seven bays and with the force applied at the middle of the structure. The response is plotted for four bays, that is bays 0, 1, 2, 3 and 4 (see fig. 7.2). The skin is only supported by a stringer at the ends of the structure. Damping is zero.

The frequencies of exictation are 18.175 and 0.10 as in figs. 7.3 and 7.4.

The response of the finite and infinite structures are virtually the same for $\Omega_o^* = 0.10$. This is expected for this is a heavily attenuating frequency, which means that there is almost no reflection at the boundaries.

Now, the response at 18.175 is radically different from that of the infinite structure. This again is expected because this is a propagating frequency and there is full reflection at the end supports (stringers).

Since damping causes the amplitude of the propagating waves to decay along the structure (and, consequently, decrease the effect of the reflections at the boundaries) one should expect that above a certain amount of damping the responses of the infinite and finite structures (with many bays) will be almost equal.

This is in fact true as figs. 7.11 and 7.12 clearly demonstrate. These figures show the response of the above described finite structure with some damping ($\eta = 0.15$) in the skin and for the frequency 18.175. Comparison between these two figures with figs. 7.7 and 7.8 show how close these results for finite and infinite structures are.

It is also interesting to notice the dramatic change in the distribution along the structure of the amplitude response when some damping is added to the finite structure (compare figs. 7.9 and 7.10 with 7.11 and 7.12, respectively).

The computation of the response of the infinite stringer-stiffened structure took 17 seconds at the ICL 1907 computer. The same computations performed for a finite structure took 35 seconds. In both cases the response was computed at a hundred points in each bay and for two different frequencies.

One could safely say that the method developed in this chapter is very efficient both in time and in storage (29k for finite and 14k for

infinite structure).

So, an infinite periodic structure can represent with advantage (from the computational point of view) a finite one, provided it has many bays away from the excitation point and a moderately high amount of damping. Therefore, considering that these assumptions hold, it is more convenient (from the computational point of view) to compute frequency response curves for the infinite structure and assume that they are representative of a finite one, no matter what sort of boundary conditions there are at the ends.

Figs. 7.13 and 7.14 show frequency response plots for non-dimensional displacement and moment for an infinite stringer-stiffened plate with $\eta = 0.25$. It is shown in these graphs that deflection and moment have a peak at around $\Omega_0^* = 17.222$, that is the lower limit of the first propagation band. If the structure had no damping the steady state response at 17.222 would be theoretically infinite, as was stated before.

7.5.2 Stringer-stiffened shell

The results to be shown here are restricted to infinite stringer-stiffened shells. This decision was taken because, as it happened for plates, one should expect that above certain levels of damping and with the force applied sufficiently away from the boundaries a finite shell structure would produce a response very close to that of the infinite structure.

For cases where damping is not sufficiently high or the force is too close to one of the extreme bays the infinite model no longer can represent the finite one and the theory developed in this chapter for finite periodic structures must be applied. Most of what was said for flat plate structures could now be repeated in connection with stiffened cylindrical shells.

Figures 7.15 and 7.16 show the amplitude response of the undamped stringer-stiffened shell for the frequencies $\Omega_o^* = 22.10$ (falling within the first propagation band) and 0.65 (an attenuating frequency). Amplitude response along the structure when the shell is damped has also been obtained but is not shown here. In fact there is nothing dramatically new in these curves in relation to those obtained for the flat structure except that amplitude of displacement and moment are comparatively smaller, which is expected. Figs. 7.17 and 7.18 are the counterparts of figs. 7.13 and 7.14. They represent amplitude response of the cylindrical shell at the middle of a bay to the harmonic force applied at the same point. The peak response occurs very close to the non-dimensional frequency 20.72 which in turn is very close to the lower limit of the first passing band.

CHAPTER VIII

RESPONSE OF PERIODIC STRUCTURES TO CONVECTED PRESSURE FIELDS

8.1 GENERAL

This chapter sets out to establish a general wave theory to compute the response of spatially periodic structures to a convected harmonic pressure field. The knowledge of the frequency response of the structure to such fields is basic to find the response to more complex ones, such as convected random acoustic fields and boundary layer fluctuations.

The power spectral density function of the response to a random pressure field can be computed when the power spectral density of the exciting field and the frequency response functions are known |42|, |11|, |34|.

This chapter will be concerned only with the computation of the frequency response function, that is, the response of the periodic structure to a convected simple harmonic pressure field of unit amplitude.

The method to be developed here can be considered as a generalisation of that presented by Mead |37|.

8.2 RESPONSE OF AN INFINITE PERIODIC STRUCTURE TO A CONVECTED HARMONIC PRESSURE FIELD

Assume an infinite periodic structure excited by convected harmonic pressure field of the form:

$$p(x,y,t) = \sum_{r=1}^{\infty} (p_{or} \sin \frac{r\pi x}{b}) e^{i(\Omega t - ky)} \qquad ..(8.2.1)$$

where k is the wave number.

The phase velocity of the convecting pressure field is $CV = \Omega/k$, and this is identical in this case with the convection velocity of the pressure field. This convected pressure field exerts pressures of equal magnitude at all points of the structure but with a phase difference of -ky between two points distant y apart.

The state equation can be written as

$$\{z(y)\}'_r = [A]_r \{z(y)\} - \{p_{or}\} e^{-iky} \qquad ..(8.2.2)$$

The forcing vector appearing in (8.2.2) will have different forms, depending on the circumstances. For instance for the stringer-stiffened plate considered in chapter IV $\{p_{or}\}$ will be

$$\{p_{or}\} = \begin{Bmatrix} 0 \\ 0 \\ 0 \\ p_{or} \end{Bmatrix}$$

and for the shell structure

$$\{p_{or}\} = \lfloor 0 \quad 0 \quad 0 \quad 0 \quad 0 \quad p_{or} \quad 0 \quad 0 \rfloor^T$$

To solve equation (8.2.2) assume a solution as given by expression (8.2.3):

$$\{z(y)\} = [U] \{\varsigma(y)\} \qquad ..(8.2.3)$$

where $[U]$ is the modal matrix of $[A]$.

The subscript r has been dropped from expression (8.2.3). Taking expression (8.2.3) into equation (8.2.2) and pre-multiplying both members by $[U]^{-1}$ the result is

$$\{z(y)\}' = [U]^{-1}[A]\,[U]\,\{\zeta(y)\} - \{\theta\}\; e^{-iky}$$

where

$$\{\theta\} = [U]^{-1}\{p_o\}.$$

Noting that $[U]^{-1}[A]\,[U] = \left[\lambda_j\right]$ the above expression is transformed into equation (8.2.4):

$$\{z(y)\}' = \left[\lambda_j\right]\{\zeta(y)\} - \{\theta\}\, e^{-iky} \qquad ..(8.2.4)$$

Expression (8.2.4) represents a set of 2n ordinary differential equations of the form:

$$\zeta'_j(y) = \lambda_j \zeta_j(y) - \theta_j\, e^{-iky}, \qquad j = 1, 2n \qquad ..(8.2.5)$$

It is very easy to solve the equations (8.2.5) |38| and their solutions are:

$$\zeta_j(y) = \theta_j \frac{e^{-iky}}{\lambda_j + ik} + C_j\, e^{\lambda_j y}, \qquad \lambda_j \neq ik \qquad ..(8.2.6)$$

where C_j is an arbitrary constant.

Expressions (8.2.6) can now be rearranged in matrix form:

$$\{\zeta(y)\} = e^{-iky}\left[\frac{1}{\lambda_j + ik}\right]\{\theta\} + \left[e^{\lambda_j y}\right]\{C\}, \qquad \lambda_j \neq ik \qquad ..(8.2.7)$$

When expression (8.2.7) is taken into (8.2.3) and it is noticed that

$$[U]\left[\frac{1}{\lambda_j + ik}\right][U]^{-1} = \left[[U]\left[\lambda_j\right][U]^{-1} + [U]\left[ik\right][U]^{-1}\right]^{-1}$$

$$= \left[[A] + ik\,[I]\right]^{-1} = [\chi]^{-1},$$

the final solution to equation (8.2.2) is

$$\{z(y)\} = e^{-iky}\,[\chi]^{-1}\{p_o\} + \left[T_F(y,0)\right]\{C_u\} \qquad ..(8.2.8)$$

where $\{C_u\} = [U]\{C\}$ and $[\chi] = [A] + ik[I]$. Notice that $\{C_u\}$ is an arbitrary constant vector. This vector can be found by noticing that the phase difference of the response at two different points of the structure separated by the periodic length is equal to the phase difference of the exciting pressure field at the same points. When this property is applied for the extremes of a period of the structure the following expression applies:

$$[P]\{z(\ell)\} = e^{ik\ell}\{z(0)\} \qquad ..(8.2.9)$$

By making use of expressions (8.2.8) and (8.2.9) the following system of linear equations is found:

$$\left[[P]\,[T_F(\ell,0)] - e^{-ik\ell}[I]\right]\{C_u\} = -e^{-ik\ell}\left[[P] - [I]\right][\chi]^{-1}\{p_o\}$$

..(8.2.10)

Alternatively expression (8.2.10) can be written:

$$\left[[P]\,[T_F(\ell,0)] - e^{-ik\ell}[I]\right]\{z(0)\} = [P]\left[[T_F(\ell,0)] - e^{-ik\ell}[I]\right][\chi]^{-1}\{p_o\}$$

..(8.2.11)

Solving the system of equations (8.2.10) for the vector $\{C_u\}$ and taking this vector into expression (8.2.8) the response is found.

Instead of inverting the matrix $[\chi]$ it is more convenient to follow the procedure below:

Call $\{z_p\} = [\chi]^{-1} \{p_o\}$ so that

$$[\chi] \{z_p\} = \{p_o\} \qquad ..(8.2.12)$$

It is enough now to solve system (8.2.12) and take $\{z_p\}$ into equation (8.2.10) or (8.2.11).

When the response $\{z(y)\}$ is computed for a certain range of frequencies for $p_o = 1$ the result is the frequency response function for that same range of frequencies.

Since the frequency response function is a function of both frequency and convection velocity a more adequate notation will be adopted, that is:

$$\{H(\Omega_o^*, CV)\} = e^{-iky} [\chi]^{-1} \{p_o\} + \left[T_F(y,0)\right] \{C_u\} \qquad ..(8.2.13)$$

When the frequency response is known the power spectral density of the random response $\{S_Z(\Omega)\}$ is related to the power spectral density of the excitation by

$$\{S_Z(\Omega_o^*)\} = \left\{ \left| H(\Omega_o^*, CV) \right|^2 \right\} S_p(\Omega_o^*) \qquad ..(8.2.14)$$

The non-dimensional mean-square response is given by

$$\left\langle \left\{ z^2(t) \right\} \right\rangle = \int_0^{\Omega_o^{*\,max}} \left\{ S_Z(\Omega_o^*) \right\} d\Omega_o^* \qquad ..(8.2.15)$$

Expression (8.2.14) applies only for pressure fields with a frozen wave-form with only one convection velocity. Such excitation does occur, for instance, in the far field of a jet noise.

When the pressure field is not frozen as it occurs in the near field of a jet noise it has a spectrum of wave number components at each frequency and can be represented by the wave number/frequency spectrum $S_p(\Omega_o^*,k)$ |11|, |39|. In these cases the response spectrum at any frequency can be obtained by integrating the wave number/ frequency spectrum over all wave numbers:

$$\{S_Z(\Omega_o^*)\} = \int_{-\infty}^{+\infty} \left\{ \left| H(\Omega_o^*,k,CV) \right| \right\} \quad S_p(\Omega_o^*,k)\, dk \qquad ..(8.2.16)$$

Looking back now at expressions (8.2.7) and (8.2.10) (8.2.11) it can be seen that large responses are expected when one (or both, simultaneously) of two things occurs:

First, when $\lambda_j = ik$, for some λ_j. This is the normal coincidence phenomenon of the unsupported structure combined with the harmonic pressure field.

Second, when $k\ell$ is equal to one of the propagation constants of the structure. In this case the square matrix appearing in the left hand side of (8.2.10) (8.2.11) becomes singular. This means that, at that particular frequency, the phase difference $k\ell$ between pressure distance ℓ apart is equal to the phase difference μ_o between free wave motion at points ℓ apart. The convection velocity of the harmonic pressure field is then equal to the phase velocity of one of the free wave components.

This second coincidence pheonomenon can occur at much lower frequency than the ordinary coincidence phenomenon ($\lambda_j = -ik$).

8.3 RESPONSE OF FINITE PERIODIC STRUCTURES TO A CONVECTED HARMONIC PRESSURE FIELD

The response of finite periodic structures to a convected harmonic pressure field can be computed by following the same approach as used in chapter VII, that is, it consists of the response of the infinite structure plus the effects of the boundaries. These effects are the free waves due to the reflections at the boundaries.

In mathematical form (see fig. 8.1):

$$\{z(y)\}_j = \{z_\infty(y)\}_j + \sum_{k=1}^{2n} \alpha_k \{\psi_k(y)\} e^{-(j-1)\mu_k} \qquad ..(8.3.1)$$

In this section a finite structure with one of the periodic supports at each end will be considered as a way of illustration. It will become clear, nevertheless, that the derivation to be shown below could have been carried out for any other boundary conditions.

Consider an N bay finite periodic structure (see fig. 8.1). The particulars of this structure (apart from being periodic with N bays and with a support at each end) are not relevant to the following derivations.

For $j = 1$ and $y = 0$ (that is, at the right hand side of the first support) eq. (8.3.1) becomes:

$$\{z(0)\}_1 = \{z_\infty(0)\}_1 + \sum_{k=1}^{2n} \alpha_k \{\psi_k(0)\} \qquad ..(8.3.2)$$

At the right hand side of the N^{th} bay (left hand side of the imaginary $(N+1)^{th}$ bay) one has:

$$\{z(0)\}_{N+1} = \{z_\infty(0)\}_{N+1} + \sum_{k=1}^{2n} \alpha_k \{\psi_k(0)\} e^{-iN\mu_k} \qquad ..(8.3.3)$$

Note that

$$\{z(0)\}_1 = [P]\,\{z(\ell)\}_0 \qquad ..(8.3.4)$$

where $[P]$ is the point transfer matrix.

The generalised forces at the left of the first support and at the right of the last one are zero. These conditions when applied to expressions (8.3.2), (8.3.3) and (8.3.4) lead to a system of 2n linear equations for which the constants α_k are found. In the following two sub-sections two cases will be considered, a stringer-stiffened plate and a stringer-stiffened shell.

8.3.1 Finite stringer-stiffened plate

Equation (8.3.3) gives:

$$\begin{Bmatrix} 0 \\ 0 \end{Bmatrix} = \begin{Bmatrix} M_\infty(0) \\ M_\infty(0)_{N+1} \end{Bmatrix} + \sum_{k=1}^{4} \alpha_k \begin{Bmatrix} \psi_{3,k}(0) \\ \psi_{4,k}(0) \end{Bmatrix} e^{-iN\mu_k} \qquad ..(8.3.5)$$

From (8.3.4) one can take:

$$\begin{Bmatrix} M \\ V \end{Bmatrix}_1 = \begin{bmatrix} K_{w\theta} & K_\theta \\ K_w & -K_{w\theta} \end{bmatrix} \begin{Bmatrix} w \\ \theta \end{Bmatrix}_1 \qquad ..(8.3.6)$$

and from (8.3.2):

$$\begin{Bmatrix} w \\ \theta \end{Bmatrix}_1 = \begin{Bmatrix} w_\infty(0) \\ \theta_\infty(0) \end{Bmatrix}_1 + \sum_{k=1}^{4} \alpha_k \begin{Bmatrix} \psi_{1,k}(0) \\ \psi_{2,k}(0) \end{Bmatrix}$$

$$\begin{Bmatrix} M \\ V \end{Bmatrix}_1 = \begin{Bmatrix} M_\infty(0) \\ V_\infty(0) \end{Bmatrix}_1 + \sum_{k=1}^{4} \alpha_k \begin{Bmatrix} \psi_{3,k}(0) \\ \psi_{4,k}(0) \end{Bmatrix} \qquad ..(8.3.7a,b)$$

Combining equations (8.3.5) and (8.3.7a,b) the result is:

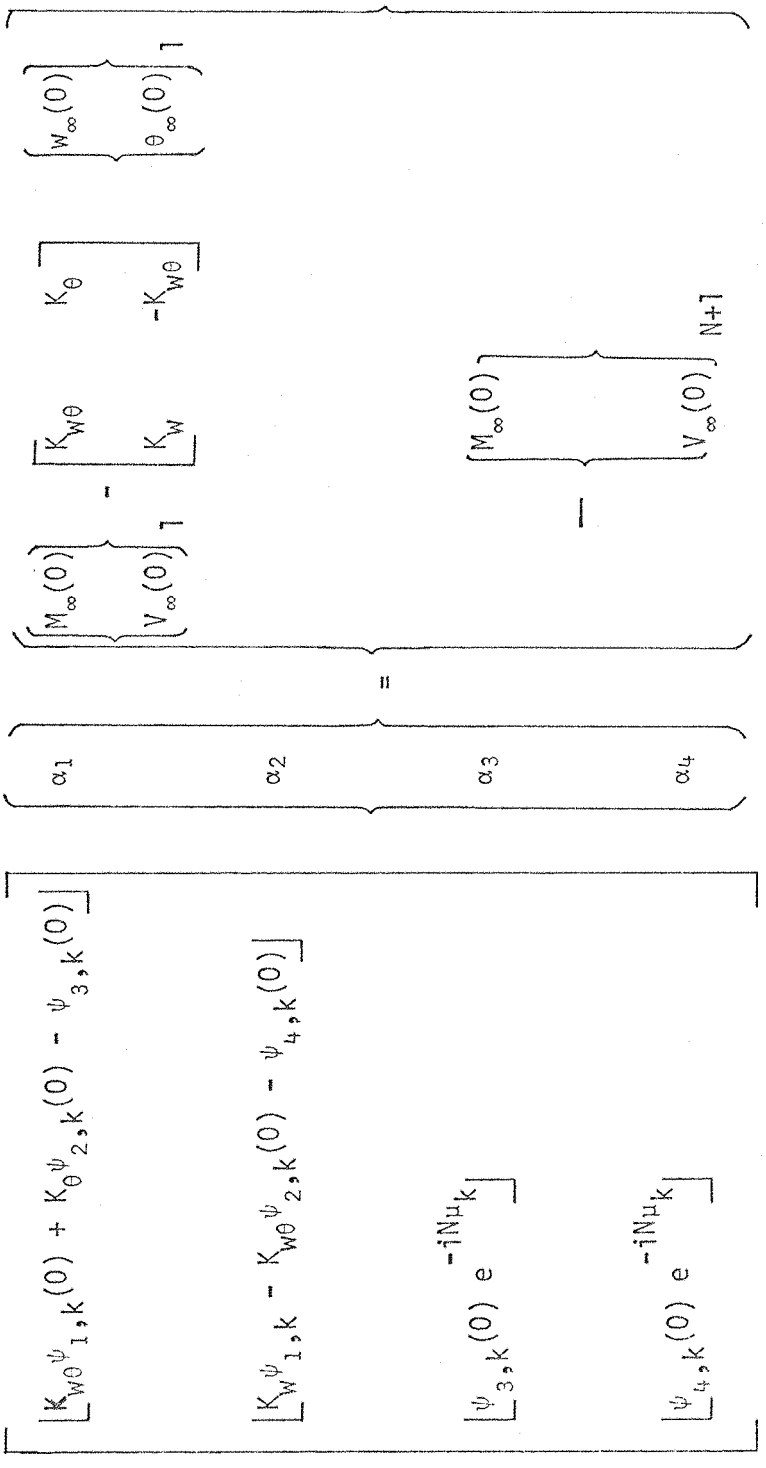

$$\therefore \quad (8.3.8)$$

Expression (8.3.8) is a system of four equations in the unknowns α_1, α_2, α_3, α_4.

Solving this system and taking the α coefficients to expression (8.3.1) the response of the stringer-stiffened structure to the convected harmonic pressure field is found.

8.3.2 Finite stringer-stiffened shell

A system of equations similar to (8.3.8) can be found for the shell case. The steps are the same given in the previous sub-section and will be omitted here.

The system of equations for the shell structure is:

$$
\begin{bmatrix}
\left[K_{\theta v}\psi_{2,k}(0) + K_{\theta w}\psi_{3,k}(0) + K_{\theta}\psi_{4,k}(0) - \psi_{5,k}(0)\right] \\
\left[K_{wv}\psi_{2,k}(0) + K_{w}\psi_{3,k}(0) - K_{w\theta}\psi_{4,k}(0) - \psi_{6,k}(0)\right] \\
\left[K_{v}\psi_{2,k}(0) + K_{vw}\psi_{3,k}(0) + K_{0v}\psi_{4,k}(0) - \psi_{7,k}(0)\right] \\
\left[-\psi_{8,k}(0)\right] \\
\left[\psi_{5,k}(0)\, e^{-iN\mu k}\right] \\
\left[\psi_{6,k}(0)\, e^{-iN\mu k}\right] \\
\left[\psi_{7,k}(0)\, e^{-iN\mu k}\right] \\
\left[\psi_{8,k}(0)\, e^{-iN\mu k}\right]
\end{bmatrix}
\begin{Bmatrix} \alpha_1 \\ \alpha_2 \\ \alpha_3 \\ \alpha_4 \\ \alpha_5 \\ \alpha_6 \\ \alpha_7 \\ \alpha_8 \end{Bmatrix}
=
\left\{
\begin{Bmatrix} M_\infty(0) \\ V_\infty(0) \\ N_\infty(0) \\ T_\infty(0) \end{Bmatrix}_1
\begin{bmatrix} K_{\theta v} & K_{\theta w} & K_{\theta} \\ K_{wv} & K_{w} & -K_{\theta w} \\ K_{v} & -K_{wv} & K_{\theta v} \\ 0 & 0 & 0 \end{bmatrix}
\begin{Bmatrix} v_\infty(0) \\ w_\infty(0) \\ \theta_\infty(0) \end{Bmatrix}_1
-
\begin{Bmatrix} M_\infty(0) \\ V_\infty(0) \\ N_\infty(0) \\ T_\infty(0) \end{Bmatrix}_{N+1}
\right\}
$$

In chapter VII it was seen that above a certain moderate amount of damping the response of the infinite and finite structures are practically equal, provided the force is sufficiently far from the extreme bays. In these circumstances the infinite periodic structure model is a good representation of the finite one (no matter the kind of boundaries) and indeed more convenient for computations.

When a finite periodic structure is being excited by a convected harmonic pressure field the picture of the excitation 'sufficiently far away' from the extremes cannot exist. Nevertheless, the infinite model can still be a good representation of the finite one, as has been shown by Mead |37|. In his paper Mead compares the greatest rms response (see expression 8.2.15) in any one bay centre of a five bays beam with that of the infinite beam.

The beams were damped with $\eta = 0.25$ and they rested on simple supports with torsional elastic constraint. The exciting field was a convected random noise of constant power spectral density.

Mead found that the rms curve for the infinite beam was very close to the curve of maximum rms in any bay centre of the finite beam.

When the mean square responses at the five bay centres were averaged and plotted against the convected velocities the resulting curve was extremely close to that of the infinite beam. This comparison has been repeated for many other values of damping with the same conclusion.

Since this sort of average is often enough for design Mead concluded that the infinite structure is a good representation of the finite one.

In this chapter results for infinite stringer-stiffened plates and shells are presented and discussed.

8.4 NUMERICAL RESULTS

As was stated in the last section only results concerning infinite structures will be presented here.

More specifically, two kinds of structures will be considered : an infinite stringer-stiffened plate (Example I in chapter IV) and an infinite stringer-stiffened shell (the same dealt with in chapters VI and VII) with a pressure field convected around the circumference.

A stringer-stiffened cylindrical shell is not, of course, infinite in the circumferential directions. However, the assumption that it is infinite can be justified provided there is enough damping, or wave attenuations, present to cause a wave generated at one point to be negligible by the time it has travelled completely around the circumference back to its starting point.

Also, the concept of a random pressure field convecting around a circular stringer-stiffened shell, with a uniform amplitude and convection velocity, is idealistic. In practice, a real noise field would approximate to this only over a limited segment of the shell structure. If the structure damping (or wave attenuation) is large enough the response of the segment will depend mainly on the pressure field over that segment. This will be the same (or nearly so) as the response of an 'infinite' shell to a uniform pressure field of uniform convection velocity over an infinite shell structure.

8.4.1 Stringer-stiffened plate

Figures 8.2 and 8.3 show the displacement and moment amplitude frequency response for the stringer-stiffened plate at the middle of a bay. The peaks of these curves represent coincidence effects. Note, for instance, that CV = 5.842 in the primary free wave velocity of the structure corresponding to the frequency $\Omega_0^* = 17.222$ ($\mu_0 = \pi$) (see fig. 4.12).

In other words, the phase difference of the pressure field between two points ℓ apart is equal to the phase difference of the primary free wave between the same points. This situation represents a sort of coincidence that tends to make the structure respond strangely. If the structure had no damping the response would be infinite (theoretically). The other pair of convection velocity/frequency for which peaks occur in the other curves also represents coincidence (see fig. 4.12). For instance CV = 8.265 is the speed of a free travelling wave component with the frequency of 18.175. Therefore, if a harmonic pressure field has a convection velocity of 8.265 and a frequency of 18.175 coincidence will occur.

Also if a random pressure field is convected along the structure with a convected speed of 5.842 the response spectrum will have a peak at the frequency 17.222.

Figures 8.4 and 8.5 show the amplitude response at the right hand side of a stringer ($\varsigma = 0$).

The same values of convected velocities have been used to compute these curves.

One can see that at the supports the displacement response peaks decrease with the convection velocity, a fact not observed in fig. 8.3. This same observation applies to the moment response.

Note that the highest response at the supports do occur when CV = ∞ and $\Omega_0^* = 21.641$, which represents another coincidence ($\mu_0 = 0$).

Fig. 8.6 shows the moment amplitude response at the left hand side of a stringer.

One can see that at these points the amplitude response peaks do not increase with the convection velocity. The highest peak occurs when CV = 14.19 and $\Omega_0^* = 20.160$ which again is a coincidence situation (see fig. 4.12). Another fact to be observed is that at the upstream side of

the stringers the moment amplitude peaks are slightly higher than those occurring at the downstream side.

8.4.2 Stringer-stiffened shell

The computations presented in the previous sub-section have been repeated for an infinite stringer-stiffened shell. The convection velocities have been selected to provide the strongest coincidence possible and to check the rate of damping in attenuating the responses. All the co-ordinates of a station vector have been computed but only curves for transverse displacement and bending moment are shown. The shell is considered damped with $\eta = 0.25$.

Fig. 8.7 and 8.8 represent the amplitude response for the transverse displacement and bending moment at the middle of a bay respectively. As for the plate case the curves show peaks where coincidence occurs.

As expected the maximum amplitude of displacement and moment are smaller than those found for the flat structure (see figs. 8.2 and 8.3). Notice again that 6.370 is the non-dimensional velocity of the primary wave component (see fig. 6.6) at the frequency $\Omega_o^* = 19.997$ ($\mu = \pi$). If the structure had no damping the response would be infinite (theoretically) The same can be said for the other peaks within propagation bands for they also represent coincidence. The presence of damping makes these peaks finite. For instance when CV = 2.124 and $\Omega_o^* = 19.997$ (see point E in fig. 6.6) one has a coincidence but the peak shown in figs. 8.7 and 8.8 is comparatively small.

Figures 8.9 and 8.10 show the transverse displacement and moment amplitude responses at the right hand side ($\varsigma = 0$) of a stringer. In these figures one can notice that the displacement and moment amplitudes no longer increase with the convection speed as happened in the plate case.

One can also see that this particular shell structure can show strong moment response at the stringers at relatively high frequencies.

Fig. 8.11 shows the moment amplitude response for the shell at the left hand side of a stringer.

A common feature of both flat and shell structures is that the response at the left hand side of a stringer (i.e. on the 'upstream' side) is higher than the response at the right hand side (i.e. on the 'downstream' side). But, contrary to what happened to the flat structure, the moment is higher in the middle of a bay.

CHAPTER IX

GENERAL CONCLUSIONS AND SUGGESTIONS FOR FURTHER STUDY

The basic ideas of free wave propagation in spatially periodic structures have been reviewed and the transfer matrix terminology introduced in connection with a specific example.

A general theory of free wave propagation in periodic structures was then constructed. This theory fully employs the transfer matrix technique and is general in the sense that it completely bypasses all the particulars of the structure (other than spatial periodicity and linearity). It is also computer oriented requiring only little algebraic effort for derivation of the state matrix. For systems with two degrees of freedom it has been possible to fully write down the field transfer matrix but for greater numbers of degrees of freedom one of the three numerical methods discussed in chapter V should be used. It was found that all these methods give virtually the same numerical results but the method based on the truncated series requires more computing time than the other two (which in turn require about equal computing time). But it has the inherent advantage of not requiring complex algebra when the field is non-damped.

When the field transfer matrix has to be computed at many points along the field the two other methods are far more advantageous.

Comparison was made between the lower limit of the first propagation band of an infinite ring-stiffened cylinder and the lowest frequency of the first group of modes of a 15 bay finite structure with the same elements, and simply supported on two 'half-rings' placed at both ends (as calculated by Wah [25]). It was found that for a number of circumferential waves greater than 3 both results are very close (within 1%). For smaller numbers of circumferential waves (say one or two) there

is little inter-ring motion and the potential energy of the finite structure is due mainly to the overall semi-sinusoidal displacement between the end supports. In these conditions comparison between finite and infinite structures have little meaning.

Comparison of the lower limit of the first propagation band of an 'infinite' stringer-stiffened cylindrical shell with the first natural frequency of a 56 bay closed stringer-stiffened cylindrical shell [4] has shown that they are very close.

On the other hand, the two first propagation bands have not shown the overlap produced by Lin's approximate method [1]. Indeed the numerical values of the two first band limits produced by Lin are not quite in agreement with those computed in this work. This overlap has not been found by increasing the values of the shell radius either. This has produced, instead, a gradual convergence to the flat plate results. Lin's band limits computed by his 'exact' method for plates are virtually identical to those produced by the present method.

The concept of complex wave components has been established and a matrix technique to compute them has been developed. It was shown that the response of finite and infinite structures to harmonic forces can be computed as a linear combination of these complex wave components.

Response along the structure and frequency response functions have been computed for stringer-stiffened plates (finite and infinite) and stringer-stiffened shells.

Computing storage and time requirements were kept very low (less than 13 sec. in the CDC 7600 to compute the single point frequency response function for the stringer-stiffened shell at 101 values of the frequency).

A general matrix theory of the response of finite and infinite periodic structures to a convected harmonic pressure field has been

developed. This theory has been applied to a stringer-stiffened plate and to a stringer-stiffened cylindrical shell.

Frequency response functions have been computed and the effect of coincidence phenomena pointed out.

The largest moments have been found at the upstream side of a stringer for the particular plate structure taken. For the particular stringer-stiffened shell the moment at the middle of a bay was higher than both upstream and downstream moments.

The main features of the methods developed in this work are:

a) generality,

b) computer oriented,

c) time and computer storage required are very small,

d) algebra required kept to a minimum.

These features are in addition to those inherent to the wave propagation approach commented on in chapter I which make it so convenient to be applied to periodic structures.

All the characteristics of the methods established in this work make it adequate for future applications to more complicated structures, for instance, sandwich structure.

The existence of bi-dimensional transfer matrices has been shown by Pestel [43]. This fact can be used to further extend the theories dealt with in this work to bi-dimensional periodic structures.

Experiments on models representing complex engineering structures (ships hulls, etc.) are urgently required. It is hoped that the theories presented in chapters VII and VIII would provide great help in assisting the analysis and interpretation of the results from such experiments.

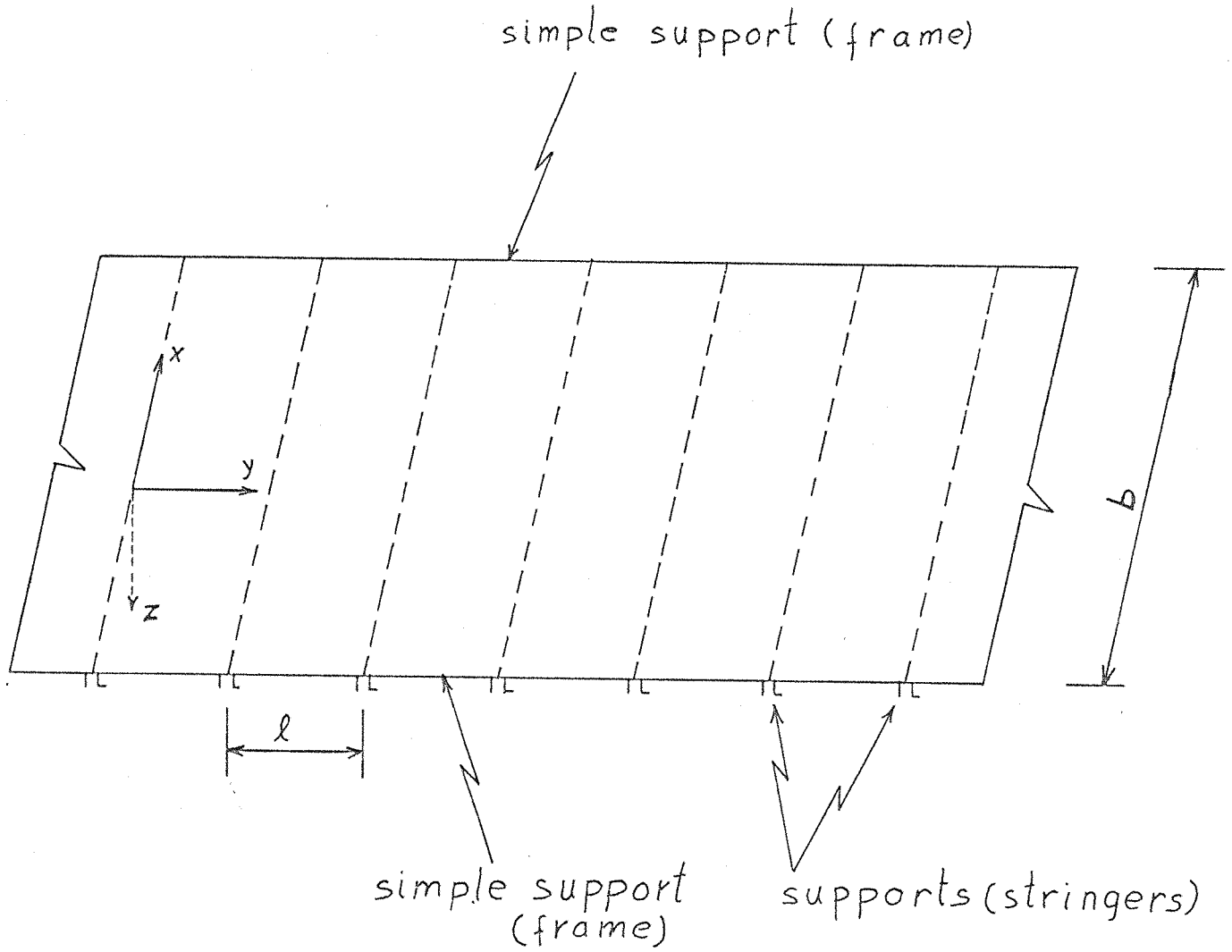
simple support (frame)
x
y
z
b
ℓ
simple support
(frame)
supports (stringers)

fig. 2.1

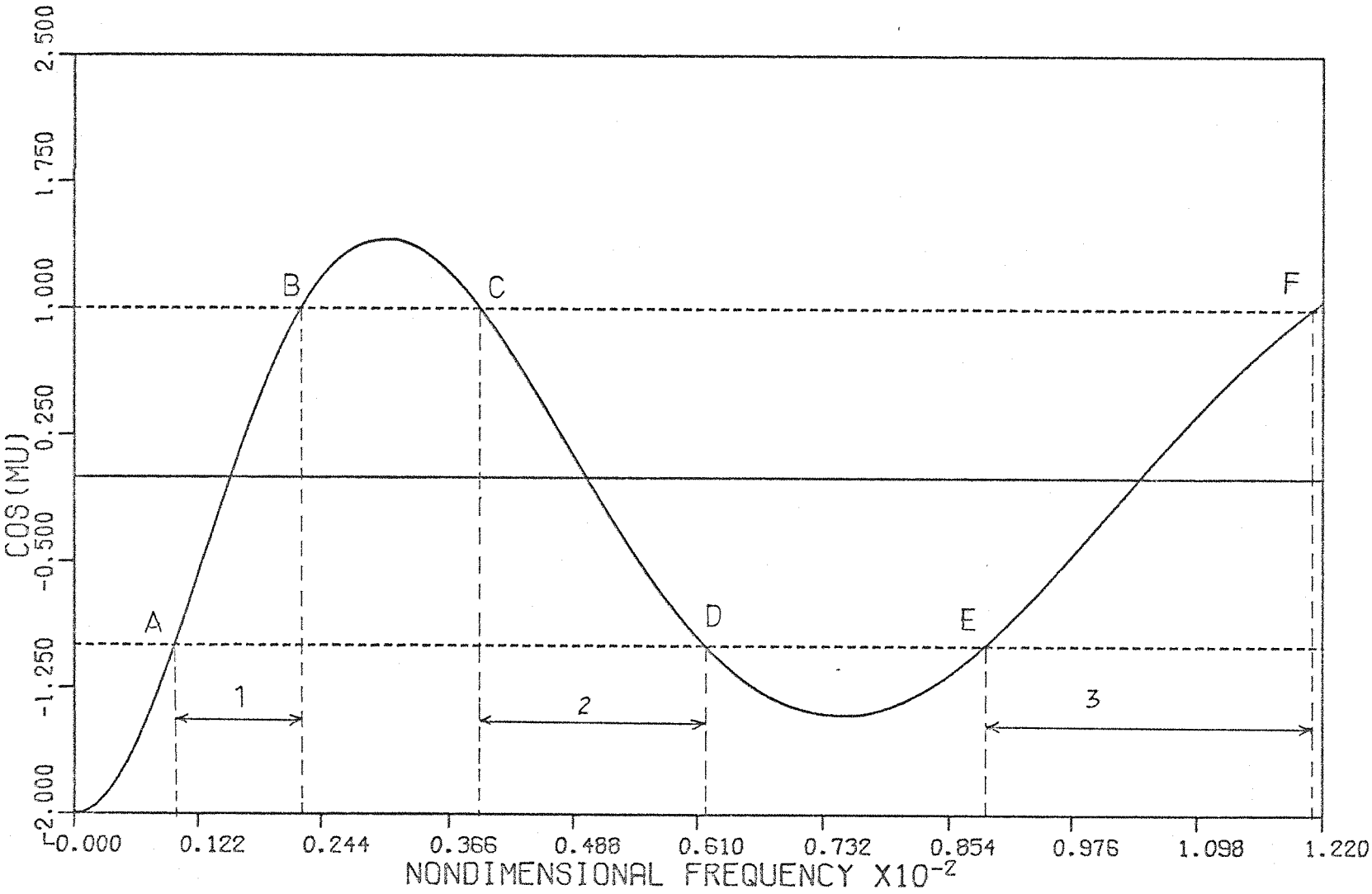
2.500
1.750
1.000
0.250
-0.500
-1.250
-2.000
COS(MU)
A
B
C
D
E
F
1
2
3
0.000
0.122
0.244
0.366
0.488
0.610
0.732
0.854
0.976
1.098
1.220
NONDIMENSIONAL FREQUENCY X10^{-2}

fig. 2.2

μ_o-Ω_o curves for a beam on simple periodic supports

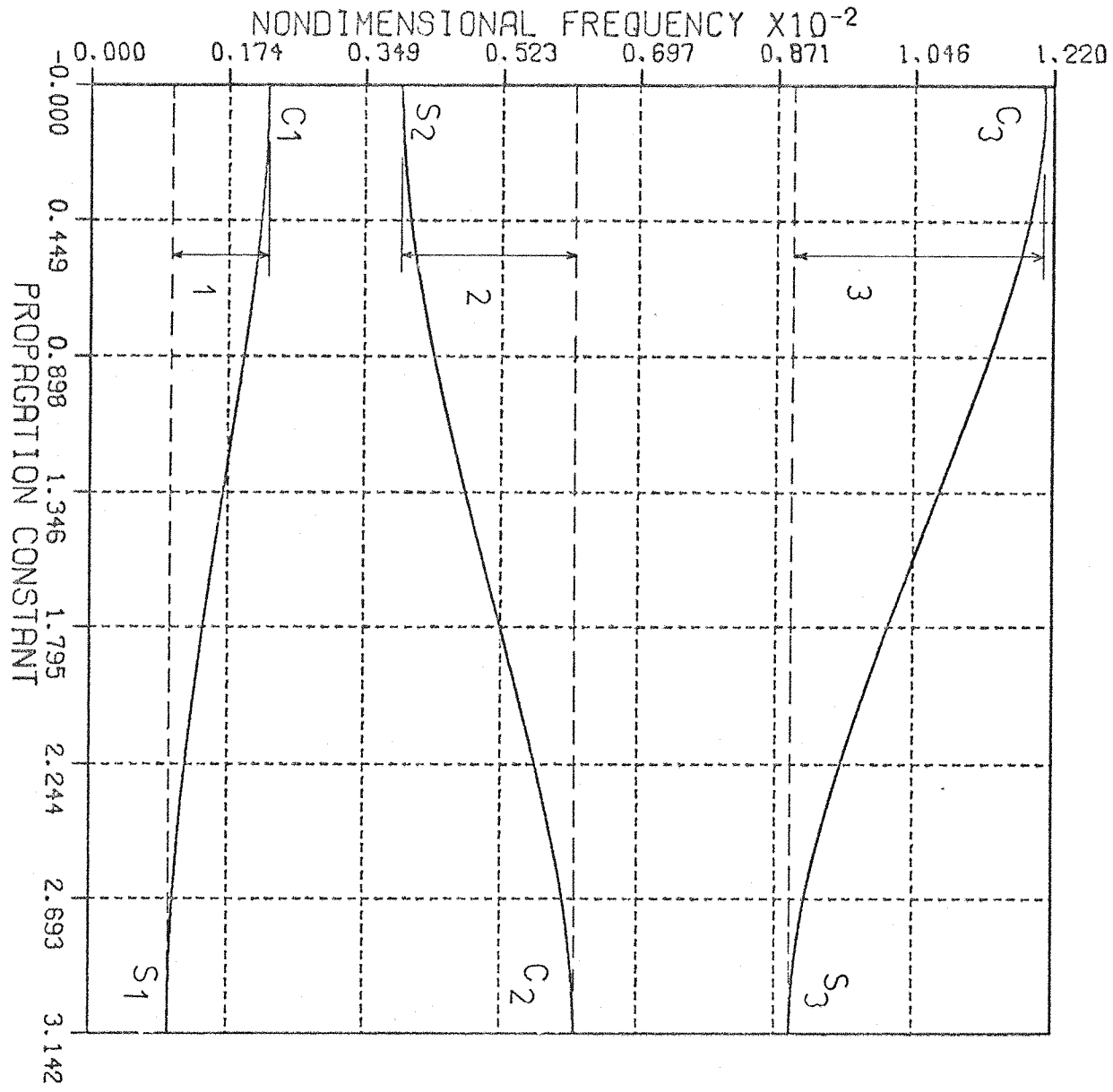

fig. 2.3

$\Omega_0^* - \mu$ curves for a beam on simple periodic supports

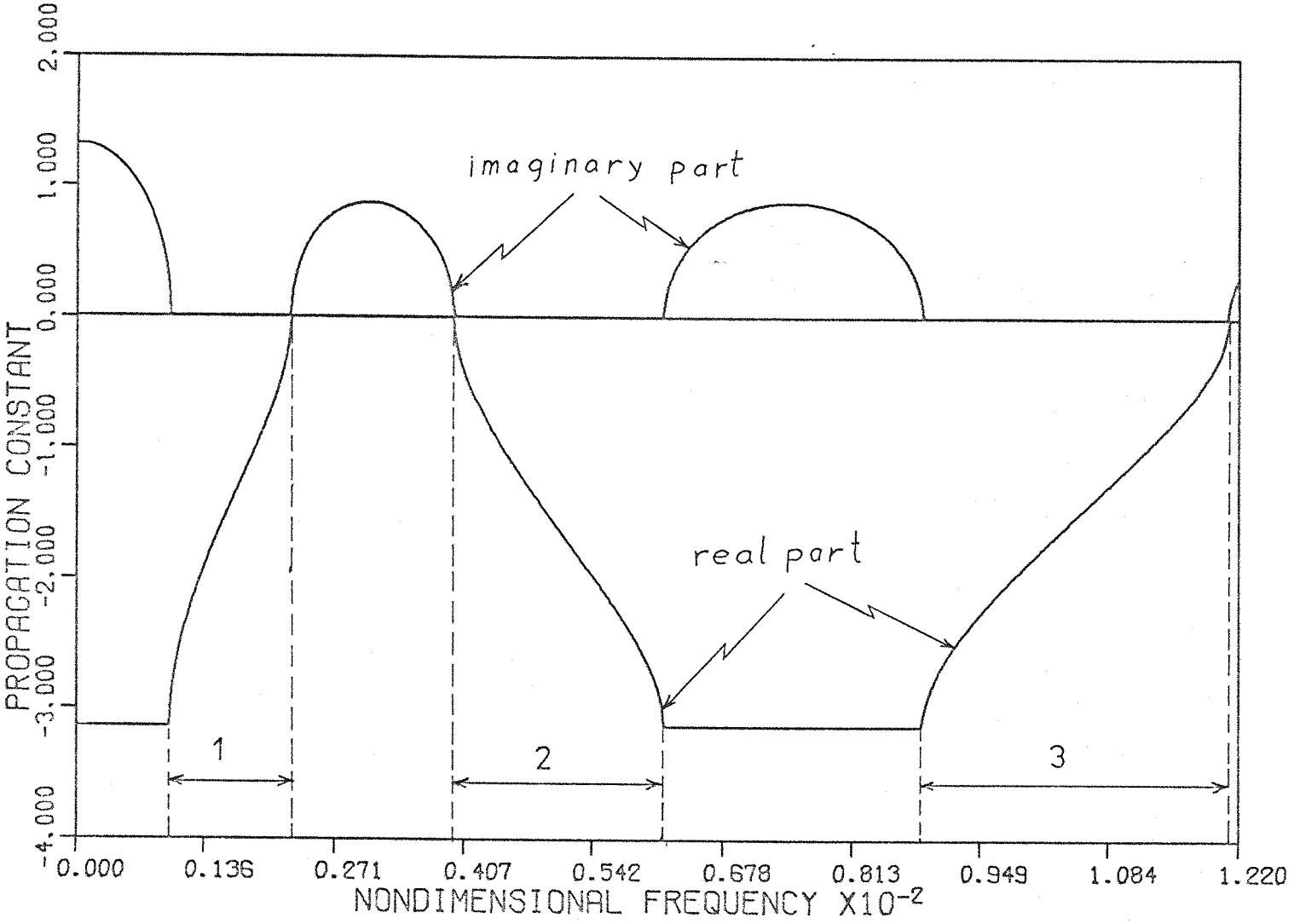

fig. 2.4

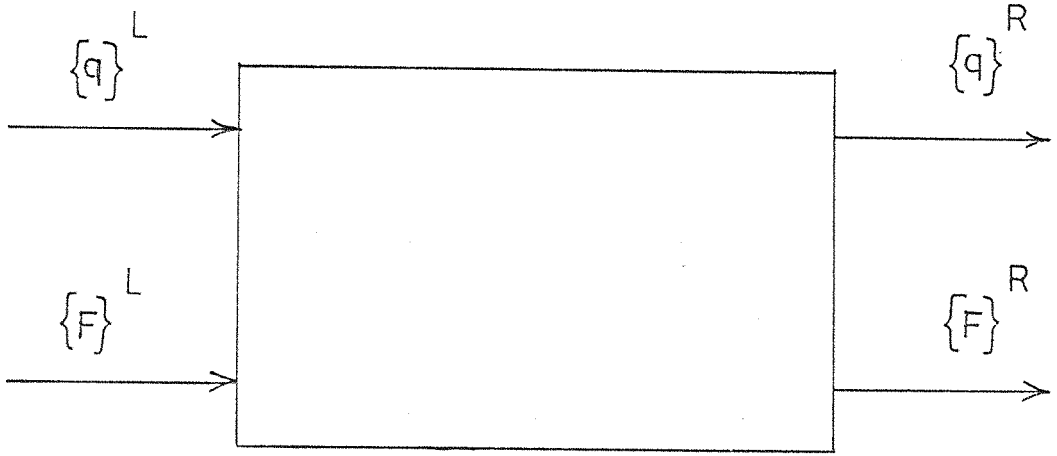

fig. 3.1

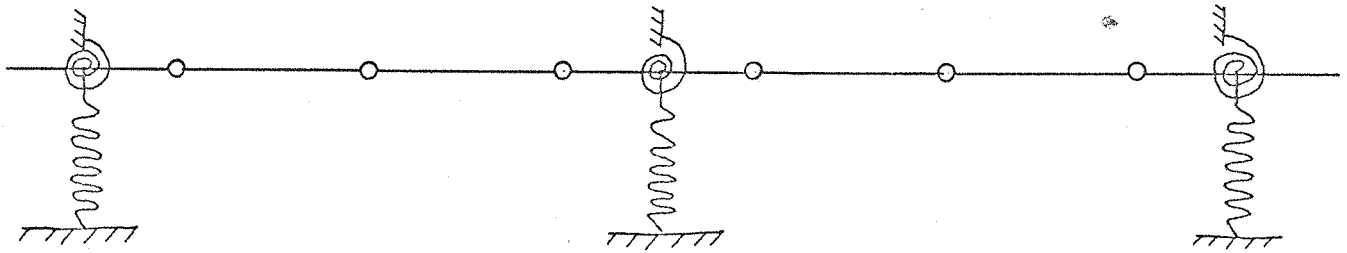

fig. 3.2

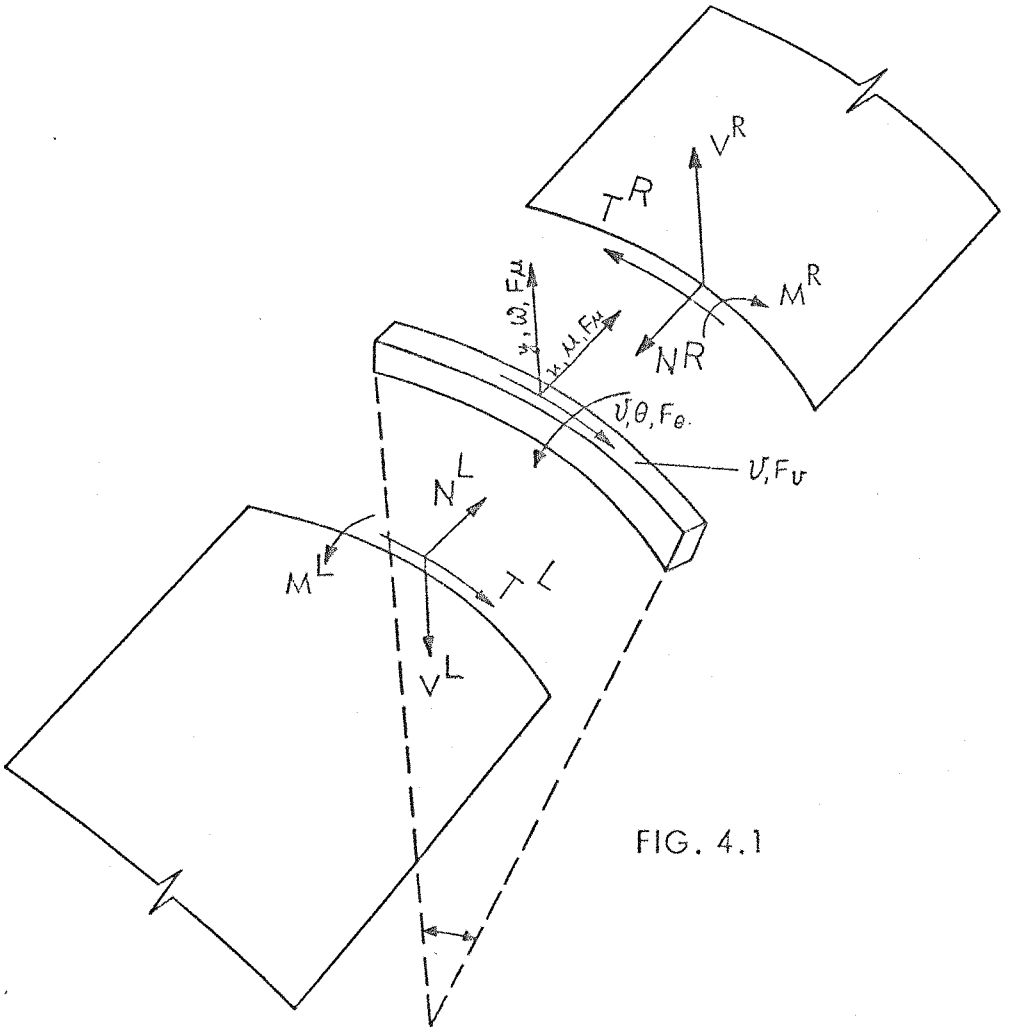

FIG. 4.1

FIG. 4.2

DEFINITION OF A STRUCTURAL PERIOD.

$\mu_0 - \Omega_0^*$ curves for

Example 1

$r = 1$

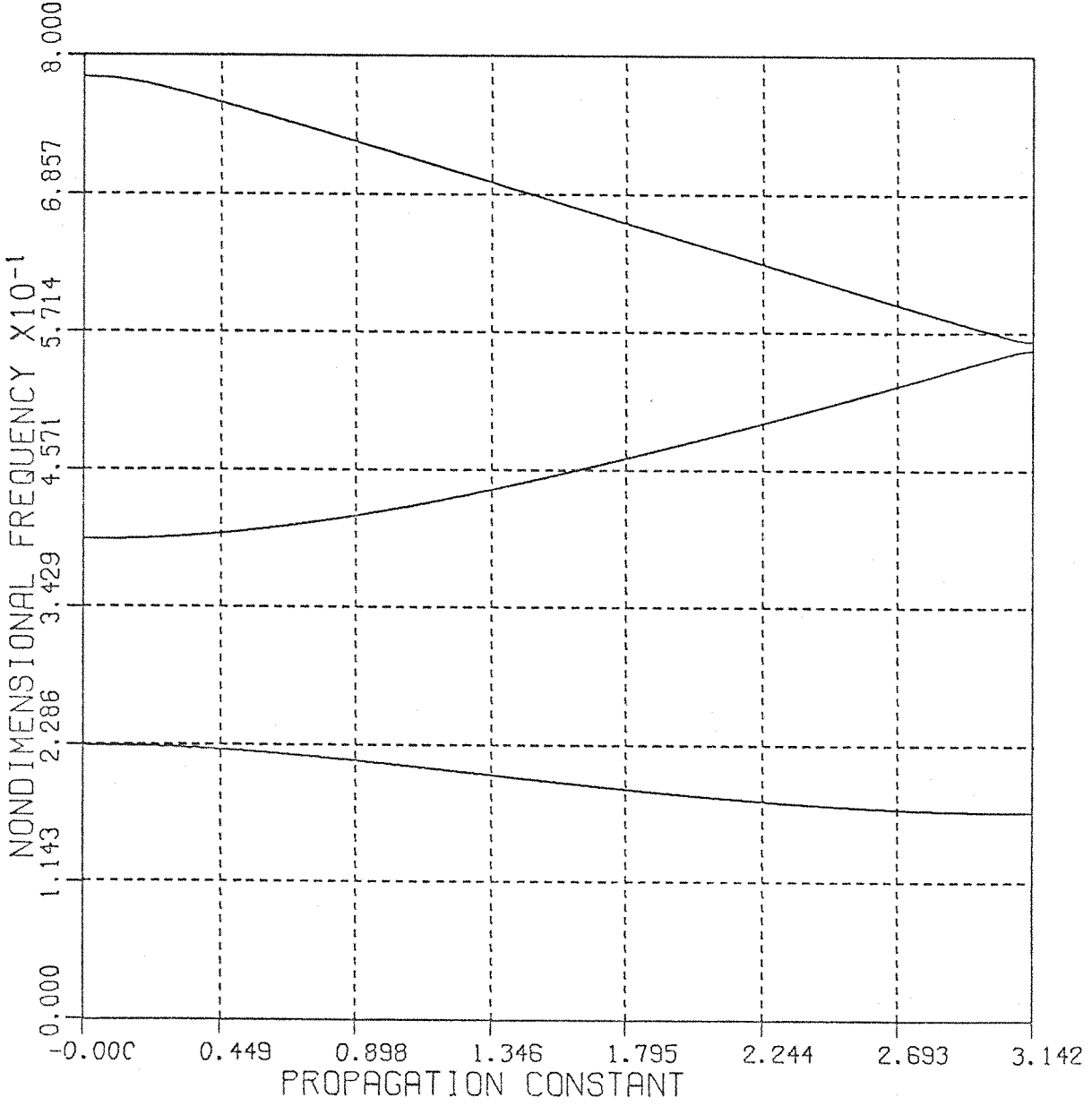

fig. 4.3

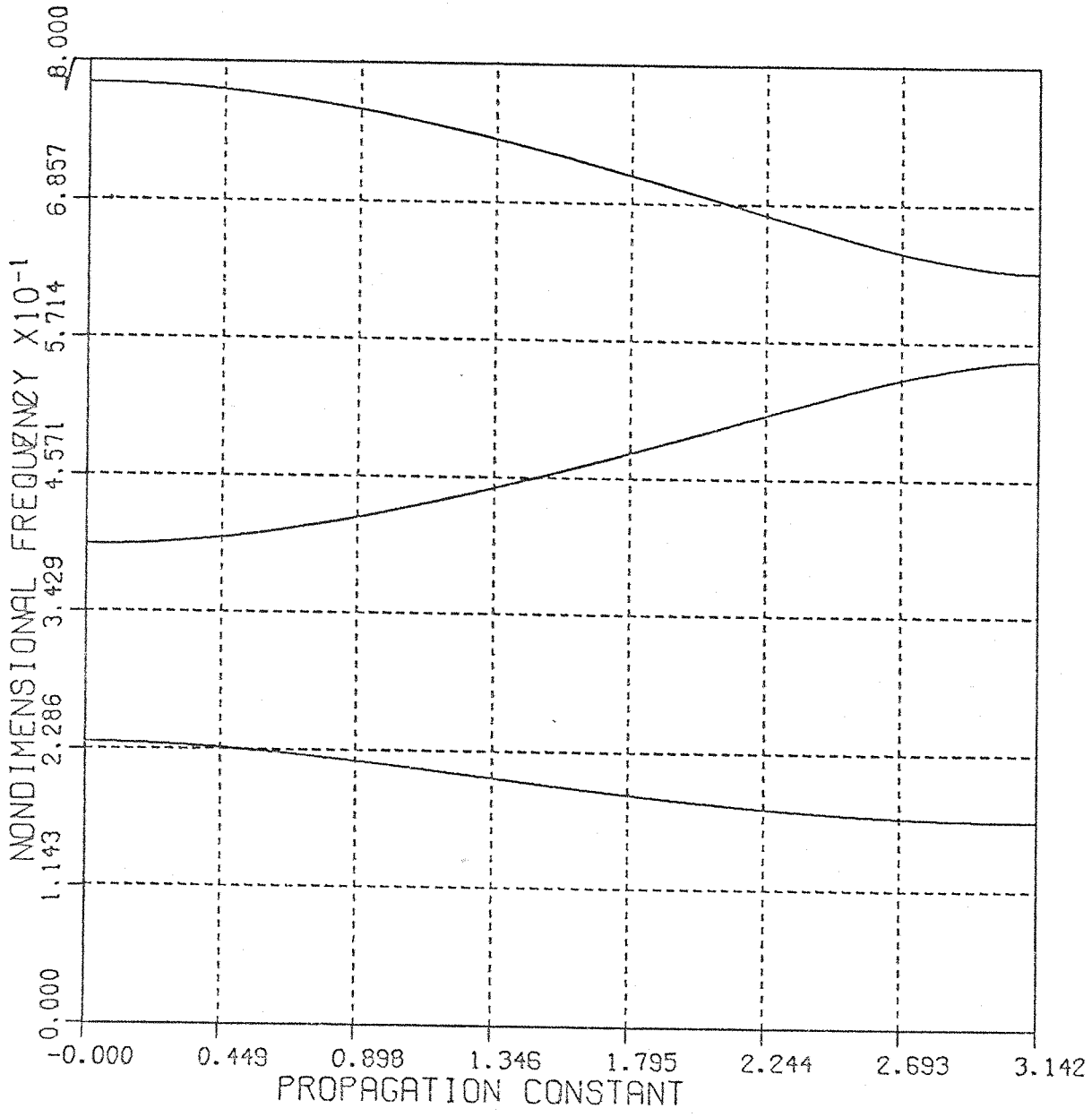

μ_0-$\mathcal{S}_0^*$ curves for Example I modified with $K_w = \infty$
$r = 1$

fig. 4.4

μ_0-Ω_0^* curves for Example I modified with $K_0 = \infty$.

$r = 1$

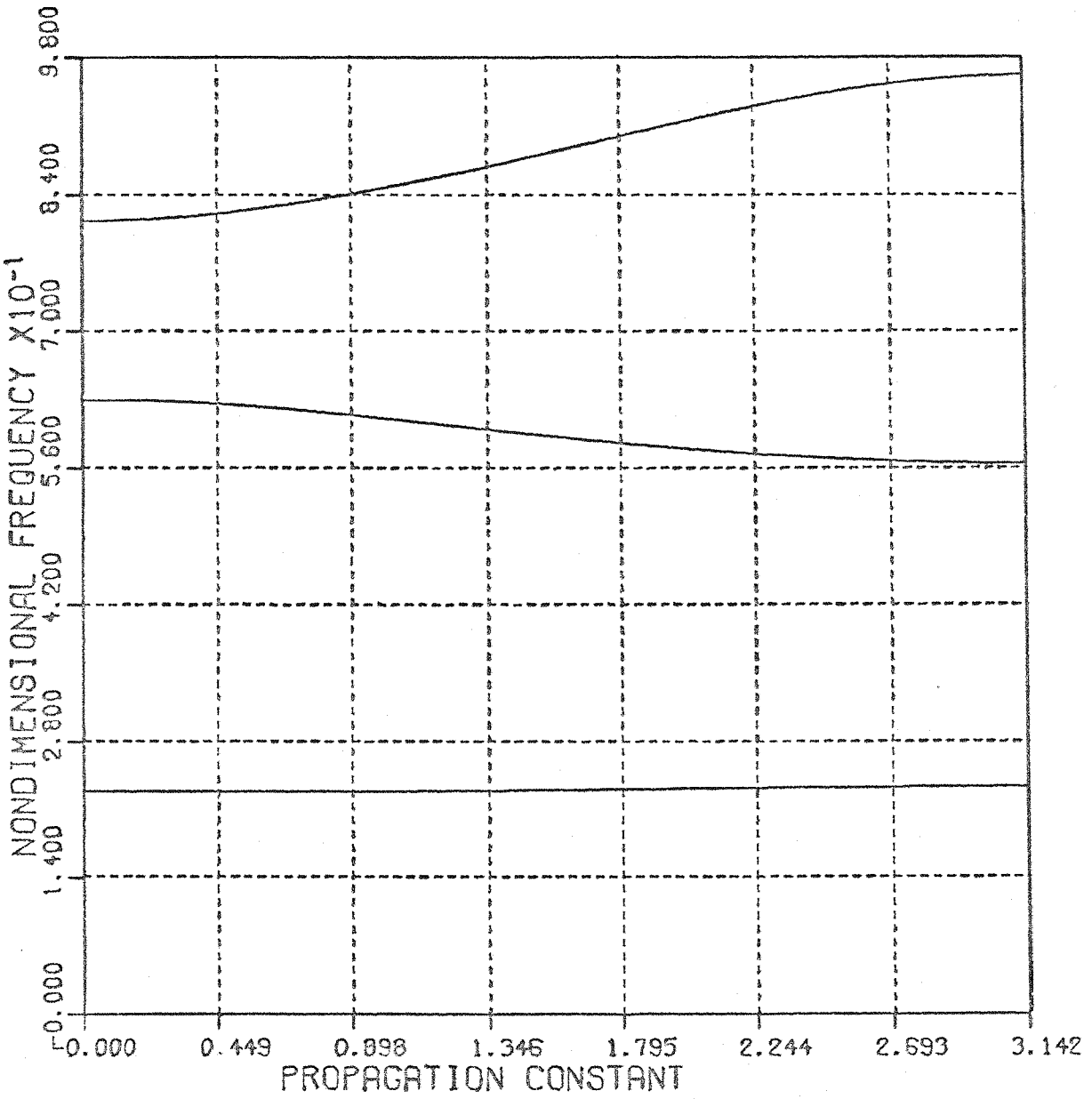

fig. 4.5

$\mu_0 - \Omega_0^*$ curves for

Example II

r=1

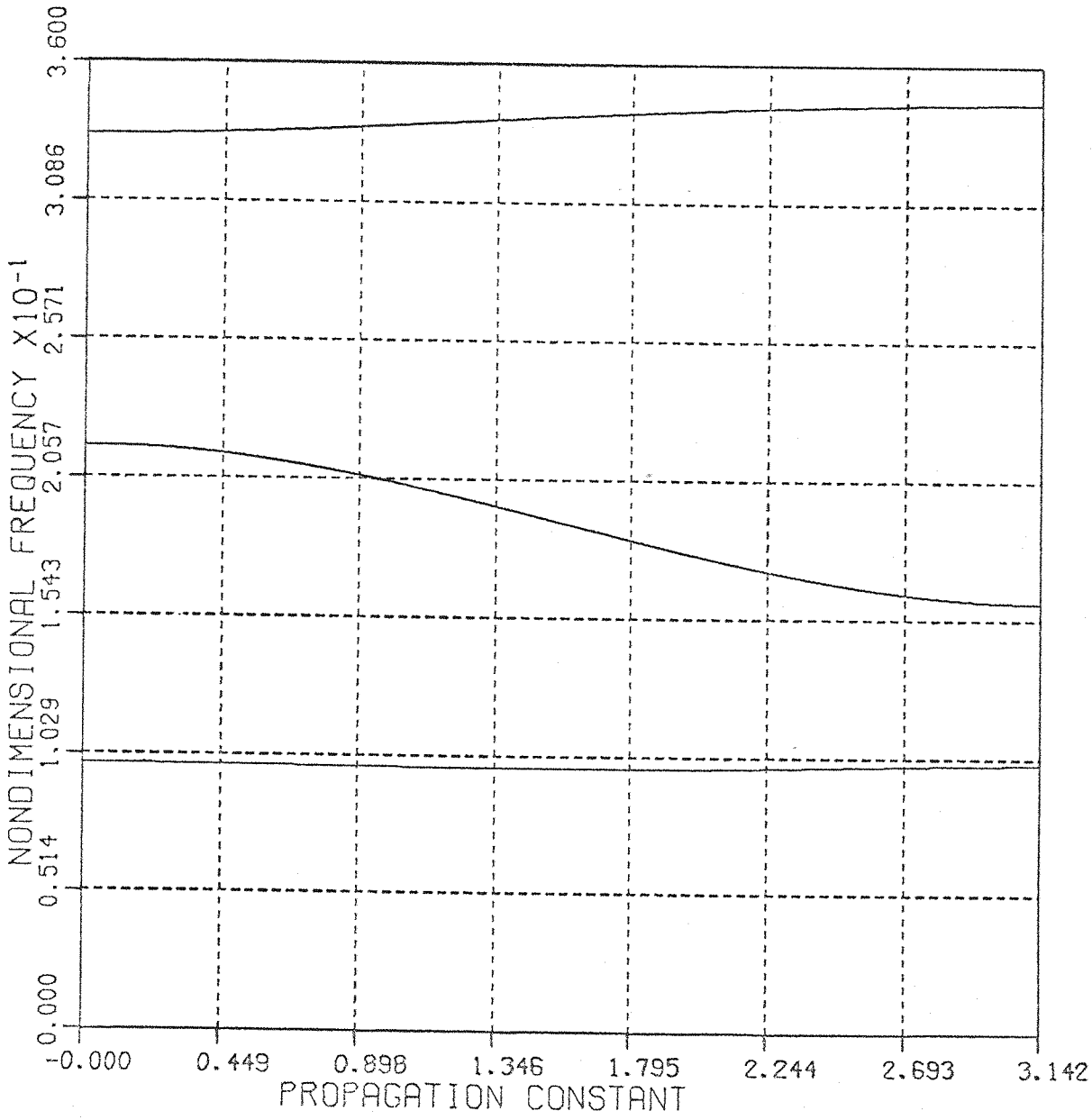

fig. 4.6

μ_o-δ_o^* curves for Example II modified with $K_w = \infty$

$r = 1$

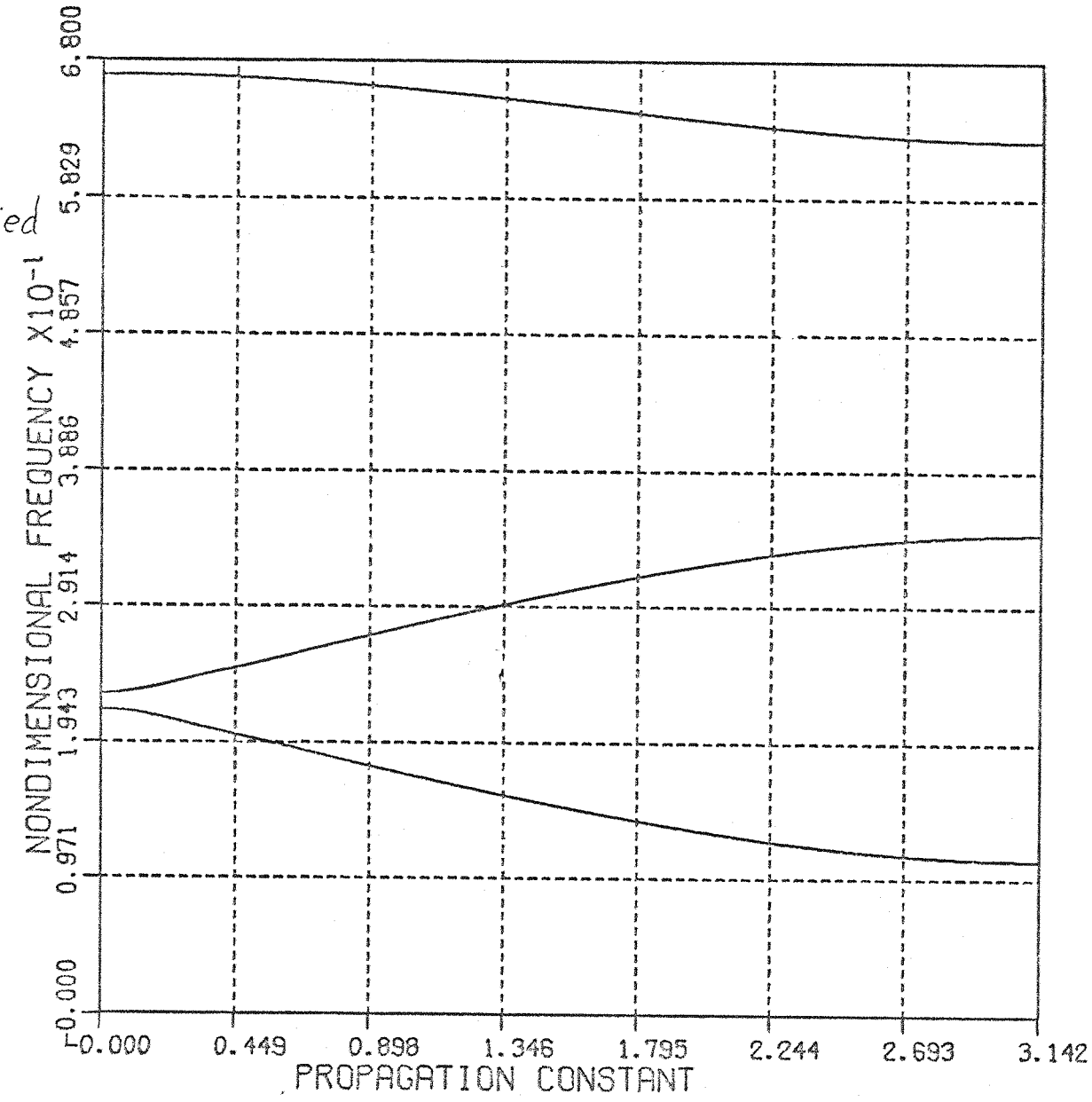

fig. 4.7

μ_0-Ω_0^* curves for Example II modified with $K_{w\theta}=0$.

$r=1$

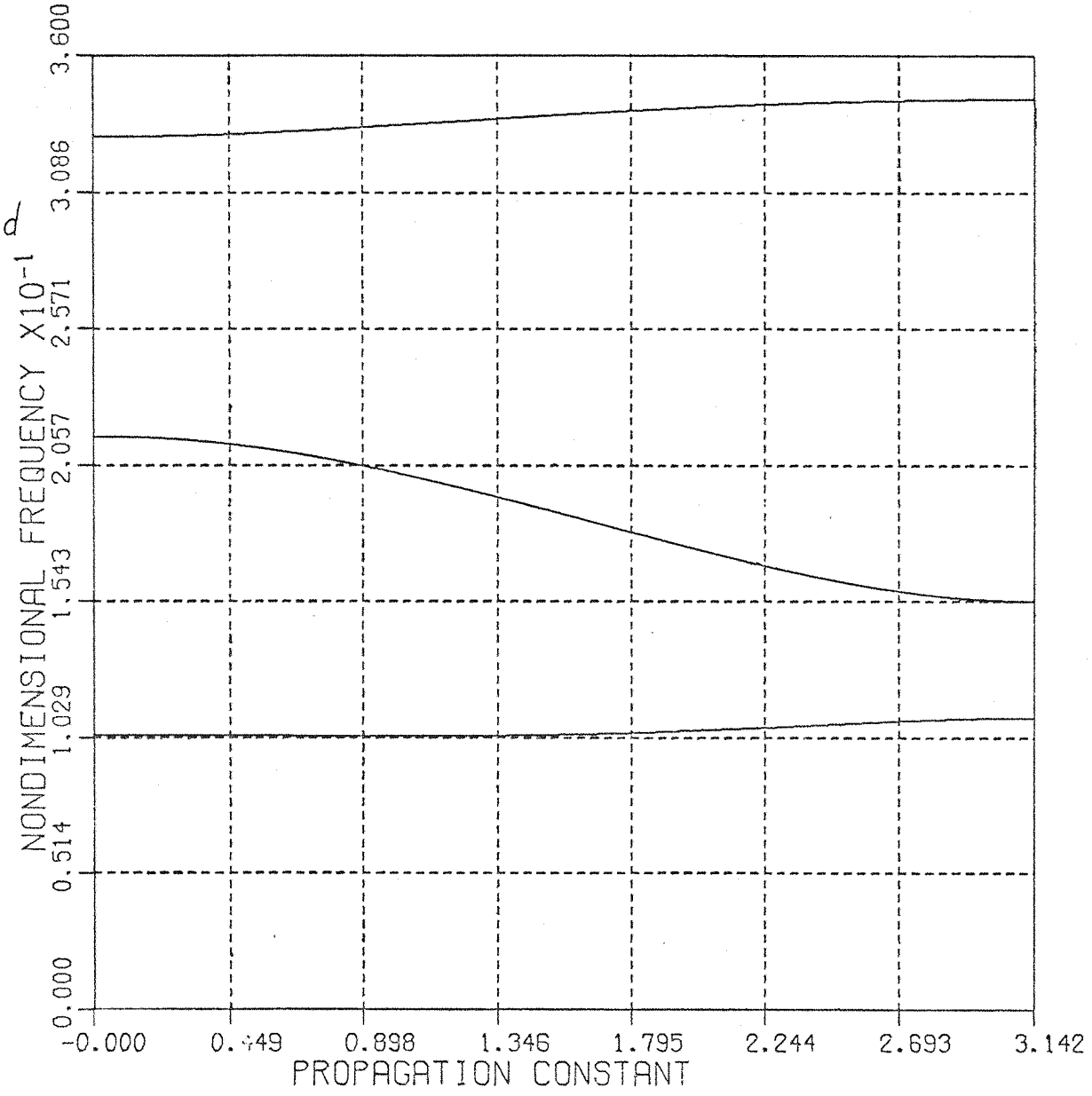

fig. 4.8

Ω_o^*-μ curves for Example I

$r=1$, $\eta=0.0$

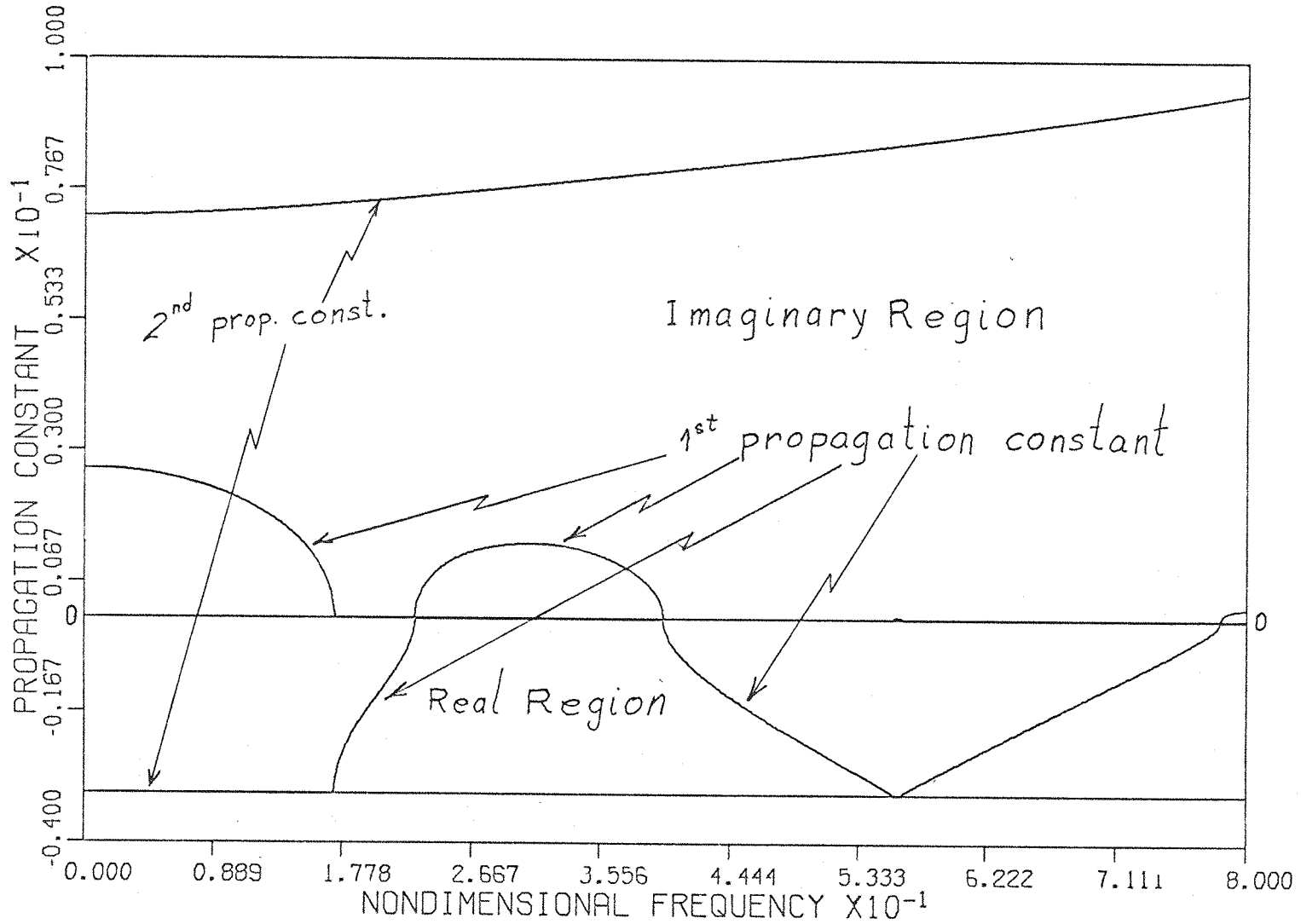

fig. 4.9

$\Omega_0^* - \mu$ curves for Example I

$r = 1$, $\eta = 0.15$

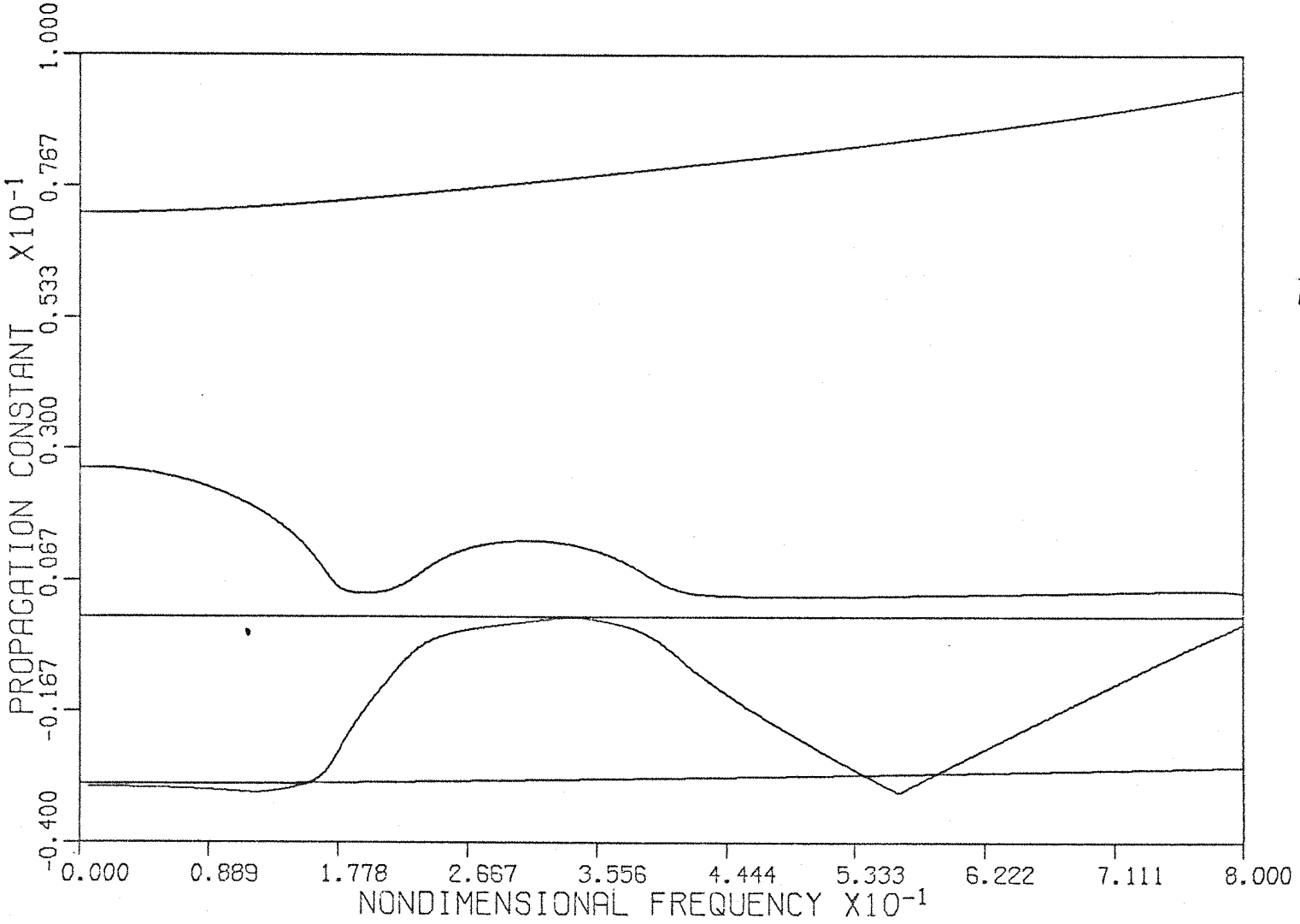

fig. 4.10

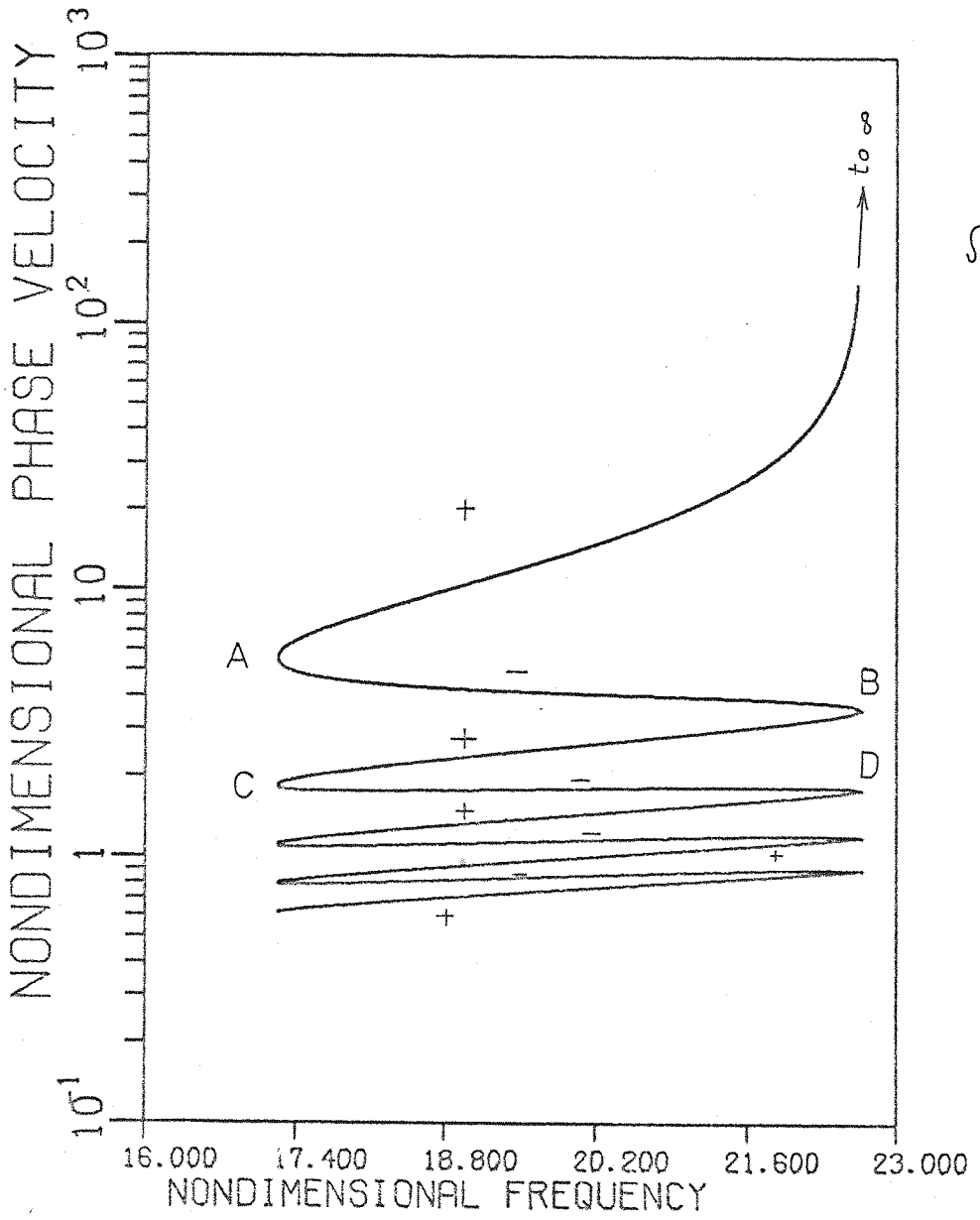

Ω_o^*-v^* diagram for Example I

1^{st} band , $r=1$

fig. 4.11

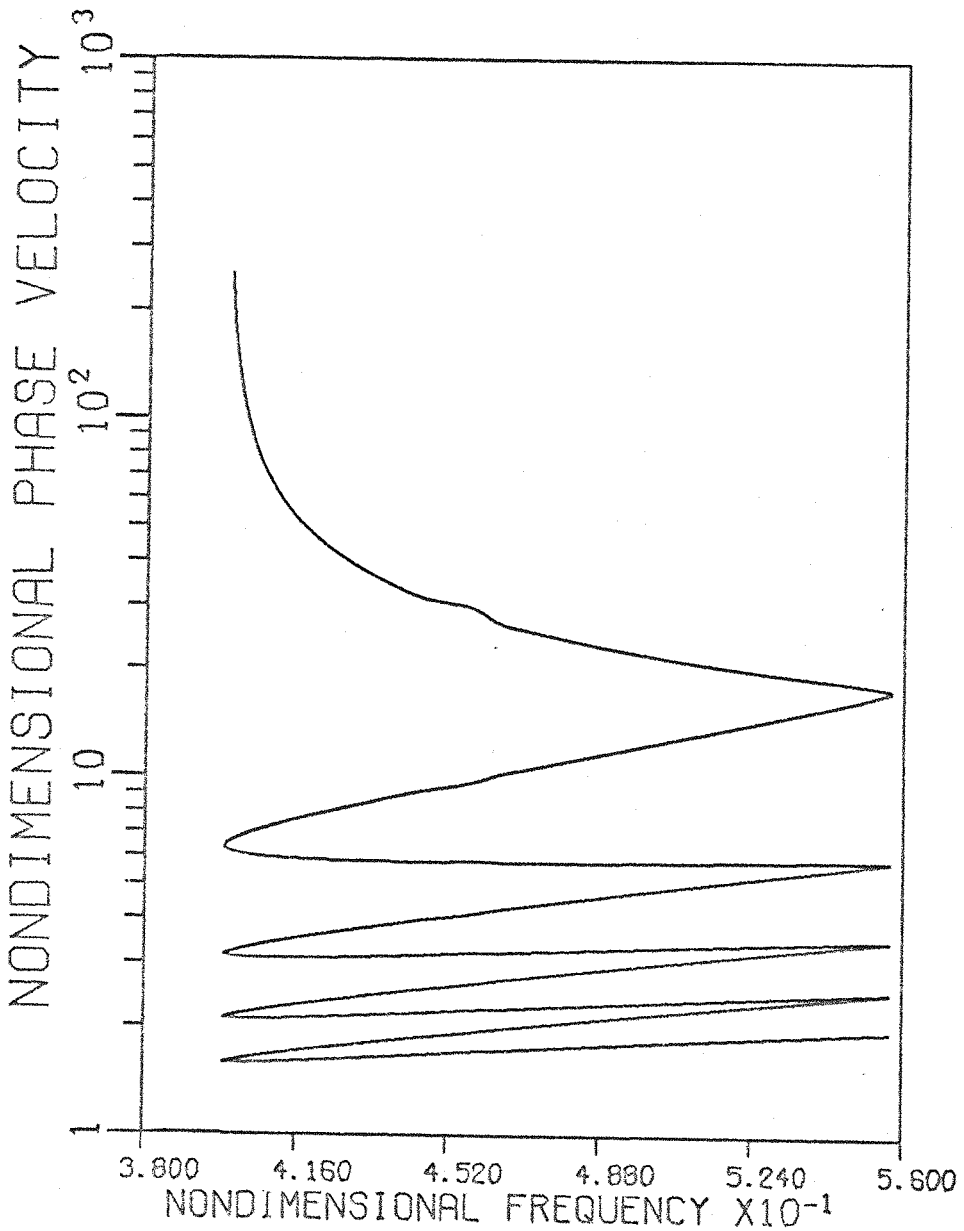

Ω_o^*-v^* diagram for Example I

2nd band, r=1

fig. 4.12

Ω_o^*-v^* diagram for Example I 3rd band, r=1

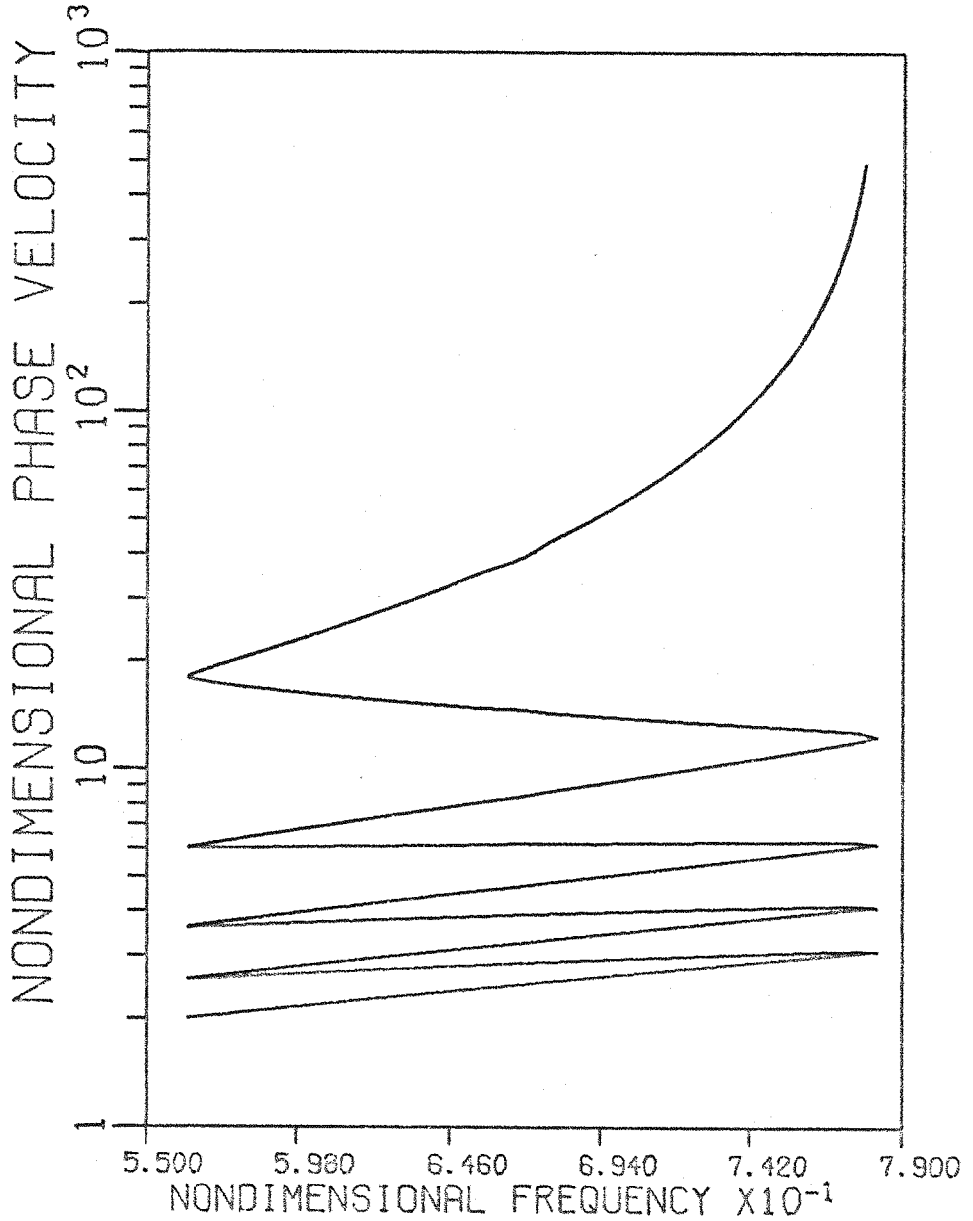

fig. 4.13

μ_0-Ω_0^* curves for Example III

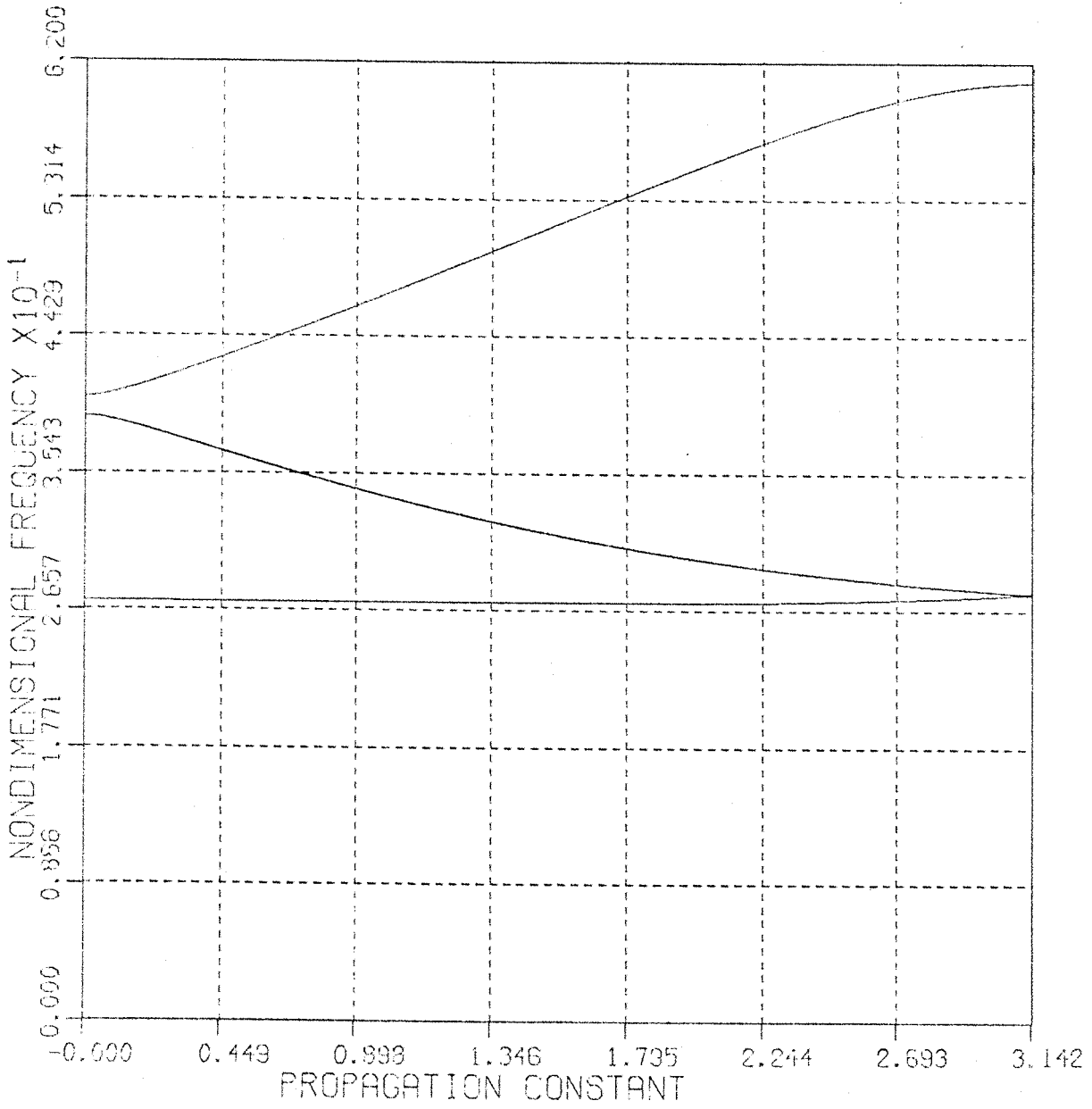

fig. 4.14

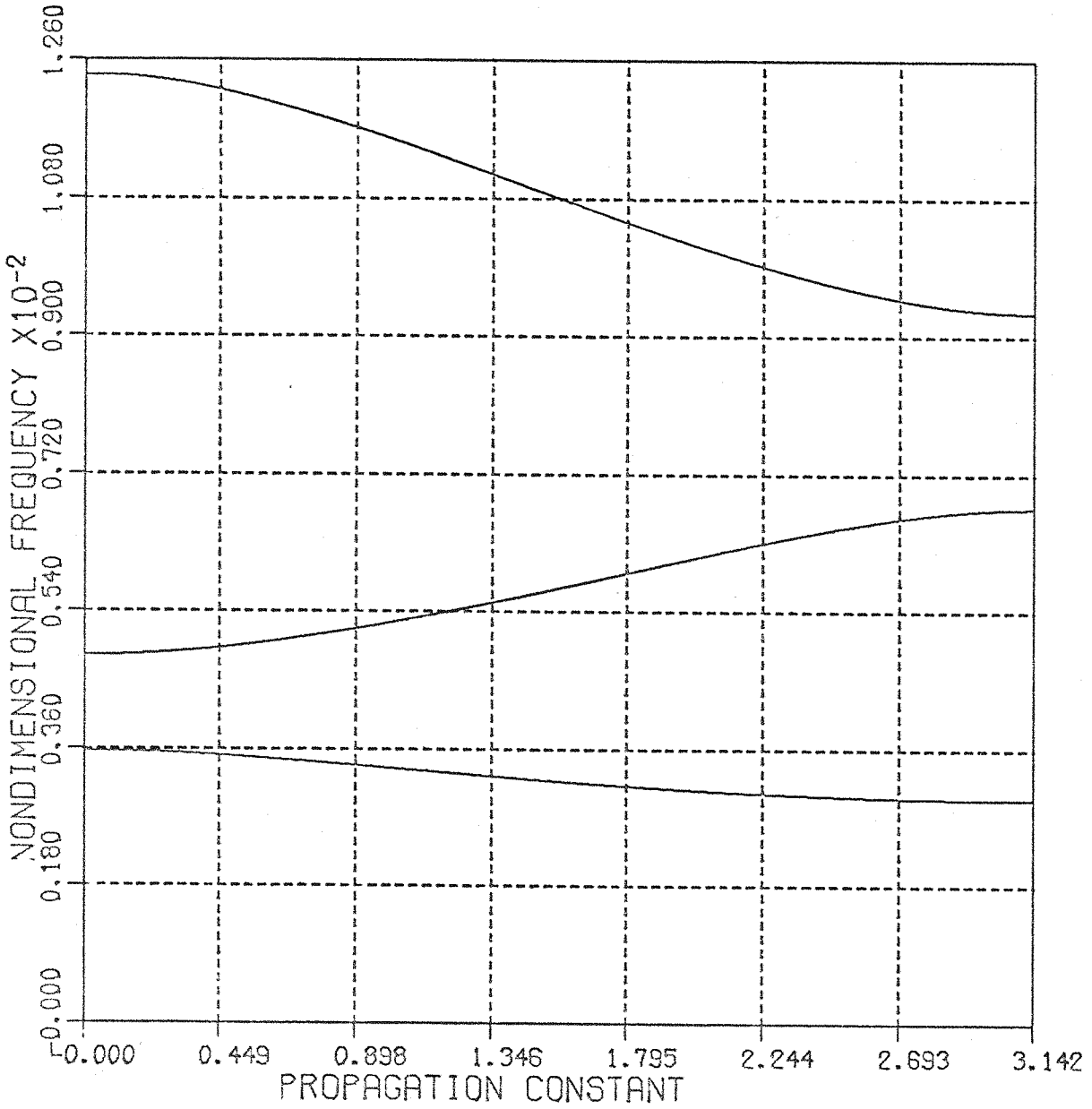

μ_0-Ω_0^* curves for Example III modified with $K_w = \infty$

fig. 4.15

Ω_o^*-μ curves for Example III

$\eta = 0.0$

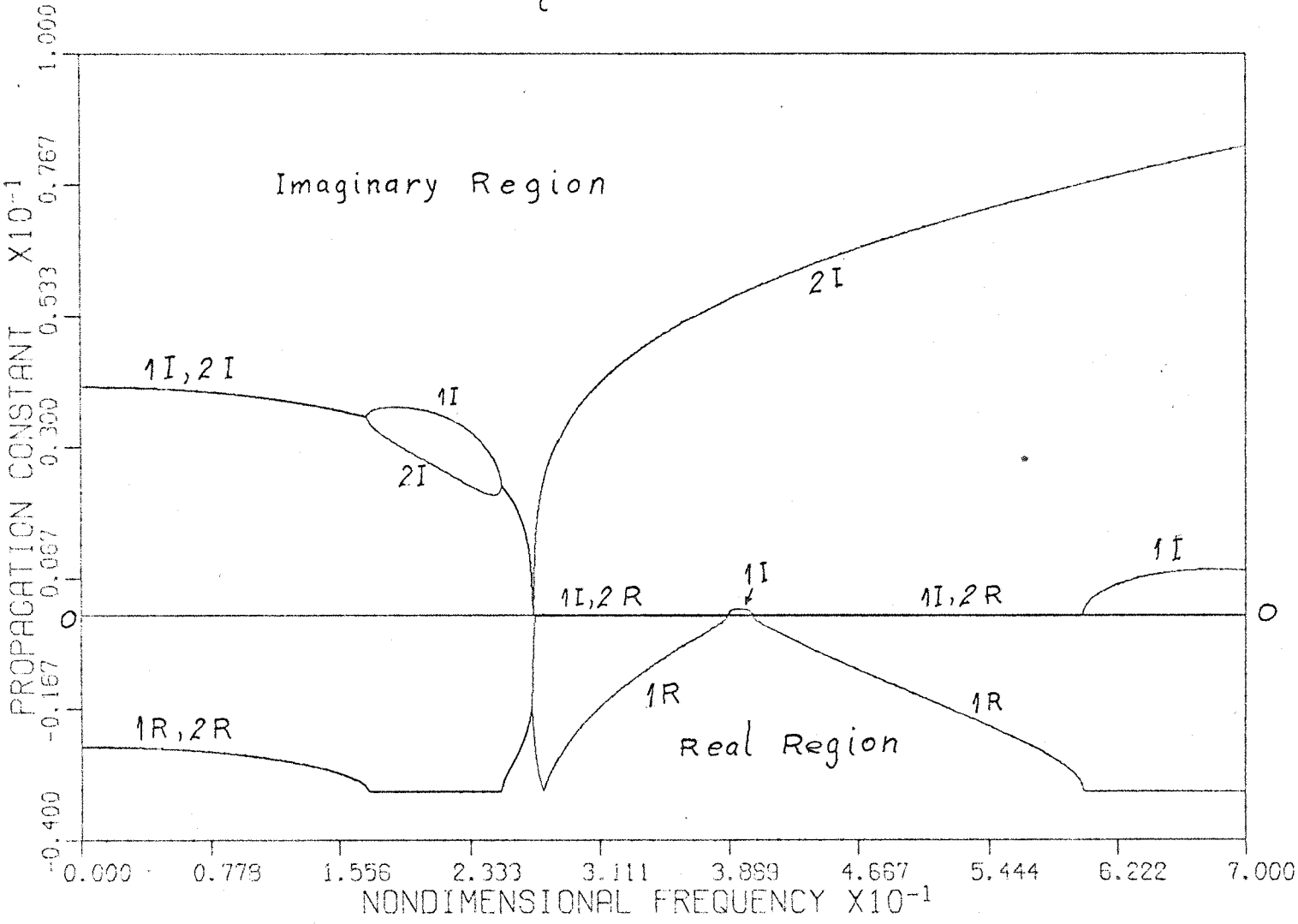

fig. 4.16

$\Omega_0^* - \mu$ curves for Example III

$\eta = 0.15$

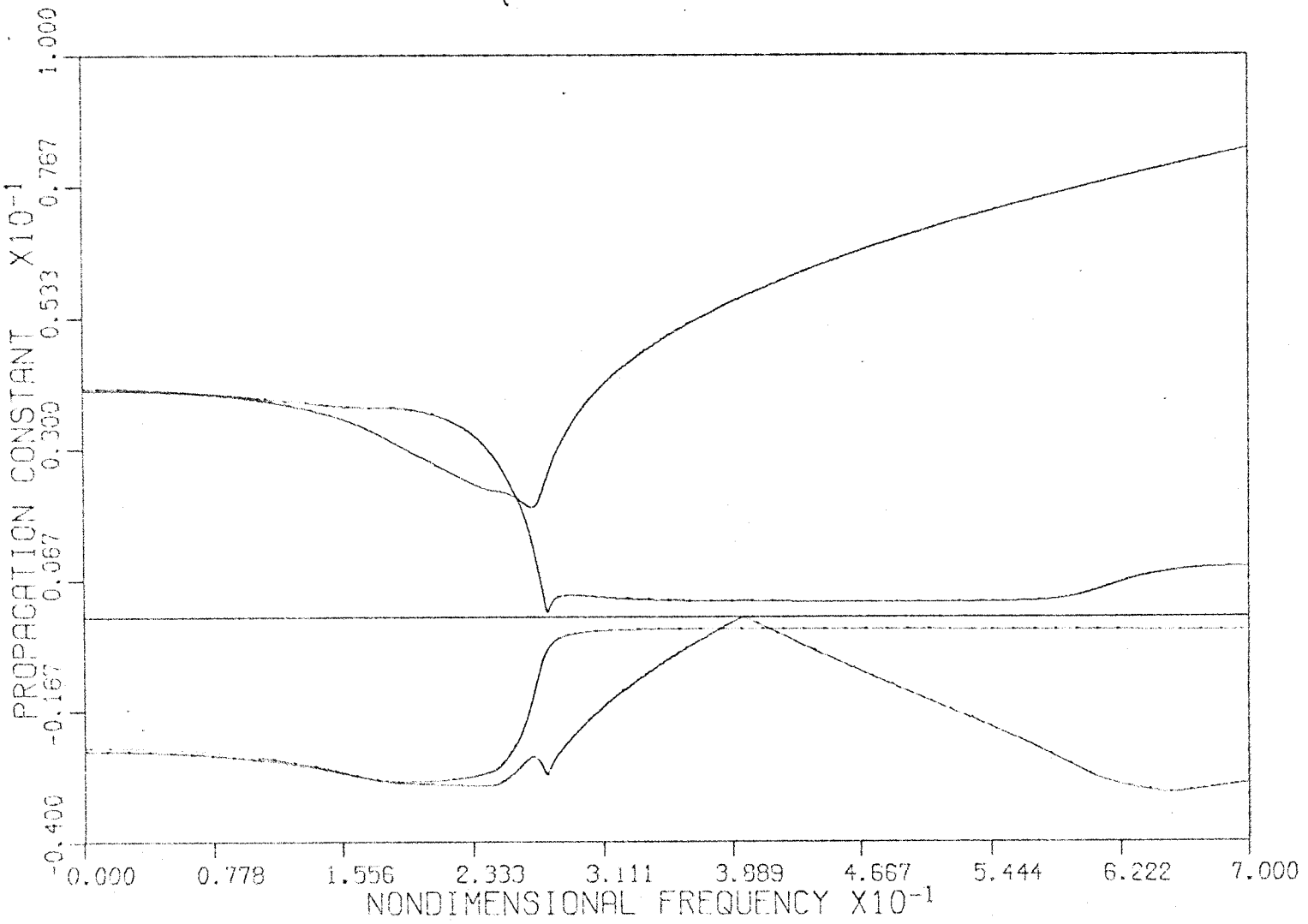

fig .4.17

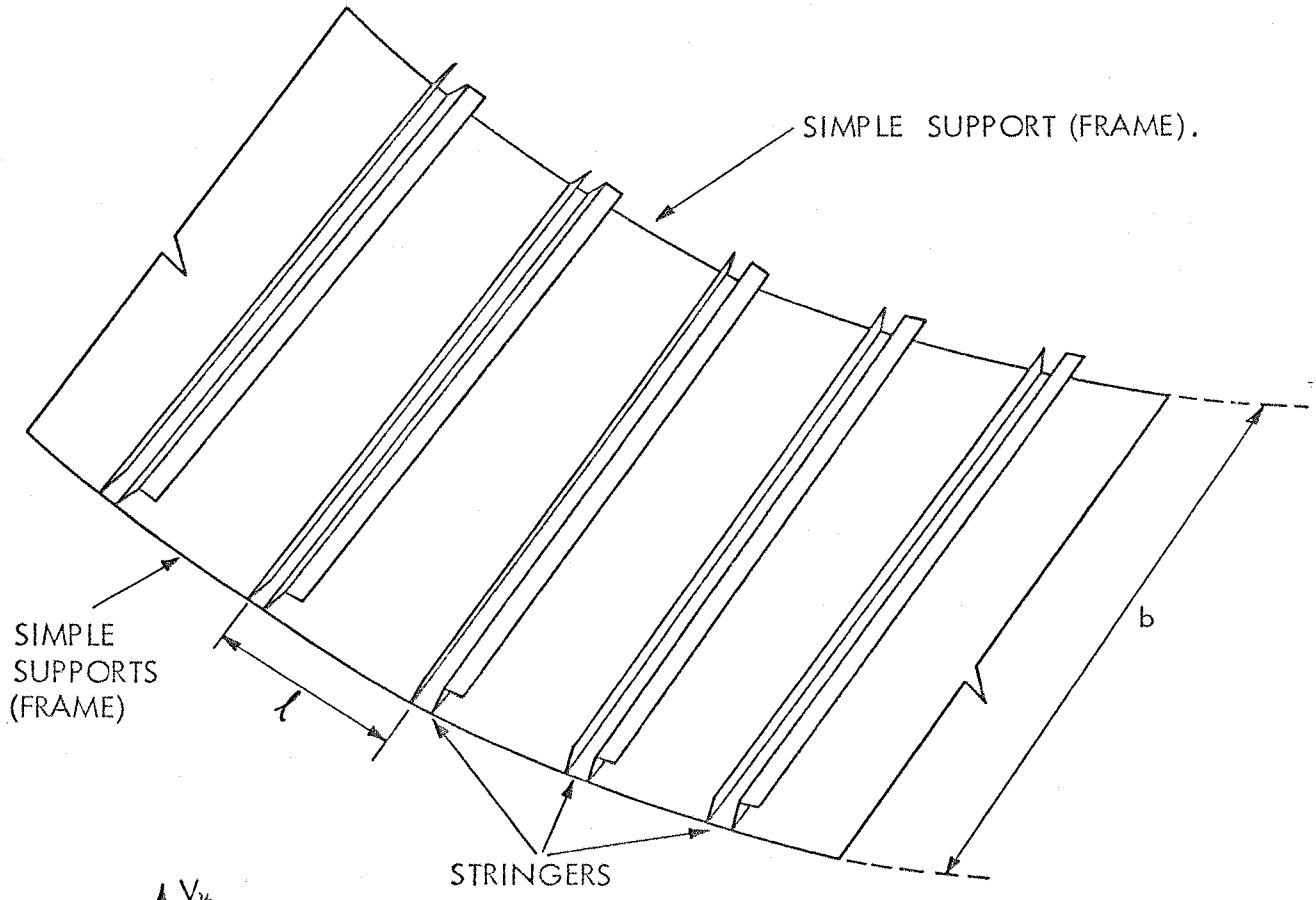

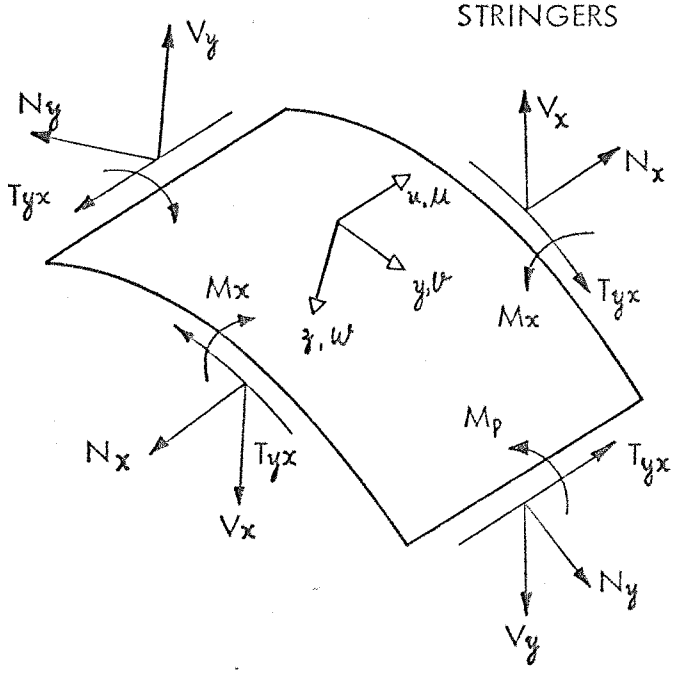

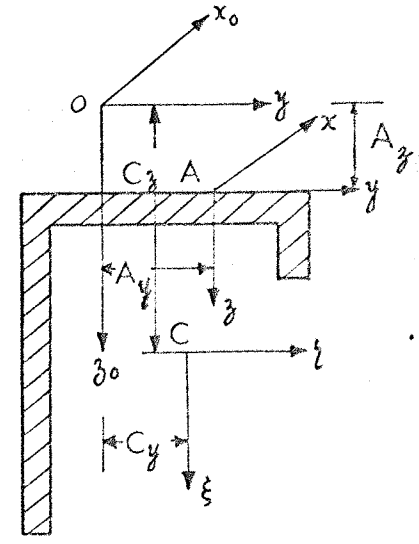

? O SHEAR CENTRE.
A ATTACHMENT POINT.
C CENTROID.

FIG. 6.1

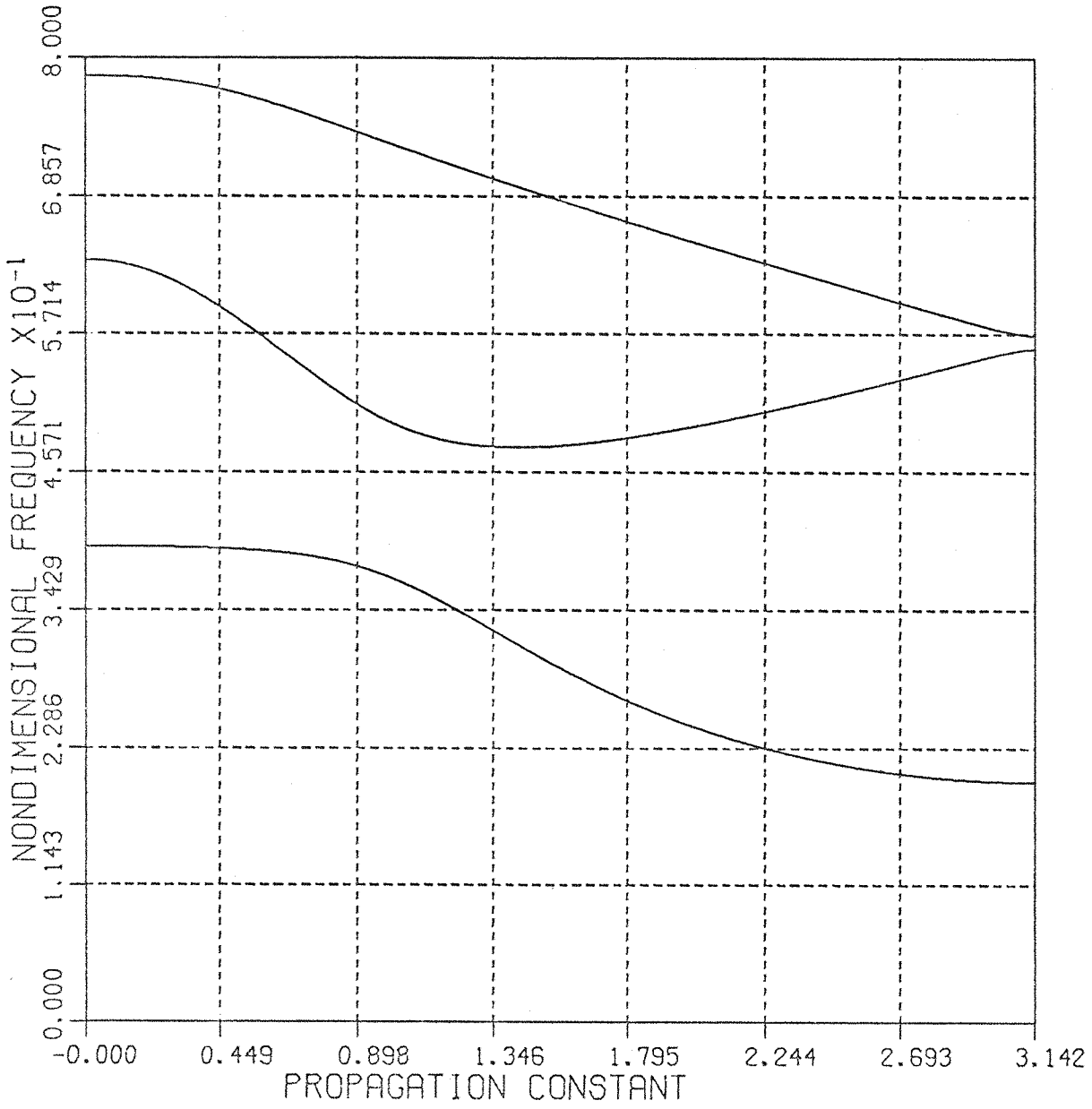

$\mu_0 - \Omega_0^*$ curves for a stringer-stiffened shell

ASP = 2.44

fig. 6.2

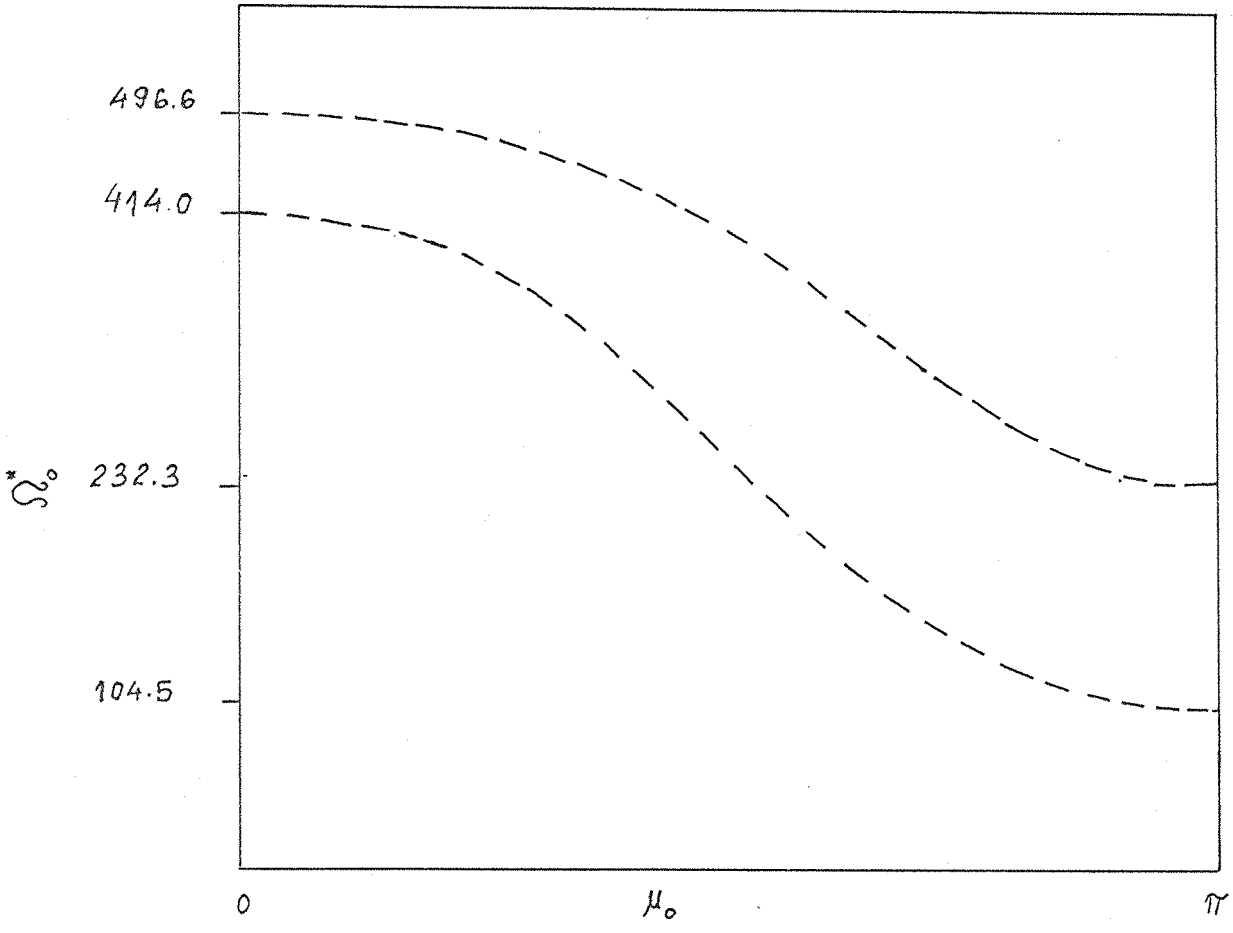

Lin's band limits [11]

fig. 6.3

$\Omega_0^* - \mu$ curves for a stringer-stiffened shell

$ASP = 3.0$, $\eta = 0.0$

fig. 6.4

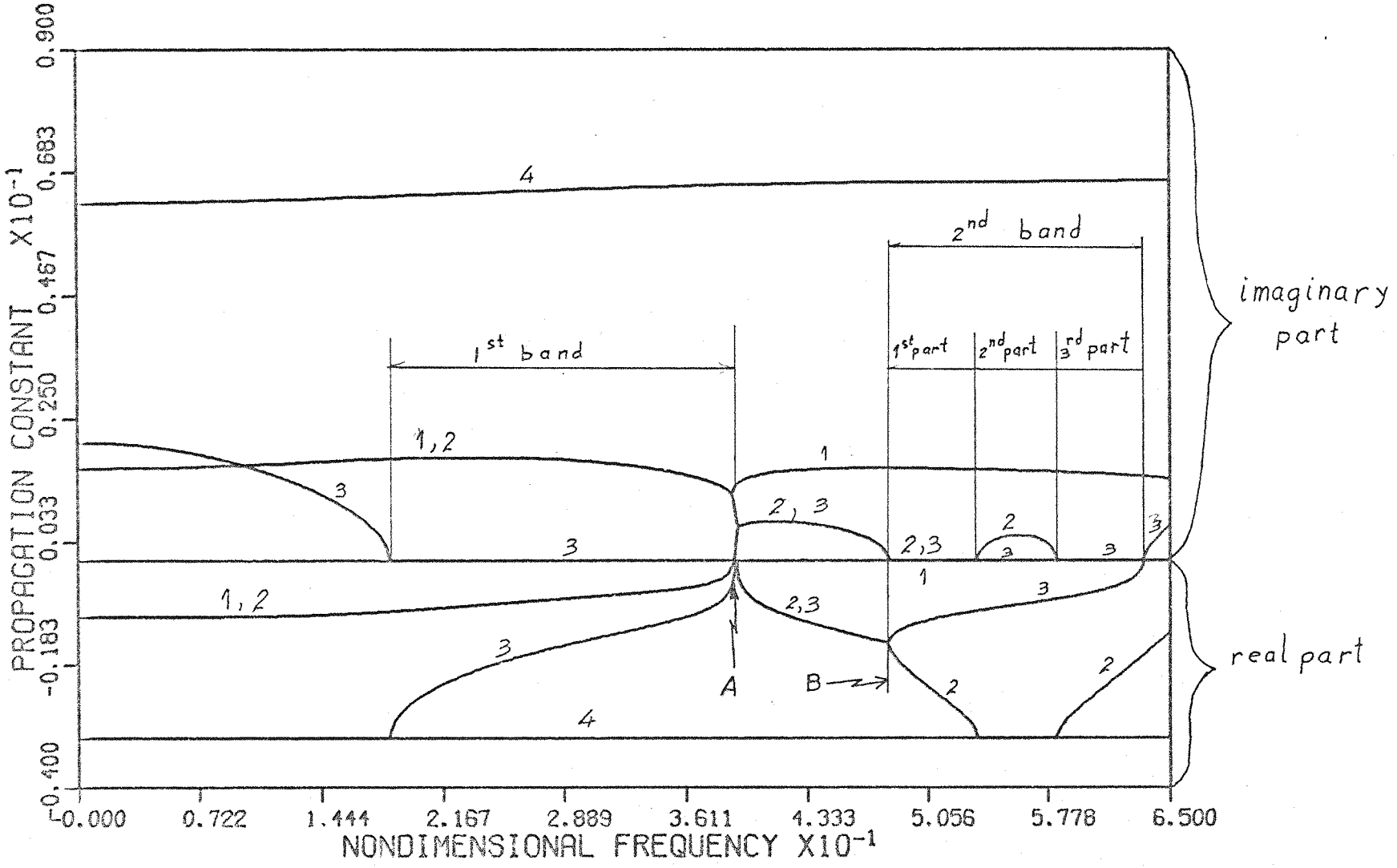

fig. 6.5

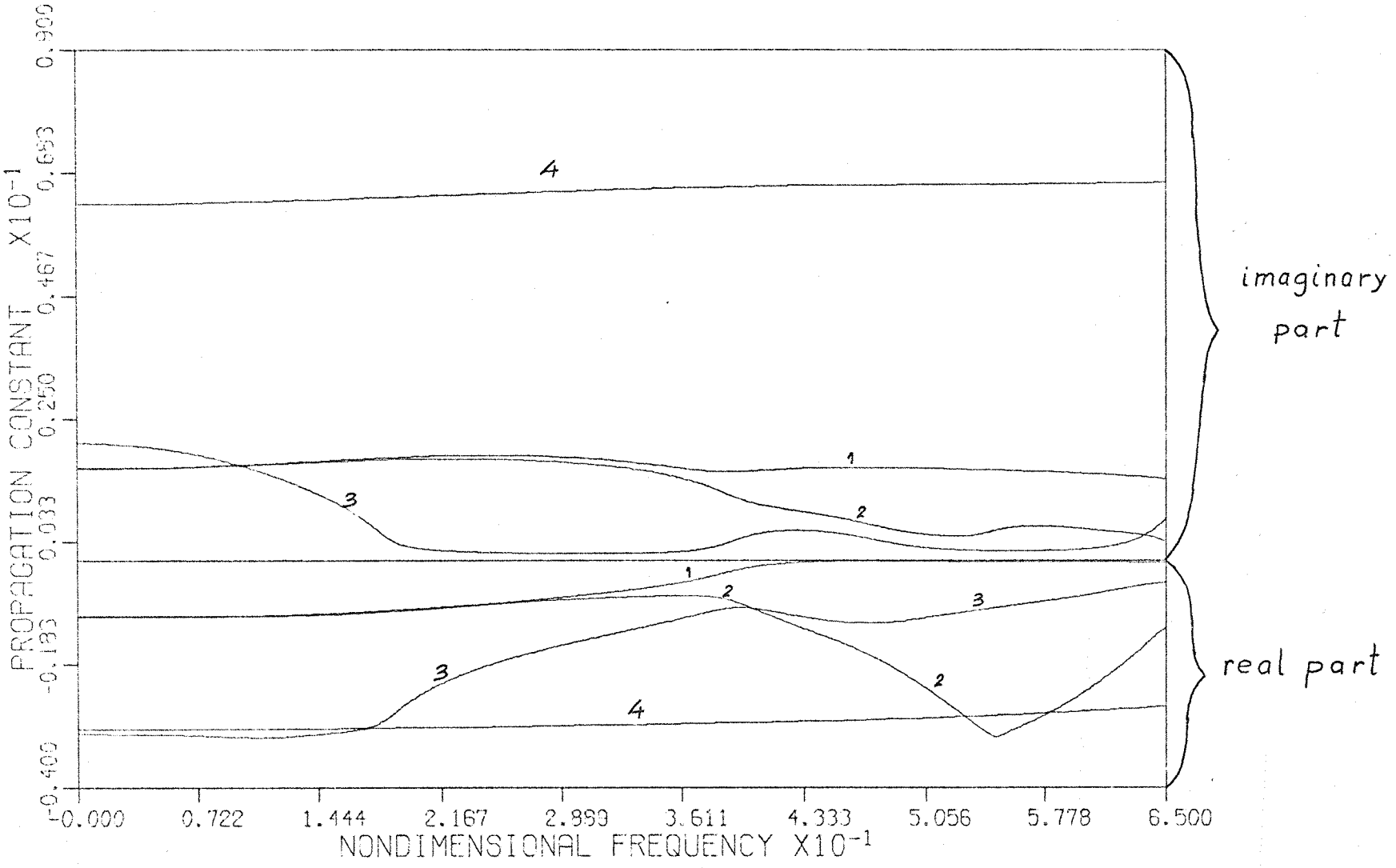

Ω_o^*-μ curves for a stringer-stiffened shell

$ASP = 3.0$, $\eta = 0.15$

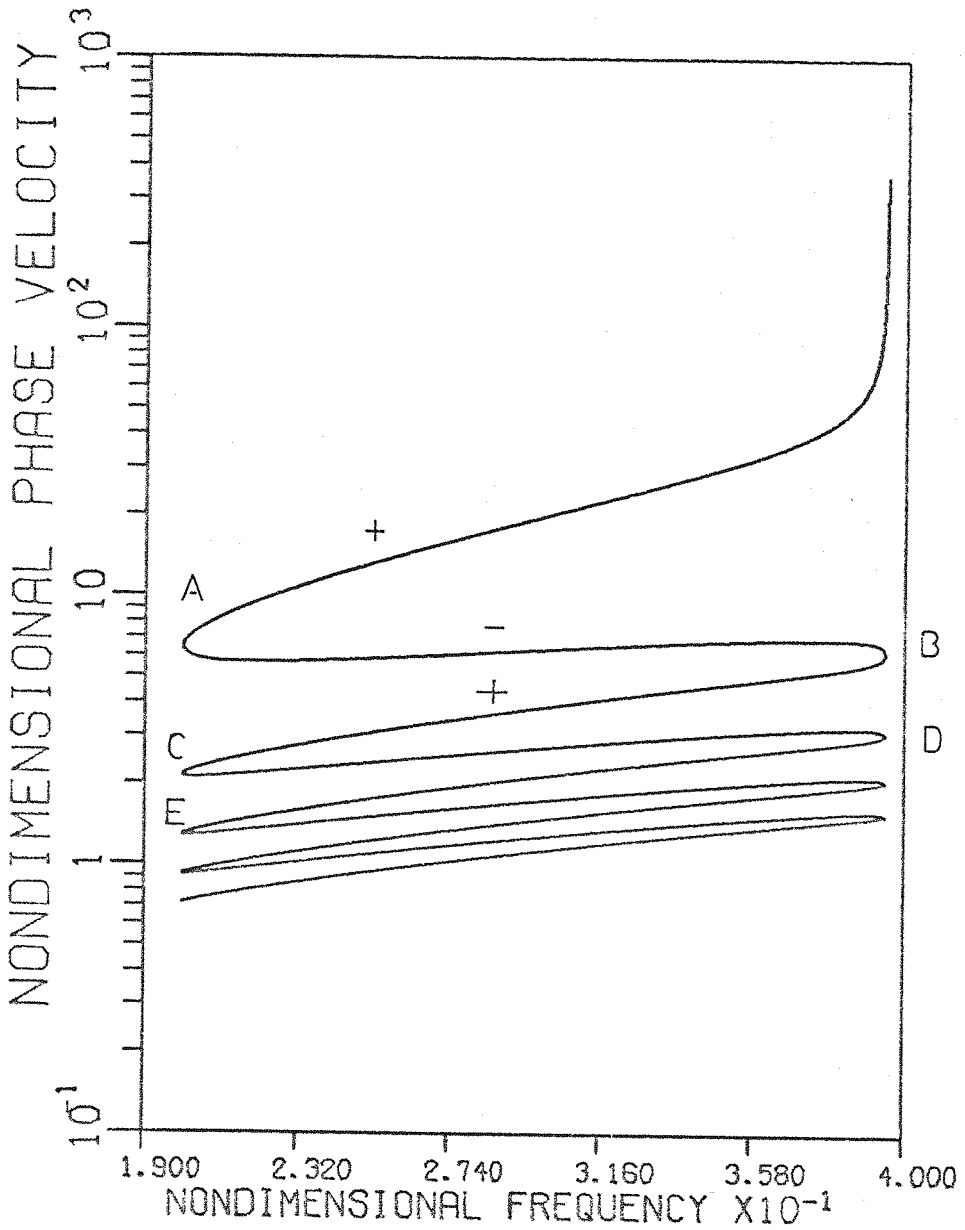
NONDIMENSIONAL PHASE VELOCITY
10^3
10^2
10
1
10^{-1}
A
B
C
D
E
+
−
+
1.900
2.320
2.740
3.160
3.580
4.000
NONDIMENSIONAL FREQUENCY X10^{-1}

fig. 6.6

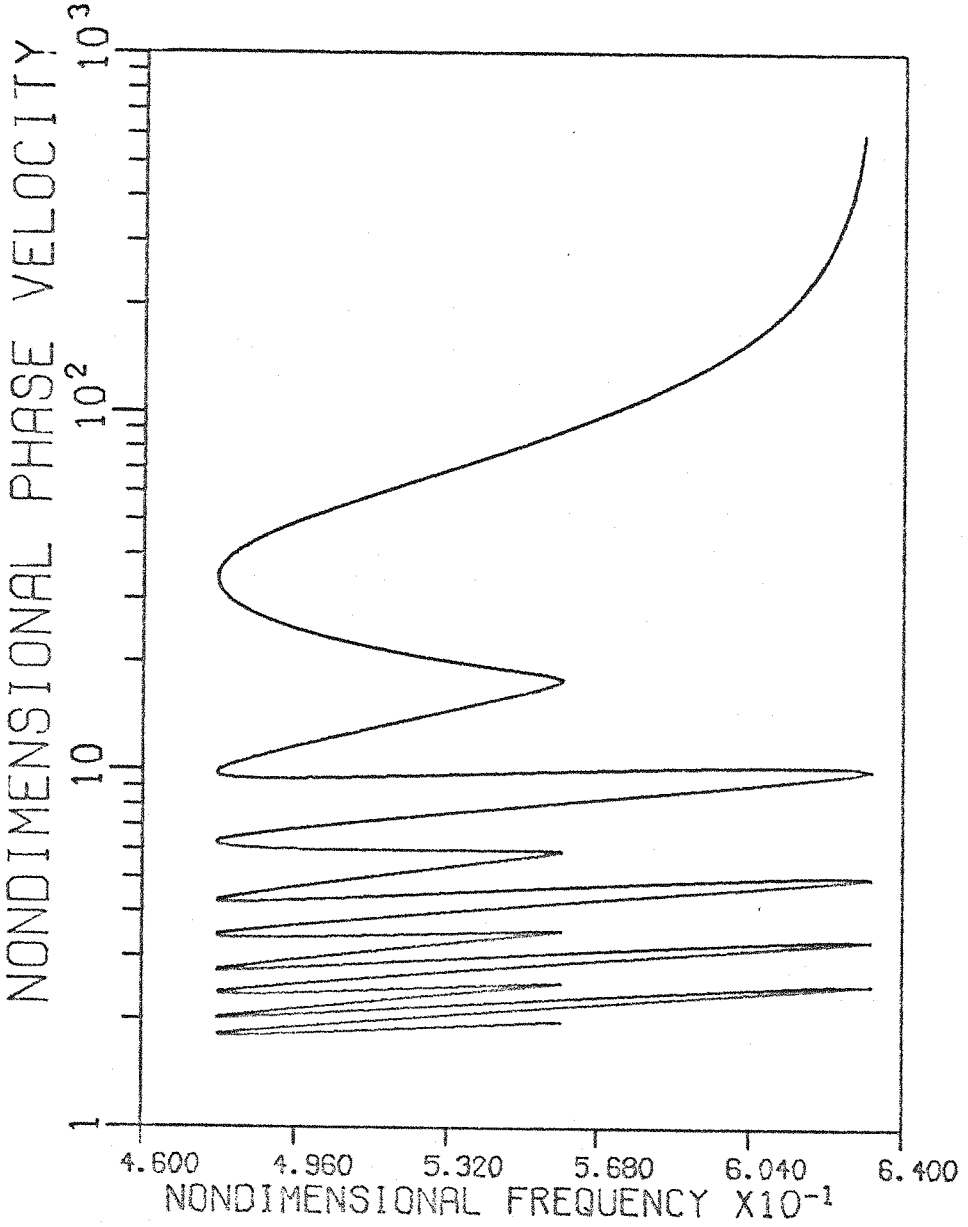
NONDIMENSIONAL PHASE VELOCITY
10^3
10^2
10
1
4.600
4.960
5.320
5.680
6.040
6.400
NONDIMENSIONAL FREQUENCY $X10^{-1}$

fig. 6.7

μ_0-Ω_0^* curves for a ring-stiffened cylinder

$r=5$

fig 6.8

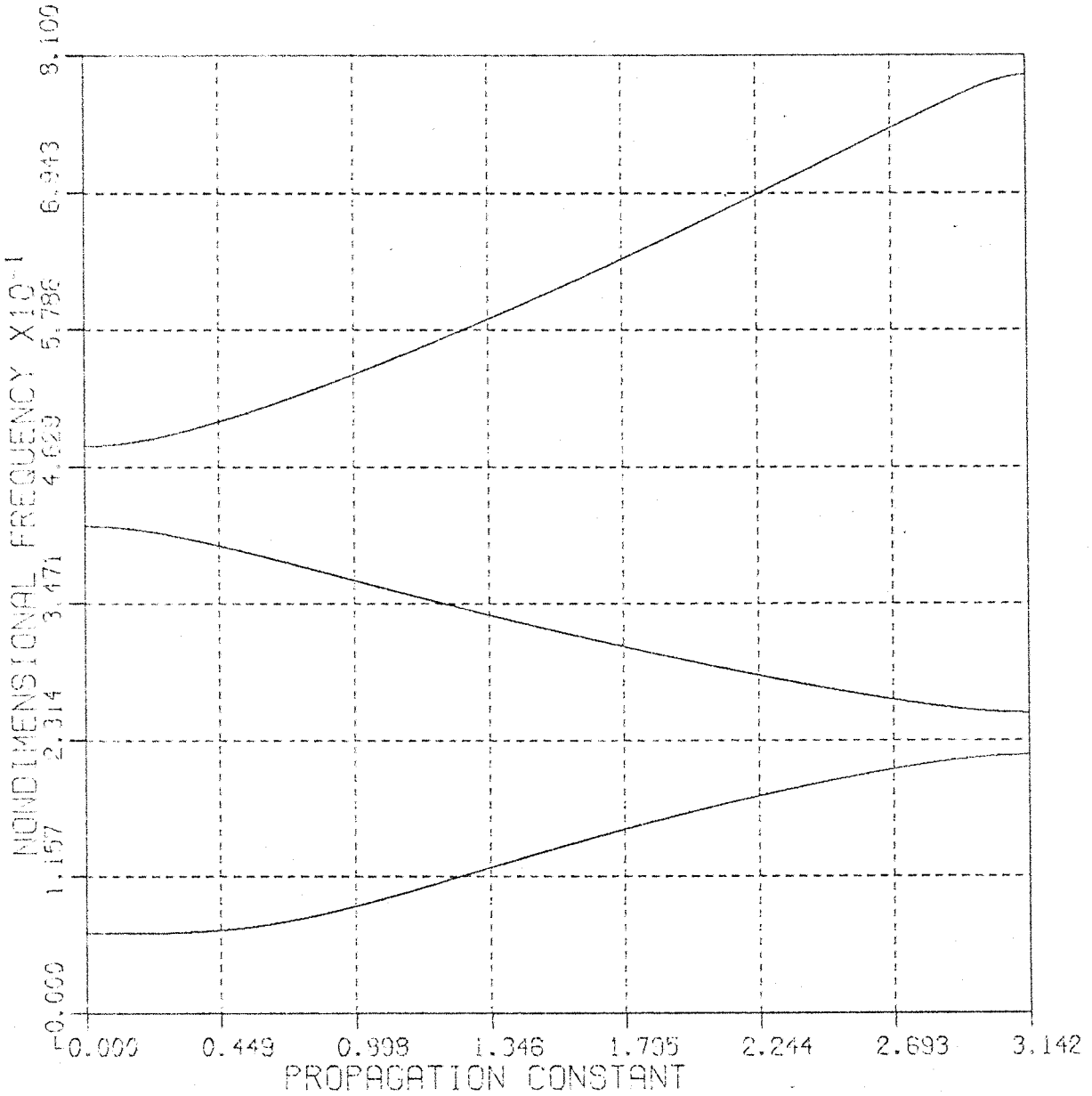

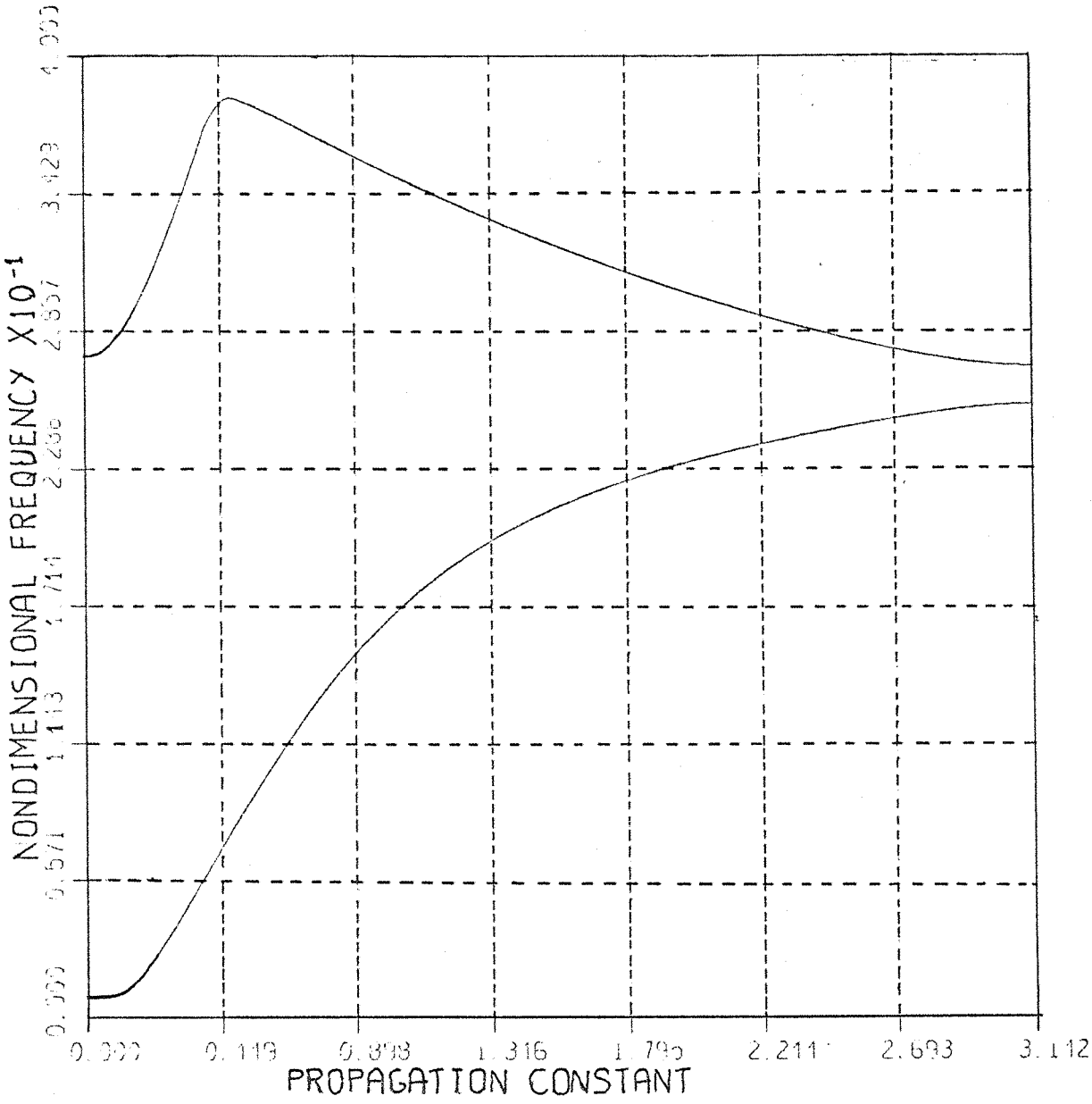

μ_o-Ω_o^* curves for a ring-stiffened cylinder

$r = 2$

fig 6.9

fig. 6.10

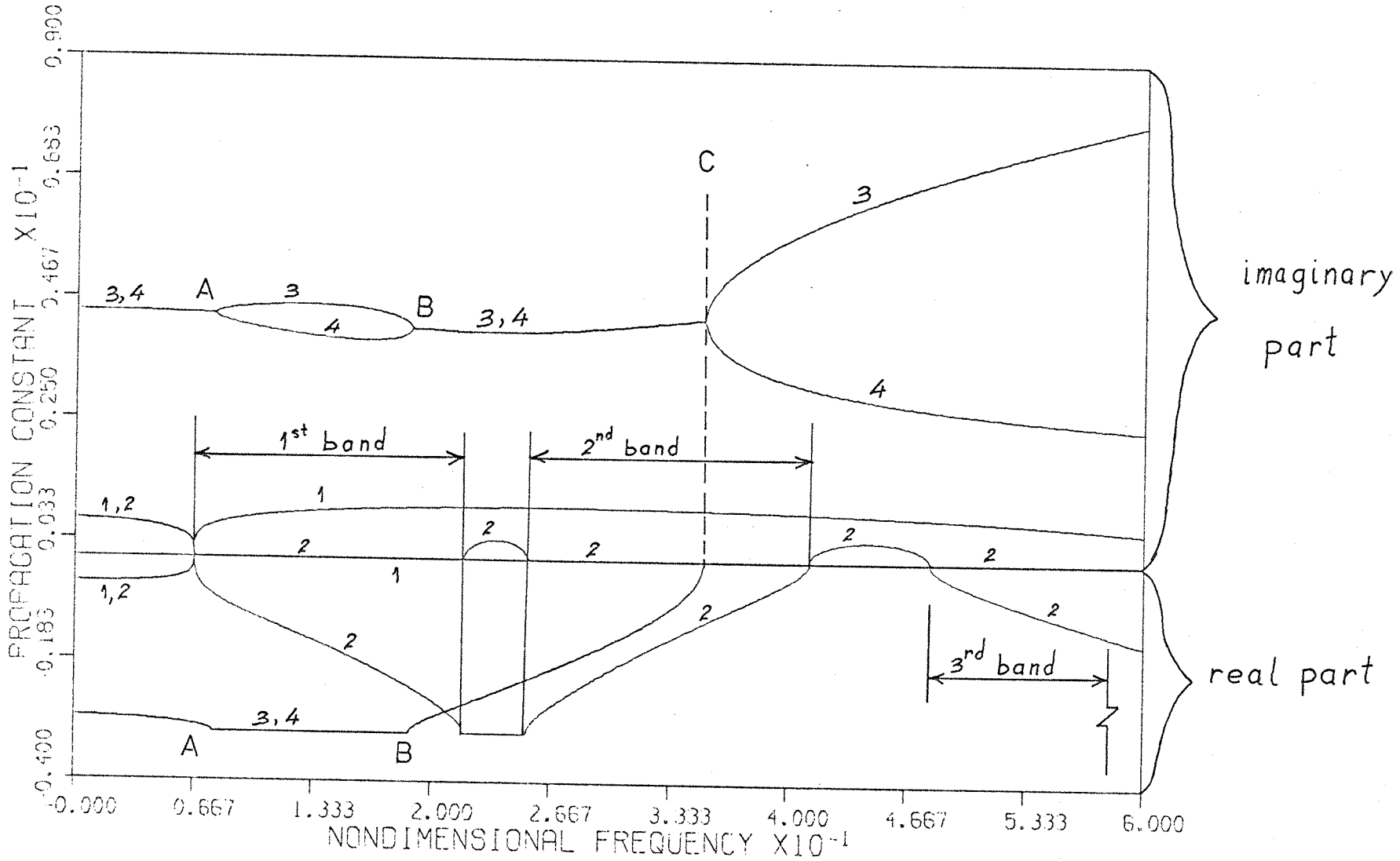

$\Omega_0^+ - \mu$ curves for a ring-stiffened cylinder

$r = 5$, $\eta = 0.0$

fig. 6.11

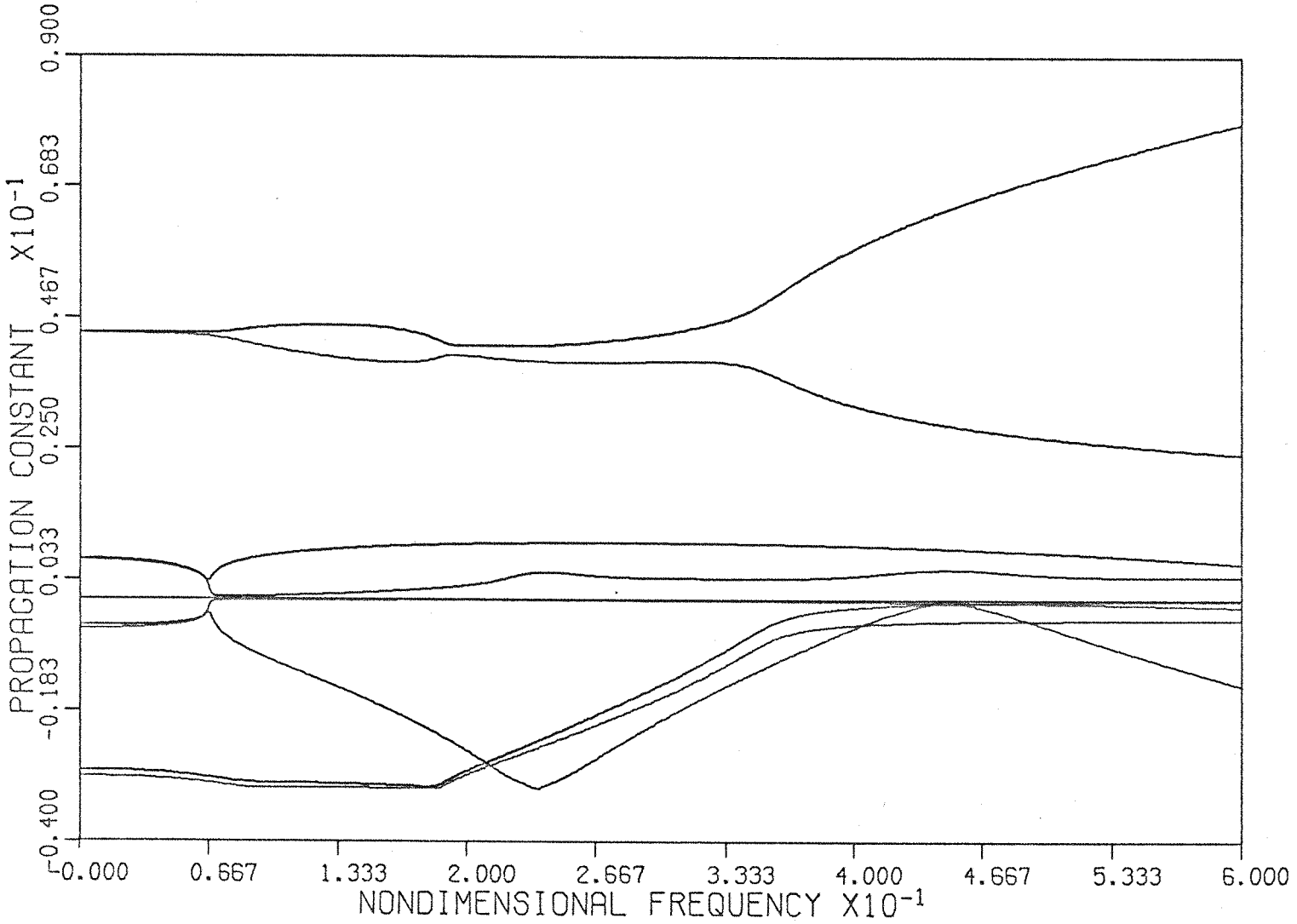

Ω_o^*-μ curves for a ring-stiffened cylinder

$r = 5$, $\eta = 0.15$

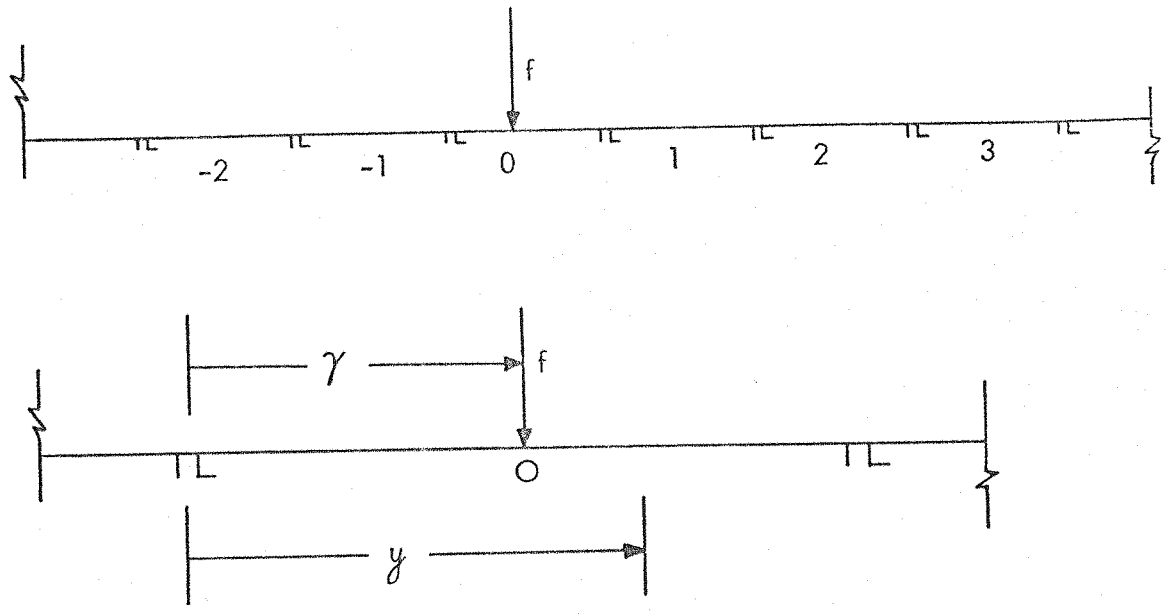

FIG. 7.1

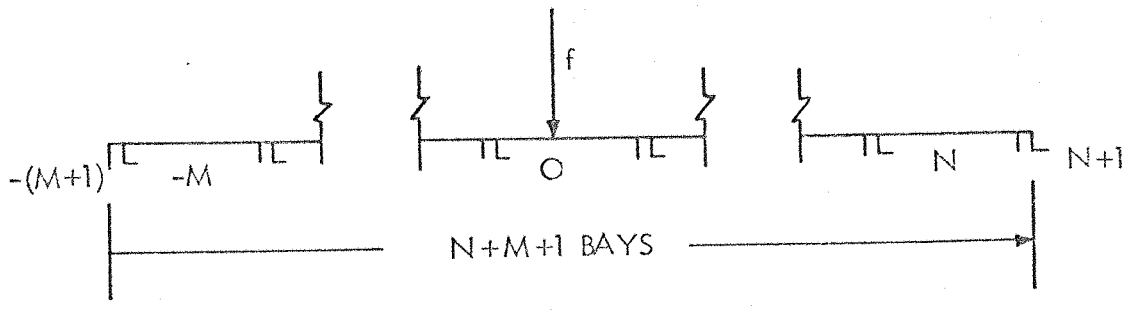

FIG. 7.2

Amplitude response of an infinite stringer-stiffened plate to a concentrated harmonic force applied at the middle of a bay.

curve 1: $\Omega_o^* = 18.175$, curve 2: $\Omega_o^* = 0.10$

$\eta = 0.0$, $r = 1$

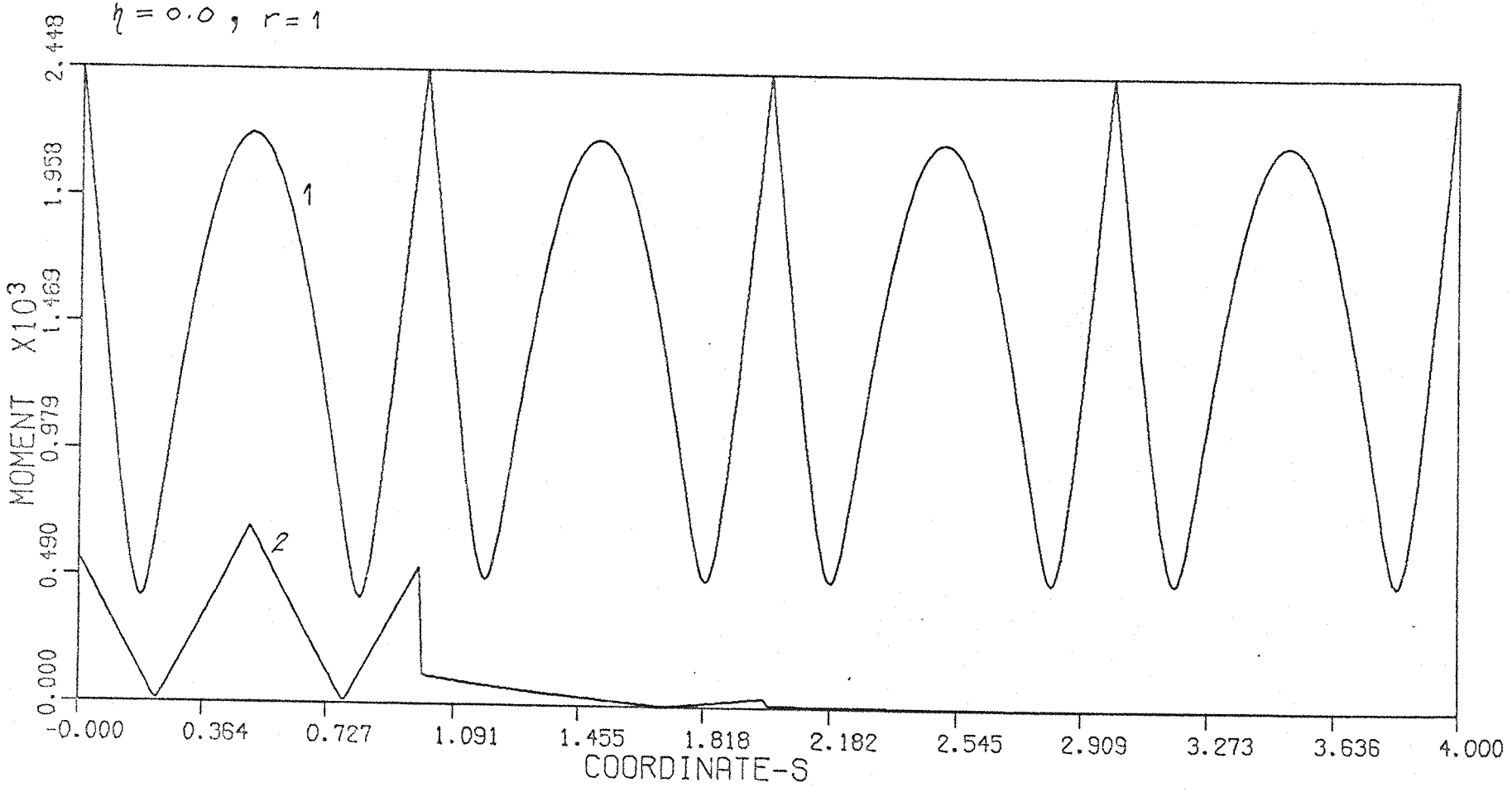

fig. 7.3

Amplitude response of an infinite stringer-stiffened plate to a concentrated harmonic force applied at the middle of a bay.

Curve 1: $\Omega_o^* = 18.175$, Curve 2: $\Omega_o^* = 0.10$.

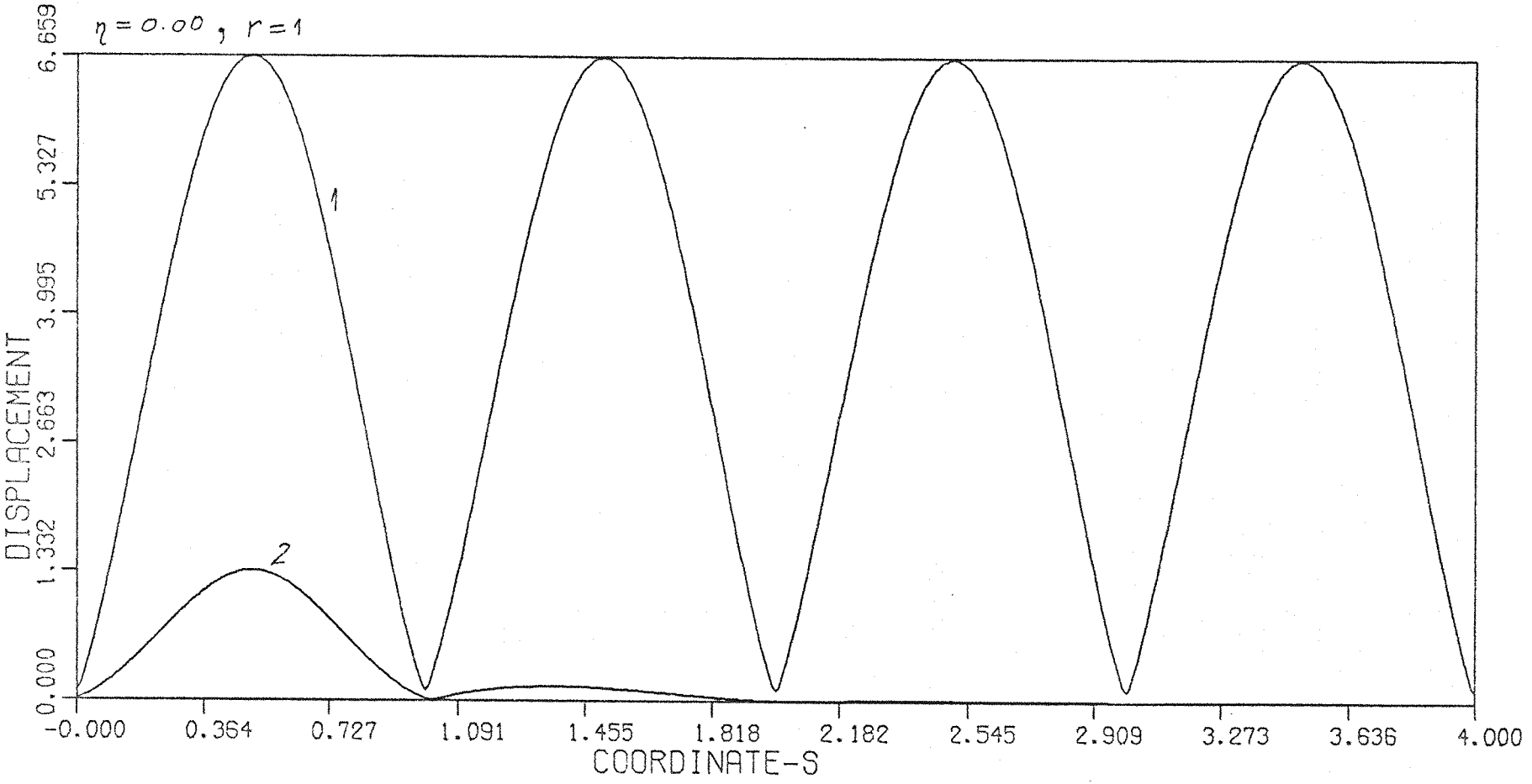

fig. 7.4

fig. 7.5

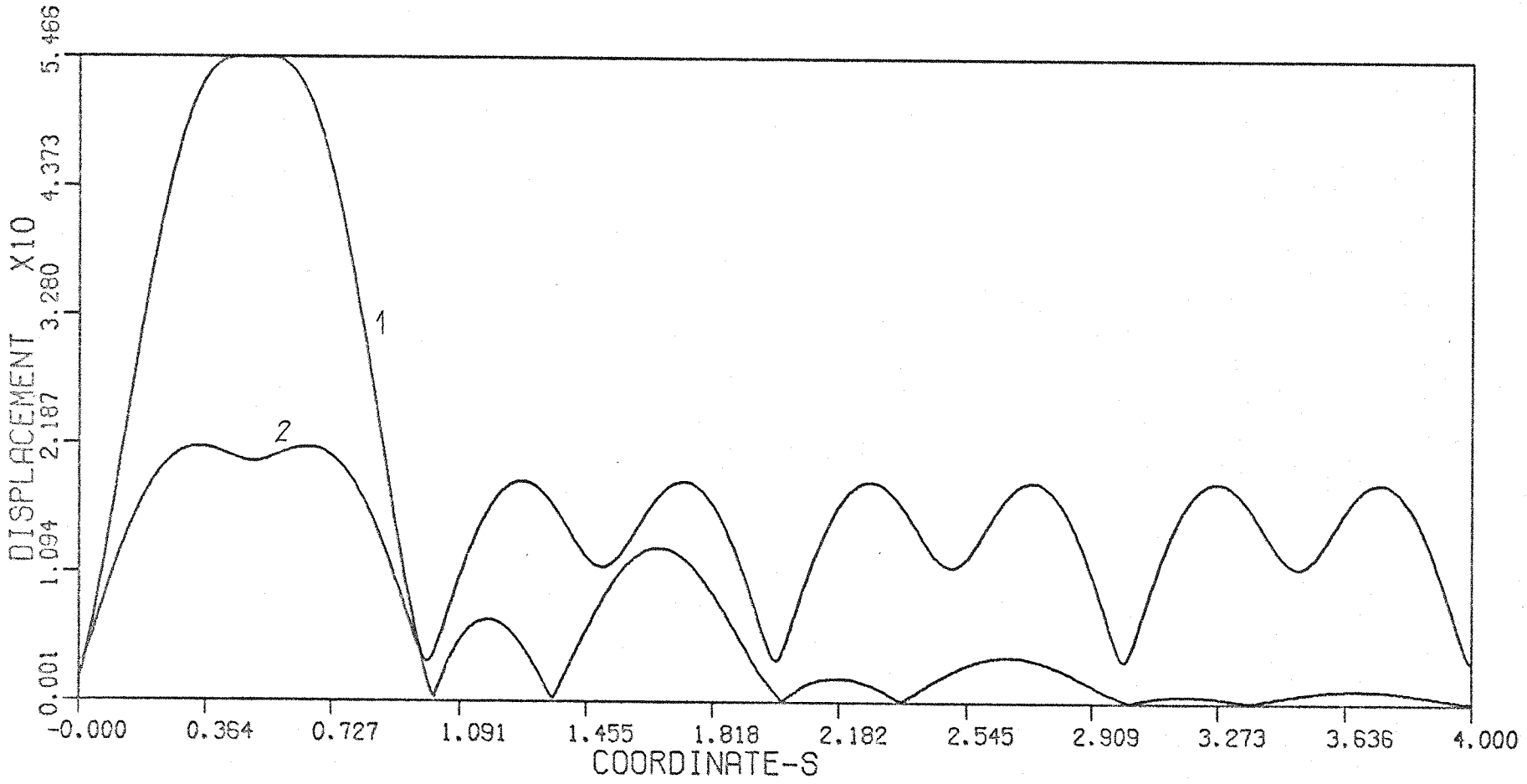

Amplitude response of infinite stringer-stiffened plate to a harmonic force applied at middle of a bay.

Curve 1: $\Omega_o^* = 49.363$, Curve 2: $\Omega_o^* = 34.10, \eta = 0.0, r = 1$

fig. 7.6

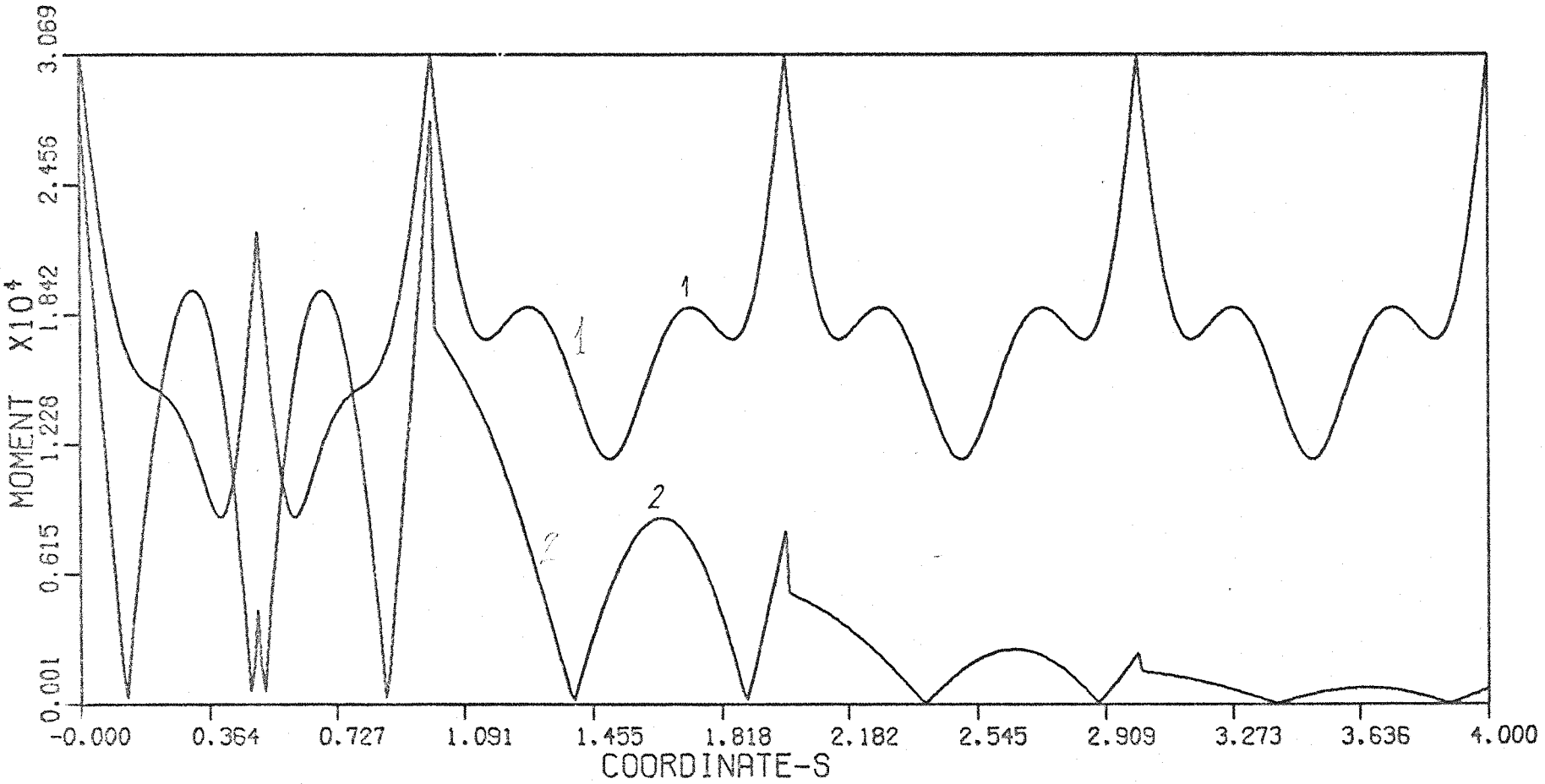

Amplitude response of an infinite stringer-stiffened plate to a concentrated harmonic force applied at the middle of a bay.

Curve1 : $\Omega_0^* = 49.363$, Curv2 : $\Omega_0^* = 34.10$, $\eta = 0.0$, $r = 1$

fig. 7.7

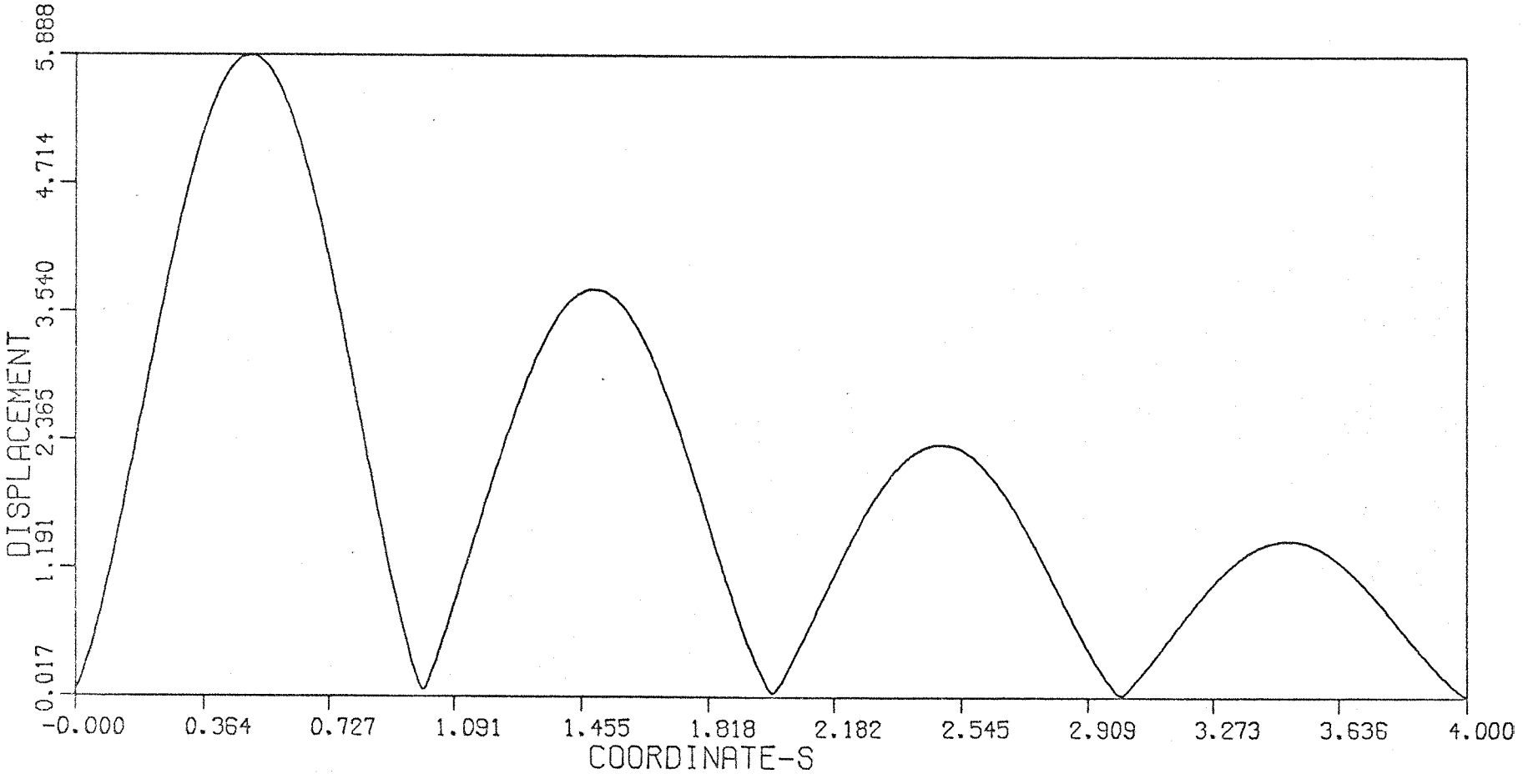

Amplitude response of infinite stringer-stiffened plate to a harmonic force applied at the middle of a bay.

$\Omega_o^* = 18.176$, $\eta = 0.15$, $r = 1$

fig. 7.8

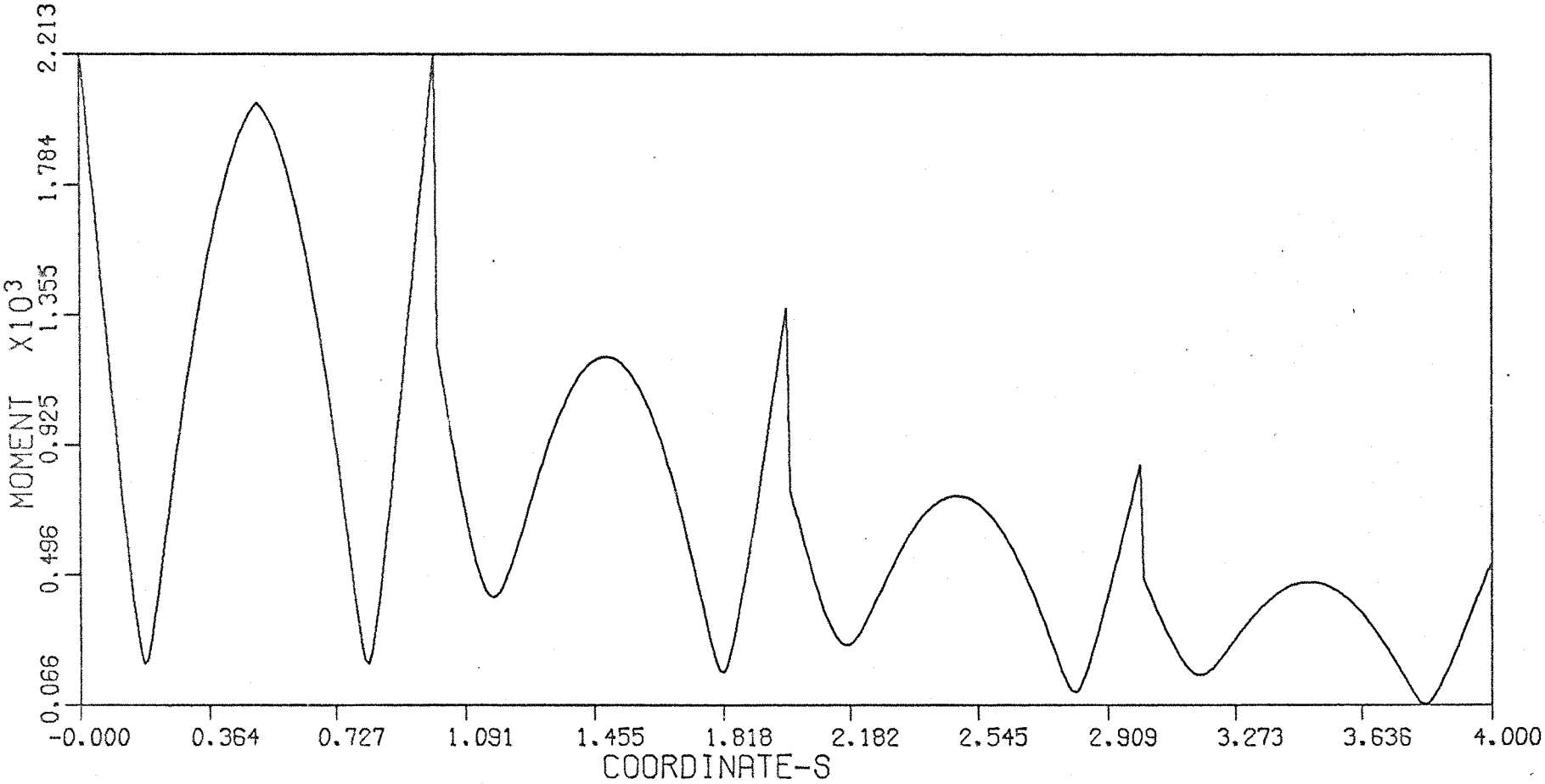

Amplitude response of an infinite stringer-stiffened plate to a harmonic force applied at the middle of a bay.

$\Omega_o^* = 18.176$, $\eta = 0.15$

fig.7.9

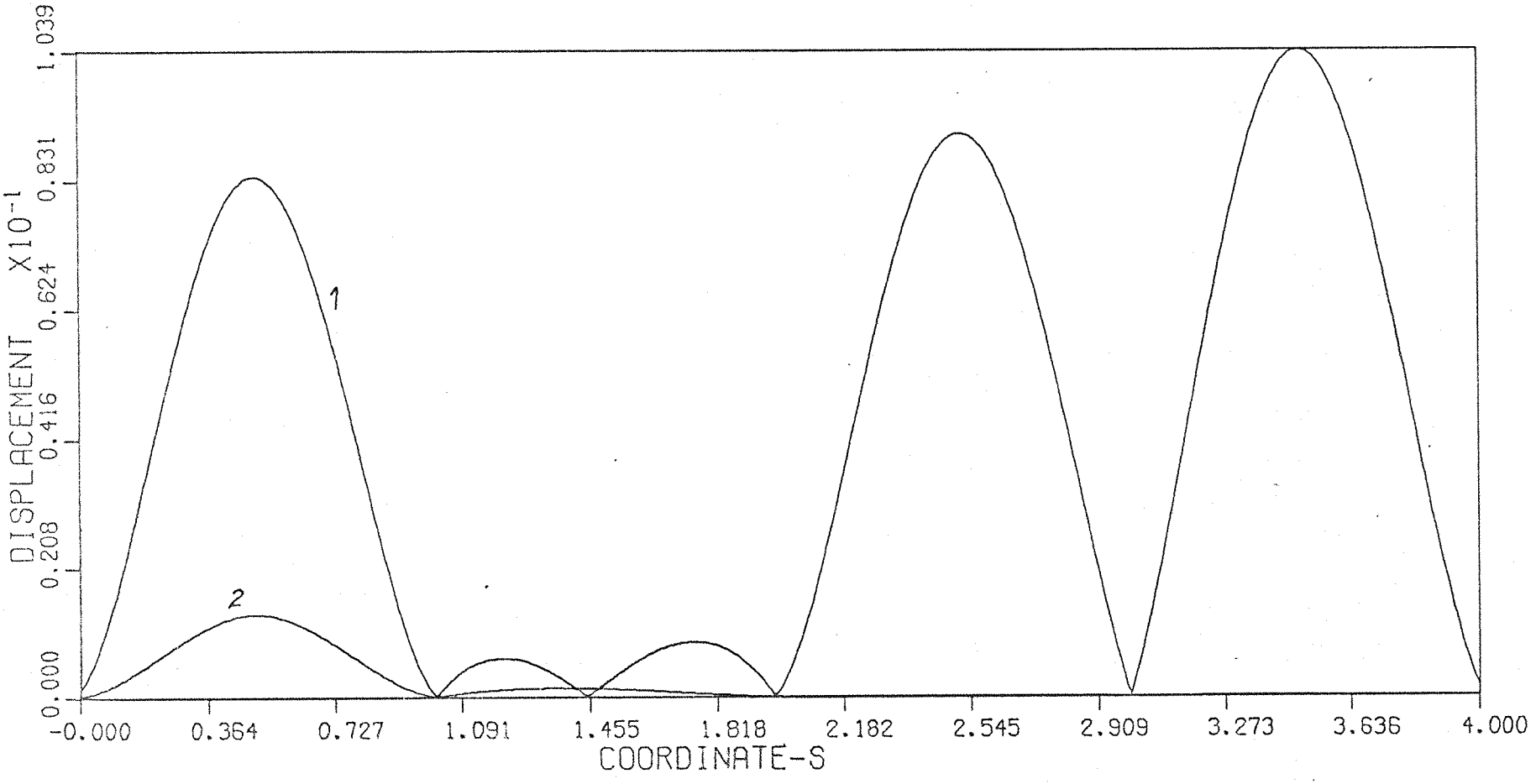

Amplitude response of a 7 bay stringer-stiffened plate to a harmonic force applied at the middle of the structure.

Curve 1: $\Omega_o^* = 18.175$, Curve 2: $\Omega_o^* = 0.10$, $\eta = 0.0$, $r = 1$

Amplitude response of a 7 bay stringer-stiffened plate to a harmonic force applied at the middle of structure.

Curve : $\Omega_o^* = 18.175$, Curve 2 : 0.10 , $\eta = 0.0$, $r = 1$

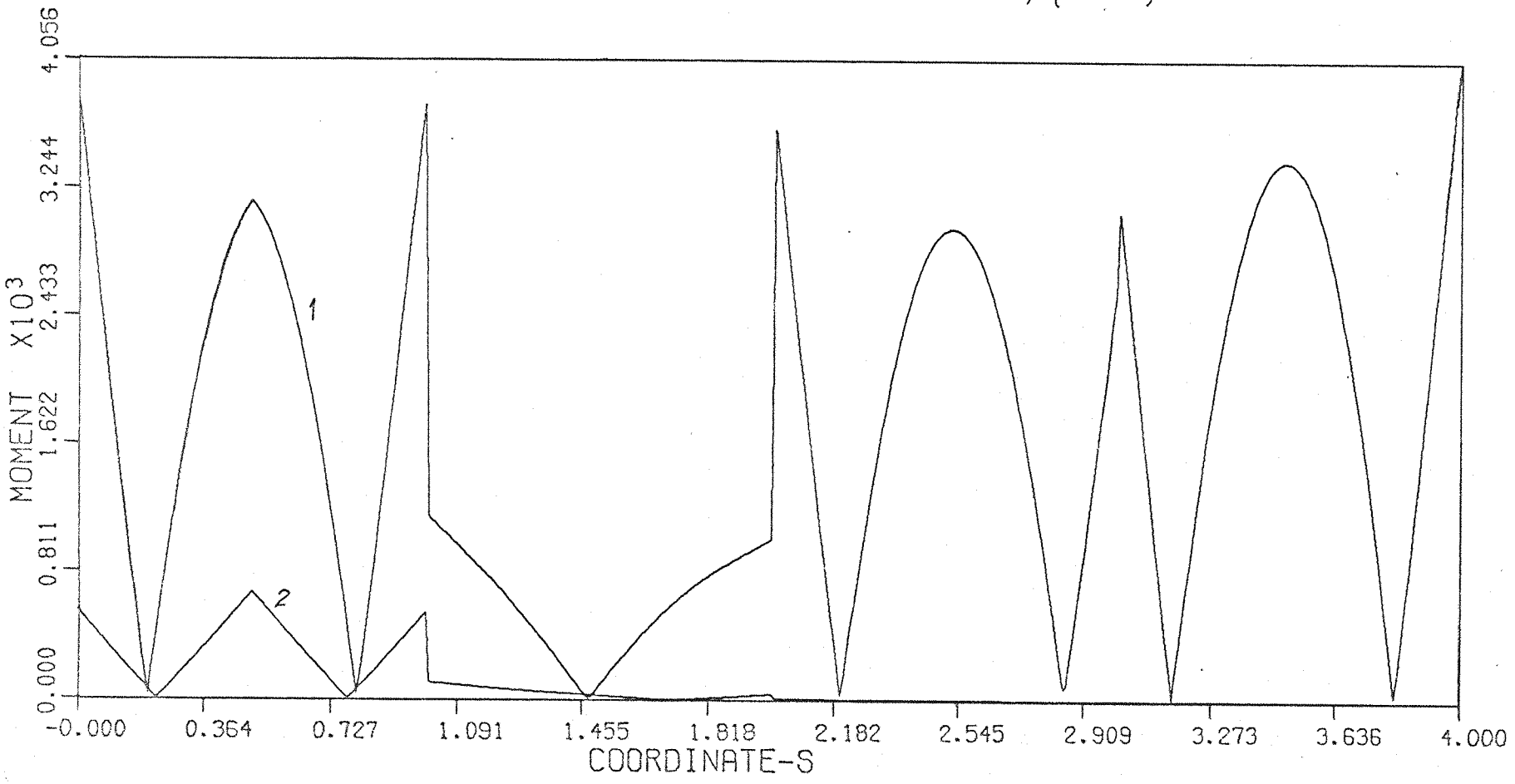

fig. 7.10

fig. 7.11

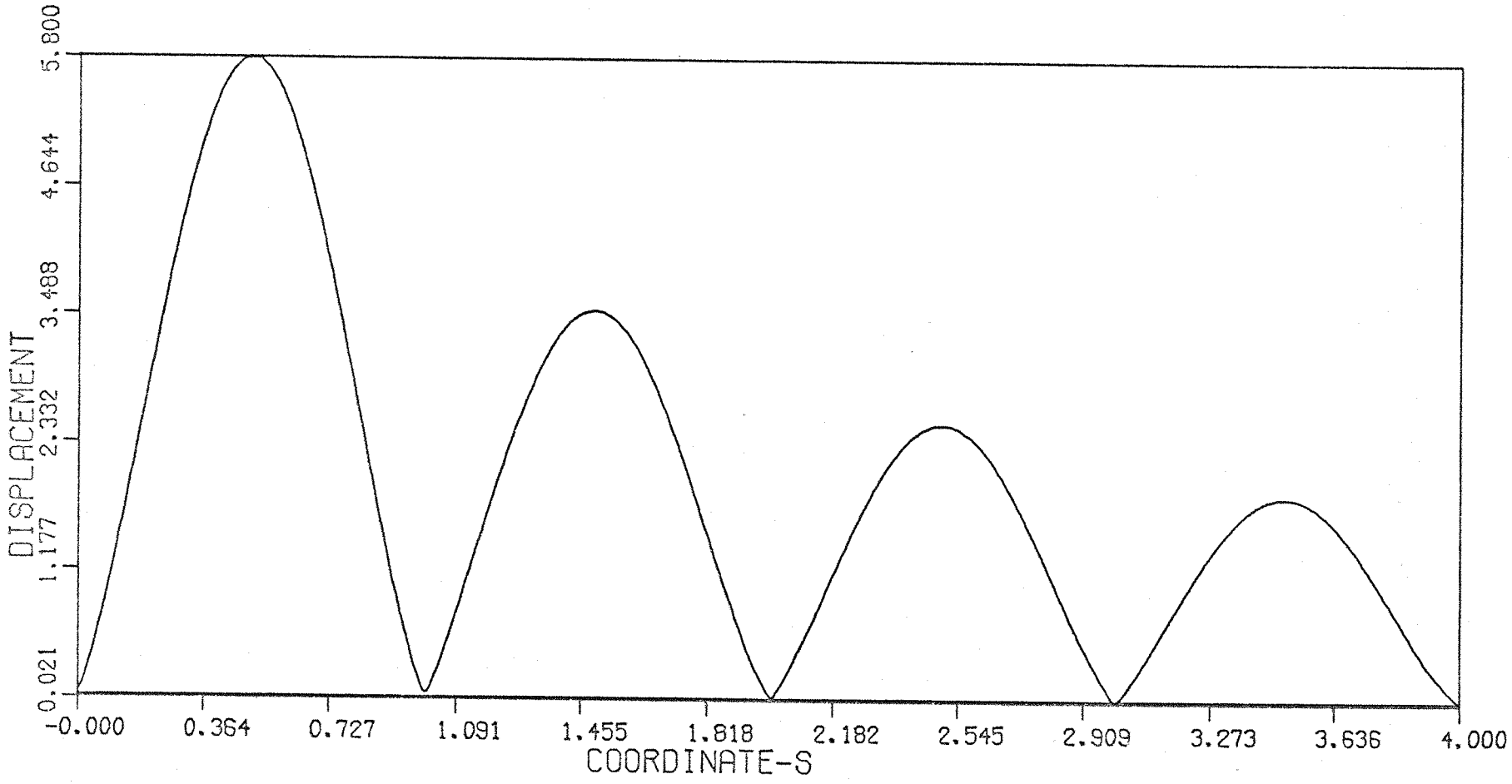

Amplitude response of a 7 bay stringer-stiffened plate to a harmonic force applied at the middle of the structure.

$\Omega_o^* = 18.175$, $\eta = 0.15$, $r = 1$

fig. 7.12

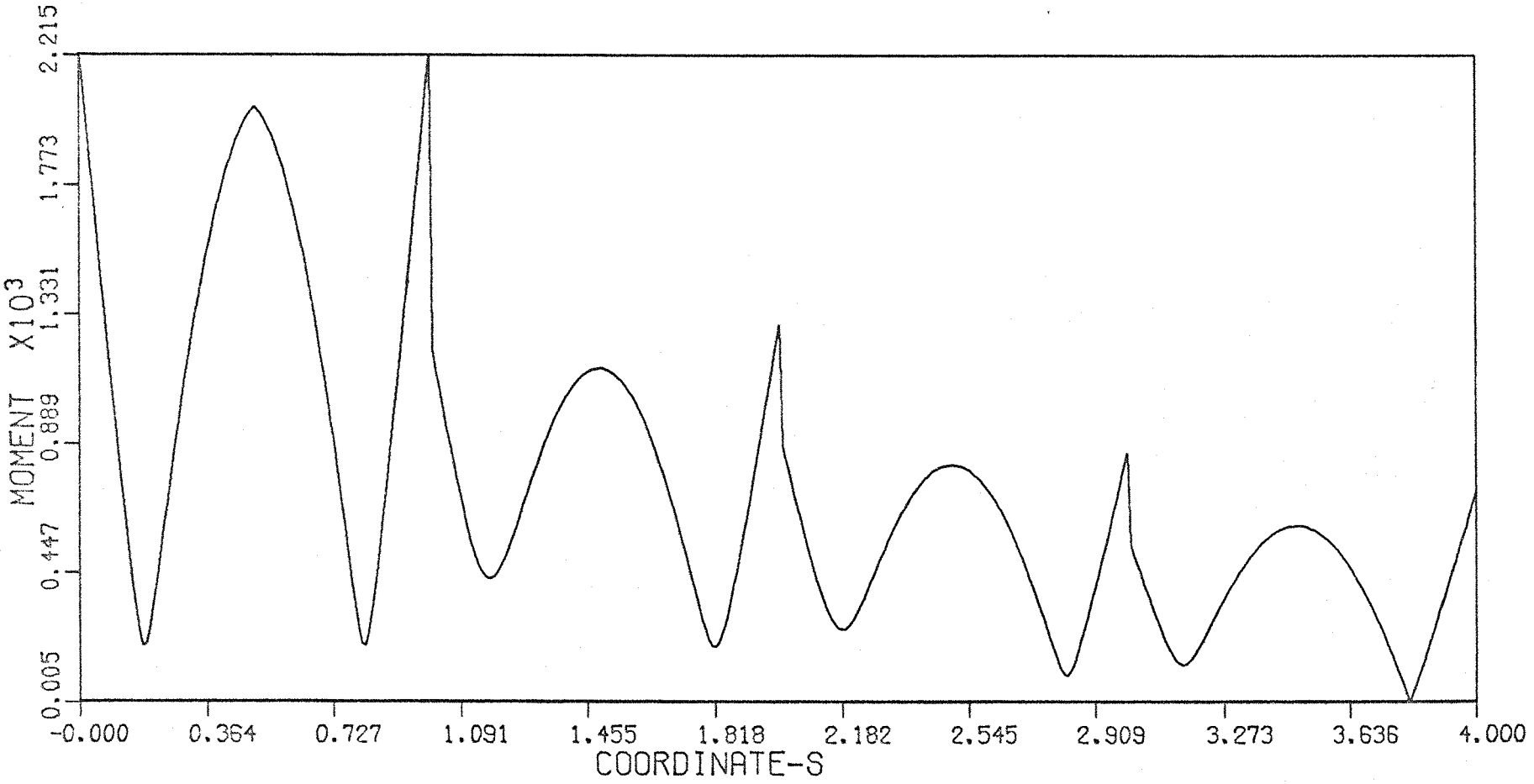

Amptitude response of a 7 bay stringer-stiffened plate to a harmonic force applied at the middle of the structure.

$\Omega_0^* = 18.175$, $\eta = 0.15$, $r = 1$

fig. 7.13

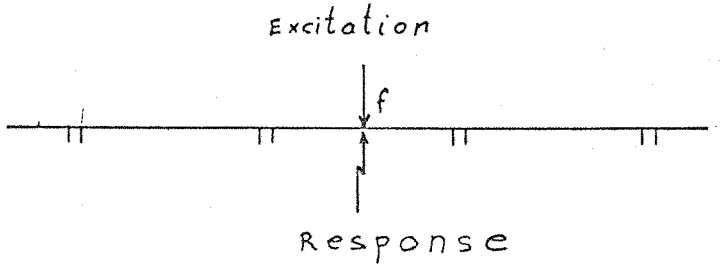

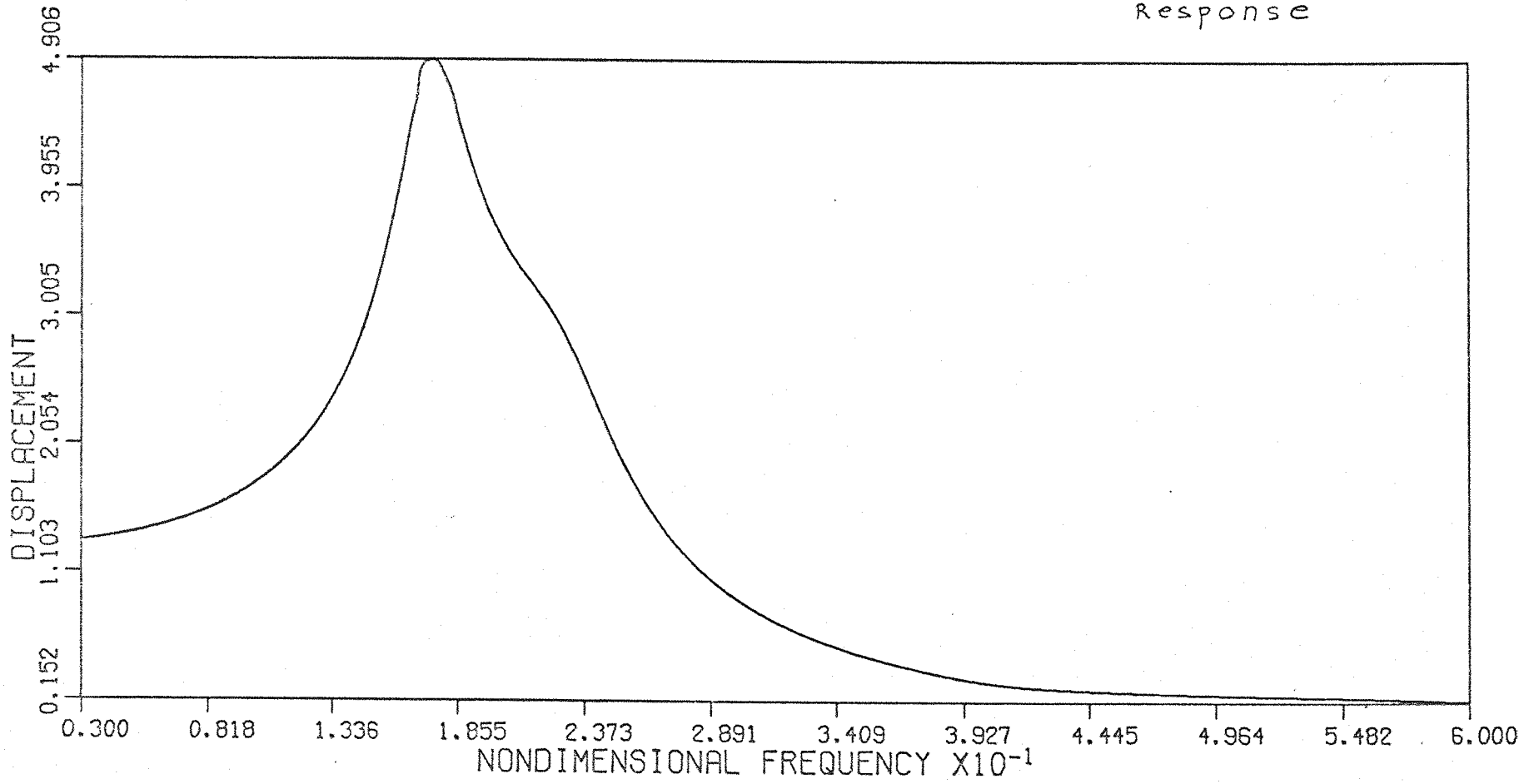

Magnitude of transverse displacement versus frequency for an infinite stringer-stiffened plate. $\eta = 0.25$, $r = 1$

fig. 7.14

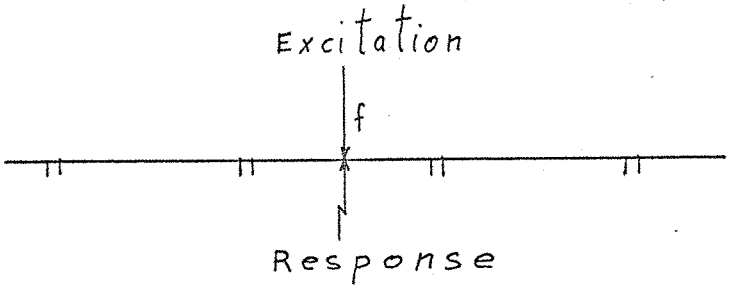

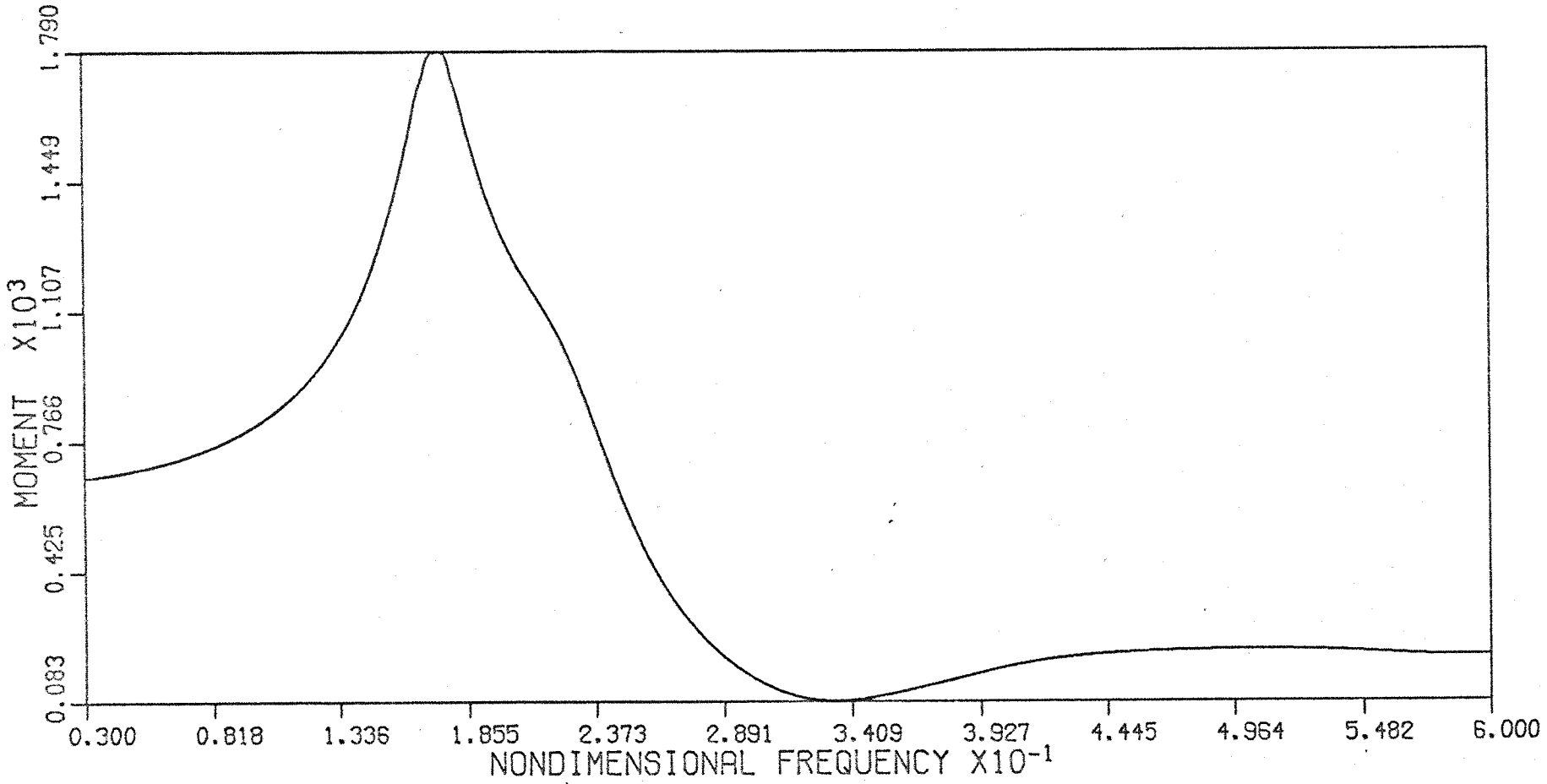

Magnitude of the bending momont versus frequency for an infinite stringer-stiffened plate. $\eta = 0.25$, $r = 1$

fig. 7.15

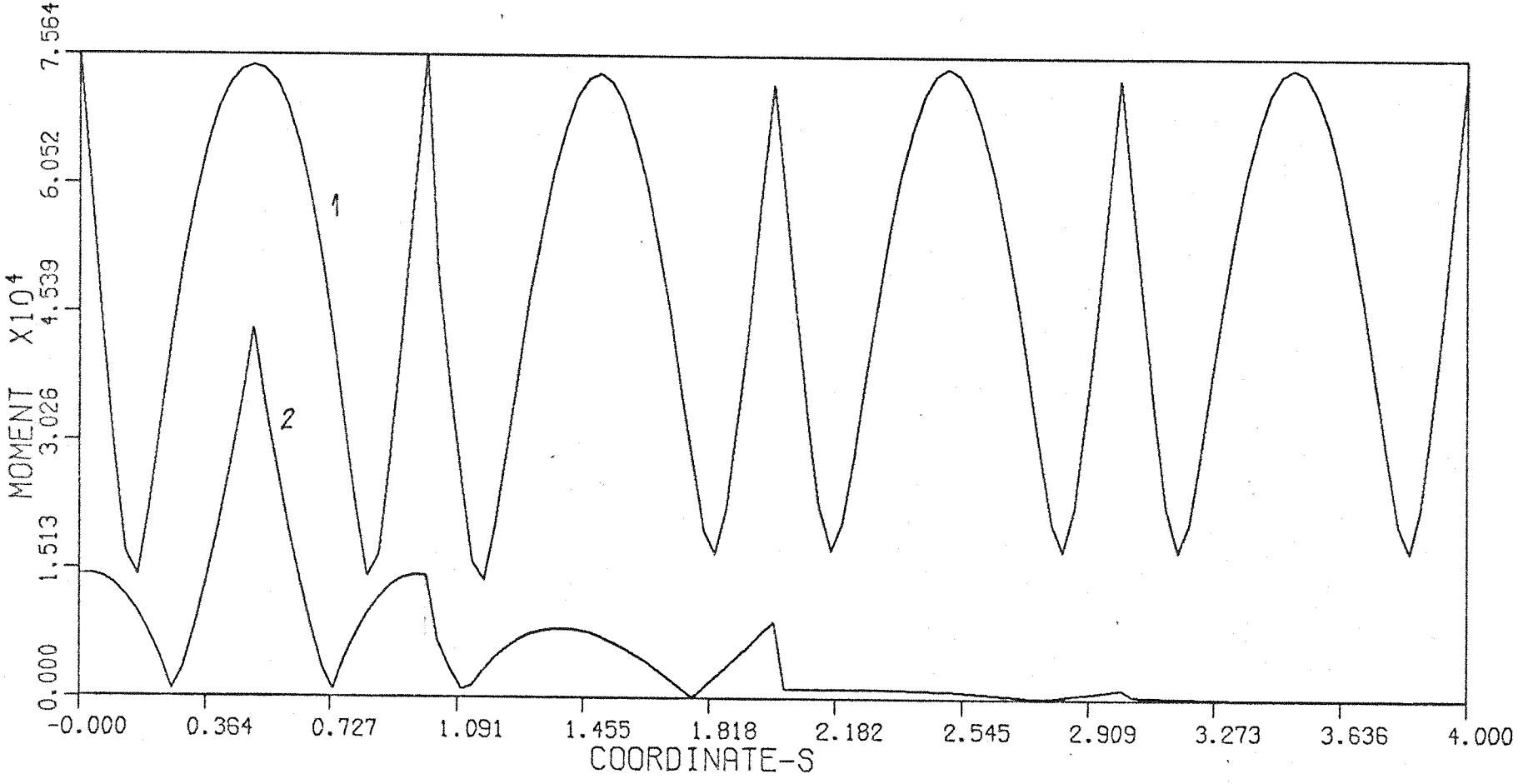

Amplitude response of an infinite stringer-stiffened shell to a harmonic force applied at the middle of a bay.

Curve1: $\Omega_o^* = 22.10$, Curve2: $\Omega_o^* = 0.65$, $\eta = 0.0$, $r = 1$.

fig. 7.16

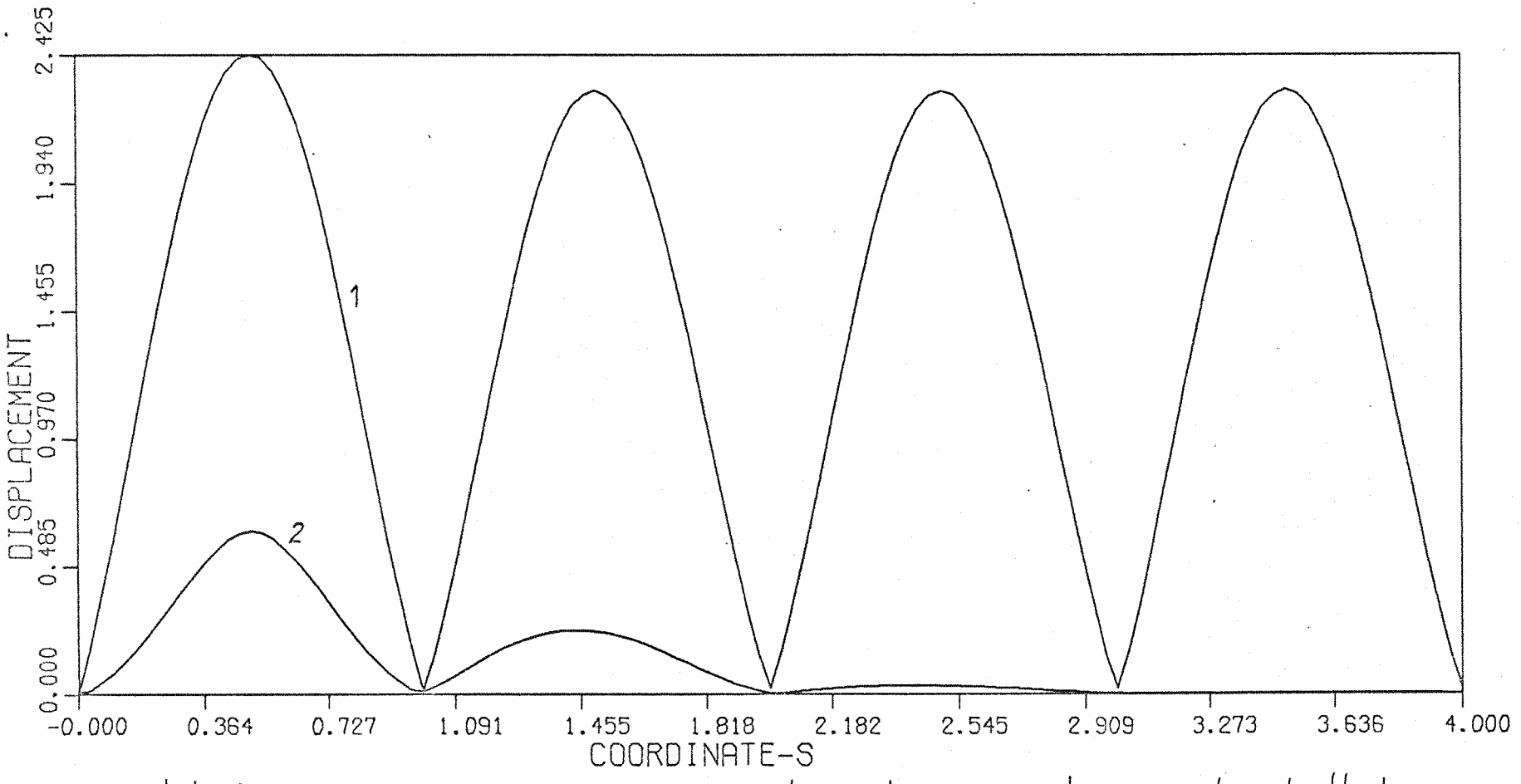

Amplitude response of an infinite stringer-stiffened shell to a harmonic force applied at the middle of a bay

Curve 1: $\bar{\Omega}_0^* = 22.10$, Curv 2: $\bar{\Omega}_0^* = 0.65$, $\eta = 0.0$, $r = 1$

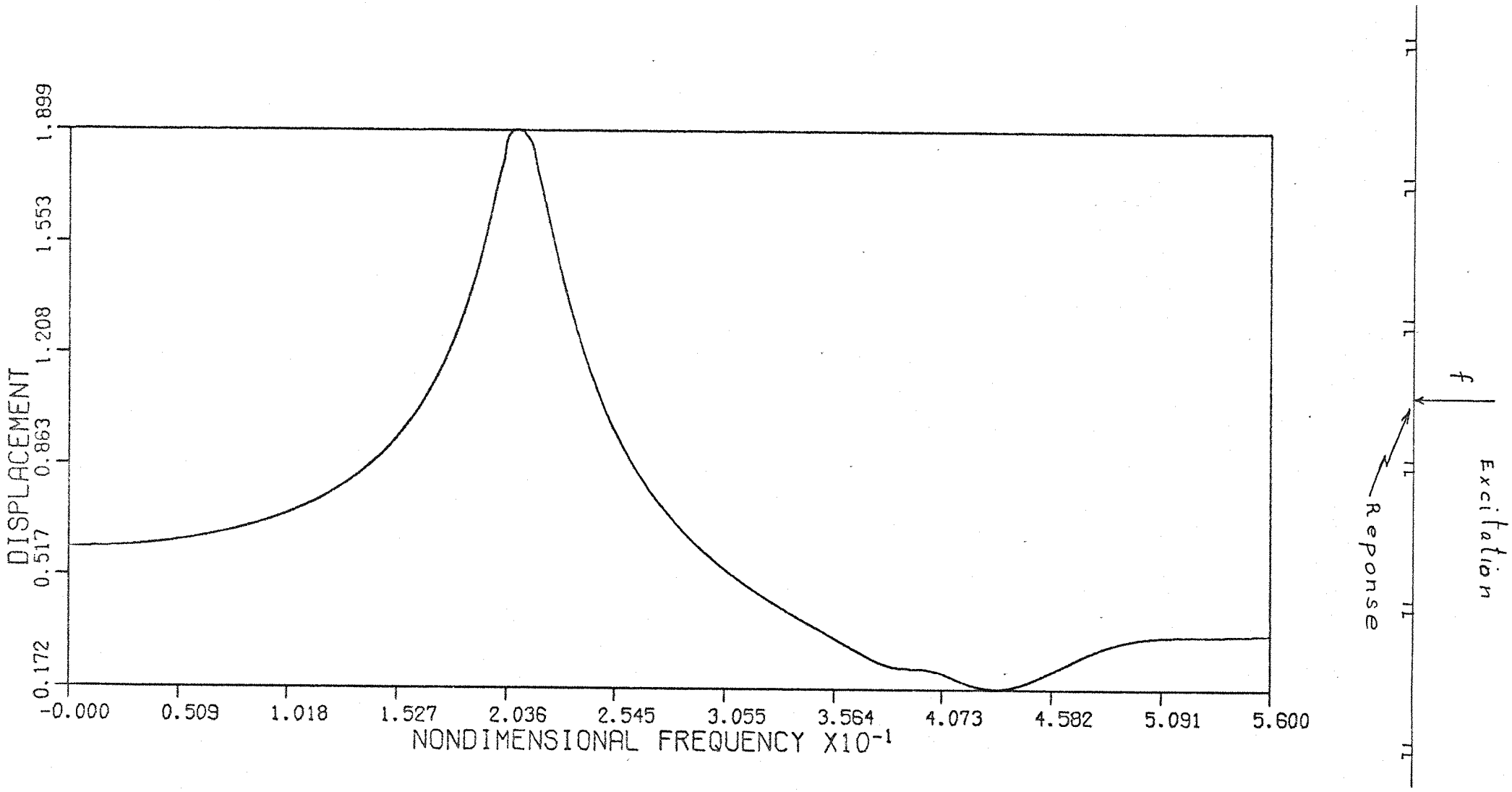

Magnitude response versus nondimensional frequency for a stringer-stiffened shell excited by a harmonic force. $\eta = 0.25$, $r = 1$

fig. 7.17

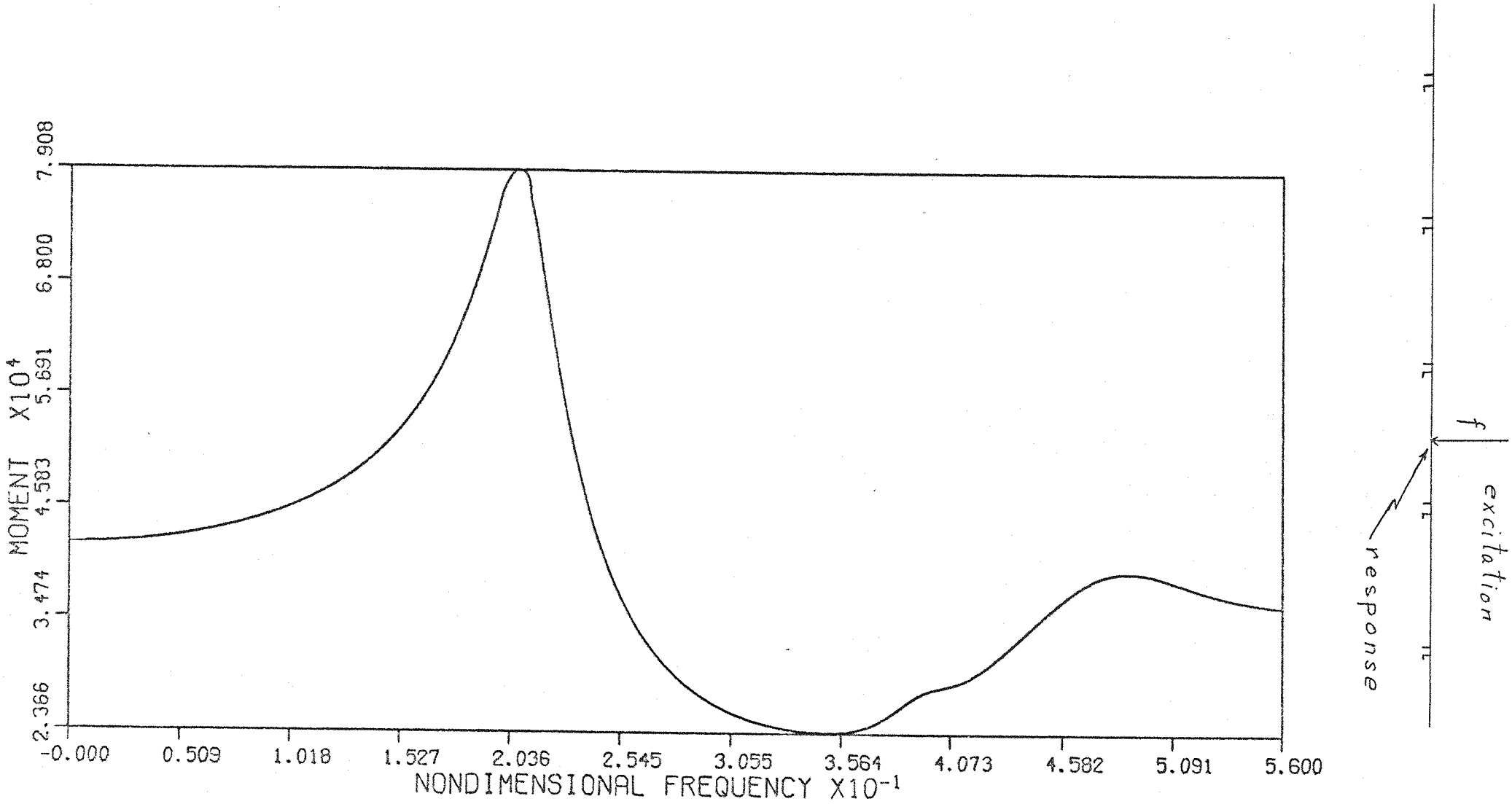

Magnitude response versus nondimensional frequency for a stringer-stiffened shell excited by a harmonic force. $\eta = 0.25$, $r = 1$

fig. 7.18

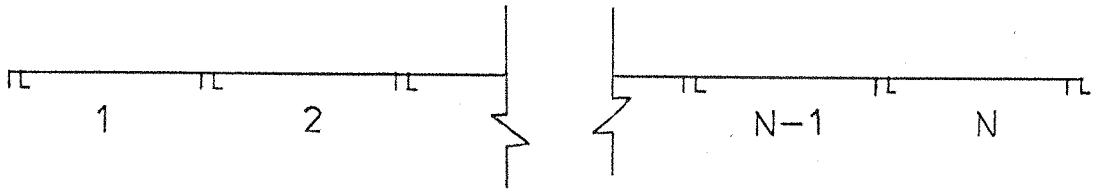

fig. 8.1

Magnitude response of an infinite stringer-stiffened plate to a convected harmonic pressure field. (middle of a bay).

$\eta = 0.25$, $r = 1$.

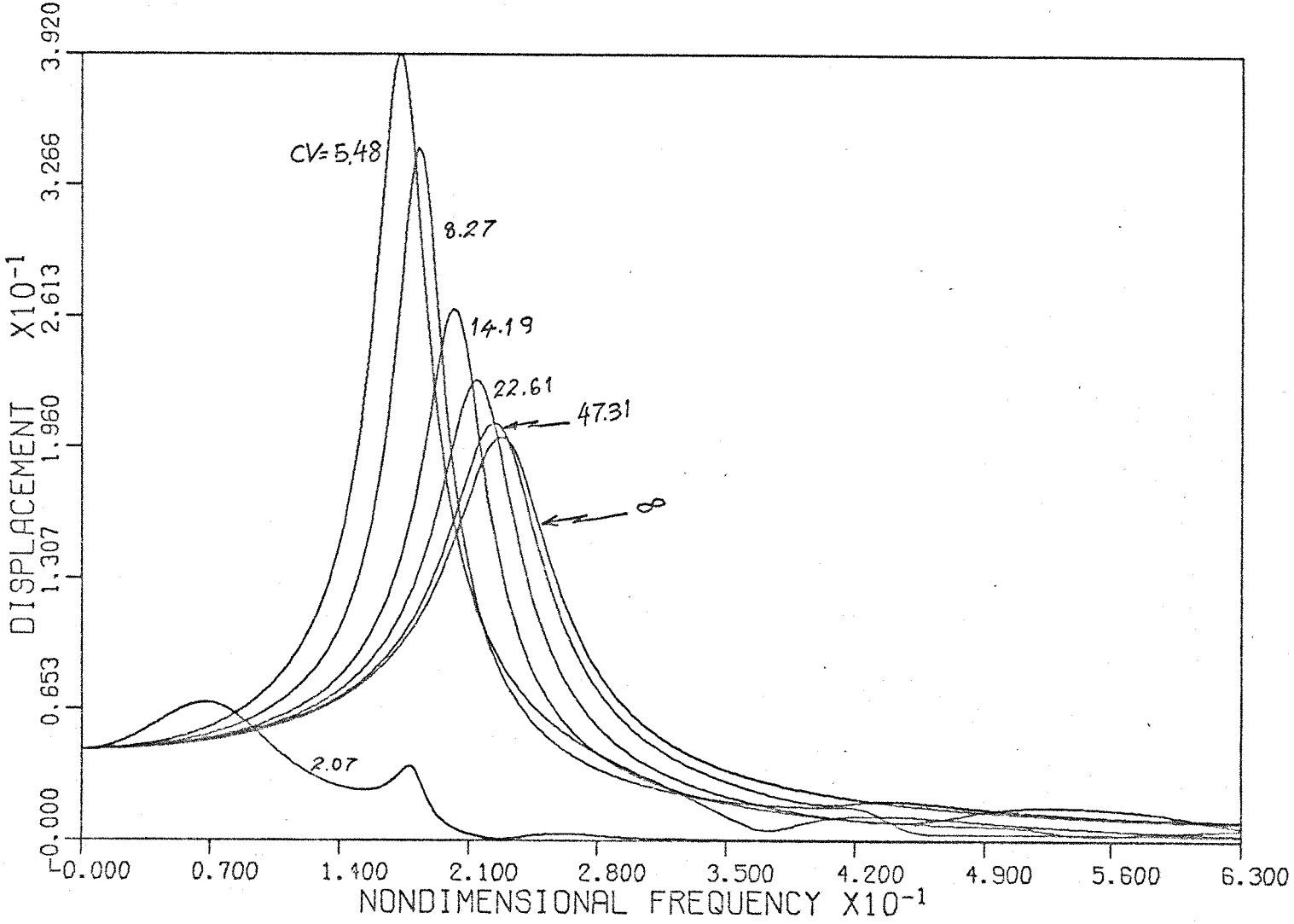

fig. 8.2

Magnitude response of an infinite stringer-stiffened plate to a convected harmonic pressure field. (middle of a bay).

$\eta = 0.25$, $r = 1.$

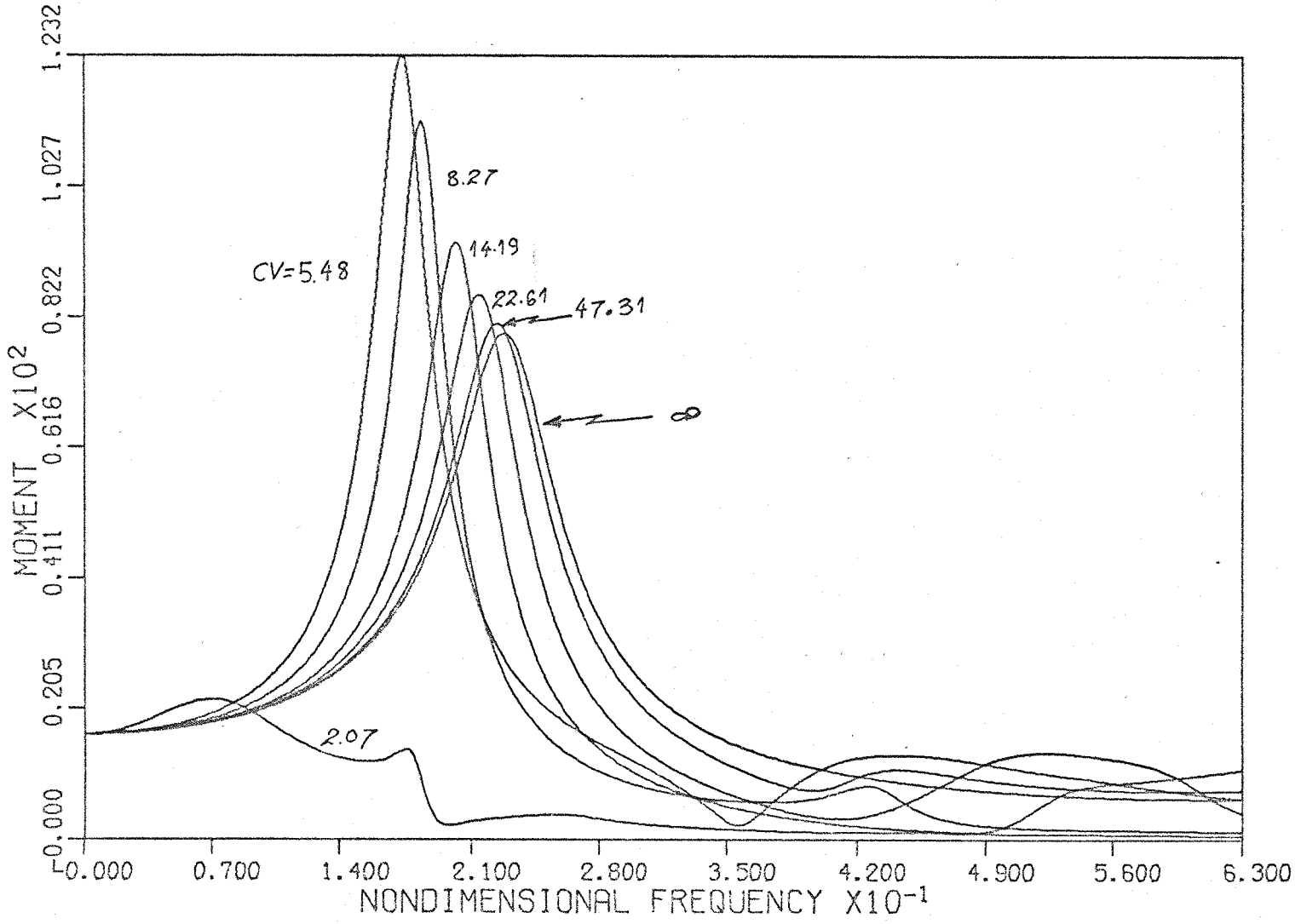

fig. 8.3

Magnitude response at the downstream side of a stringer of a stringer–stiffened plate (infinite) to a convected harmonic pressure field.

$\eta = 0.25$, $r = 1$

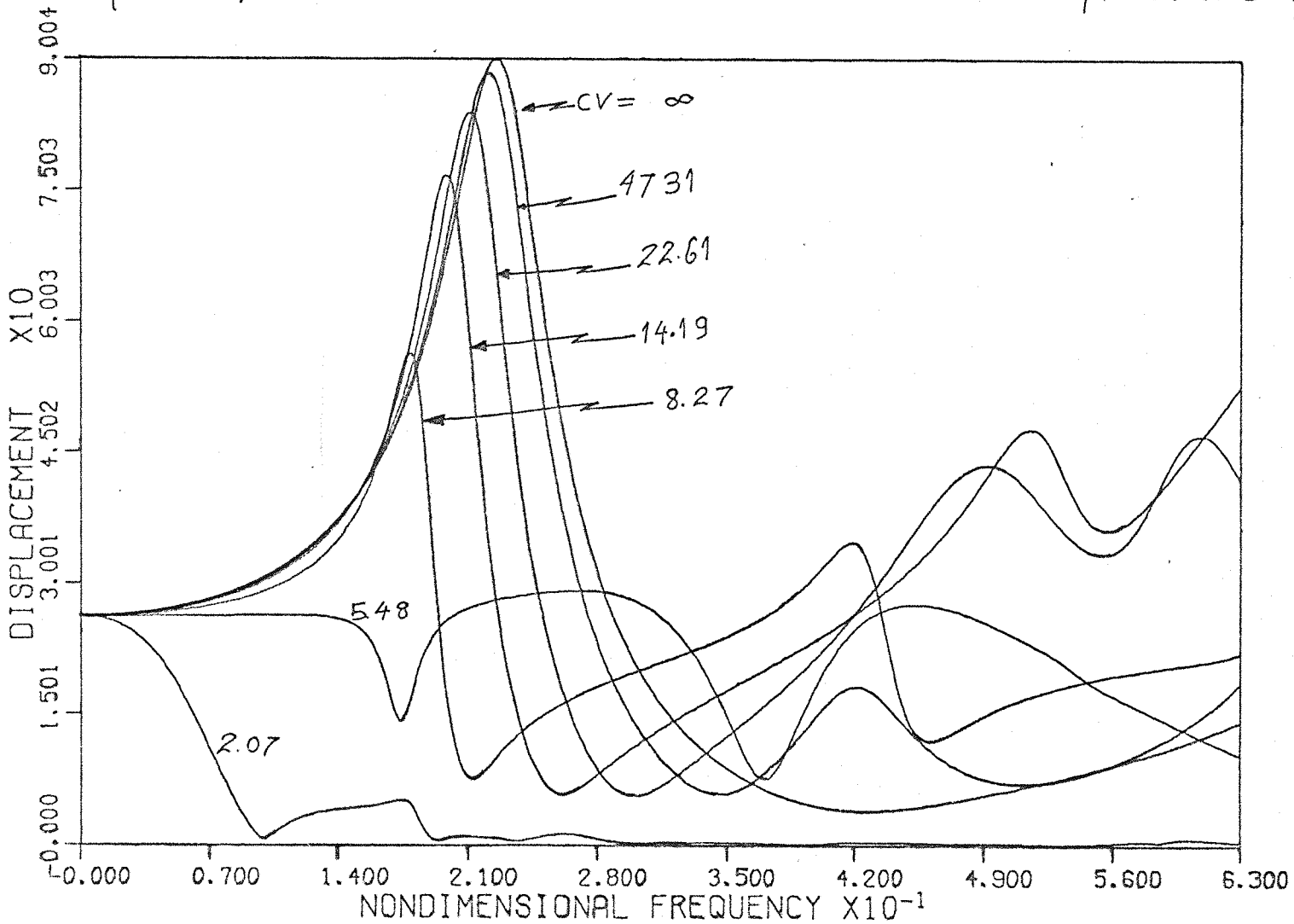

fig. 8.4

Magnitude response at the downstream side of a stringer of a infinite stringer-stiffened plate to a harmonic convected pressure field.

$\eta = 0.25$, $r = 1$.

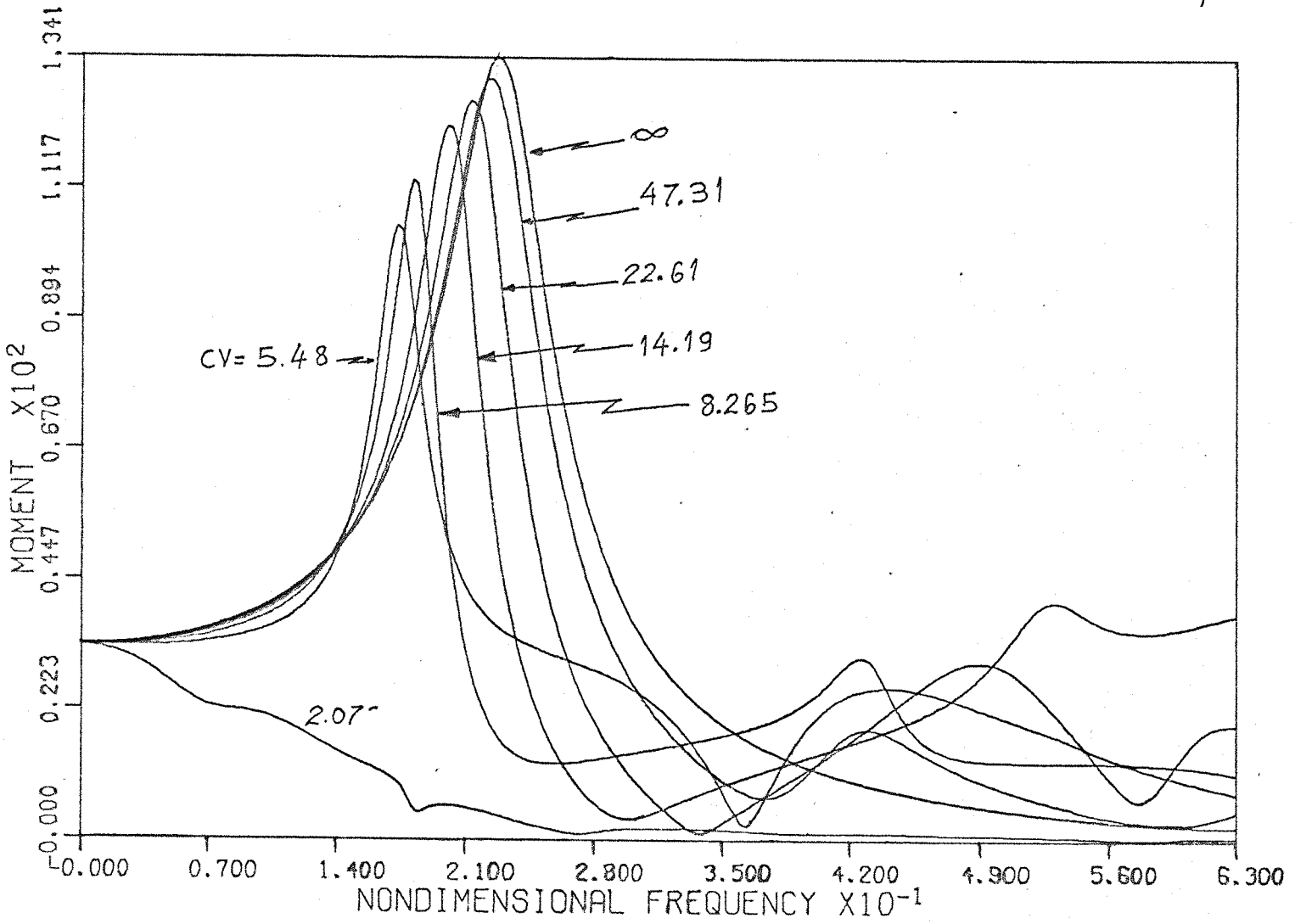

fig. 8.5

fig. 8.6

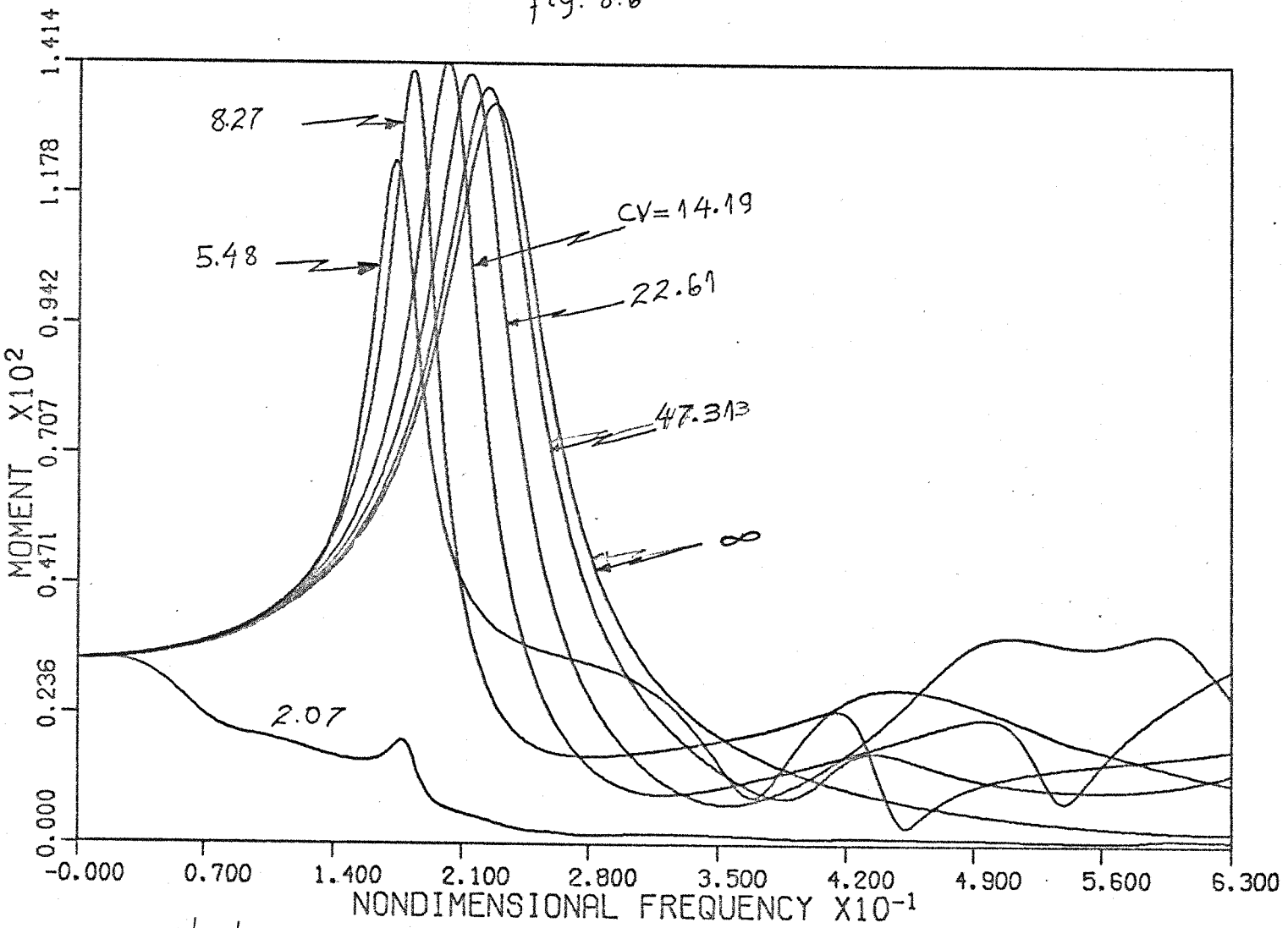

Magnitude response at the upstream side of an stringer-stiffened plate (infinite) to a harmonic pressure field.

$\eta = 0.25$, $r = 1$

Magnitude response at the middle of a bay of a stringer-stiffened shell to a convected harmonic pressure field. $\eta = 0.25$, $r = 1$

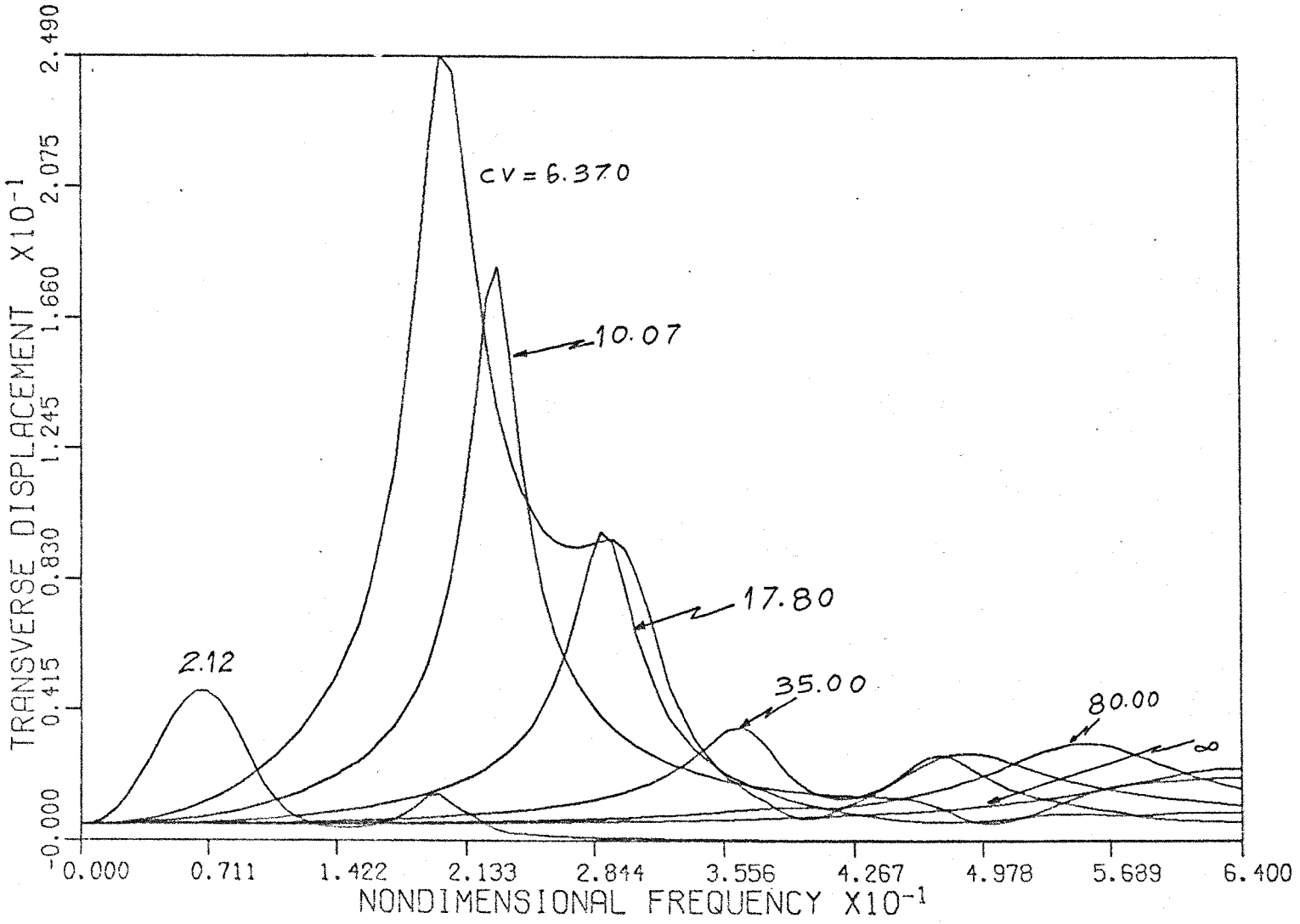

fig. 8.7

Magnitude response at the middle of a bay of a stringer-stiffened shell to a convected harmonic pressure field. $\eta = 0.25$, $r = 1$

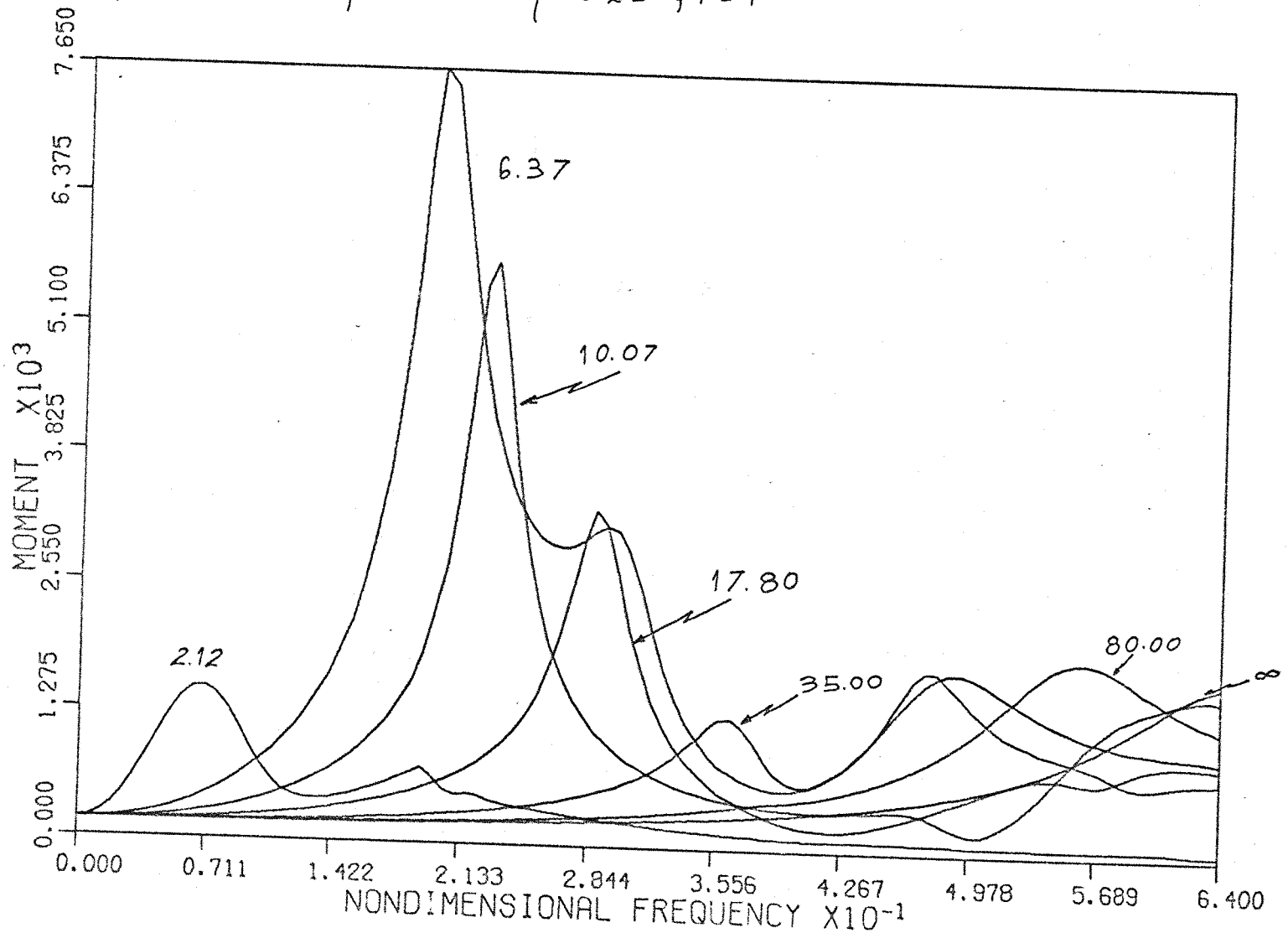

fig. 8.8

Magnitude response at the downstream side of a stringer of a stringer-stiffened shell to a convected harmonic pressure field. $\eta = 0.25$, $r = 1$

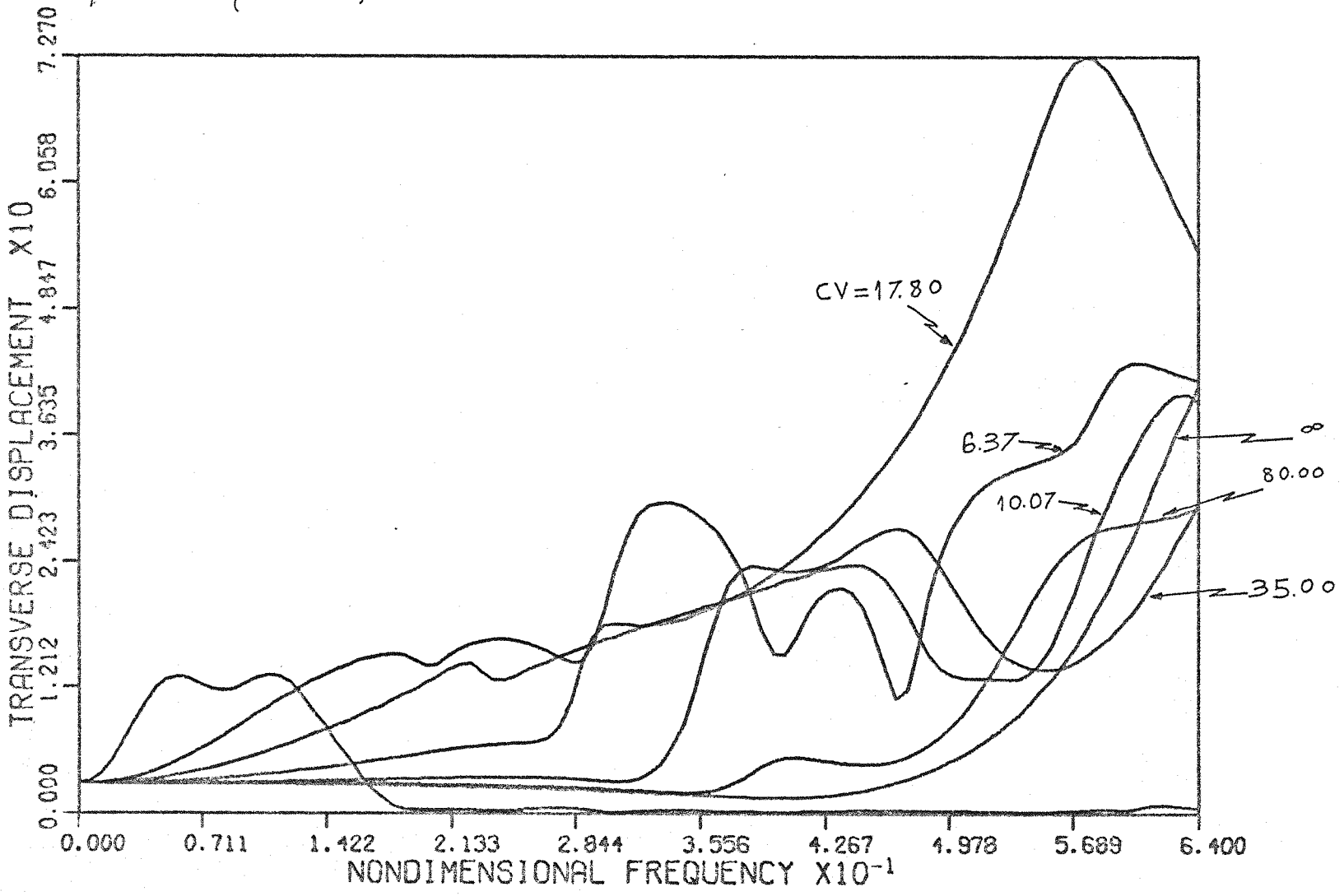

fig. 8.9

Magnitude response at the downstream side of a stringer of a stringer-stiffened shell to a convected harmonic pressure field. $\eta = 0.25$, $r = 1$

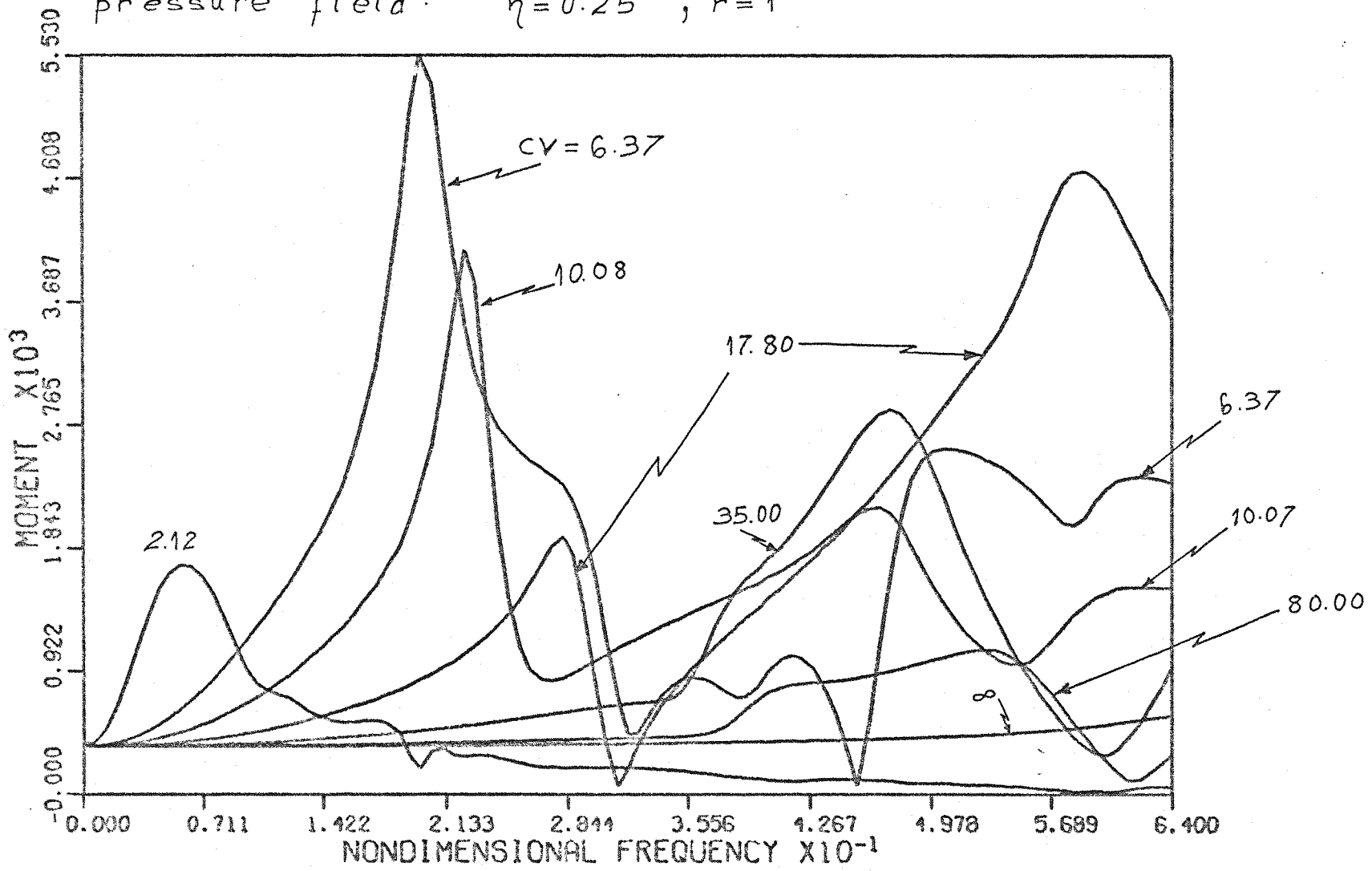

fig. 8.10

Magnitude response at the upstream side of a stringer of a stringer-stiffened shell to a convected harmonic pressure field.

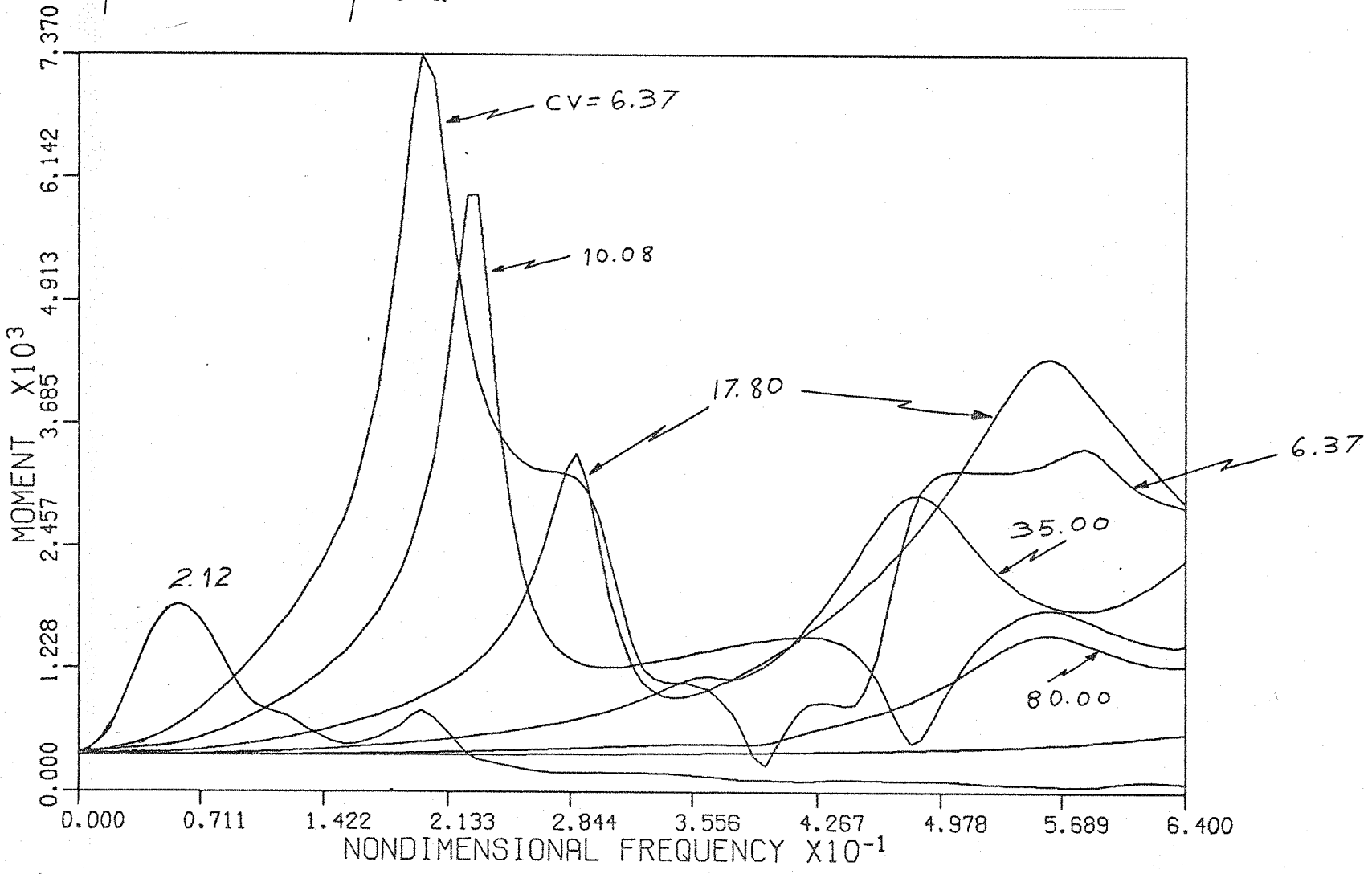

fig. 8.11

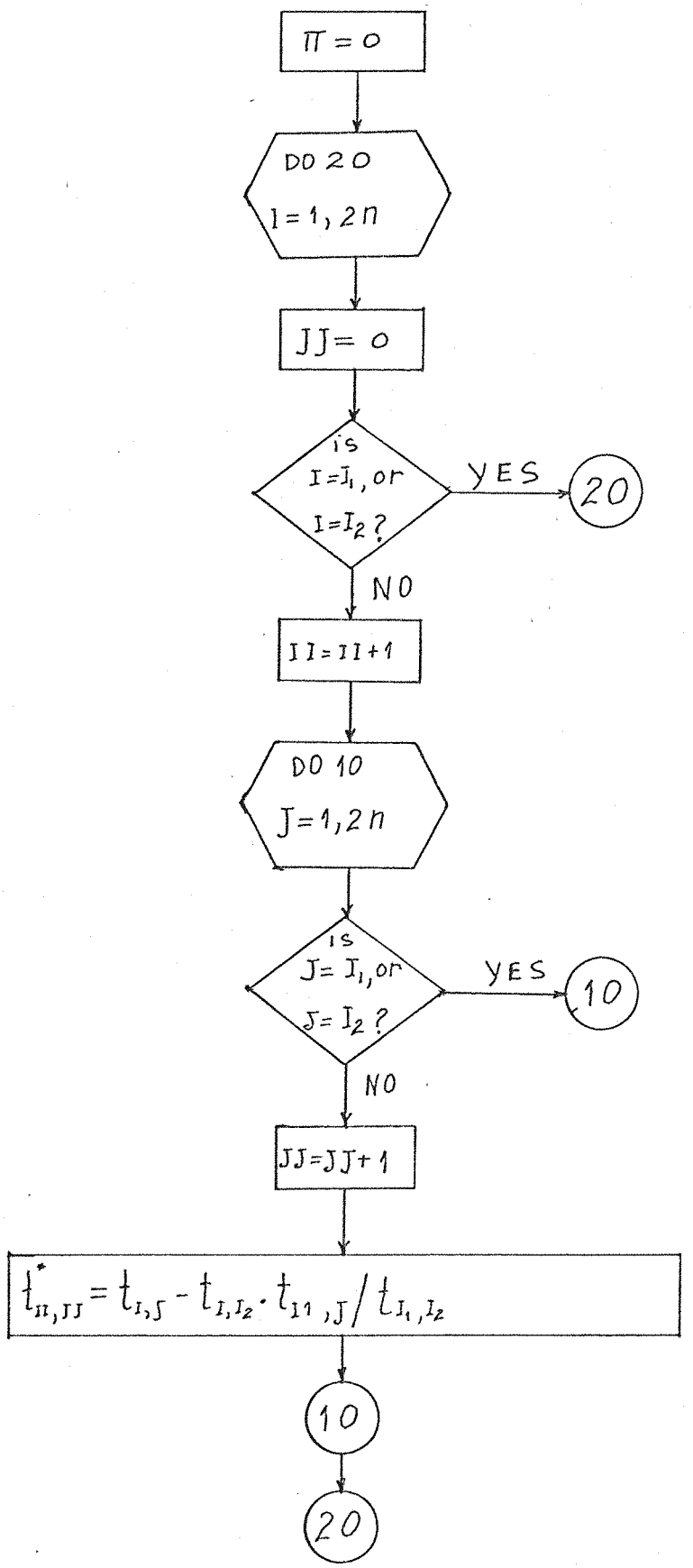
II = 0
DO 20
I = 1, 2n
JJ = 0
is
I = I1, or
I = I2 ?
YES
20
NO
II = II + 1
DO 10
J = 1, 2n
is
J = I1, or
J = I2 ?
YES
10
NO
JJ = JJ + 1
t*II,JJ = tI,J - tI,I2 · tI1,J / tI1,I2
10
20

fig. B 1

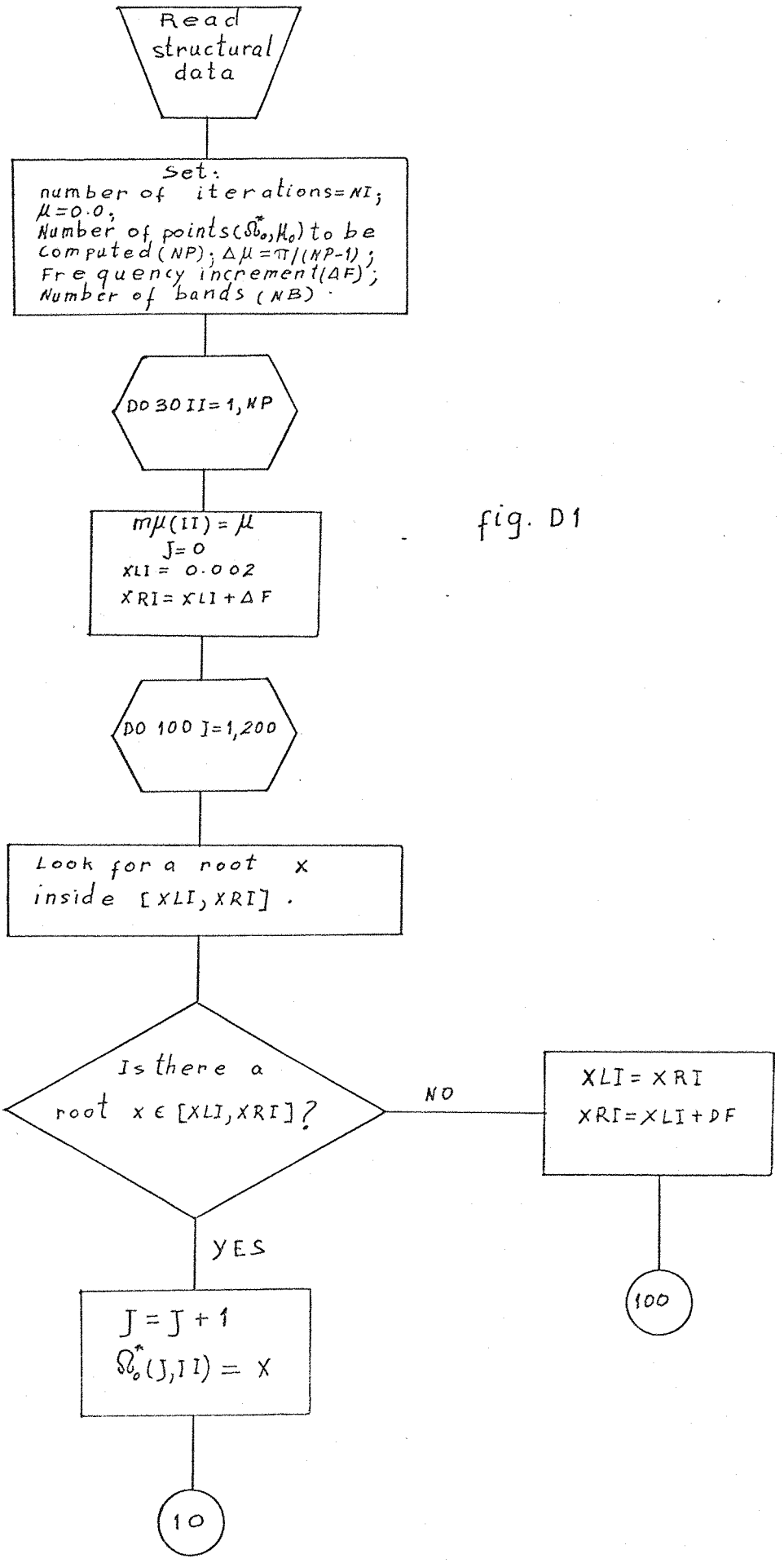
Read structural data
Set:
number of iterations=NI;
μ=0.0;
Number of points(Ω*₀,μ₀) to be computed(NP); Δμ=π/(NP-1);
Frequency increment(ΔF);
Number of bands (NB).
DO 30 II=1,NP
mμ(II)=μ
J=0
XLI = 0.002
XRI=XLI+ΔF
DO 100 I=1,200
Look for a root X inside [XLI,XRI].
Is there a root x ∈ [XLI,XRI]?
NO
XLI=XRI
XRI=XLI+DF
100
YES
J=J+1
Ω*₀(J,II)=X
10

fig. D1

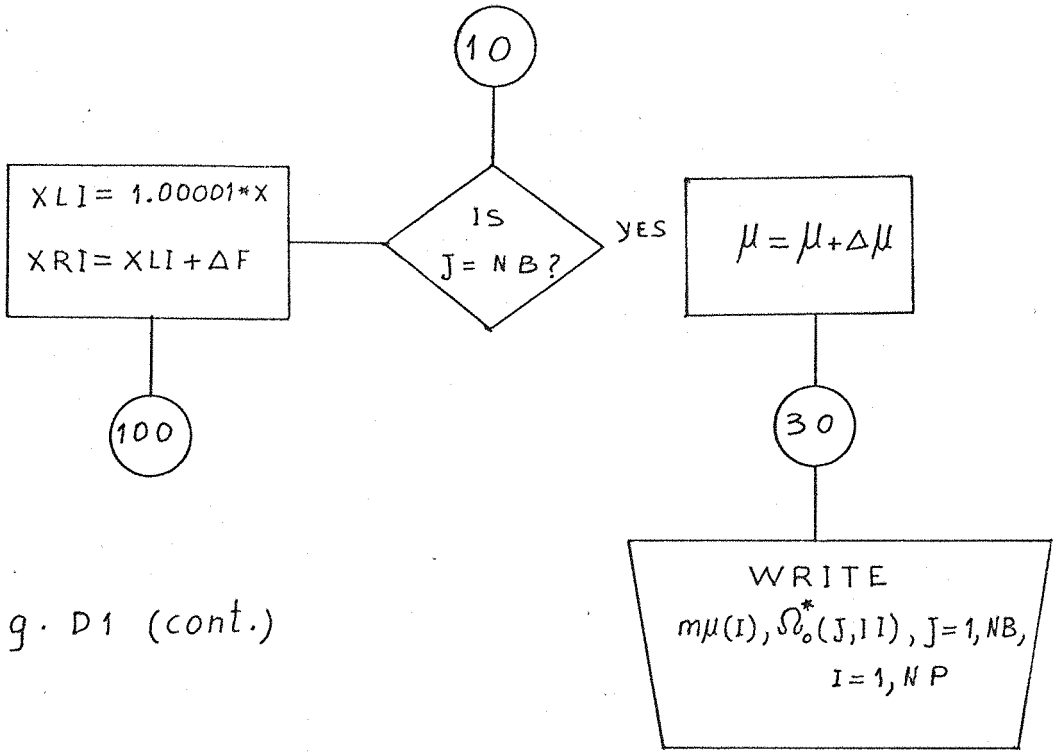

fig. D1 (cont.)

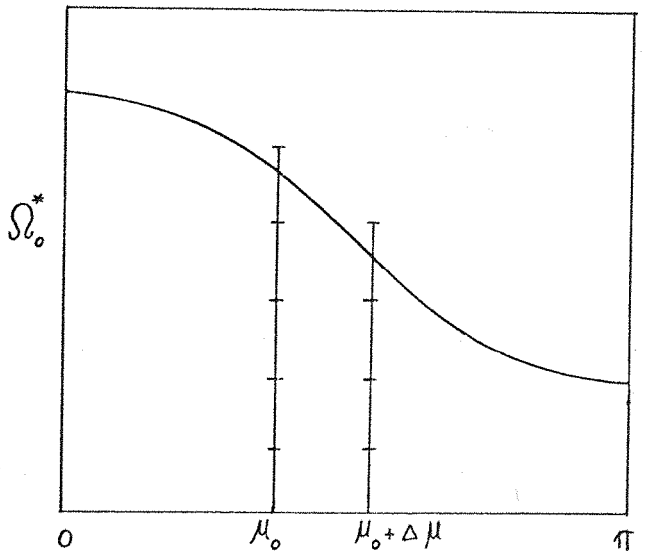

fig. D2

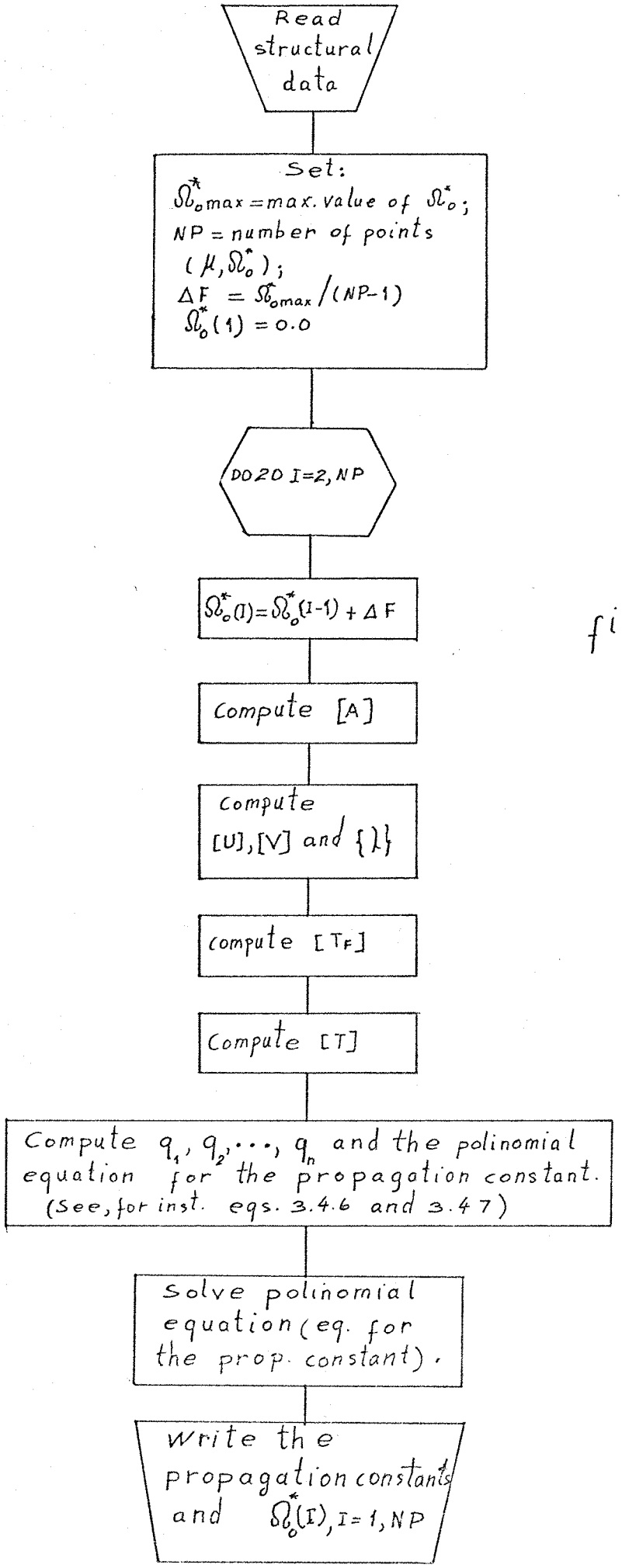
Read structural data
Set:
$\Omega_{o\,max}^{*}$ = max. value of Ω_o^*;
NP = number of points (μ, Ω_o^*);
$\Delta F = \Omega_{o\,max}^{*}/(NP-1)$
$\Omega_o^*(1) = 0.0$
DO 20 I=2, NP
$\Omega_o^*(I) = \Omega_o^*(I-1) + \Delta F$
Compute [A]
Compute [U], [V] and {λ}
compute $[T_F]$
Compute [T]
Compute $q_1, q_2, \cdots, q_n$ and the polinomial equation for the propagation constant. (See, for inst. eqs. 3.4.6 and 3.47)
Solve polinomial equation (eq. for the prop. constant).
write the propagation constants and $\Omega_o^*(I)$, I=1, NP

fig. D3

APPENDIX A

SOME PROPERTIES ASSOCIATED WITH TRANSFER MATRICES

In this appendix some properties associated with transfer matrices are listed. No proof is shown because they are either evident or have been given elsewhere |15|.

Property A1.

If [A] is a cross-symmetric state matrix and if $a_{ij} = 0$ for i + j even then the field transfer matrix is cross-symmetric.

Property A2.

If [T(y,0)] is a transfer matrix and if the state matrix is not dependent on y then:

$$[T(y,0)]^{-1} = [T(-y,0)]$$

Property A3.

The determinant of a transfer matrix is one, that is:

$$\left|[T(y,0)]\right| = 1$$

Property A4.

The characteristic equation of a 2n x 2n transfer matrix

$$\lambda^{2n} - (p_1\lambda^{2n-1} + p_2\lambda^{2n-2} + \ldots + p_{2n-1}\lambda + p_{2n}) = 0$$

enjoys the following properties:

$$p_{2n} = -1$$

$$pj = p_{2n-j}, \quad j = 1,n$$

APPENDIX B

TERMINAL SINGULARITIES : THE AUTOMATIC REDUCTION TECHNIQUE

It was said in sub-section 3.4.1 that when the period transfer matrix is known in its most general form, the period transfer matrix of any other system, derived from the former by imposing terminal constraints (singularities), can be easily obtained numerically. To deduce the technique to perform such operation, the case of a system with originally two terminal degrees of freedom is taken as an illustration. One assumes that one of the terminal degrees of freedom is eliminated so that the derived system has only one terminal degree of freedom left. More specifically still : it will be assumed that the first co-ordinate of the station vector is annihilated by a constraint. Equation (3.2.1) can be expanded for this particular example:

$$0 = t_{12}q_2^L + t_{13}F_1^L + t_{14}F_2^L$$

$$q_2^R = t_{22}q_2^L + t_{23}F_1^L + t_{24}F_2^L$$

$$F_1^R = t_{32}q_2^L + t_{33}F_1^L + t_{34}F_2^L$$

$$F_2^R = t_{42}q_2^L + t_{43}F_1^L + t_{44}F_2^L$$

Solving for F_2^L in the first equation of the above set and taking it into the second and third equations, one can write:

$$q_2^R = (t_{22} - t_{12}\frac{t_{24}}{t_{14}})q_2^L + (t_{23} - t_{13}\frac{t_{24}}{t_{14}})F_1^L$$

$$F_1^R = (t_{32} - t_{12}\frac{t_{34}}{t_{14}})q_2^L + (t_{33} - t_{13}\frac{t_{34}}{t_{14}})F_1^L \quad ..(B.1)$$

Equation (B.1) can be written in matrix form:

$$\begin{Bmatrix} q_2 \\ F_1 \end{Bmatrix}^R = \begin{bmatrix} (t_{22} - t_{12}\frac{t_{24}}{t_{14}}) & (t_{23} - t_{13}\frac{t_{24}}{t_{14}}) \\ (t_{32} - t_{12}\frac{t_{34}}{t_{14}}) & (t_{33} - t_{13}\frac{t_{34}}{t_{14}}) \end{bmatrix} \begin{Bmatrix} q_2 \\ F_1 \end{Bmatrix}^L \quad ..(B.2)$$

In condensed form:

$$\{Z\}^{*R} = [T^*] \{Z\}^{*L} \quad ..(B.2a)$$

It is worth noting that, once this particular case has been considered, the result expressed by equation (B.2) can be generalized for the n-terminal case by looking carefully at the elements of the reduced square matrix.

Perhaps it may not be easy to write down a general formula for the elements of the reduced square matrix, but one can readily establish their law of formation.

Let I_1 be the order of the annihilated generalized co-ordinate and I_2 the order of corresponding generalized force.

Probably the best way of showing how the elements of the reduced transfer matrix are formed is through a flow diagram. This is done in fig. (B.1).

In fig. (B.1) t is an element of the reduced matrix, that is, of the period transfer matrix of the derived system. The diagram is made up of quite standard symbols and the notation is very close to that used in Fortran. If more than one degree of freedom is taken from the terminals of the original system the technique established in fig.(B.1) can be applied in succession, the order of elimination being immaterial.

APPENDIX C

LEVERRIER METHOD WITH FADEEV'S MODIFICATION

Leverrier's method with Fadeev's modification is a direct method for the computation of eigenvalues and eigenvectors of a general square matrix.

Direct methods are not usually the first choice for the computation of eigenvectors and eigenvalues for large matrices because they are generally more sensitive to round-off errors and require greater computing time. The present method, nevertheless, is quite advantageous for the needs of this work because:-

a) The matrices are usually small and in such cases it requires less computing time;

b) It allows advantage to be taken from the cross-symmetry of the matrices with further saving in computing time;

c) It is completely insensitive to the peculiarities of the matrices;

d) It gives the same level of accuracy to both eigenvectors and eigenvalues;

e) It provides an extremely economical way of computing equation for the propagation constant from the period transfer matrix.

Suppose

$$P(t) = (-1)^N (\lambda^N - g_1\lambda^{N-1} - g_2\lambda^{N-2} - \ldots\ldots - g_N) \quad |18|$$

is the characteristic polinomial of the square matrix [A]. It can be proved that the coefficients g_j can be computed by constructing the following sequence:

$$[A]_1 = [A] \quad ; \quad t_r[A]_1 = g_1 \quad ; \quad [B]_1 = [A]_1 - g_1 [I]$$

$$[A]_2 = [A]\,[B]_1 \quad ; \quad \frac{t_r[A]_2}{2} = g_2 \quad ; \quad [B]_2 = [A]_2 - g_2 [I]$$

..(C.1)

$$[A]_{N-1} = [A]\,[B]_{N-2} \; ; \; \frac{t_r[A]_{N-1}}{N-1} = g_{N-1} \quad ; \quad [B]_{N-1} = [A]_{N-1} - g_{N-1} [I]$$

$$[A]_N = [A]\,[B]_{N-1} \; ; \; \frac{t_r[A]_N}{N} = g_N \quad ; \quad [B]_N = [A]_N - g_n [I]$$

By solving the characteristic equation the eigenvalues are found. As was explained in chapter III N is usually even (N = 2n) and it can be seen that $g_j = 0$, j odd, so that the characteristic equation can always be solved first for λ^2 and have its order reduced by half.

Supposing that the eigenvalues are distinct it can be shown that |18| the eigenvalue corresponding to λ_j is given by any of the columns of the square matrix

$$[U]_j = \lambda_j^{N-1} [I] + \lambda_j^{N-2} [B]_1 + \lambda_j^{N-3} [B]_2 + \ldots\ldots [B]_{N-1} \qquad ..(c.2)$$

For instance, for the flat plate structure one has:

$$[A]_1 = [A]_r \; ; \quad [B]_1 = [A]_r \; , \qquad \text{since } g_1 = 0$$

$$[A]_2 = [A]_r^2 ; \quad [B]_2 = [A]_r^2 - 2\zeta^2[I] \quad ; \quad \zeta = \frac{r\pi}{b}$$

$$[A]_3 = [A]_r[B]_2 ; \; [B]_3 = [A_r]^3 - 2\zeta^3[A] \quad ; \quad \text{since } g_3 = 0$$

Taking the expressions for $[A]_r$, $[A]_r^2$ and $[A]_r^3$ and choosing, for instance, the fourth column of $[U]_j$ one has:

$$\{u_j\} = \begin{Bmatrix} 1 \\ -D\,(\lambda_j^2 - \varsigma^2\nu) \\ \\ -D\lambda_j\,\lambda_j^2 - (2-\nu)\varsigma^2 \end{Bmatrix} \qquad ..(C.3)$$

Expression (C.3) has previously been found in Chapter VII.

To compute, say, the k^{th} column of (C.2) it is convenient to use the recurrence formula:

$$\{u\}_o = \{e\}_k$$

$$\{u\}_i = \lambda_j \{u\}_{i-1} + \{b\}_i$$

where $\{e\}_k$ is a column of zero elements except the k^{th} one, which is one and $\{b\}_i$ is the k^{th} column of matrix $[B]_i$.

APPENDIX D

NOTES ON THE COMPUTATION OF $\mu_o - \Omega_o^*$ AND $\Omega_o^* - \mu$ CURVES

Flow diagram D.1 contains the basic steps for the computation of $\mu_o - \Omega_o^*$ curves (passing bands). After reading the pertinent data for the structure it is necessary to set some constants:

NI = maximum number of iterations that are allowed to be performed to find a root, that is, a propagating frequency corresponding to a certain value of μ_o between 0 and π.

ΔF = frequency interval within which a propagating frequency is to be searched. If no root is found inside ΔF another increment ΔF is given and the search continues. If a root is found within ΔF it is stored in mu (see fig. D.2).

Δu = propagation constant increment.

NB = number of passing bands desired; J is a counter for the number of bands.

The search for a root within ΔF was made by a subroutine based on Muller's method [29]. The subroutine first compares the signs of $f(\mu_o, \Omega_o^*)$ (see expression 3.4.5) at the extremes of ΔF and if they are equals it returns giving a message of non-existence of a root within ΔF. If they are different it starts Muller's iterative process until a root is found within a pre-set accuracy.

This process may not converge if ΔF is too large (in a sense) or if round-off errors prevent it. Therefore it is very important to compute $f(\mu_o, \Omega_o^*)$ accurately which implies in the accurate computation of the field transfer matrix and in the coefficients of the equation for the propagation constant. This fact has been emphasised throughout this work.

Fig. D.3 is a flow diagram for the computation of $\Omega_o^* - \mu$ curves. The diagram is self-explanatory and needs no further comments. Perhaps

it is only worth reminding that the polinomial equation for the propagation constant has complex coefficients and was satisfactorily solved by using another subroutine based on Muller's method.

REFERENCES

1. Lin, Y.K. — Free vibration of continuous skin-stringer panels. J. Appl. Mech., Vol. 27, No. 4. (1960).

2. Clarkson, B.L. and Ford, R. — The response of a typical aircraft structure to jet noise. J. Roy. Aero. Soc., Vol. 66, No. 31 (1962)

3. Lin, Y.K., McDaniel, T. Donaldson, B.K., Vail, C.F. and Dwyer, W.J. — Free vibration of continuous skin-stringer panels with non-uniform stringer spacing and panel thickness. Part I. Air Force Materials Laboratory, TR-67-347 (1965).

4. Henderson, J.P. and McDaniel, T.J. — The analysis of curved multi-span structures. Proc. Symp. Struct. Dyn. Vol. I. Loughborough University of Technology (1970).

5. Mead, D.J. — Free wave propagation in periodically supported, infinite beams. J. Sound Vib. 11(2), (1970).

6. Miles, J.W. — Vibration of beams on many supports. Proc. Am. Soc. Civil Eng., ASCE, Vol. 82, nEM1, 1-9 (1956).

7. Brillouin, L. — Wave propagation in periodic structures. Dover Publications (1953).

8. Brillouin, L. — Wave propagation and group velocity. Academic Press (1960).

9. Mead, D.J. and Wilby, E.W. — The random vibrations of a multi-supported heavily damped beam. Shock and Vibration Bulletin, 35, Part 3, (1966).

10. Sen Gupta, G. — Natural flexural waves and normal modes of periodically supported beams and plates. J. Sound Vib. 13(1) (1970).

11. Mead, D.J. and Sen Gupta, G. — Wave group theory applied to the analysis of forced vibrations of rib-skin structures. Paper No. D-3, Proceedings Symp. Struct. Dynamics, Loughborough (1970).

12. Mead, D.J. and Sen Gupta, G. — Wave-group theory applied to the response of finite structures. Paper No. Q. Proc. Conf. on Current Developments in Sonic Fatigue, Southampton (1970).

13. Pestel, E.C. and Leckie, F.A. — Matrix methods in elastomechanics. McGraw-Hill, New York, N.Y. (1963).

14. Lin, Y.K. and McDaniel, T.J. — Response of multi-spanned beam and panel systems under noise excitation. Air Force Systems Command Report No. AFML-TR-64-348, Part II, Wright Patterson Air Force Base, Ohio (1967).

15. Lin, Y.K. and McDaniel, T.J. — Dynamics of beam-type periodic structures. J. of Engineering for Industry, Series B, No. 4, vol. 91 (1969).

16. Mercer, C.A. and Seavey, C. (Miss) — Prediction of natural frequencies and normal modes of skin-stringer panel rows. J. Sound Vib. (1967) 6(1).

17. Leverrier, V.J.J. — Sur les variations seculaires des elements des orbites. J. Math. (1840).

18. Faddeev, D.K. and Faddeeva, V.H. — Computational methods of linear algebra. W.H. Freeman and Co.

19. Sen Gupta, G. — Natural frequencies of periodic skin-stringer structures using a wave approach. J. Sound Vib, 16(4) (1971).

20. Henderson, J.P. and Nashif, A.D. — The effect of stringer width and damping of the response of skin-stringer structures. Trans. ASME, paper no. 71-Vibr-101 (1971).

21. Donnell, L.H. — Stability of thin-walled tubes under torsion. NACA Report No. 479 (1933).

22. Porter, B. — Synthesis of dynamical systems. Thomas Nelson & Son Ltd. (1969).

23. Whitehead, D.S. — A symmetry property of transfer matrices. Aero. J. Roy. Aero. Soc. August (1969).

24. Flugge, Wilhelm — Stresses in shells. Springer-Verlag, New York Inc. (1967).

25. Wah, T. and Hu, W.C.L. — Vibration analysis of stiffened cylinders including inter-ring motion. J. Acoust. Soc. Am., Vol. 43, No. 5 (1968).

26. Mead, D.J. — Acoustically excited modes of vibration. Noise and Acoustic Fatigue in Aeronautics, edited by E.J. Richards and D.J. Mead. John Wiley & Sons Ltd. (1968).

27. Frame, J.S. — Matrix functions and applications, Parts I to V. IEEE spectrum (1964).

28. Lin, Y.K. and Donaldson, B.K. — A brief survey of transfer matrix techniques with special reference to the analysis of aircraft panels. J. Sound Vib. 10(1) (1969).

29. Muller, D.E. — A method of solving algebraic equations using an automatic computer. MTAC 10:208-215 (1956).

30. Aitken, A.C. — Determinants and matrices. Oliver and Boyd (1939).

31. Bushnell, D. — Buckling and vibration of ring-stiffened, segmented shells of revolutions. Internat. J. of Solids and Structures (1969).

32. Forsberg, K. — Exact solution for natural frequencies of ring-stiffened cylinders.

33. Warburton, G.B. — Dynamics of Shells. Proc. Symp. of Structural Dynamics, Loughborough (1970).

34. Warburton, G.B. — Current developments in theoretical dynamics. Proc. Symp. on Applications of Experimental and Theoretical Structural Dynamics, Southampton (1972).

35. Lin, Y.K. — Probabilistic Theory of Structural Dynamics. McGraw-Hill, New York (1967).

36. Hartog, J.P. — Mechanical Vibrations, Fourth Edition. McGraw-Hill Book Co., New York (1956).

37. Mead, D.J. — Vibration response and wave propagation in periodical structures. Paper No. 70-WA/DE-3, Proc. ASME Winter Annual Meeting, New York, N.Y. (1970).

38. Hildebrand, F.B. — Advanced Calculus for Applications. Prentice Hall Inc. (1965).

39. Mead, D.J. and Pujara, K.K. — Space harmonic analysis of periodically supported beams: response to convected random loading.

40. Ungar, E.E. — Steady state response of one dimensional periodic flexural systems. J. Acoust. Soc. Am. 39 (1966).

41. Brobovnitskii, Yu.I. Maslov, V.P. — Propagation of flexural waves along a beam with periodic point loading. Sovietic Physics-Acoustics (1966).

42. Robson, J.D. — Random Vibration. Edinburgh University Press (1963).

43. Pestel, E. — Dynamics of structures by transfer matrices. EOARDC (two reports under contracts AF61(052)-33, 1959 and AF61(052)-302, 1960).

44. Crandall, S.H. and Mark, W.D. — Random vibration in mechanical systems. Academic Press, New York and London (1963).

45. Crandall, S.H. — Random vibration, vol. 2. MIT Press (1963).

46. Kraus, H. — Thin elastic shells. John Wiley & Sons, Inc., New York, London, Sydney (1967).

47. Baker, E.H. et al — Shell analysis manual. NASA CR-912, April (1968).

48. Novozhilov, V.V. — The theory of thin shells. Erven P. Noordhoff, Ltd., Groningen, Netherlands (1959).

49. Pain, H.J. — The Physics of vibrations and waves. John Wiley & Sons (1970).

50. Lindsay, R.B. — Mechanical radiation. McGraw-Hill Book Co. (1960).